THE UNIVERSITY
of EDINBURGH

Examining the potential of rationally designed recombinant Infectious Bronchitis Virus as a vaccine against Infectious Bronchitis.

A thesis submitted in accordance with the requirements of the University of Edinburgh for the degree of Doctor in Philosophy

By Miss Sarah May Keep

June 2019

THE UNIVERSITY *of* EDINBURGH

Contents

List of figures and tables.

Chapter 1.

Chapter 2.

Chapter 3.

Chapter 4.

Chapter 5.

Chapter 6.

Chapter 8.

Declaration.

The University of Edinburgh

Thesis Declaration

See the Postgraduate Assessment Regulations for Research Degrees available via: www.ed.ac.uk/schools-departments/academic-services/policies-regulations/regulations/assessment

Name of Candidate:	Miss Sarah May Keep	*UUN*	S1584262
University email:	s1584262@sms.ed.ac.uk		

Degree Sought:	Doctorate	*No. of words in the main text of Thesis:*	60,000
Title of Thesis:	Examining the potential of rationally designed recombinant Infectious Bronchitis Virus as a vaccine against Infectious Bronchitis.		

I certify:

(a) that the thesis has been composed by me, and

(b) either that the work is my own, or, where I have been a member of a research group, that I have made a substantial contribution to the work, such contribution being clearly indicated, and

(c) that the work has not been submitted for any other degree or professional qualification except as specified.

Signature:	

Acknowledgements.

Firstly I would like to thank my supervisor, Professor Lonneke Vervelde at The Roslin Institute, University of Edinburgh, as well as Dr. Samantha Ellis who helped with the *in vivo* experiments. I would like to thank all members of the coronavirus group at The Pirbright Institute for their unwavering support with particular mention to Michael Oade and Dr. Phoebe Stevenson-Leggett, who both quite frankly deserve a medal. My family and friends deserve a mention for simply keeping me sane as does The Pirbright Institute for providing the funds! Finally I would like to thank my supervisor at The Pirbright Institute, Dr. Erica Bickerton and Professor Paul Britton for helping me secure the opportunity to study for a PhD as well as providing what can only be described as fabulous level of support!

Abstract.

Infectious Bronchitis Virus (IBV) is a gammacoronavirus that is prevalent in poultry flocks worldwide. Infection results in Infectious Bronchitis (IB), an economically important disease characterised by snicking, rales, lethargy, loss of tracheal ciliary activity, reduced weight gain and reduced egg production. Vaccination is commonly practiced using both live attenuated and inactivated vaccines. Live attenuated vaccines are generated by serial passage of a pathogenic field strain in embryonated chicken eggs; the molecular mechanism is unknown. A fine balance needs to be achieved between the loss of pathogenic *in vivo* phenotype and the retention of immunogenicity. Due to the unpredictability of the process and the time required there is a drive to rationally design and rationally attenuate recombinant IBV (rIBV) that can be subsequently utilised as live attenuated vaccines.

Vaccine induced protection is predominantly associated with the spike (S) glycoprotein, which consists of two subunits, the immunodominant S1 and the highly conserved S2. Whilst the latter is considered to be less immunogenic, it has been reported to play a role in protective immunity. In this thesis rIBVs, based on the apathogenic rIBV, Beau-R, that express heterologous S1 or S2 subunits BeauR-QX(S1), BeauR-M41(S1), BeauR-M41(S2), or S glycoproteins, BeauR-M41(S) and BeauR-4/19(S) are investigated as vaccines against either homologous or heterologous challenge. The rIBV expressing a heterologous S glycoprotein, BeauR-M41(S) offered increased protection against homologous challenge as defined by the retention of ciliary activity in comparison to those expressing heterologous S1 or S2 subunits, BeauR-M41(S1) and BeauR-M41(S2) respectively. The protection induced however fell short of the standards set by the European Pharomopiea and further investigation demonstrated that rIBV expressing heterologous S glycoproteins, BeauR-M41(S) and BeauR-4/91(S) could not protect against a heterologous QX challenge. One possible explanation is the limited replication of the vaccine viruses *in vivo*. Investigation of the Beau-R vaccine backbone determined that replication is temperature sensitive and highly restricted at 41°C, the core body temperature of a chicken. As a consequence a rIBV based on the laboratory strain M41-CK was subsequently investigated for its potential to act as a vaccine backbone.

Lay summary of thesis.

Infectious Bronchitis Virus (IBV) is a virus that is prevalent in poultry flocks worldwide. Infection results in Infectious Bronchitis (IB), an economically important disease characterised by snicking (sneezing), rales (rattle in the lungs), lethargy, reduced weight gain as well as reduced egg production, in terms of both quantity and quality. The virus also renders infected birds susceptible to secondary bacterial infections which can lead to mortality. Vaccination is commonly practiced using both live attenuated and inactivated vaccines. Live attenuated vaccines are traditionally generated by serial passage of a pathogenic field strain in embryonated chicken eggs; the molecular mechanism is unknown. A fine balance needs to be achieved between loss of a pathogenic *in vivo* phenotype and the retention of immunogenicity. Due to the unpredictability of the process and the time required there is a drive to rationally design and rationally attenuate recombinant IBV (rIBV) that can be subsequently utilised as live attenuated vaccines.

Research detailed in this thesis investigates the potential for rationally designed rIBVs to act as vaccine viruses. The research involves characterisation through vaccine-challenge experiments in specific pathogen free (SPF) chickens as well as characterisation through *in vitro* experiments in cell culture. Research assessing temperature sensitive replication is also included in these *in vitro* experiments. The information provided in this thesis will help in the design of the next generation of rationally designed, rationally attenuated rIBVs for use as vaccine viruses.

Abbreviations.

µg - Microgram

µl - Microlitre

aa - Amino acid

Ab - Antibody

ACE2 - Angiotensin I converting enzyme 2

ACE2 - Human Angiotensin converting enzyme 2

ADRP - ADP-ribose-1”-phosphate phosphatase

Ala - Alanine

ANOVA - Analysis of variance

APHA - Animal Health and Plant agency

APN - Aminopeptidase N

Arg - Arginine

Asn - Asparagine

Asp - Aspartic Acid

BAC - Bacterial Artificial Chromosome

BcoV - Bovine coronavirus

BES - N,N-bis(2-hydroxyethyl)-2-aminoethanesulphonic acid

BHK - Baby Kidney Hamster

BSA - Bovine Serum Albumin

$C_2H_{20}BrN_3$ - Ethidium Bromide

CALT - Conjunctival-associated lymphoid tissue

CoV - Caninie Coronavirus

CD - Cilostatic dose

CDC - Centers for Disease Control

CEACAM1 - Carcinoembryonic antigen-cell adhesion molecule

CEF - Chicken Embyo Fibroblast

CK - Chicken kidney

CLT – Cytotoxic T cell

CMV - Cytomegalovirus

CO_2 - Carbon dioxide

CoV - Coronavirus

CPE - Cytopathic effect

Cryo-EM - Cryogenic electron microscopy

CSU - Central Services Unit

CT - Cytoplasmic tail

ct - Cycle threshold

CTD - Carboxyl terminal domain

Cys - Cysteine

Da - Dalton

DF1 - Immoratized chicken embryo fibroblasts

DMEM - Dulbecco's minimum essential medium

DMV - Double membrane vesicle

dpc - Days post challenge

dpi - Days post infection

DPP4 - Dipeptidyl peptidase 4

dppv - Days post primary vaccination

dpsv - Days post secondary vaccination

dpv - Days post vaccination

dsRNA - Double-stranded RNA

E - Envelope

E.coli - Escherichia coli

EAH/BSU - Experimental animal house

EDTA - Ethylenediaminetetraacetic acid

ELISA - Enzyme linked immunosorbent assay

EMEM - Eagle's minimum essential medium

ER - Endoplasmic reticulum

ERGIC - Endoplasmic reticulum Golgi intermediate compartment

ExoN - Exoribonuclease

FCoV - Feline coronavirus

FCS - Foetal Bovine Serum

FIPV - Feline infectious peritonitis virus

FP - Fusion Peptide

FPV - Fowlpox virus

g - Gram

Gln - Glutamine

Glu - Glutamic Acid

Gly - Glycine

GMEM - Glasgow's minimum essential medium

GPT - Escherichia coli guanine phosphoribosyltransferase

GTase - Guanylyltransferase

h - Hour

HCoV - Human coronavirus

HE - Haemagglutinin Esterase

HG - Harderian Gland

His - Histidine

hpi - Hours post infection

HPIV3 - Human parainfluenza virus type 3

hpv - Hours post vaccination

HR - Heptad repeat

HVR - Hypervariable region

HδR - Hepatitis delta antigenome ribozyme

i.m. - Intramuscular

IB - Infectious bronchitis

IBV - Infectious bronchitis virus

ICTV - International Committee for the Taxonomy of Viruses

IFN - Interferon

IIe - Isoleucine

Il18 - Interleukin I18

IR - Intergenic Region

kb - Kilobases

LB - Luria-Bertani broth

Leu - Leucine

Lys - Lysine

M - Membrane

MDA – Maternally derived anitbody

MDA5 - Melanoma differentiation associated protein 5

MERS-CoV - Middle East respiratory syndrome coronavirus

Met - Methioninie

Mg - Magnesium

mg - Milligram

MgCl2 - Magnesium Chloride

MHV - Mouse hepatitis virus

min - Minute

ml - Milliliter

MOI - Multiplicity of infection

MPA - Mycophenolic acid

Mtase - N7 Methyltransferase

N - Nucleocapsid

NaOH - Sodium hydroxide

NARF - National Avian Resource Facility

NBBS - Newborn Calf Serum

NDV - Newcastle disease virus

NendoU - Manganese-dependant endoribonuclease

NK – Natural Killer cell

ns - Not significant

nsp - Non-structural protein

nt - Nucleotide

NTD - Amino terminal domain

ORF - Open reading frame

PBS - Phosphate buffered saline

PBSa - Phosphate buffered saline a

PCR - Polymerase chain reaction

PDCoV - Porcine delta coronavirus

PEDV - Porcine epidemic diarrhoea virus

PFU - Plaque forming unit

Phe - Phenylalanine

PLPro/PLP - Papain-like protease

pp - Polypeptide

PPU - Poultry production unit

PRCV - Porcine respiratory coronavirus

Pro - Proline

qRT-PCR - Quantitative real time polymerase chain reaction

RBD - Receptor binding domain

RdRp - RNA-dependent RNA polymerase

rFPV - Recombinant fowlpox virus

RFS – Ribsomal Frame Shift

rIBV - Recombinant infectious bronchitis virus

RIR - Rhode Island Red

rN - Recombinant N

rNDV - Recombinant Newcastle Disease Virus

RNP - Ribonucleoprotein

rph - Revolutions per hour

rpm - Revolutions per minute

rS - Recombinant S

rS1 - Recombinant S1

RSV - Respiratory syncytial virus

RTC - Replication-transcription complex

RT-PCR - Reverse transcription polymerase chain reaction

s - Second

S - Spike

s/pratio - Sample/positive ratio

SAM - S-adenosyl methionine

SARS-CoV - Severe acute respiratory syndrome coronavirus

SD - Standard deviation

SDS - Sodium Dodecyl Sulfate

SEM - Standard error of mean

Ser - Serine

sg - Sub-genomic

sgmRNA - Sub-genomic messenger RNA

SIII - Superscript III

SPF - Specific pathogen free

ss - Single stranded

SSIV - Superscript IV

TAE - Tris-acetate EDTA

TBE - Tris Borate EDTA

TCoV - Turkey coronavirus

TDS - Transient dominant selection

TE buffer - Tris-EDTA buffer

TGEV - Transmissible gastroenteritis virus

Thr - Threonine

TK - Thymidine Kinase

TM - Transmembrane

TOC - Tracheal organ culture

TPB - Tryptose phosphate broth

Tris-HCl - Tris(hydroxymethyl)aminomethane hydrochloride

Trp - Tryptophan

TRS - Transcription regulatory sequence

Tyr - Tyrosine

U - Unit

Ubl - Ubiquitin-like domain

UTR - Untranslated region

Val - Valine - Val

VN - Virus neutralising

VV - Vaccinia virus

WT - Wild type

Chapter 1: Introduction

1.1 Classification: the Coronavirinae.

The *Orthocoronavirinae* is a subfamily of the family *Coronaviridae* that is part of the *Nidovirales* order (Figure 1.1). The subfamily *Orthocoronavirinae* is divided into four genera including *Alphacoronavirus*, *Betacoronavirus*, *Gammacoronavirus* and *Deltacoronavirus* (International Committee for the Taxonomy of Viruses, ICTV, October, 2018). Members across each of the genera pose significant threats to human health, animal health and welfare, as well as food security. Notable members of each genera are listed in Table 1.1. Despite the identification of coronaviruses across all four genera that infect over 30 species, the most widely researched and characterised viruses are that of the betacoronavirus genus and include the zoonotic human pathogen Severe Acute Respiratory Syndrome Coronavirus (SARS-CoV) and Middle East Respiratory Syndrome Coronavirus (MERS-CoV) as well as the mouse pathogen, Murine Hepatitis Virus (MHV).

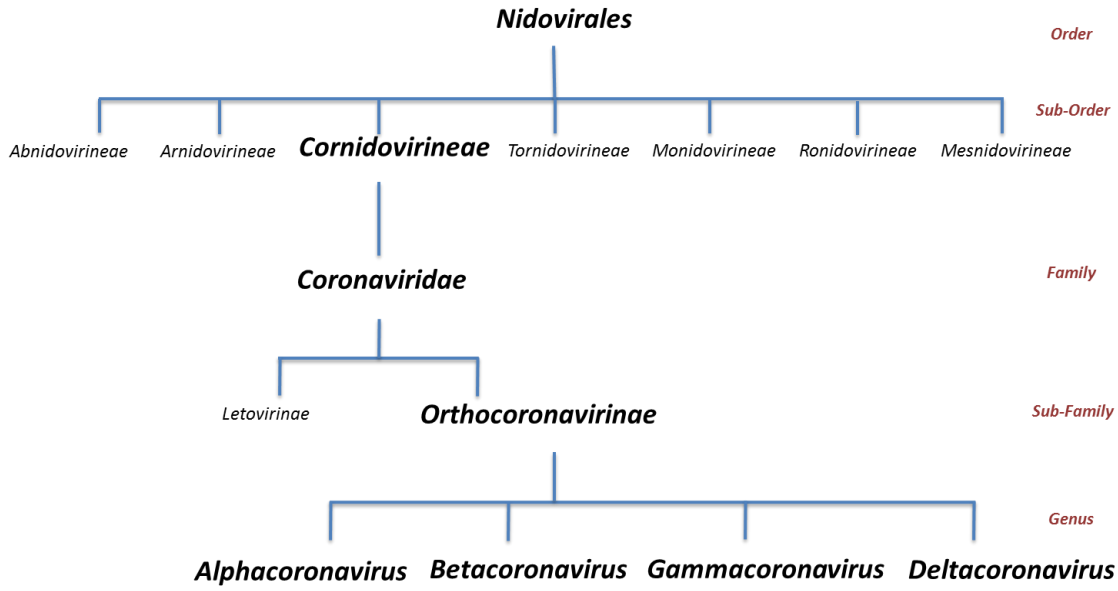

Figure 1.1: Classification of the Nidovirales order as determined by the ICTV, 2018.

Table 1.1 Members of the four genera of the *Orthocoronavirinae* subfamily as determined by the ICTV, 2018.

Genus	***Species***	***Host species***
Alphacoronavirus	Porcine epidemic diarrhoea virus (PEDV)	Pigs
	Human coronavirus 229E (HCoV-229E)	Human
	Human coronavirus NL63 (HCoV-NL63)	Human
	Feline Coronavirus (FCoV)	Cats
	Canine Coronavirus (CCoV)	Dogs
	Transmissible gastroenteritis virus (TEGV)	Pigs
Betacoronavirus	Murine Coronavirus (MHV)	Mouse
	Human coronavirus HKU1 (HCoV-HKU1)	Human
	Severe Acute Respiratory syndrome related coronavirus (SARS-CoV)	Human
	Middle East Respiratory syndrome related coronavirus (MERS-CoV)	Human
	Bovine Coronavirus (BCoV)	Cows
Gammacoronavirus	Beluga whale coronavirus SW1	Beluga Whale*
	Avian coronavirus (IBV)	Poultry (domestic fowl)
	Turkey Coronavirus (TCoV)	Turkey
Deltacoronavirus	Munia coronavirus	Bird *(Estrildidae)**
	Bulbul coronavirus	Bird *(Pycnonotidae)**
	Thrush coronavirus	Bird *(Turdidae)**

Notes: * Viruses were identified from genome screening, and no known infectious virus has been isolated (Mihindukulasuriya *et al.,* 2008; Woo *et al.,* 2009).

1.2 Infectious Bronchitis Virus.

Infectious bronchitis virus (IBV) is the prototype *gammacoronavirus* that was first identified in 1937 (Beaudette and Hudson, 1937). IBV infects domestic fowl (*Gallus gallus*), is spread by droplet transmission and is the aetiological agent of Infectious Bronchitis (reviewed by Cavanagh, 2007). There is a wide variety of both circulating and non-circulating strains, which is unusual in comparison to other known coronaviruses (Valastro *et al.,* 2016). Notably strains include Beaudette, an apathogenic commonly utilised laboratory strain and M41, a pathogenic field strain with global distribution, that is also commonly used in the laboratory. Both M41 and Beaudette are of the Massachusetts serotype. Other notable field strains include 4/91 which appeared in the UK in the 1990's (Gough *et al.,* 1992) and has spread globally although not to the USA, Australia or New Zealand (reviewed by de Wit *et al.,* 2011). Similarly, the QX strain first identified in China in the later 1990's (Lui and Kong, 2004; Liu *et al.,* 2006) and subsequently spread through Russia into Europe is also not circulating in the USA, Australia nor New Zealand.

Although new IBV strains appear continuously, not all these strains are able to spread and become global problems. The Connecticut and Arkansas strains that appeared in the USA in the 1950's and 1970's respectively, remain still largely confined to the USA (reviewed by de Wit *et al.,* 2011). The strain B1648, that first appeared in Belgium in the 1990's remained confined to neighbouring countries and did not become endemic throughout Europe. Common IBV strains circulating in Egypt and Israel have also not established infection outside of their current geographical location. A further example is D1466, first reported in the 1970's, which remains a concern in Europe but not for the rest of the world (reviewed by de Wit *et al.,* 2011). This variety of IBV strains and the associated geographical dispersal means that each country/area has strains of interest and/or concern. Research and vaccine development projects, therefore, are tailored to reflect these interests.

1.3 The coronavirus genome.

The coronavirus (CoV) genome consists of a linear non-segmented positive sense single stranded RNA molecule that possesses a methylated cap structure (cap-1) at the 5′ end and is polyadenylated at the 3′ end. Each CoV genome therefore resembles eukaryotic mRNA (reviewed by Britton and Cavanagh, 2008). In addition each genome contains an

untranslated region (UTR) at both the 5′ and 3′ end which have roles in both genome and subgenomic mRNA (sgmRNA) synthesis (Hsue and Masters, 1997; Williams *et al.,* 1999; Liu *et al.,* 2001). The genomes of coronaviruses are the largest recorded of all the known RNA viruses ranging from approximately 26 kb to 32 kb (reviewed by Gorbalenya *et al.,* 2006); the genome of IBV is 27.6 kb (Boursnell *et al.,* 1987).

General genome organisation is shared between coronaviruses; 5′ UTR – replicase gene – structural and accessory genes – 3′ UTR (Figure 1.2A). The replicase gene comprises approximately the 5′ most proximal two thirds of the genome, and is divided into two open reading frames (ORF), ORF1a and ORF1b. Translation of the replicase gene results in the generation of two polypeptides, pp1a, approximately 3950 amino acids (aa) in length and pp1ab, 6630 aa, of which the latter is a result of -1 programmed ribosomal frame shift (Brierley *et al.,* 1987; Brierley *et al.,* 1989). Both polypeptide pp1a and pp1ab are proteolytically cleaved by virus encoded proteinases into 16 or in the case of IBV, 15 non-structural proteins (nsps; Ziebuhur *et al.,* 2000; Sawicki *et al.,* 2007). Of note, the genome of IBV is missing nsp 1. The resulting nsps assemble into replication-transcription complexes (RTC) which during viral replication synthesis genome and sgmRNAs (reviewed by Fehr and Perlman, 2015).

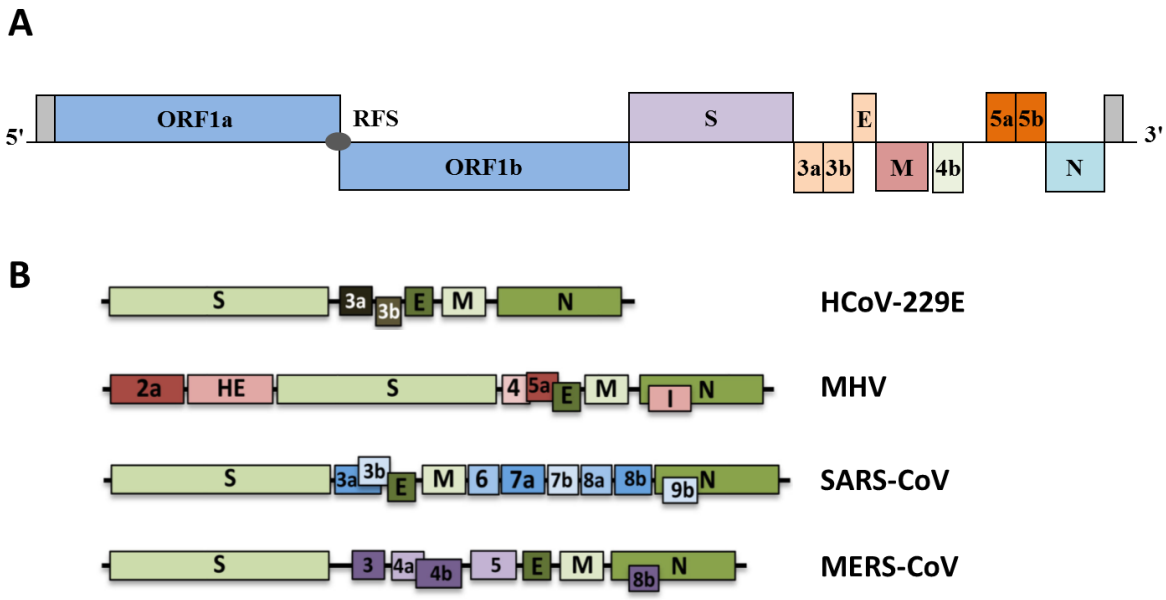

Figure 1.2 Coronavirus genome organisation. (A) Schematic of IBV genome. The 5′ two thirds of the genome consists of two ORFs that are translated as two polyproteins, via a -1 ribosome frameshift site (RFS). The 3′ third of the genome contains the structural genes spike (S), envelope (E), membrane (M) and nucleocapsid (N) genes as well as the accessory genes 3a, 3b, 4b, 5a and 5b. At each end of the genome is an untranslated region (UTR) denoted in grey. (B) Schematic detailing the organisation of the structural and accessory genes of HCoV-229E, MHV, SARS-CoV and MERS-CoV. Image adapted from Fehr and Perlman (2015).

The 3′ proximal end of the genome encodes the structural genes, Spike (S), Envelope (E), Membrane (M) and Nucleocapsid (N) as well as several small non-structural genes referred to as either the accessory or group specific genes (Figure 1.2A). The location and quantity of the accessory genes varies from one coronavirus to another (Figure 1.2B). It must be noted that the naming of the accessory genes/proteins is related to genome location and not biological function. The IBV genome is widely accepted to encode four accessory proteins, designated 3a, 3b, 5a and 5b, encoded by gene 3 and gene 5 respectively (Figure 1.1A). A fifth accessory protein, 4b, has been proposed from a previously unidentified ORF often referred to as the intergenic region (IR) that is located between gene M and gene 5 (Bentley *et al.,* 2013B).

1.4 Virion structure.

The coronavirus virion has been studied by both cryo-electron tomography and cryo-electron microscopsy (Neuman *et al.,* 2006; Barcena *et al.,* 2009). The characteristic feature is the distinct solar corona-like morphology, which is the result of the S glycoprotein protomers protruding outward from the virion surface (Figure 1.3). The membrane of the virion which houses a helically symmetrical nucleocapsid contains at least the S, M and E proteins. The virion membrane of the betacoronavirus, MHV, also contains haemagglutinin esterase (HE). The nucleocapsid constitutes the N protein which complexes with the RNA genome.

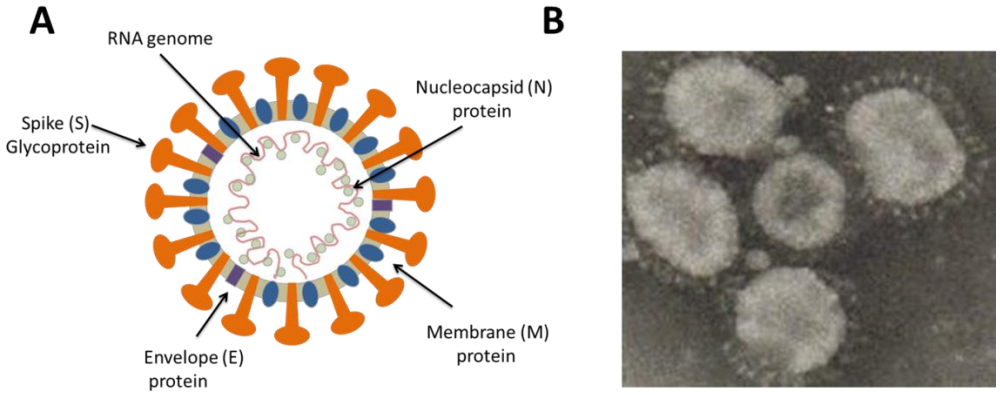

Figure 1.3: Coronavirus virion morphology. (A) Schematic detailing the structural organisation of a coronavirus virion. (B) Electron micrograph of IBV. Image taken from the Centers for Disease Control and Prevention (CDC) Public Health Image Library, ID number 4814.

1.5 Replication cycle.

All coronaviruses including IBV replicate solely in the cell cytoplasm (Figure 1.4). Attachment and entry of the virus particle to the host cell is mediated by the S glycoprotein. The exact mechanism of IBV entry is not completely understood; the coronavirus entry process is complex, exhibits differences between coronavirus species and strains and additionally is dependent on the host cell (reviewed by Belouzard *et al.,* 2012). It is thought that IBV enters via endocytosis where pH dependant viral to membrane fusion occurs releasing the nucleocaspid into the cells cytosol (Chu *et al.,* 2006). It must be noted, and will be discussed further in Chapter 1 and Chapter 3, that after receptor binding, the S glycoprotein undergoes extensive conformational changes which exposes a fusion peptide (FP) allowing the fusion of viral and host cell membranes (Walls *et al.,* 2017; Shang *et al.,* 2018). These conformational changes are not only driven by receptor binding but are thought to require additional triggers such as pH acidification and/or proteolytic cleavage (reviewed by Belouzard *et al.,* 2012). The IBV S glycoprotein is cleaved by furin like proteases.

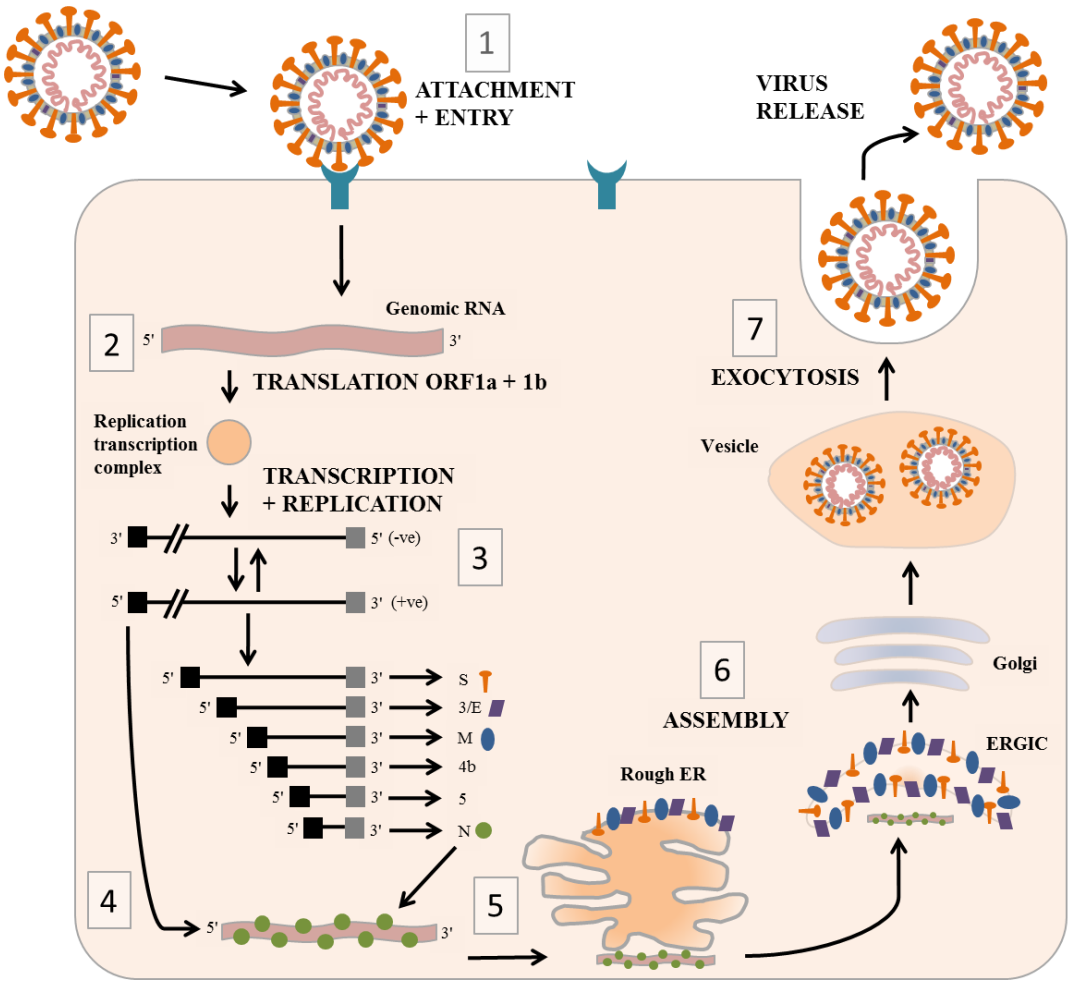

Figure 1.4: Schematic representation detailing the main events in the replication cycle of IBV. (1) The virus particle attaches to the host cell via a receptor; this event is mediated by the S glycoprotein. (2) The virus particle is thought to enter the cell via endocytosis, where membrane fusion results in the release of the nucleocapsid containing the viral genome into the cell cytoplasm initiating the translation of ORF1a and ORF1b. (3) The resulting nsps form the replication transcription complexes (RTCs) which mediate both genome replication and sg mRNA synthesis. (4) Newly synthesised RNA genomes are encapisated by the N protein. (5) The structural proteins are transported to the endoplasmic reticulum (ER) via the secretory pathway. (6) Progeny virions are assembled at the ER-Golgi Intermediate Compartment (ERGIC) with mature virion particles released (7) from the cell via exocytosis.

Once the nucleocaspid has been released into the cytoplasm the genomic RNA acts directly as mRNA for the translation of the replicase polyproteins, pp1a and pp1ab. Expression of the latter is the result of a slippery sequence and an RNA pseudoknot that causes a -1ribosomal frameshift from ORF1a to ORF1b (Brierley *et al.,* 1989; Baranov *et al.,* 2005). The polyproteins are proteolytically cleaved by virus encoded proteinases, notably papain-like proteases encoded by nsp 3 and nsp 5, generating 16 or for IBV, 15 nsps (Ziebuhr *et al.,* 2000). The frameshift event is thought to be a method of regulating production of the nsps, as those encoded by ORF 1b are produced less than those encoded by ORF 1a. Once produced, some of the resulting nsps assemble to form replication-transcription complexes (RTCs). Despite extensive research the exact composition of the coronavirus RTC remains undetermined however it is thought the core structure will include nsp 7, 8, 9, 10, 12, 13 and 14 (reviewed by Sola *et al.,* 2015). Individual roles of the nsps can be found in Table 1.2.

Table 1.2: Known functions of the coronavirus non-structural proteins.

Protein	Function
1	• Promotes cellular mRNA degradation and blocks host cell translation. • Blocks innate immune response. • The IBV genome does not contain nsp 1.
2	• No known function, binds to prohibitin proteins
3	Large, multi-domain transmembrane protein with several functions: • Ubiquitin-like domain 1 (Ubl1); interacts with N protein. • ADP-ribose-1"-phosphate phosphatase or otherwise known X domain; promotes cytokine expression and has been demonstrated to be a pathogenicity factor although the ADRP domain alone from the pathogenic IBV strain M41-CK cannot confer a pathogenic phenotype to Beau-R.* • Papain-like protease (PLPro or PLP) domain; cleaves viral polyprotein at nsp 1/2, 2/3 and 3/4 junctions. PLP2 may interact with the ADRP domain.* • Deubiquitinase activity; blocks host innate immune response. • Ubl2, NAB, G2M, SUD, Y domains, unknown functions.
4	• Potential transmembrane scaffold protein, important for proper structure of double membrane vesicles (DMV) that are possibly the site of viral replication. • Nsp 4 from IBV can induce membrane pairing.*
5	• Protease activity, cleaves viral polyprotein.
6	• Potential transmembrane scaffold protein.
7	• Forms hexadecameric complex with nsp8, may act as processivity clamp for RNA polymerase.
8	• Forms hexadecameric complex with nsp7, may act as processivity clamp for RNA polymerase; may act as a primase.
9	• RNA binding protein.
10	• Cofactor for nsp16 and nsp14.
11	• Unknown.
12	• RNA dependant RNA polymerase (RdRp).
13	• RNA helicase and 5′ triphosphatase activity.
14	• Consists of two domains: • N7 Methyltransferease (MTase) activity; involved in 5′ capping of viral RNA • 3′-5′ exoribonuclease (ExoN) activity, important for RNA proofreading
15	• Manganese-dependent endoribonuclease (NendoU); preferentially cleave 3′ of uridylates on both single and double-stranded RNA.
16	• 2'O-methyltransferase; involved in capping of viral RNA which shields viral RNA from Melanoma differentiation associated protein 5 (MDA5) recognition.

Notes: Adapted from Fehr and Perlman (2015), with further specific information (*) added from Deng *et al., (*2019), Doyle *et al.,* (2018) and Keep *et al.,* (2018).

The RTC performs both RNA-dependant RNA synthesis for genome replication as well as subgenomic mRNA (sgmRNA) synthesis for the production of the structural and accessory proteins. Genome replication is a process of continuous synthesis from full length negative copies of the genomic RNA. Synthesis of the negative strand copies is initiated from the very 3′ end of the genome, a process which will involve the RTC as well as RNA sequences and RNA structures including stem loops and pseudoknots present in the 3′ UTR (Hsue and Masters, 1997; Williams *et al.,* 1999). A positive sense copy is then generated from the negative strand template generating new genomic RNA that is encapsidated into newly formed progeny virions.

Unlike genomic RNA synthesis the production of the sgmRNAs occurs via a process of discontinuous RNA synthesis (Figure 1.5). The process, referred to as discontinuous transcription during negative strand synthesis was proposed in the mid 1990's by Sawicki and Sawicki (1995). The model relies on the presence of two complementary transcription regulatory sequences (TRS), one, TRS-L, located at the 5′ end of the genome within what is referred to as the leader sequence and the second, TRS-B, in the body of the genome, upstream of each structural and accessory gene. Each TRS-B essentially acts a pause signal for the RTC during negative strand synthesis, and when a TRS-B is encountered one of two events occurs; either the RTC will continue to the next TRS-B or, the now complementary TRS-B of the newly synthesised negative-strand RNA will translocate and hybridize to the TRS-L present at the 5′ end of the genome. This hybridisation event facilitates a template switch resulting in RNA synthesis continuing to the very 5′ end of the genomic template thereby adding the anti-leader sequence to each negative sense sub genomic (sg) RNA. The negative sense sg RNA is subsequently copied by the RTC into a positive sense sgmRNA. A defining characteristic of this transcription process is the production of a nested set of sequentially smaller sgmRNAs all sharing common 5′ and 3′ sequences.

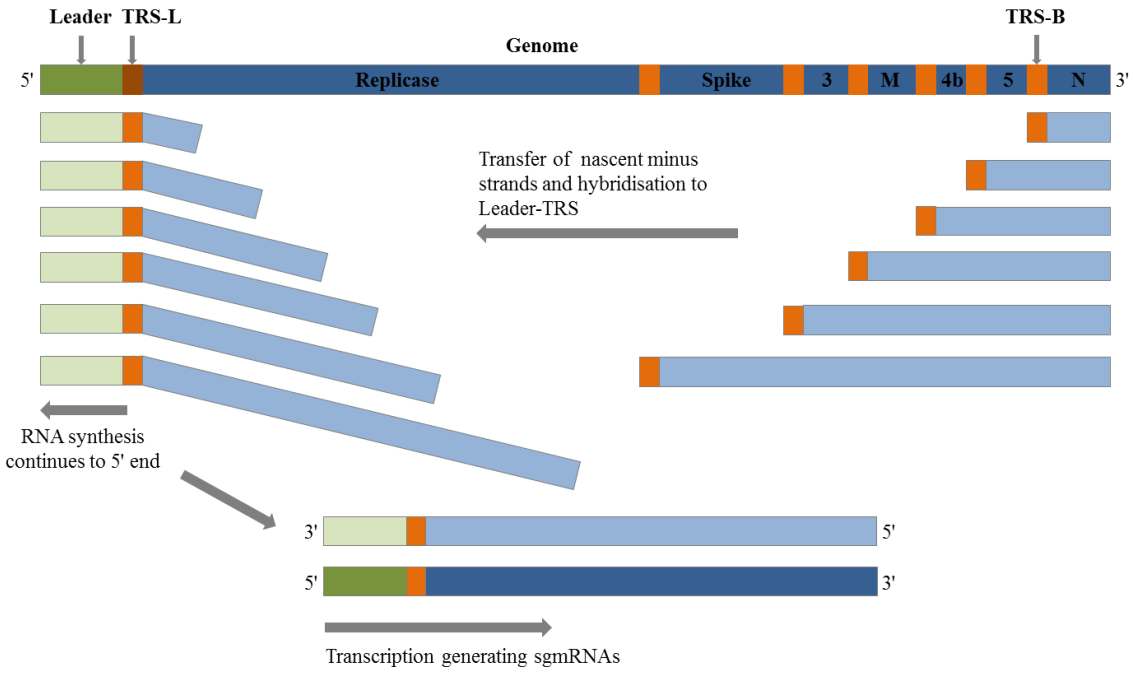

Figure 1.5: Schematic detailing the process of discontinuous transcription during negative strand synthesis. RNA synthesis is initiated at the 3′ -end of the genome, generating a negative sense copy of the positive sense viral genome. RNA synthesis continues until a transcriptional regulatory sequence (TRS) is reached within the body of the genome (TRS-B). Once a TRS-B is encountered RNA synthesis either continues until the next TRS-B or undergoes a translocation event after hybridisation to the TRS located within the Leader sequence (TRS-L) at the 5′ end of the viral genome. RNA synthesis continues so that the newly synthesised RNA contains an anti-leader sequence. The negative sense copies act as templates for the transcription of positive sense sgmRNAs which are subsequently translated into viral proteins.

The synthesis of the sgmRNAs is a complicated process which is not fully understood, however it has been demonstrated that the presence of a TRS is essential. For IBV the accepted consensus sequence of the TRS is CUUAACAA (Bentley *et al.,* 2013; reviewed by Armesto *et al.,* 2013). Whilst the model proposed by Sawicki and Sawicki (1995) suggests the need for complementary TRS-L and TRS-B, this is not necessarily the case as in IBV there are naturally occurring variations in the TRS-B for the S gene and gene 5. Bentley *et al.,* (2013) demonstrated further flexibility by identifying the presence of a sgmRNA, relating to gene 4b, which is transcribed from a shortened, non-canonical TRS-B of only 3 nucleotides, CAA. It is likely therefore that the production of the sgmRNAs also involves regulatory RNA-RNA interactions as well as protein-RNA interactions (reviewed by Sola *et al.,* 2015).

Once synthesised, the sgmRNAs are translated by cellular machinery producing the structural and accessory proteins. The structural proteins are subsequently transported the endoplasmic reticulum (ER), and then to the ER-Golgi intermediate compartment (ERGIC), via the secretory pathway (reviewed by Fehr and Perlmann, 2015). The structural proteins embed into the membranes of the ERGIC and encapsulated viral progeny genomes bud from these membranes forming mature virions which are released from the cell by exocytosis (Tooze *et al.,* 1987; Klumperman *et al.,* 1994; Krijnse-Locker 1994). Several viral proteins have been implicated in the assembly and release process including E and M (Vennema *et al.,* 1996). Unsurprisingly the process of coronavirus replication is accompanied by extensive membrane re-arrangements including double membrane vesicles, zippered ER and spherules (Knoops *et al.,* 2008; Ulasli *et al.,* 2010; Maier *et al.,* 2013; Maier *et al.,* 2016). There are several hypothesised reasons for the observed membrane re-arrangements; they may provide a scaffold for the RTC and genome replication and/or shield potential replication derived immunogenic molecules such as double-stranded RNA thereby providing a method of evading of host immune responses and/or aid in virion assembly by concentrating the necessary viral proteins.

1.6 Non-structural proteins.

Numerous functions have been attributed to the coronavirus nsps which are summarised in Table 1.2. Although much is known about certain nsps, the function of others remains elusive. In addition, the interactions between certain nsps are still poorly understood. Despite the many unknowns however, there is increasing evidence surrounding the fundamental role of the nsps in viral replication and pathogencity (reviewed by Weiss and Navas-Martin, 2005;

Sevajol *et al.,* 2014; Enjuanes *et al.,* 2016) however, it must be noted that much of this research focuses on MHV and SARS-CoV and not IBV. Research by Armesto *et al.,* (2009) has however identified the replicase gene as a pathogenic determinant in IBV. Continuing research in the coronavirus field has identified several of the nsps as promising antiviral and vaccine targets and it is those nsps which will be discussed further in this Chapter.

1.6.1 Nsp 3.

Nsp 3 is the largest of the nsps, and is a multi-functional protein containing a number of domains which are found to be conserved amongst members of the *orthocoronavirinae* (reviewed by Lei *et al.,* 2018). One such domain, which has been investigated in the context of vaccine development is the macrodomain/X domain, or otherwise termed ADRP domain due to its ADP-ribose-1"-phosphate phosphatase activity (Putics *et al.,* 2005; Saikaterdu *et al.,* 2005; Egloff *et al.,* 2006). Mutations of key residues in SARS-CoV, MHV and HCoV-229E has demonstrated that ADRP activity is not required for RNA synthesis and viral replication *in vitro* (Putics *et al.,* 2005; Eriksson *et al.,* 2008; Kuri *et al.,* 2011). In support of this, the non-pathogenic IBV strain Beaudette, presumed to have an inactive ADRP due to a Glycine (Gly) to Serine (Ser) mutation at residue 48 (Xu *et al.,* 2009; Piotrowski *et al.,* 2009) is also able to replicate efficiently in cell culture (Casais *et al.,* 2003). The role of the ADRP domain has been investigated in terms of pathogenicity. Although modification of residue 48 to a Gly in the infectious Beaudette based clone, recombinant IBV (rIBV) Beau-R, did not confer a pathogenic phenotype (Casais *et al.,* 2001; Keep *et al.,* 2018), Eriksson *et al.,* (2008) modified the ADRP domain in MHV at the conserved residue 1348 (Aspartic acid, Asp, to Alanine, Ala) with the resulting recombinant virus not causing acute viral hepatitis *in vivo*. Incorporating the equivalent mutation in mouse adapted SARS-CoV, Fehr *et al.,* (2016) demonstrated an inactive ADRP domain resulted in reduced viral load and reduced pathology *in vivo*. Further research has identified a possible role for the ADRP domain in the regulation of innate immune responses (Kuri *et al.,* 2011; Fehr *et al.,* 2015) which alongside the *in vivo* data generated by Eriksson *et al.,* (2008) and Fehr *et al.,* (2016) identifies the ADRP domain as a promising target for vaccine development.

1.6.2 Nsp 10.

Nsp 10 is a small 15 k Da protein which belongs to the zinc protein family (Joseph *et al.,* 2006). The protein consists of two zinc fingers, which in SARS-CoV, one is co-ordinated by the following residues Cysteine (Cys) 74, Cys 77, Histidine (His) 83, Cys 90 and the other by

Cys 117, Cys 120, Cy 128 and Cys 130 (Joseph *et al.,* 2006). Interestingly despite the crystal structure being solved (Joseph *et al.,* 2006; Su *et al.,* 2006), the protein has no known enzymatic function, however due to the presence of zinc finger Joseph *et al.,* (2006) hypothesised an RNA binding function. The protein has since been identified to act as a stimulatory co-factor to both nsp 16 (Chen *et al.,* 2011; Wang *et al.,* 2015, Decroly *et al.,* 2011, Bouvet *et al.,* 2010) and the EXoN activity of nsp 14 (Bouvet *et al.,* 2012; Bouvet *et al.,* 2014). No stimulatory effect on the N7-MTase activity of nsp 14 *in vitro* has been demonstrated (Bouvet *et al.,* 2010). Mutagenesis studies have identified that nsp 10 is essential for viral replication (Donaldson *et al.,* 2007; Bouvet *et al.,* 2014) whether that is through direct action or indirectly through stimulation of another nsp, remains undetermined.

Several key residues have been identified including a Tyrosine (Tyr) at position 96 and either a Lysine (Lys) or Arginine (Arg) at position 93, which were found to be critical for the interaction with nsp 16 (Lugari *et al.,* 2010) as well as Phenylalanine (Phe) at position 19 that is critical to the interaction with nsp 14 (Bouvet *et al.,* 2014). Alanine scanning mutagenesis in MHV of residues that were deemed to be conserved within the coronavirus family identified a central core in which modification resulted in a lethal phenotype; this included residues Ser 72, Gly 69, Phenylalanine (Phe) 68, Aspartic acid (Asp) 123, His 113, Lysine (Lys) 104, Glutamic acid (Glu) 82 and Arginine (Arg) 78 (Donaldson *et al.,* 2007). Similar alanine mutagenesis studies in SARS-CoV identified modification of Phe 19, His 80 and Tyr 96 also resulted in a lethal phenotype (Bouvet *et al.,* 2014). Interestingly these lethal phenotypes were not attributed to a reduction in nsp 14 EXoN activities raising the distinct possibility that additional functions of nsp 10 have yet to be identified. Nsp 10 is therefore an appealing target for vaccine and antiviral therapy.

1.6.3 Nsp 14.

Nsp 14 is a 59 kDa protein that is bifunctional, consisting of two distinct domains. Encoded by amino terminal residues is a 3′-5′ exoribonuclease (ExoN), and by the residues at the C terminal a S-adenosyl methionine (SAM)-dependent (guanine-N7) methyl transferase (N7-MTase; Minskaia *et al.,* 2006; Chen *et al.,* 2009; Chen *et al.,* 2013). Interactions with nsp 10 have been demonstrated to enhance ExoN activity by ~35 fold (Bouvet *et al.,* 2012) but seemingly has a minimal effect on N7-MTase activity (Bouvet *et al.,* 2010; Bouvet *et al.,* 2104). Whilst it is simpler to consider the functions of the two domains as separate, both the ExoN and N7-MTase domains are interlinked, interacting through hydrophobic interactions (Ma *et al.,* 2015). Structural analysis of nsp 14 from SARS-CoV identified a number of

residues important for these interactions including Isoleucine (Ile) 80, Valine (Val) 83, Leucine (Leu) 177, Val 282, Phe 286, Val 294, Tyr 296, Pro 297, Ile 299, Leu 411, Pro 412, and Leu 419. Notably all these residues are highly conserved between members of the *orthcoronavirinae.*

Mutations in nsp 14, notably in the ExoN domain have been investigated for vaccine development (Graham *et al.,* 2012; Menachery *et al.,* 2018). The ExoN active core encompasses three motifs, I (DE), II (E) and III (D), with *in vitro* studies of nsp 14 derived from SARS-CoV demonstrating that Ala substitutions in these motifs either reduced or abolished ExoN activity (Minskaia *et al.,* 2006). Ala mutations in motif I engineered into infectious clones of both SARS-CoV and MHV, as well as in motif III in MHV resulted in modest replication defects in cell culture as well as increases in mutation frequency within the viral genome (Eckerle *et al.,* 2007; Eckerle *et al.,* 2010). Of note, infectious progeny SARS-CoV could be recovered with Ala substitutions in motif III however the mutations were deemed not stable enough to warrant further investigation by Eckerle *et al.,* (2010). Interestingly, engineered ExoN mutations within the TGEV genome, despite limited effects on viral RNA synthesis were lethal to the production of infectious progeny virus therefore indicating that ExoN activity is essential for productive viral replication (Becares *et al.,* 2016). Mouse adapted SARS-CoV containing the ExoN I motif mutations were assessed for pathogenicity *in vivo*; no mortality was reported and young mice showed no signs of clinical disease, although aged mice did exhibit weight loss, (Graham *et al.,* 2012). This therefore indicates that ExoN activity may be a pathogenicity factor. Vaccine-challenge experiments in aged mice demonstrated that vaccination with the engineered ExoN I motif mutant could induce protection against virulent challenge (Graham *et al.,* 2012).

The other role of nsp 14 is in the capping process of viral RNAs (Figure 1.6). The cap-1 structure located on the 5′ end of all viral RNAs both assists in translation and in the evasion of host defences, primarily the innate immune response (reviewed by Savajol *et al.,* 2014). Four sequential reactions are required; nsp 13 hydrolyzes nascent RNA to yield pp-RNA, which then is modified by a yet unidentified guanylyltransferase to generate Gppp-RNA. The N7-MTase activity of nsp 14 then methylates the 5′ guanine molecule at the N7 position resulting in a final substrate that is further methylated by nsp 16 (Ma *et al.,* 2015). The conserved residue Asp 331 in SARS-CoV has been identified as essential for N7-MTase activity (Chen *et al.,* 2009). Due to the importance of the capping process in viral replication several inhibitors of N7-MTase have been investigated as antiviral drugs (Bouvet *et al.,* 2010).

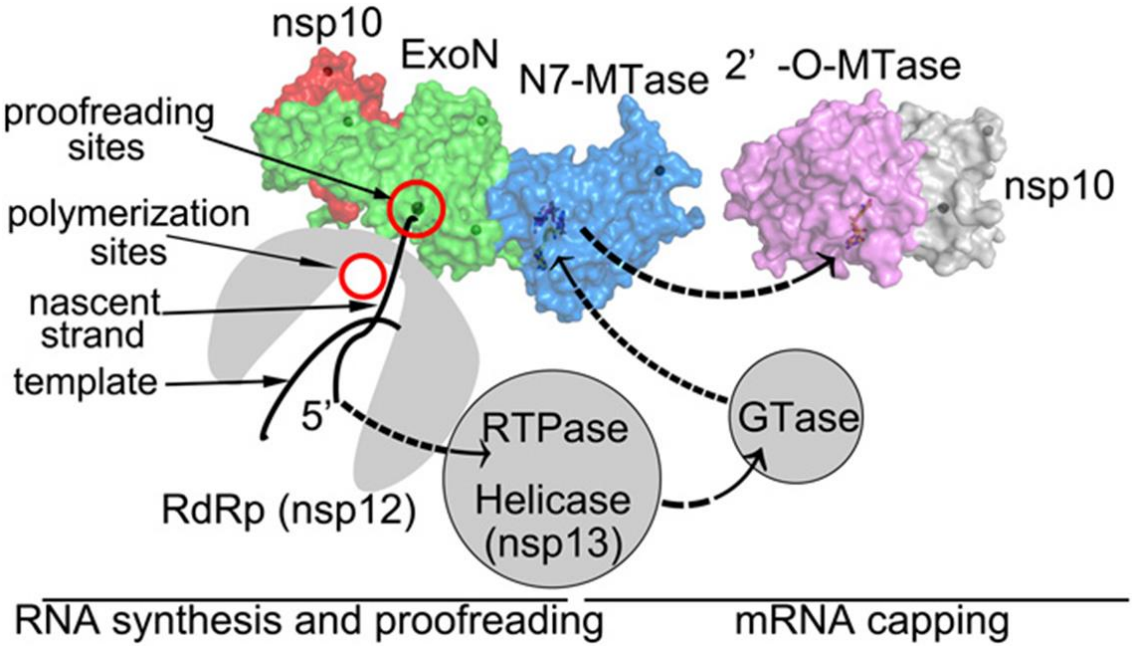

Figure 1.6: Capping of viral RNA in a process mediated by several viral proteins. Viral RNA is synthesized by the RNA dependant RNA polymerase (RdRp) encoded by nsp 12; the polymerization site is denoted by a red circle. The Exon domain (green) of nsp 14 provides a proof-reading function to the RNA synthesis step, which is enhanced through the nsp10/nsp 14 interaction. A cap-1 structure is added to the 5′ end of all newly synthesised RNA molecules which involves several sequential activities including an RTPase activity provided by nsp 13, GTase activity from a currently unknown source, N7-MTase activity provided by nsp 14 (blue), and 2′-O–MTase activity (purple) provided by nsp 16. Nsp 10 has been shown to stimulate the activity of nsp 16. Figure taken from Ma *et al.,* (2015).

1.6.4 Nsp 15.

Nsp 15 is a highly conserved manganese-dependent endoribonuclease (NendoU) that has been shown to preferentially cleave 3′ of uridylates on both single and double-stranded RNA (Ivanov *et al.,* 2004; Bhardwaj *et al.,* 2004; Cao *et al.,* 2008; Snijder *et al.,* 2003). RNA substrates that are 2′-O-ribose- methylated are resistant to cleavage by NendoU, therefore implying a functional link in the coronavirus replication cycle with the 2′-O-ribose methyltransferase encoded in nsp 16 (Ivanov *et al.,* 2004; reviewed in Deng and Baker, 2018). In IBV the NendoU core domain is reported to be between aa position 221 and 338, with catalytic residues predicted at position 223 and 238 (Deng and Baker, 2018). In addition, a threonine (Thr) at position 232 and a Tyr at position 234 may be involved in substrate specificity (Deng and Baker 2018).

It was thought originally that NendoU activity was essential for viral RNA synthesis (Snijder *et al.,* 2003; Ivanov *et al.,* 2004). Neither HCoV-229E nor MHV could be successfully rescued with an engineered Asp to Ala mutation in the non-catalytic residue 298 (HCoV-229E) or the equivalent residue, 324 (MHV) (Kang *et al.,* 2007; Ivanov *et al.,* 2004). Expression of the mutated protein in *Escherichia coli* (*E.coli*) demonstrated that the Asp324Ala mutation resulted in the MHV nsp 15 protein being insoluble (Kang *et al.,* 2007). Interestingly Ala substitutions at three key residues in the catalytic pocket, His 262, His 277 and Gly 275 resulted in three recombinant MHV viruses which exhibited a subtle defect in RNA synthesis and only a slight reduction in progeny viral titres (Kang *et al.,* 2007). A double mutant MHV was also constructed, His262Pro and His277Ala, which also exhibited reductions in both RNA synthesis and viral titres (Kang *et al.,* 2007). The ablity of these mutatant viruses to replicate *in vitro* indicated to Kang et al., (2007) that NendoU activity may not be essential for viral replication.

Overexpression studies have identified that nsp 15 stimulates an interferon (IFN) response (Frieman *et al.,* 2009) and can inhibit cellular responses (Lei *et al.,* 2009; Wang *et al.,* 2015). These studies however do not take in to account that nsp 15 exist as part of the RTCs in wild type (WT) infection. Differences in the cellular localisation of over expressed nsp 15, and nsp 15 expressed from natural infection have been reported (Heusipp *et al.,* 1997; Shi *et al.,* 1999; Deng *et al.,* 2017; Athmer *et al.,* 2017; Cao and Zhang 2012). Recent research has identified that replication of MHV with deficiency in NendoU activity as a result of either a Threonine (Thr) to Methionine (Met) mutation at residue 98 or His to Ala at 262, was highly restricted in bone marrow macrophages yet not in fibroblasts (Deng *et al.,* 2017). It was

determined that the inoculation of the macrophages stimulated higher levels of type I interferon in early infection compared to WT, which restricted viral replication. A similar study utilised an MHV virus containing the mutation His277Ala (Kindler *et al.,* 2017); the replication of the mutant virus was also restricted in murine bone marrow derived macrophages, and viral replication was hampered in IFN treated murine L929 cells. HCoV-229E with the corresponding mutation His250Ala also exhibited reduced replication in human blood derived macrophages as well as in IFN treated human MRC5 lung fibroblasts. Deng and Baker (2018) theorised that the difference in viral replication of the NendoU mutant viruses in the different cell types may be a consequence of differences in basal gene expression.

As well as a potential role in mediating antiviral responses, both Kindler *et al.,* (2017) and Deng *et al.,* (2017) demonstrated that nsp 15 plays a role in pathogenicity as in both studies the mutant viruses were attenuated *in vivo*. Kindler *et al.,* (2017), could not detect the mutant MHV in the livers or spleens of experimental infected mice and concluded that NendU is required for efficient viral replication and dissemination *in vivo*. Interestingly Deng *et al.,* (2017) demonstrated that mice infected with the mutant viruses were protected against challenge, highlighting a potential role for nsp 15 mutants in coronavirus vaccine development.

1.6.5 Nsp 16.

Nsp 16 functions as part of the 5′ capping process on coronavirus RNAs. Computational studies first predicted that nsp 16 was a 2′O-methyltransferase (Snijder *et al.,* 2003), with functional activity confirmed in FCoV (Decroly *et al.,* 2008). Nsp 16 works in conjunction with several other enzymes as part of the capping process, which is summarised in Figure 1.6. Notably, nsp 16 mediated methylation is sequence dependent, with methylation occurring on the exposed 2'OH on the N7 position of the guanyl cap (Chen *et al.,* 2011). This indicates that a functional nsp 14 must be present in WT infection in order for viral RNAs to be capped properly (Bouvet *et al.,* 2010). In addition several studies have identified nsp 10 as a necessary stimulatory co-factor (Chen *et al.,* 2011; Wang *et al.,* 2015B, Decroly *et al.,* 2011, Bouvet *et al.,* 2010).

Mutagenesis studies have identified a role for nsp 16 in both viral replication *in vitro* and *in vivo*, as well as pathogenicity (Zust *et al.,* 2011; Menachery *et al.,* 2014; Wang *et al.,* 2015B). The conserved Lys-Asp-Lys-Glu (KDKE) motif has been identified as essential for 2′O-

methyltransferase activity (Chen *et al.,* 2011). HCoV-299E with the mutation Asp129Ala in the conserved KDKE motif, was found to have altered growth kinetics in fibroblasts, and induced greater levels of IFN in macrophages (Zust *et al.,* 2011). The corresponding mutation in MHV, Asp130Ala also resulted in reduced viral replication in macrophages and increased levels of IFN. The Asp130Ala MHV was also found to be attenuated in experimentally infected mice demonstrating that nsp 16 has a role in coronavirus pathogenicity (Zust *et al.,* 2011). Similarly Menachery *et al.,* 2014 constructed three SARS-CoV mutant viruses with individual alanine substitution at KDKE motif residues Lys 46, Lys 170, and Asp 130. Interestingly replication in IFN lacking Vero cells was unaltered however replication in IFN competent Calu3 respiratory cells was reduced. Furthermore vaccination of mice with a mouse adapted SARS-CoV containing the Asp130Ala mutation protected against lethal challenge.

One other way to reduce nsp 16 activity is to interfere with the nsp10/16 interaction (Chen *et al.,* 2011; Wang *et al.,* 2015). Biochemical activity assays demonstrated that nsp 16 activity increased in a dose dependant manner with nsp 10 (Wang *et al.,* 2015B). A number of residues have been identified as important for the nsp 10/16 interaction; using SARS-CoV numbering, these include Lys 93 and Tyr 96 in nsp 10, and residues Ala 83, Val 84, Arginine (Arg) 86, Glutamine (Gln) 87, Ser 105, Asp 106, in nsp 16 (Decroly *et al.,* 2011; Chen *et al.,* 2011; Lugari *et al.,* 2010). Interestingly a small peptide, p29, derived of residues 68 to 96 of the MHV nsp 10 was found to act as a competitive inhibitor which reduced both the *in vitro* replication of MHV and a SARS-CoV replicon. Mice inoculated with MHV and immediately treated with p29 did not exhibit clinical disease. It was theorised that competitive inhibition with p29 induced an IFN response in early infection which reduced viral replication (Wang *et al.,* 2015B).

1.7 Structural proteins.

1.7.1 The Spike glycoprotein.

The S protein is a large, ~180 kDa, highly glycosylated type I transmembrane, class I fusion protein. The structure of the S glycoprotein is complex as each S promoter or monomeric unit, 1162 aa in IBV, consists of a globular head sat upon a stalk like structure which complexes with two other S protomers forming a trimeric S glycoprotein (Walls *et al.,* 2016; Kirchdoerfer *et al.,* 2016; Shang *et al.,* 2018). Literature referring to the S glycoprotein refers to the trimeric arrangement of three individual S promoters which as mentioned above

protrude outwards from the viral membrane (Figure 1.7A and 1.7B). The main role of the S glycoprotein during infection is to mediate attachment to the host cell receptor, and subsequently the fusion of host cell and viral membranes. During this process, the S glycoprotein undergoes major conformational changes and as such structures are divided into pre-fusion (Figure 1.7A) and post-fusion states (Walls *et al.,* 2016; Walls *et al.,* 2017; Kirchdoerfer *et al.,* 2016; Shang *et al.,* 2018, Shang et al., 2018B). A cryo-EM structure has been published for the IBV S glycoprotein (Shang *et al.,* 2018), which will be discussed further in Chapter 3. The remainder of this section will detail the domains within each S protomer and the role of the S glycoprotein in tropism and pathogenicity. The S glycoprotein also has a major role in protective immunity which will be discussed further in a later section during this Chapter.

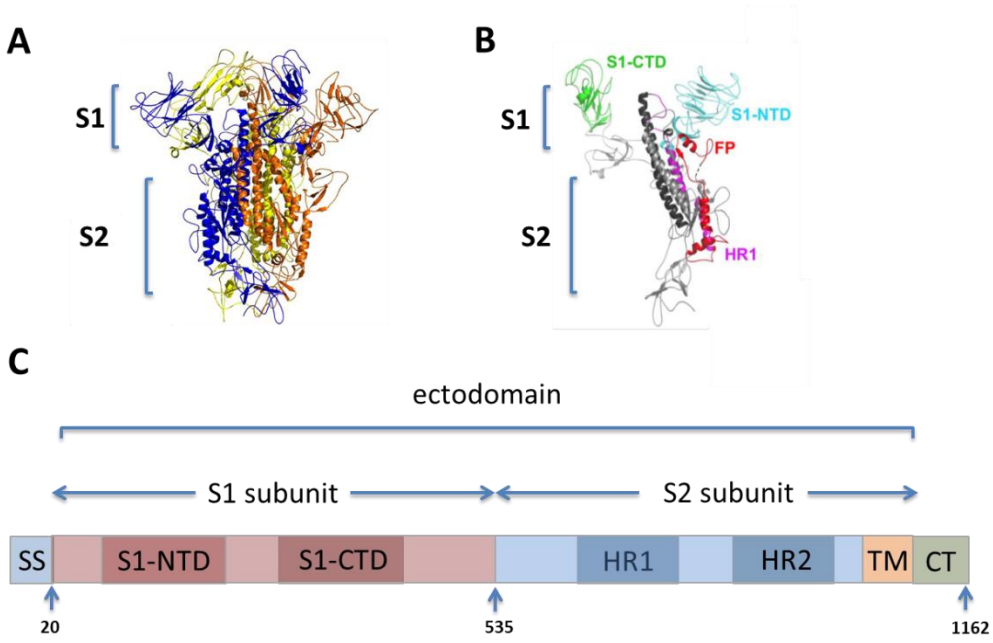

Figure 1.7: The S glycoprotein. (A) Cryo-EM structure of IBV spike ectodomain in the pre-fusion conformation as determined by Shang *et al.,* (2018). Each colour represents a different S protomer. The pre-fusion structure contains an S1 globular head sat upon an S2 stalk like structure. (B) Structure of a single S protomer in the pre-fusion conformation as determined by Shang *et al.,* (2018). S1-NTD and S1-CTD are receptor binding domains located in the S1 subunit. The S2 subunit contains heptad repeats (HR1 and HR2) as well as the fusion peptide (FP). (C) Schematic representation of the coronavirus S gene. The S gene consists of a large ectodomain flanked by a single sequence (SS) and a cytoplasmic tail (CT). The ectodomain is divided into two subunits, S1 and S2. The exact genome location of FP is unknown. Highlighted gene sections are not to scale and noted amino acid location are taken from Bickerton *et al.,* 2018.

Each S protomer can be broadly divided into three sections; a signal sequence (SS), a large ectodomain followed by a cytoplasmic tail (CT; Figure 1.7C). The ectodomain can be further divided in two, the amino terminal (NTD) S1 subunit and the carboxyl terminal (CTD) S2 subunit. The S1 domain has been shown to mediate receptor binding, and is further divided into two subdomains (SD), both containing receptor binding abilities; the amino terminal domain (S1-NTD) encompassing residues 21-237 and the carboxy terminal domain (S1-CTD) encompassing residues 269 – 414 (Shang *et al.,* 2018). The IBV S1 subunit is noted to contain three hypervariable regions (HVR), which are areas of concentrated amino acid differences between IBV strains, with HVR1 and HVR2 located in the S1-NTD, and HVR3 in the S1-CTD; residues 38 – 51, 99 – 115 and 274 – 387 respectively (Niesters *et al.,* 1986; Cavanagh *et al.,* 1988; Moore *et al.,* 1997; Valstro *et al.,* 2016). Typically it is thought that S1-NTD binds sugar based receptors and S1-CTD binds protein receptors (Liu *et al.,* 2015; Promkuntod *et al.,* 2014; Wong *et al.,* 2004). The receptors for several coronaviruses are known (Table 1.3) however the receptor for IBV remains undetermined although research has implicated sialic acids (Bingham *et al.,* 1975; Cavanagh *et al.,* 1986; Winter *et al.,* 2006; Winter *et al.,* 2008) and lectins (Zhang *et al.,* 2012). Promkuntod *et al.,* (2014) mapped the RBD for the M41 strains to residues 19-272 in the S1-NTD, highlighting residues Asparagine (Asn) 38, His 43, Pro 63 and Thr 69 as critical. This research was however completed using chimeric S1 subunits expressed from *E.coli*, and not whole S glycoproteins expressed from chicken cells. The glycosylation of the S glycoprotein may have a role in receptor binding (Jeffers *et al.,* 2004; Jeffers *et al.,* 2006; Han *et al.,* 2007), and such post translational modifications may not be comparable between bacteria and chicken cells (reviewed by Goh and Ng, 2018).

Table 1.3: Known receptors utilised for coronavirus entry.

Genus	Species	Host receptor
Alphacoronavirus	FCoV	Aminopeptidase N (APN)
	TEGV	
	CCoV	
	HCoV-NL63	Human angiotensin I converting enzyme 2 (ACE 2)
Betacoronavirus	BCoV	Carbohydrate, Neu 5,9 Ac2
	HCoV-OC43	
	MHV	Carcinoembryonic antigen-cell adhesion molecule (CEACAM1)
	SARS-CoV	ACE 2
	MERS-CoV	Dipeptidylpeptidase 4 (DPP4)

Notes: Table adapted from Belouzard *et al.,* (2012) and Raj *et al.,* (2013).

Similarly to the S1 subunit, the S2 subunit also contains several subdomains and notable features. One such feature is the presence of two regions of extended α helices, referred to as heptad repeats (HR1 and HR2); a typical feature of class I fusion proteins (Bosch *et al.,* 2003; Shang *et al.,* 2018). Both HR1 and HR2 have a role in cellular entry of the nucleocapsid by drawing the virus and cell membrane together as a result of conformational changes in the S glycoprotein upon receptor binding (Sainz *et al.,* 2005, Walls *et al.,* 2017). The S2 subunit also contains a transmembrane domain (TM), and a fusion peptide (FP). FPs are typically 15 to 25 amino acids in length, apolar, and highly conversed within virus families (reviewed by Belouzard *et al.,* 2012). Experiments utilising SARS-CoV, MERS-CoV and MHV support the notion that the FP resides in the S2 domain (Madu *et al.,* 2009; Basso *et al.,* 2016; Ou *et al.,* 2016). Furthermore Shang *et al.,* (2018) identified a potential region on the cryo-EM structure of the S glycoprotein from M41, in which the FP is thought to be located. Interestingly despite the S2 not containing an RBD, the extended tropism of the Beaudette strain, and notably the ability to replicate in Vero cells is conferred by the S2 subunit (Bickerton *et al.,* 2018, Bickerton *et al.,* 2018b). This result has been attributed to a secondary cleavage site, Arg-Arg-Arg, referred to as the S2′ site, located at position 690 therefore highlighting a role for the S2 subunit in host tropism (Madu *et al.,* 2007; Yamada and Liu 2009; Bickerton *et al.,* 2018; Bickerton *et al.,* 2018b). As well as the secondary cleavage site, a primary cleavage site exists some coronaviruses, including IBV, located between the S1 and S2 domain. Cleavage at this site is typically mediated by furin or furin like host cell proteases resident in the Golgi apparatus during assembly and exocytosis (de Haan *et al.,* 2004; reviewed by Belouzard *et al.,* 2012). This means the S1 and S2 subunits are non-covalently linked in the pre-fusion structure. IBV is cleaved at amino acid residues Arg-Arg-Phe-Arg-Arg although there is some variability in this sequence between individual strains (Cavanagh *et al.,* 1986; Jackwood *et al.,* 2001). It must be noted that the S glycoprotein of some coronaviruses including SARS-CoV and MHV is not cleaved during viral exit (Rota *et al.,* 2003; Frana *et al.,* 1985).

As expected due to its role in viral entry, and eluded to in the above paragraph, the S glycoprotein determines cellular tropism and host range (Sanchez *et al.,* 1999; Tekes *et al.,* 2010; Casais *et al.,* 2003; Armesto *et al.,* 2011). This has been demonstrated for several coronaviruses including porcine respiratory coronavirus (PRCV), TGEV, SARS-CoV, MHV, feline infectious peritonitis virus (FIPV) and IBV (reviewed by Belouzard *et al.,* 2012). The difference in tissue tropsim between PRCV and TGEV was the result of a deletion in the S gene (Rasschaert *et al.,* 1990; Schultze *et al.,* 1996). The ablity of SARS-CoV to jump the species barrier from palm civets to humans was mapped to two mutations with the S glycoprotein, Lys479Asn and Ser487Thr respectively (Li *et al.,* 2005). MHV was found to be able to replicate in feline cells, when the ectodomain of the S gene was exchanged for the

counterpart seqeunce derived from FIPV (Kuo *et al.,* 2000). In addition Haijema *et al.,* (2003), generated the reciprocal virus, FIPV with the S ecotodomain from MHV which was found to be able to replicate in murine cells. Sequence differences between S glycoproteins are also responsible for the range of *in vitro* tropisms exhibited by IBV strains (Casais *et al.,* 2003; Armesto *et al.,* 2011). Several strains, often those isolated from field conditions, are restricted to replication in *ex vivo* tracheal organ cultures (TOCs) and embryonated eggs; this includes strains such as 4/91 and QX (Armesto *et al.,* 2011; Bickerton *et al.,* 2018b). Laboratory strains such as M41-CK and Beaudette as well as the vaccine strain H120 are able to be propagated in primary chicken kidney (CK) cells (Casais *et al.,* 2003; Bickerton *et al.,* 2018b). The Beaudette strain is particularly unusual as it exhibits extended tropism and is able to replicate in Vero cells, a continuous cell line derived from African Green Monkey kidney epithelial cells, immortalized chicken embryo fibroblasts (DF1 cells) and Baby hamster kidney (BHK) cells (Casais *et al.,* 2003; Keep *et al.,* 2018).

The role of the S glycoprotein in pathogenicity is less established for IBV. Research utilising MHV, SARS-CoV and FIPV has indicated the S gene as a pathogenicity factor (Phillips *et al.,* 1999; Li *et al.,* 2005; Miura *et al.,* 2008; Chang *et al.,* 2012), however both Hodgson *et al.,* (2004) and Armesto *et al.,* (2011) demonstrated that this was not necessarily the case for IBV. The ectodomain of recombinant IBV (rIBV) Beau-R, a Beaudette based molecular clone, was exchanged for either the ectodomain of a pathogenic strain M41-CK or 4/91, generating rIBV BeauR-M41(S) and BeauR-4/91(S) respectively; both viruses were apathogenic *in vivo* (Hodgson *et al.,* 2004; Armesto *et al.,* 2011). The incorporation of the S gene from Beau-R into a pathogenic IBV was however found to be attenuating indicating that the S glycoprotein of IBV is a pathogenicity factor (Stevenson-Leggett, P. 2018).

1.7.2 The Envelope protein.

The E protein is small, 76 to 109 aa, 12.4 kDa and contains a single hydrophobic domain and a charged CT (reviewed by Ruch and Machamer, 2012 and DeDiego *et al.,* 2014). Unusually the protein is present in only small quantities in the viral membrane. Ion channel activity has been reported which is hypothesised to require the oligomerisation of individual E proteins (Wilson *et al.,* 2004; Wilson *et al.,* 2006). E is thought to be involved in several viral processes during infection, including virus assembly and egress (Lim and Liu, 2001; Ye and Hogue, 2007; reviewed by Ruch and Machamer, 2012 and DeDiego *et al.,* 2014). The IBV E protein has been reported to localise to the Golgi during infection (Corse and Machamer, 2000). Despite the role of the E protein in viral replication not being fully

understood, E has been implicated in the pathogenesis of SARS-CoV (DeDiego *et al.,* 2011; DeDiego et al., 2014; DeDiego *et al.,* 2014B; Jimenez-Guarideno *et al.,* 2014; Regla-Nava *et al.,* 2014).

1.7.3 The Membrane protein.

The M protein is a small, 200aa, 25-30 kDa, protein that contains three hydrophobic TM domains as well as a short NTD that is exposed on the outside of the viral envelope. Within the viral envelope, a long tail, located at the CTD contains both an amphiphilic domain and a hydrophilic domain (Klumperman *et al.,* 1994; reviewed by Hogue and Machamer 2008). The M protein is glycosylated at the NTD, is the most abundant of all the structural proteins and is a key player in virion assembly (de Haan *et al.,* 1999; Neuman *et al.,* 2011; reviewed by Fehr and Perlman, 2015). Virion assembly involves both M-M interactions that are thought to exclude host membrane proteins from the viral envelope (de Hann *et al.,* 2000; Neuman *et al.,* 2008) and M-S interactions that mediate assembly of the S protomers into the virion particle (de Hann *et al.,* 1999; Neuman *et al.,* 2011). Interactions with N and E, as well as genomic RNA packaging signals have also been demonstrated (Vennema *et al.,* 1996; Opstelten *et al.,* 1995; Narayanan *et al.,* 2000; Lim and Liu, 2001; Kuo and Masters, 2002). It has been hypothesised that M exists in two conformations during infection with each conformation mediating specific interactions and/or tasks during assembly (Neuman *et al.,* 2011).

1.7.4 The nucleocapsid protein.

The N protein is a phosphorylated protein that has several functions throughout the viral life cycle but its primary purpose is the encapsidation of genomic RNA. Each N protein consists of three distinct domains; a structured NTD and CTD, with a disordered central region situated between the two (reviewed by McBride *et al.,* 2014). All three domains have been demonstrated to bind RNA *in vitro* and in addition a dimerization function has been identified in the CTD (Surjit *et al.,* 2004) as well as the identification of residues in the disordered region that interact with nsp 3 (Verheije *et al.,* 2010; Keane *et al.,* 2013). Two specific RNA substrates have been identified including TRSs as well as the genomic packaging signals (Stohlman *et al.,* 1988; Molenkamp *et al.,* 1997). In addition to a role in nucleocapsid formation, the N protein is therefore involved viral transcription and translation (Baric *et al.,* 1988; Zuniga *et al.,* 2004). Interestingly the development of reverse genetics systems for coronaviruses in the early 2000s highlighted the pivotal role of N in viral replication as it was

found that the N protein was either essential, or significantly enhanced the recovery of infectious progeny virions (Yount *et al.,* 2000, Casais *et al.,* 2001; Almazan *et al.,* 2004).

1.8 Accessory proteins.

The coronavirus genome encodes several accessory proteins of the which the number and location is virus specific. IBV encodes four known accessory proteins, 3a, 3b, 5a, and 5b of 58, 65, 66, and 83 aa in length respectively (reviewed by Cavanagh, 2007). Neither of these proteins is required for viral replication in cell culture or *in ovo* (Casais *et al.,* 2005; Hodgson *et al.,* 2006; Laconi *et al.,* 2018; van Beurden *et al.,* 2018). There is however some evidence suggesting a role of 3a and 3b during replication in *ex vivo* tracheal organ cultures (TOCs), as rIBVs not expressing these proteins exhibited lower titres 24 hpi in comparison to WT (Hodgson *et al.,* 2006). Although overall the functions of the accessory proteins are still poorly understood, research has identified potential roles in mediating IFN responses as well as in host cell translation shut off (Kint *et al.,* 2015, Kint *et al.,* 2016, Laconi *et al.,* 2018). All four accessory proteins have been implicated as pathogenicity factors (Laconi *et al.,* 2018). In addition the IBV strain H52 lacking either 3a and 3b or 5a and 5b or all four proteins, has been shown to protect chickens against homologous challenge with the level of protection determined by ciliary activity comparable to the H52 vaccinated control group (van Beurden *et al.,* 2018).

The genome of IBV also encodes a potential fifth accessory protein of 94 aa, termed 4b. This protein is translated from a sgmRNA that utilises a non-canonical TRS-B from what was previously considered a non-coding IR located between gene M and gene 5 (Bentley *et al.,* 2013B). Despite the function remaining undermined, 4b has been detected during viral infection and deletion of 4b has been shown to have no effect on viral replication in CK cells (Bentley *et al.,* 2013B, Hall., 2017).

1.9 Reverse genetics systems for coronaviruses.

The advent of reverse genetics systems has opened up the possibility to investigate pathogenic and immunogenic determinants in the context of live viral infections. Subsequently this information can be used for the development of rationally designed vaccine viruses. There are several technologies that have been used, and are still used to generate infectious clones of coronaviruses including IBV, SARS-CoV, MERS-CoV, HCoV-

299E, HCoV-OC43, TEGV, FIPV and MHV. These systems have been independently developed and employ several different strategies to generate infectious recombinant virus including *in vitro* ligation, RNA recombination and the use of both Bacterial Artifical Chromosome (BAC) and Vaccinia virus (VV) vectors for the generation of infectious cDNA copies of the RNA genome (Koetaner *et al.,* 1992; Kuo *et al.,* 2000; Almazan *et al.,* 2000; Yount *et al.,* 2000; Casais *et al.,* 2001; Thiel *et al.,* 2001; Gonzalez *et al.,* 2002; Yount *et al.,* 2002; Haijema *et al.,* 2003; Yount *et al.,* 2003; Coley *et al.,* 2005; Youn *et al.,* 2005; St-Jean *et al.,* 2006; Tan *et al.,* 2006; Fang *et al.,* 2007; Becker *et al.,* 2008; Donaldson *et al.,* 2008; Tekes *et al.,* 2008; Pfefferle *et al.,* 2009; Tylor *et al.,* 2009; Balint *et al.,* 2012; Tekes *et al.,* 2012; van der Worm *et al.,* 2012; Almazan *et al.,* 2013; Scobey *et al.,* 2013; van Beurden *et al.,* 2017). The number of reverse genetic systems in use does portray the illusion that development was easy, however the large size of the RNA genome paired with the toxicity of some virus derived cDNAs in bacteria presented a magnitude of problems that required out of the box thinking to solve. As with all reverse genetics systems, there are advantages and disadvantages in all the developed strategies.

The first reverse genetic strategy employed for a coronavirus was targeted RNA recombination, which involves homologous recombination events between donor RNA molecules and a recipient RNA molecule. One of the RNA molecules must contain a selective marker to differentiate between parental and recombinant virus, often this is temperature sensitivity or host range (Koetzner *et al.,* 1992; Kuo *et al.,* 2000; Haijema *et al.,* 2003). One of the main disadvantages of this system is it allows for only the modification of the structural and accessory genes, and not the replicase. Targeted RNA recombination has been successfully used for the H52 vaccine strain of IBV (van Beurden *et al.,* 2017), however several non-coding mutations had to be incorporated into the RNA molecules for cloning purposes; although silent these may impact secondary RNA structure and transcription of viral ORFs.

Another strategy used is *in vitro* ligation, which was originally utilised for TGEV (Yount *et al.,* 2000) but has also been successfully applied for the Beaudette strain of IBV (Fang *et al.,* 2007; Tan *et al.,* 2006; Youn *et al.,* 2005). The process involves the assembly of a full length infectious cDNA from several contiguous cDNA fragments that collectively span the entire genome. Each fragment is flanked by naturally occurring or engineered restriction sites, which allowed ligation to proceed in an ordered fashion. The full length cDNA is under the control of a T7 RNA promoter allowing for *in vitro* transcription, and the resulting transcripts are transfected into a susceptible cell line along with N gene transcripts. The *in vitro* cDNA assembly approach is both simple and straightforward; the process does however rely on

continuous amplification of the individual cDNA fragments either in bacteria or from PCR, both of which can introduce error. Also if using engineered restriction sites this may introduce coding or non-coding mutations into the viral genome. Finally using *in vitro* ligation for the recovery of recombinant virus is very much a one shot approach, and additionally cannot be used to study lethal mutations.

Several groups have combined *in vitro* ligation with a vector such as BAC or vaccinia virus (VV), of which the latter has been utilised for HCoV-229E (Thiel *et al.,* 2001), MHV (Coley *et al.,* 2005), SARS-CoV (Van den Worm *et al.,* 2012), FIPV (Tekes *et al.,* 2008; Tekes *et al.,* 2012), and IBV (Casais *et al.,* 2001). The use of a vector removes the need for plasmid intermediates, and allows for unlimited production of the full length cDNA with vaccinia virus introducing fewer errors compared to BAC. Although there is a risk of error, BAC vectors have been used for TGEV (Almazon *et al.,* 2000), SARS-CoV (Almazan *et al.,* 2006), HCoV-OC43 (St-Jean *et al.,* 2006), FIPV (Balint *et al.,* 2012) and MERS-CoV (Almazan *et al.,* 2013). The majority of BAC based reverse genetic systems utilise a Cytomegalovirus (CMV) late early promoter allowing for transcription in the cell nucleus, however this process does come with a risk of splicing as the RNA exits the cell nucleus. An alternative approach is to use a T7 promoter and use *in vitro* transcription to produce RNA that is then subsequently transfected into susceptible cells (Pfefferle *et al.,* 2009). For vaccinia vectors there are two strategies that have been used for the recovery of infectious virus including *in vitro* transcription followed by transfection into a susceptible cell line as well as the method used in this PhD project in which a fowlpox virus delivers the T7 RNA polymerase into cells that are subsequently transfected with IBV cDNA (Casais *et al.,* 2001). Notably this method also works with a BAC vector, as Tylor *et al.,* (2009) transfected cells infected with a vaccinia virus encoding the T7 polymerase.

1.10 Infectious Bronchitis.

Infectious bronchitis (IB) is primarily an acute highly contagious respiratory disease of poultry. The diesease was first descibed in the 1930s (Schalk and Hawn, 1931) though at this time the aetiological agent, IBV, was unknown. Classical clinical signs include snicking (the chicken version of a sneeze), rales (vibration in the bronchi), watery eyes, nasal discharge and lethargy (Dhinaker and Jones, 1997). In addition reduced cillia movement, or complete cessation of ciliary activity (cilostasis), is observed in trachea of infected birds. This IBV inflicted damage renders infected birds susceptible to secondary bacterial infections,

and it is often these secondary infections, for example colibacillosis, that result in mortality (Matthijs *et al.,* 2003; Cavanagh and Naqi 2003).

The primary replication site of IBV is epithelial cells that line the respiratory tract however several strains can infect epithelial cells that line the enteric tract, oviducts and kidneys (Jones and Jordan, 1970; Jones and Jordan, 1971; Ambali and Jones, 1990; Benyeda *et al.,* 2009). In addition to classical IB symptoms, extensive pathology including inflammation of the kidneys and oviducts is often observed in birds infected with nephropathogenic and enterotropic strains (Cook *et al.,* 2001; Bayry *et al.,* 2005; Liu and Kong, 2004). The nephropathogenic strain B1648 first isolated in 1984 caused large outbreaks in Belgium, Holland and France, with infected birds exhibiting enlarged pale kidneys with urates in collecting tubules (Cook *et al.,* 2012; Reddy *et al.,* 2016). The IBV strain QX, first identified in the Qingdao region in China in 1996, caused the abdomen of infected birds to swell to such an extent that birds developed a hunched “penguin like” posture (YuDong *et al.,* 1998). In addition, infection of the oviducts of young birds resulted in false-layer syndrome (Gough *et al.,* 2008; Benyeda *et al.,* 2009).

IBV and the resulting IB is not only a welfare concern but an economic concern for countries with industrialised poultry industries. As reviewed by Cavanagh (2007) IBV infected broilers exhibit reduced weight gain and poor meat quality, whilst infected layers produced fewer eggs, as well as poor quality eggs including those with soft shells and watery albumens. A report by the Department for Envirmonent, Food and Rural Affairs (DEFRA) in 2005 estimated the ecomonic burden of IB to the UK to be in the region of £20 million per annum (DEFRA, 2005).

1.11 Current vaccination practices.

Attempts to control IBV were employed as early as the 1940’s using a crude “controlled exposure” method in which birds deliberately infected with attenuated IBVs were introduced into the naïve flock during the rearing period. As the IBV strain naturally spread, birds were “protected” against IBV infection during the laying period, thereby reducing the economic consequences of IB (Cook *et al.,* 2012). Today, live attenuated vaccines administered by eye or nasal drop or *en masse* through sprays or in the drinking water are routinely used to control IBV infection in poultry flocks (Jordan, 2017). Breeders and layers are subsequently boosted at defined intervals during the course of their lifetime with a mixture of live

attenuated or inactivated vaccines (reviewed by de Wit *et al.,* 2011). Inactivated vaccines are administered intramuscularly or via subcutaneous infection and often birds receive a series of vaccinations following a live-attenuated vaccination prime. Typical timings of vaccinations are as follows: Broilers are mass vaccinated with live attenuated vaccines at one day of age and may subsequently receive secondary or otherwise termed booster vaccinations between 14 and 18 days of age. Breeders and layers receive live attenuated vaccines at two, four and six weeks of age followed by the administration of inactivated vaccines after 20 weeks of age (Jordan, 2012).

Unfortunately, a single IBV serotype vaccine does not provide adequate cross-protection against the wide variety of circulating strains, discussed further is section 1.14 as well as in Chapter 4. Poultry produces therefore use a multi-monovalent strategy for vaccination in which vaccinations of at least two serotypes are administered, e.g. H120 + D274, although if administered at the same time, there is a risk of recombination events between the vaccine viruses, and a risk that adequate immune responses toward both strains will not be induced equally. The other strategy is to vaccinate with different serotypes at different times, for example for broilers, one vaccine serotype, H120, will be administered at one day of age and then a second, CR88, at 14 days of age. Poultry producers either pick IBV vaccines suitable against known circulating strains or pick vaccines known to induce an adequate level of cross-protection (reviewed by Jordan, 2012). Both strategies require knowledge of known circulating strains and unfortunately may not be effective if a novel strain emerges, such as seen with QX in the early 2000's (Lui and Kong, 2004). In addition, the chicks vaccinated via the latter method remain susceptible during the two-week period between the primary and secondary/booster vaccinations.

Both the use of live attenuated vaccines and inactivated vaccines come with advantages and disadvantages. Inactivated vaccines or otherwise termed killed vaccines offer minimal risk of vaccine reversion or the potential for vaccine related IB-like symptoms. However, manufactures need to develop protocols for the optimal method of destroying virus infectivity whist retaining antigenicity as well as developing suitable adjuvants. As a result, killed vaccines typically have higher manufacturing costs than their live attenuated counterparts, as well as a more laborious method of administration. Despite these downsides, killed vaccines when administered correctly do result in the slow release of antigen and long lasting immunity (reviewed by Cook et al., 2012).

All current live attenuated vaccine viruses are generated through serial passaging of a virulent field isolate through embryonated hens' eggs, typically up to 100 passages (Bijenga *et al.,* 2004; Geerlings et al., 2011). The most well used vaccines are H120 and H52, both of the Massachusetts serotype, with the respective number denoting the passage number in embryonated eggs, 120 and 52 passages, respectively (Bijlenga *et al.,* 2004). Other well used live-attenuated strains are D1466 and D274, both of which were generated in the 1980's and CR88 (4/91 serotype) developed in the 1990s (reviewed by Cook *et al.,* 2012). All these vaccines, and all live attenuated IBV vaccines in general, in order to be effective, must be able to replicate in the respiratory tract to stimulate protective immune responses and as a result some damage to the epithelial lining will occur. A balance needs to be achieved between a vaccine virus that is attenuated to such a degree that it can no longer replicate sufficiently to induce the relevant immune responses and one that is not attenuated enough that it causes serious damage, and IB associated symptoms, after administration. Live attenuated vaccines therefore have varying degrees of pathology and may not be suitable for all flocks dependant on age and immune status; the vaccines H120 and H52 provide a classic example of this consideration. H120 is acknowledged as a mild vaccine and can be used on chicks as young as one day of age, whilst H52 due to the lower number of passages in embryonated hens' eggs is "hotter" and is only used for booster vaccination in older chicks (Hoekstra and Rispens, 1960; reviewed by Bijlenga *et al.,* 2004 and Cook *et al.,* 2012).

Although live attenuated vaccines are well used, cheap and relatively easy to produce and administer, there are some notable disadvantages including vaccines that can render the birds more susceptible to *cobibacillosis* (Smith *et al.,* 1985; Matthijis *et al.,* 2003) due to excessive epithelial damage and the process also renders the vaccine virus embryo lethal and therefore unsuitable for *in ovo* administration. In addition, and more importantly a fine balance needs to be achieved between the loss of pathogenicity and the retention of immunogenicity which can only be achieved through trial and error. Despite this process being a well-established method of vaccine preparation, the exact molecular mechanisms that result in attenuation are unknown. Each batch of vaccine virus therefore needs to be thoroughly tested to ensure that administration *in vivo* will not result in any adverse IB like symptoms. Recent research has indicated that only a few consensus level mutations are acquired over the passaging process thereby presenting a short possible route back to virulence (Oade *et al.,* 2019). The risk of reversion is a notable disadvantage of current live attenuated vaccines and is heightened when live attenuated vaccines are administered incorrectly, and either accidentally or purposely overdiluted (reviewed by Bijlenga *et al.,* 2004). As a result of this risk, there is consequently a drive to rationally attenuate IBV, and subsequently rationally design IBV vaccines which have a significantly reduced risk of

reverting to a virulent phenotype *in vivo*, and the added advantage that they can be potentially administered *in ovo*, thereby allowing the chick to be protected from the point of hatch.

1.12 Immune responses to IBV.

There are several immune responses to IBV infection and IBV vaccination that despite several decades of research only remain partially understood. IBV vaccination is predominantly associated with humoral immunity and the generation of virus neutralising (VN) antibodies (reviewed by Bijlenga *et al.,* 2004; Cavanagh *et al.,* 2007, de Wit and Cook, 2014). This immunity is largely associated with the S glycoprotein and this association will be discussed further in Chapter 3 and Chapter 4. In terms of humoral immunity both systemic IgM and IgG and mucosal IgA responses have been demonstrated to be determinants in viral clearance (reviewed by Bande *et al.,* 2015). IgM has been shown to appear at five days post infection (dpi) and reaching a peak between eight and ten days. Viral replication in the Harderian Gland (HG) influence the development of mucosal IgA responses which have been demonstrated to be important in birds vaccinated via the intraocular route (Meir *et al.,* 2012). Maternally derived antibodies (MDAs) have also been shown to be important in the early protection of IBV with MDA shown to protect around 97% of birds at one day of age declining to 30% by seven days of age (Mondal and Naqi, 2001). MDA is however an important consideration for vaccine strategies as MDA is considered to have a negative impact on vaccine efficacy (Klieve and Cumming, 1988).

As well as humoral immunity, cell mediated and innate immune responses also have roles during IBV infection. Innate immune responses are considered the first line of defence and include the type I and type II interferon (IFN) response, characterised by the secretion of both IFN alpha (IFN α) and IFN beta (IFN β), and IFN gamma (IFN γ) respectively (reviewed by Bande *et al.,* 2015). The IFN I response, and specifically IFN α has been shown to inhibit IBV infection *in vitro* (Pei *et al.,* 2004). The administration of IFN α *in vivo* one day prior to IBV challenge was shown to partially protect birds from clinical disease (Pei *et al.,* 2004). The onset of IFN β production is delayed during *in vitro* IBV infection, and in IBV infected cells the early accumulation of double stranded RNA does not correlate with early onset of IFN β induction (Kint *et al.,* 2015). IBV and coronaviruses in general, have employed several strategies of evading and modulating the host IFN responses including cellular membrane rearrangements that shield viral RNA replication (Maier *et al.,* 2013; Maier *et al.,* 2016), the presence of a methylated cap structure at the 5’ end of all viral RNAs, and viral proteins that

directly and indirectly affect the IFN response. For SARS-CoV the accessory proteins have been shown to modulate the IFN response (reviewed by Liu *et al.,* 2014). Similarly, for IBV, the accessory proteins 3a and 3b have also been demonstrated to modify the IFN response at both the transcriptional and translation level (Kint *et al.,* 2015). Roles for the coronavirus N and nsp 3 proteins have also been implicated in the IFN response pathways (Kuri et al., 2011; reviewed by Zhong *et al.,* 2012; Fehr *et al.,* 2015).

The IFN response feeds into both cell mediated immunity and humoral immunity. The type I IFN response provides a rapid response to viral infection through the activation of macrophages and natural killer (NK) cells which in turn leads to the activation of humoral immunity (reviewed by Bande *et al.,* 2015). Similarly, the type II response also activates both cell mediated responses and humoral responses (reviewed by Bande *et al.,* 2015). For cell mediated immunity, cytotoxic T cells (CTLs) have been shown to be responsible for the clearance of IBV infection, and both the S and N protein has been associated with the stimulation of such responses (Seo *et al.,* 1997; reviewed by Collison *et al.,* 2000; Seo *et al.,* 2000). Additionally, the adoptive transfer of T cells harvested from chicks 10 dpi to naïve chicks prior to IBV challenge demonstrated that IBV primed CD8+ lymphocytes could induce protection against acute infection (Seo *et al.,* 2000). A role for NK cells has also been indicated in the clearance of IBV infection (Pardo *et al.,* 2004; Vervelde *et al.,* 2013).

1.13 The role of S in protective immunity and the design of rationally attenuated rIBV for use in vaccination.

The S glycoprotein is the main target for vaccine development as it has been demonstrated by several studies to induce virus neutralising (VN) antibodies (Abs; Cavanagh *et al.,* 1984; Cavanagh *et al.,* 1986; Kock *et al.,* 1990; Kant *et al.,* 1992; reviewed by Jordan, 2017). As such the serotype of any IBV is determined by the S glycoprotein. A complicated relationship exists, however, between the sequence of the S gene, the resulting genotype classification, and the serotype grouping. As reviewed by de Wit, (2011) different serotypes can have remarkably high similarity between their genomes and conversely viruses within the same serotype grouping can exhibit large variations within the S gene sequence. This complicated relationship is further is exacerbated by the lack of consensus to which areas of the S1 are compared as well as the criteria used to distinguish genotypes (Valastro *et al.,* 2016). Despite advances in sequencing methods, serotype groupings remain the common method of IBV classification with regards to vaccine research.

The S glycoprotein has been demonstrated that it is capable of inducing a protective immune response (reviewed by de Wit *et al.,* 2011; Jordan, 2017). Reverse genetics has been used to generate recombinant IBVs (rIBVs) based on the apathogenic Beaudette strain expressing heterologous S genes, from either the pathogenic strain M41-CK or 4/91 (Casais *et al.,* 2003; Armesto *et al.,* 2011). Vaccination with these rIBVs, BeauR-M41(S) and BeauR-4/91(S), was demonstrated to offer protection against homologous challenge with the wild type (WT) IBV corresponding to the donor S, M41-CK and 4/91(UK) respectively (Hodgson *et al.,* 2004; Armesto *et al.,* 2011). This research therefore highlighted the possibility of using rationally designed rIBV as a vaccine virus. Both the viruses used by Hodgson *et al.,* (2004) and Armesto *et al.,* (2011) contained the full ectodomain of the S gene from the donor virus. In a similar study Shirvani *et al.,* (2018) used a recombinant Newcastle disease virus (rNDV) to express the IBV S glycoprotein; the authors concluded that vaccination protected the birds against clinical disease but had no effect on viral shedding.

The two subunits that make up the S glycoprotein (Figure 1.7) however are not reported to play equal contributions in protective immunity. The S1 subunit has been shown to induce the majority of VN Abs and therefore is considered to play the dominant role (Mockett *et al.,* 1984; Cavanagh *et al.,* 1986a, Cavanagh *et al.,* 1986B, Ignjatovic and Galli, 1994; Moore *et al.,* 1997; Song *et al.,* 1998; Johnson *et al.,* 2003). This is not unexpected as the S1 contains the RBD (S1-CTD and S1-NTD), and consists of 3 hyperviable regions (HVRs) which have been reported to correlate to VN Abs (Cavanagh *et al.,* 1988; Shang *et al.,* 2018). Predictably the amino acid sequence of the S1 subunit is less conserved between IBV strains than the S2 (Cavanagh *et al.,* 1984; Cavanagh *et al.,* 1986b; Binns *et al.,* 1985; Kusters *et al.,* 1989; Valastro *et al.,* 2016).

Several groups have demonstrated a level of protection induced *in vivo* by recombinant S1 (rS1) protein (Song *et al.,* 1998; Johnson *et al.,* 2003; Yan *et al.,* 2013; Toro *et al.,* 2014; Zhao *et al.,* 2017). Research groups have taken several alternative routes at producing the S1 antigen, with some vaccinating birds with rS1 protein (Song *et al.,* 1998) and others vaccinating with S1 expression vectors including fowl adenovirus, FPV, DNA plasmids and NDV (Johnson *et al.,* 2003; Chen *et al.,* 2010; Yan *et al.,* 2013; Toro *et al.,* 2014; Zhao *et al.,* 2017; Shirvani *et al.,* 2018); these studies will be discussed further in Chapter 3. There has been some investigation into the S2 subunit with Shirvani *et al.,* (2018) vaccinating birds with a recombinant Newcastle disease virus (rNDV) expressing the S2 subunit; there was no difference in viral load in comparison to the unvaccinated control group. The potential role of the S2 subunit in protective immunity will also be discussed further in Chapter 3.

1.14 Definitions of protection.

There are several methods in use to determine whether vaccinated birds are protected from challenge with the method used dependant on a variety of factors including whether the vaccine is going to be licenced in the USA and/or The European Union (reviewed by de Wit and Cook, 2011; Jordan, 2017). Surprisingly the assessment of clinical signs and therefore whether the bird is free from clinical disease is rarely taken into account for vaccine efficacy in licencing terms but is used by researchers in academic settings. For license in the USA, vaccinated/challenged birds must be free of the challenge virus, and that is determined by virus re-isolation in specific pathogen free (SPF) embryonated hens' eggs from tracheal swabs taken post challenge (reviewed by de Wit and Cook, 2011). Whilst virus isolation in embryonated hens' eggs is regarded as the gold standard technique for determination of the presence of IBV, molecular methods including quantitative real time polymerase chain reaction (PCR) and enzyme-linked immunosorbent assay (ELISA) are commonly used by researchers.

Vaccines to be licenced in the European Union have to meet the standards set by the European Pharmacopeia (2010) which uses a ciliostasis or otherwise referred to ciliary activity test as a measure of tracheal cilia function. Reduced ciliary activity is a marker of the presence of IBV (Cavanagh *et al.,* 1997; Cook *et al.,* 1999) and it has been demonstrated that increased ciliary activity correlates to increased protection against secondary bacterial infections (Jackwood *et al.,* 2015). The European Pharmacopeia (2010) states that in order for a chicken to be deemed fully protected at least 50% ciliary activity must be retained post challenge in nine out of ten tracheal rings sampled.

1.15 Cross protection.

One of the major problems faced by IBV vaccine manufacturers is the lack of cross protection induced between the different IBV serotypes (reviewed by Cavanagh, 2003; de Wit *et al.,* 2011; de Wit and Cook, 2014). In a classic study, Cavanagh *et al.,* (1997) challenged chickens with a variety of strains with varying sequence homology after vaccination with IBV 6/82. The broad conclusion was that the probabilities of successful vaccination decreased as the sequence difference in the S gene of the challenge and vaccine strain increased. However, as mentioned there is a complicated relationship between gene sequencing and serotyping and as expected cross protection is equally

complex. Abdel-Moneim *et al.,* (2006), demonstrated that vaccination with H120 could not induce protection against Egypt/F/03 challenge; the sequence of the S1 subunit between the vaccine and challenge strains differed by only 34 nucleotides (nt; 14 aa). Hodgson *et al.,* (2004) demonstrated that rIBV Beau-R could not protect against challenge with M41-CK; S1 sequence homology is 95% and both belong to the same Massachusetts serotype grouping. The problems of cross protection becomes more apparent when novel variants of IBV unexpectantly emerge such as B1648 in the mid 1980s (Lambrechts *et al.,* 1993) and QX in the late 1990s (YuDong *et al.,* 1998). With current vaccines offering little cross protection the only option is to generate a new vaccine, and as discussed the generation of vaccine virus in embryonated hen's eggs is time consuming and unpredicatable. As a consequence the industry is not able to readily react to emerging threats; a scenario that could be minimised by generating vaccine viruses through a reverse genetics approach.

1.16 Project aims and objectives.

The overall aim of this PhD project was to evaluate the protection offered by vaccine candidates based on rIBV Beau-R that have been rationally designed and generated by reverse genetics. Protection was assessed *in vivo* and is defined by the standards set by the European Pharmacopeia (2010).

Objective 1: To assess whether rIBVs based on the Beau-R backbone expressing heterologous S1 subunits can induce a fully protective immune response against homologous challenge.

Objective 2: To assess whether rIBVs based on the Beau-R backbone expressing heterologous S glycoprotein can induce a fully protective immune response against challenge with an IBV of a different serotype to both Beau-R and the expressed S glycoprotein.

Objective 3: To investigate replication of Beau-R as well as other attenuated IBVs and rIBVs *in vivo* and *in vitro* at physiologically relevant temperatures.

Chapter 2: Materials and Methods.

2.1 Viruses.

2.1.1 IBV strains.

All IBV strains were propagated in 10 or 11 day old SPF embryonated hens' eggs, and were either titrated in primary chicken kidney (CK) cells or *ex vivo* TOCs.

- **Beau-CK:** GenBank accession number AJ311317. A laboratory strain that has been serially propagated in embryonated chicken eggs and *in vitro* (Cavanagh *et al.,* 1986). The exact history of Beau-CK is unknown with reports stating that Beau-CK has been passaged up to 300 times (Cavanagh *et al.,* 1988). Beau-CK is attenuated *in vivo*, and displays extended tropism *in vitro*, notably the ability to replicate in Vero, DF1 and BHK-21 cells (Casais *et al.,* 2001). Beau-CK belongs to the Massachusetts serotype and the GI-1 genotype (Valastro *et al.,* 2016).
- **Beau-R:** A molecular clone of Beau-CK that likewise displays extended tropism in cell culture (Casais *et al.,* 2003; Bickerton *et al.,* 2018), Beau-R is attenuated *in vivo* but is embryo lethal (Hodgson *et al.,* 2004). Beau-R belongs to the Massachusetts serotype and can be distinguished from Beau-CK by two marker mutations located in the nsp 16 and N genes respectively, C19666U and A27087G.
- **M41-CK:** GenBank accession number MK728875.1. A laboratory pathogenic strain that has been adapted for propagation in primary chicken cells through an unknown number of passages. M41-CK does not display the extended cell culture tropism of Beau-R and notably is unable to replicate in Vero cells but belongs to the same Massachusetts serotype and the same GI-1 genotype (Casais *et al.,* 2003; Valastro *et al.,* 2016).
- **M41-R:** A molecular clone of M41-CK that is attenuated *in vivo* as the result of four point mutations in nsp 10 (C12139T), 14 (G18119C), 15 (T19052A) and 16 (G20144A).
- **M41-K:** A pathogenic molecule clone of M41-CK. There are a number of non-coding mutations including C11682T and C11709T, both in nsp 9 that distinguish M41-CK and M41-K. Coding mutations in nsp 10, 14, 15 and 16 enable differentiation of M41-K from M41-R.
- **4/91(UK):** GenBank accession number JN192154. A pathogenic field isolate that was a gift from Intervet (UK). Birds infected with 4/91 display classical IB respiratory symptoms (Armesto *et al.,* 2011). 4/91 has restricted tropism *in vitro* and can only be propagated in embroynated hens' eggs and *ex vivo* TOCs. The virus belongs to the 4/91 serotype and the GI-13 genotype (Valastro *et al.,* 2016).

- **QX (L1148):** GenBank accession number KY933090. The field strain QX, first detected in China in 1995 (Liu and Kong, 2004; Liu *et al.,* 2006), has restricted host range in cell culture, and can replicate in neither CK cells nor Vero cells (Bickerton *et al.,* 2018B). QX is noted for its pathogenicity in chickens, with a range of clinical symptoms observed including respiratory disease, nephritis and in young birds damage to the developing reproductive tract leading to false layer syndrome (Gough *et al.,* 2008). If the latter occurs, the swelling of the oviducts leads to an extended abdomen often resulting in the infected bird adopting a “penguin”-like posture. QX is of a different serotype to 4/91, M41-CK and Beau-R, and also a different genotype, GI-19 (Valastro *et al.,* 2016). This strain of QX was a gift from Professor Richard Jones at University of Liverpool (Worthington *et al.,* 2008).
- **D388:** A strain belonging to the QX genotype, first isolated in the Netherlands in 2004 (de Wit *et al.* 2011B; Valastro *et al.,* 2016). Induces clinical disease comparable to the QX strain (de Wit *et al.,* 2011B). This strain was a gift from Sjaak de Wit at GD Animal Health, Deventer, The Netherlands.
- **H120:** A commonly used vaccine virus of the Massachusetts serotype that was produced via 120 serial passages in embryonated hens’ eggs. This strain was a gift from Professor Richard Jones at University of Liverpool. H120 is able to replicate in primary CK cells but not Vero cells (Bickerton *et al.,* 2018B). H120 is part of the GI-1 genotype (Valastro *et al.,* 2016).
- **BeauR-M41(S):** This rIBV has previously been described by Casais *et al.,* (2003). Briefly the virus contains the 5′ UTR, replicase gene as well as the structural and accessory genes from Beau-R except that the signal sequence, the ectodomain and the transmembane domain of the S gene is derived from M41-CK. The cytoplasmic tail sequence of the S gene is derived from Beau-R rather than M41-CK, and was maintained to preserve interactions with the other Beaudette-derived viral proteins. This virus is attenuated *in vivo* and displays comparable tropism *in vitro* to M41-CK.
- **BeauR-M41(S1):** This rIBV has the S1 domain of the S gene from M41-CK, with the S2 domain derived from Beau-R. All other structural, non-structural and accessory genes are derived from Beau-R. This virus exhibits extended tropism *in vitro* due to the incorporation of the Beaudette S2 domain, and is notably able to be propagated in Vero cells (Bickerton *et al.,* 2018).
- **BeauR-M41(S2):** This rIBV has the S2 domain, except the cytoplasmic tail from M41-CK, with the S1 domain derived from Beau-R. All other viral genes are derived from Beau-R (Bickerton *et al.* 2018). This virus displays *in vitro* tropism comparable to M41-CK.
- **BeauR-QX(S1):** This virus is similar to BeauR-M41(S1) in that all viral genes except the S1 are derived from Beau-R. The S1 sequence is derived from QX (L1148).

Similarly to BeauR-M41(S1) this virus has extended tropism *in vitro* due to the presence of the Beaudette S2 domain (Bickerton *et al.,* 2018B).

- **BeauR-4/91(S):** A rIBV that contains the signal sequence, the ectodomain and transmembrane domain of the S gene from the field strain 4/91 (UK). The remaining genome sequence is derived from Beau-R. As with BeauR-M41(S) the cytoplasmic tail sequence of the S gene is derived from Beau-R and was maintained to preserve interactions with the other Beaudette-derived viral proteins. This virus is attenuated *in vivo* and has restricted tropism *in vitro*, in which it can only be propagated in embroynated hen's eggs and *ex vivo* TOCs (Armesto *et al.,* 2011).
- **BeauR-M41-Struct:** A rIBV previously described by Armesto *et al* (2009). The genome of this rIBV contains Beau-R derived sequence coding for the 5′UTR through to, and including nsp 16. The remaining genome sequence from the S gene through to and including the 3′ UTR is derived from M41-CK. This virus has an attenuated phenotype *in vivo*.
- **M41-SK-106A, M41-SK-106A1, M41-SK-106C and M41-SK-106D:** Serially passaged isolates of M41-CK. Each isolate, A, A1, C and D has been passaged 110 times in embroynated hens' eggs, and all isolates display an attenuated phenotype *in vivo* (Oade *et al.,* 2019).

2.1.2 Vaccinia viruses.

- **M41R-del-S:** a recombinant vaccinia virus (rVV) containing a cDNA copy of the M41-R genome, with the S gene deleted (Keep, 2013).
- **M41R-4/91(S):** an rVV containing a cDNA copy of the M41-R genome, with the ectodomain of the S gene of 4/91 (UK) sequence instead of M41-R.
- **M41R-4/91(S1):** an rVV containing a cDNA copy of the M41-R genome with a chimeric S gene. The S1 domain, except from the signal sequence is derived from 4/91 (UK) and the S2 domain consists of M41-R sequence.
- **M41-R**: an rVV containing a cDNA copy of the M41-R genome.

2.1.3 Fowlpox virus.

- **rFPV-T7:** a recombinant fowlpox (rFPV) virus that expresses the bacteriophage T7 RNA polymerase under the control of a vaccinia virus P7.5 promotor (Britton *et al.,* 1996).

2.2 Cells, eggs and tracheal organ cultures.

All cell cultures were maintained at 37°C, 5% carbon dioxide (CO_2) unless otherwise stated. All embryonated eggs were maintained at 37°C. TOCs were incubated at 37°C without CO_2 rotating at 7 to 8 revolutions per hour (h). All TOCs were incubated for a full 48 h before use.

2.2.1 Primary cell lines.

- **Chicken kidney (CK) cells:** generated by the removal and trypsinization of kidneys from SPF Valo chickens or SPF Rhode Island Red (RIR) chickens, at 2- to 3-weeks old by a method previously described by Hennion and Hill, 2015. CK cell suspensions were prepared either by the Microbiological Services department of the Animal and Plant Agency (APHA) or the Central Services Unit (CSU) at the Pirbright Institute. The suspensions provided were subsequently used to seed plates or flasks containing CK cell medium (Table 2.1).

Table 2.1: CK cell medium.

Ingredient	Volume (ml)	Final Concentration
1x Eagle's minimum essential medium (EMEM) (Sigma, M2279)	500	0.8 x
Newborn Calf Serum (NBBS) (Sigma, N4762)	55	8.8 %
Tryptose Phosphate Broth (TPB) (Sigma, T8159)	55	8.8 %
1 M Hepes (Gibco, Life Technologies, 15630-056)	5.5	8.8 mM
200mM L-Glutamine (Sigma, G7513)	5	1.6 mM
Penicillin/Streptomycin (Gibco, Life Technologies, 15140: Penicillin 10,000 U/ml and streptomycin 10,000µg/ml).	1	Penicillin 16 U/ml Streptomycin 16 µg/ml
Nystatin (Sigma, N1638, 10,000 U/ml)	2.5	40 U /ml
Final volume	624	

- **Chicken embryo fibroblast (CEF) cells:** generated from 9 day old SPF embryonated hens' eggs (Valo) by CSU at The Pribright Institute. Briefly embryos are decapitated, eviscerated and trypsinised. The resulting cell suspensions are used to seed plates of flasks containing 1 x 199 medium (Table 2.2).

Table 2.2: 199 medium for CEF preparation.

Ingredient	Volume (ml)	Final concentration
1 x 199 medium (Sigma, M4530)	500 ml	0.8 x
Foetal Bovine Serum (FCS) (Sigma, F0926)	50	8.29 %
TPB	50	8.29 %
Penicillin/Streptomycin	1	16.6 U/ml Penicillin 16.6 µg/ml Streptomycin
Nystatin	2.5	41.4 U /ml
Final volume	603.5	

2.2.2 Continuous cell lines.

- **Vero cells:** A continuous cell line originally derived from kidney epithelial cells of the African Green Monkey. Cultures were maintained in 1 x EMEM supplemented with 10% FCS and 1% L-Glutamine.
- **DF1 cells:** An avian cell line derived from chicken embryo fibroblasts isolated from 10 day old East Langsing eggs (Himly *et al.,* 1998). Cultures were maintained in Dulbecco's modified essential medium (DMEM, Sigma, D5796) supplemented with 10% FCS.
- **BHK 21 cells:** A cell line originally derived from the kidneys of five 1-day old Syrian golden hamsters. Cultures were maintained in Glasgow minimum essential media (GMEM, Sigma, G5154) supplemented with 10% FCS, 5% TPB and 1% L-Glutamine.

2.2.3 Embryonated eggs.

SPF Valo embryonated hens' eggs were provided by VALO Biomedia GmbH, Germany. SPF RIR embryonated hen's eggs were provided by either the Poultry Production unit (PPU) at the Pirbright Institute, Compton Laboratory, or by the National Avian Research Facility (NARF) in Edinburgh. All eggs were set by Animal Services at room temperature for 24 h

before incubation at 37°C. Eggs containing live embryos at the desired gestation point were then delivered to the laboratories.

2.2.4 *Ex vivo* tracheal organ cultures.

Ex vivo TOCs were prepared from 19 day old SPF RIR embryos by a method previously described by Hennion (2015). Briefly embryos were decapitated and the trachea removed. The extracted trachea was sectioned using a microtome generating rings of approximately 1 mm. The resulting rings were separated by hand, and each ring was placed in a glass test tube containing 1 ml TOC medium (Table 2.3).

Ex vivo TOCs were also prepared from 2 - 3 week old SPF RIR chickens. The trachea was removed from each bird and cleaned using a scalpel blade. Each trachea was flushed with Phosphate buffered saline a (PBSa) before being sectioned as above, or by hand. As described above either 1 ring or 3 rings depending on the experiment, were placed in glass test tubes with 1 ml TOC medium (Table 2.3).

Table 2.3 Recipe for TOC medium.

Ingredient	Volume (ml)	Final Concentration
1 x EMEM	500	0.9 x
1M Hepes	20	37.8 mM
200mM L-Glutamine	5	1.9 mM
Penicillin/Streptomycin	1	Penicillin 18.9 U/ml Streptomycin 18.9 µg/ml
Nystatin	2.5	47 U /ml
Final volume	528.5	

2.3 Cell culture medium used for *in vitro* IBV, Vaccinia virus and FPV infections.

The below tables list the recipes for all cell culture medium used during experiments utilising IBV, Vaccinia Virus (VV) and rFPV.

Table 2.4: N,N-bis[2-hydroxethyl]-2-Aminoethanesulfonic acid (BES) medium, 1 x and 2 x, for IBV infections

Ingredient	1 x BES		2 x BES	
	Volume (ml)	Final concentration	Volume (ml)	Final Concentration
10 x EMEM (Sigma, M0275)	50	1 x	100	2 x
TPB	50	10%	100	20%
10% Bovine Serum Albumin (BSA, Sigma A9418)	10	0.2 %	20	0.4 %
1M BES (Sigma, B9879)	10	20 mM	20	40 mM
Sodium Bicarbonate solution, 7.5%	14	0.21 %	28	0.42 %
L-Glutamine, 200mM	5	2 mM	10	4 mM
Nystatin	2.5	50 U/ml	2.5	50 U/ml
Penicillin/Streptomycin	0.5	10 U/ml penicillin, 10 µg/ml streptomycin	1	20 U/ml penicillin, 20 µg/ml streptomycin
Sterile Water	358	N/A	218.5	N/A
Final volume	***500***		***500***	

Table 2.5: Recipe for 2 x EMEM for use in Vaccinia Virus infections.

Ingredient	2 x EMEM	
	Volume (ml)	Final Concentration
10 x EMEM (Sigma)	100	2 x
FCS	50	10 %
Sodium Bicarbonate, 7.5%	23	0.35 %
L-Glutamine, 200 mM	10	4 mM
Nystatin	2.5	50 U/ml
Penicillin/Streptomycin	1	20 U/ml penicillin, 20 µg/ml streptomycin
Sterile Water	313.5	N/A
Final volume	***500***	

Table 2.6 Recipe for 1 x GMEM for use in Vaccinia Virus infections.

Ingredient	1 x GMEM	
	Volume (ml)	Final Concentration
1 x GMEM (Sigma)	500	0.88 x
FCS	5.5	0.96 %
TPB	55	9.68 %
L-Glutamine, 200 mM	5	0.88 %
Nystatin	2.5	44 U/ml
Penicillin/Streptomycin	0.5	8.8 U/ml penicillin, 8.8 µg/ml streptomycin
Final volume	***568***	

Table 2.7 Recipe for 1 x 199 medium for FPV infections.

Ingredient	Volume (ml)	Final concentration
10 x 199 (Sigma, M0650)	20	1 x
TPB	20	1%
7.5 % sodium Bicarbonate	6	0.4%
200mM L-Glutamine	2	2 mM
Nystatin	1	50 U/ml
Penicillin/Streptomycin	0.2	Penicillin 10 U/ml, Streptomycin 10µg/ml
NBBS	4*	0.02%*
Water	146.8	N/A
Final volume	200	

Notes: * For serum free 1x199, NBBS was not added and the volume was replaced with water.

2.4 Buffers and solutions.

All buffers and solutions were stored at room temperature unless otherwise stated.

- **Phosphate buffered saline a (PBSa):** 9.55 g PBSa powder (BioWhittaker), made up to 1 l in type 1 endotoxin free water. The solution was adjusted to pH 7.2 using hydrochloric acid (HCl) followed by sterilisation in an autoclave for 20 min at 115˚C. PBSa was prepared by Central Service Unit (CSU) at The Pirbright Institute.
- **Phosphate buffered saline (PBS):** 9.55g/l DPBS powder (Sigma) adjusted to pH 7.1 – 7.5 using HCl. The solution was sterilised in an autoclave for 20 min at 115˚C. PBS was prepared by CSU at The Pirbright Institute.
- **Sterile water:** Type 1 endotoxin-free water was supplied by the Central Services Unit at The Pirbright Institute. Water was drawn from a Milli-Q system, 18.2 Ωm and autoclaved for 20 min at 121˚C.
- **DNA loading buffer:** 2 ml Glycerol (VWR International, 24388.26), 50 mg Ficoll 400 (Sigma, F2637), 25 mg Bromophenol blue (Sigma, 114391) and 3 ml water.
- **TE buffer, pH 9:** 10mM Trizma hydrochloride (Tris-HCl) solution, pH 9, Sigma, T2819), 1mM Ethylenediaminetetraacetic acid, pH 9 (EDTA; Sigma; E9884) in water.
- **30% sucrose:** 30 g sucrose (Sigma, 16104), made up to 100 ml in sterile water. Final solution filtered through 0.22 µM filtration system (Sartorius Stedim, 16534-K) and stored at 4˚C.
- **1% neutral red:** 1 g neutral red powder (Sigma, N4638), made up to 100 ml in sterile water. Final solution sterilised by autoclaving for 20 min at 121˚C.
- **2% agar:** 6 g agar (Sigma, A1296) made up to 300 ml in water. Final solution was autoclaved for 15 min at 121˚C.
- **Mycophenolic acid (MPA):** 10mg/ml MPA (Sigma, M3536) in 0.1M Sodium Hydroxide (NaOH; 30mM; Sigma, S5881); 400x concentrated. Final solution was filtered sterilised (0.22 µM filters) and stored at -20˚C.
- **Xanthine:** 10mg/ml Xanthine (Sigma, X3627) in 0.1M NaOH (66mM); 40x concentrated. Final solution was filtered sterilised (0.22 µM filters) and stored at -20˚C.
- **Hypoxanthine:** 10mg/ml Hypoxathine (Sigma, H9636) in 0.1M NaOH (73mM); 667x concentrated. Final solution was filtered sterilised (0.22 µM filters) and stored at -20˚C.
- **10% formaldehyde:** 50 ml formaldehyde solution (VWR International, 20909.29) was made up to 500 ml PBSa.
- **0.1% crystal violet:** 1 g crystal violet powder (Sigma, C6158), made up to 1 L in water. Final solution stored in the dark at room temperature (RT).
- **Proteinase K digestion buffer:** 200mM Tris-HCl pH 7.5 (Sigma), 10 mM EDTA, 0.4 % Sodium Dodecyl Sulfate (SDS; Sigma 75746), 400mM Sodium Chloride (NaCl; Sigma, S3014). Buffer was freshly prepared before use.

- **Proteinase K:** 20 mg proteinase K powder (Sigma, 2308) made up to 1 ml in sterile water. Final solution stored at -20˚C.
- **3M sodium acetate**: 24.6 g sodium anhydrous powder (Fisher Scientific, S/2080/53) made up to 100 ml in molecular grade water (Sigma, W4502).
- **10% BSA**: 10 g BSA powder (Sigma, A9418) made up to 100 ml in sterile water. Final solution was filtered (0.22µM) and stored at -20*C.
- **1M BES**: 213.25 BES powder (Sigma, B9879) made up to 1 L in sterile water. Final solution was filtered (0.22µM) and stored at 4*C in 250 ml aliquots.
- **Foetal Bovine Serum (FCS)**: Sigma, F0926. Serum was heat inactivated for 1 h at 50°C and subsequently stored at either 4˚C or -20˚C.

2.5 *In vivo* methods.

All animal experimental protocols were carried out in strict accordance with the UK Home Office guidelines and under licence granted for experiments involving regulated procedures on animals protected under the UK Animals (Scientific Procedures) Act 1986. The experiments were performed in The Pirbright Institute Home Office licensed (X24684464) experimental animal house facilities and were approved by the animal welfare and ethical review committee under the terms of reference HO-ERP-01-1.

All *in vivo* experiments used SPF RIR chickens. For experiments detailed in section 2.5.1.1 and 2.5.1.5, chickens were hatched and reared at the PPU at The Pirbright Institute, Compton site, and delivered to the Experimental Animal House (EAH) at 7 days of age. For experiments detailed in section 2.5.1.2 and 2.5.1.3 chickens were hatched at the National Avian Resource Facility (NARF) in Edinburgh and delivered to the experimental animal unit (BSU) at The Pirbright Institute at 1 day of age. NARF also provided eggs for the experiment detailed in section 2.5.1.4; these eggs were delivered to The Pirbright Institute where hatching and rearing occurred in the BSU.

2.5.1 Study design.

2.5.1.1: Homologous vaccine-challenge – Trial 1.

SPF RIR chickens were housed in raised floor pens in separate positive pressure HEPA filtered rooms in groups of thirty birds. Chickens were randomly assigned to one of five groups, sex of the birds was not considered. Eight-day old chickens were inoculated (vaccinated) with 10^5 plaque forming units (PFU) of either BeauR-M41(S1), BeauR-QX(S1) or PBS for mock infection/vaccination via the ocular nasal route. Twenty-one days post vaccination a challenge dose, equal to the vaccination dose was administered also via the ocular nasal route. Birds received either 10^5 PFU of M41-CK, $10^{2.73}$ Cilostatic dose 50 (CD_{50}) of QX or PBS for mock challenge. Clinical signs were observed from days two to seven both post vaccination and post challenge. Blood was sampled from each bird two days prior to challenge (Chapter 3, Figure 3.1). Details of the groups are listed below:

- Group A: mock vaccinated/mock challenged
- Group B: mock vaccinated/M41-CK challenged
- Group C: mock vaccinated/QX challenged
- Group D: BeauR-M41(S1) vaccinated/M41 challenged
- Group E: BeauR-QX(S1) vaccinated/QX challenged

Two and four days post vaccination (dpv), and two and four days post-challenge (dpc), five randomly selected chickens were humanely euthanized by cervical dislocation. A sample size of five birds and ten tracheal rings per bird was calculated to detect a significant difference in mean ciliary activity of 25% (95% certainty, 80% power, two-sided) between groups post IBV infection (de Wit *et al.,* 2013). All remaining birds were culled 14 dpc.

2.5.1.2: Homologous vaccine-challenge – Trial 2.

The method for trial 2 was as detailed in section 2.6.1.1 except birds were vaccinated with 10^4 PFU of either BeauR-M41(S), BeauR-M41(S1), BeauR-M41(S2) or PBS. Birds were challenged with either 10^4 PFU of M41-CK or PBS for mock challenge. Two additional sampling points, 4 hour post vaccination (hpv) and one dpv were included in this trial (Chapter 3, Figure 3.2) with the aim of identifying the *in vivo* dissemination pattern of each vaccine virus. Details of the groups are listed below:

- Group A: mock vaccinated/mock challenged
- Group B: mock vaccinated/M41-CK challenged
- Group C: BeauR-M41(S) vaccinated/M41-CK challenged
- Group D: BeauR-M41(S1) vaccinated/M41-CK challenged
- Group E: BeauR-M41(S2) vaccinated/M41-CK challenged

2.5.1.3: Heterologous vaccine-challenge.

SPF RIR chickens were housed in raised floor pens held within separate positive-pressure HEPA-filtered rooms in groups of 20, 30 or 35 birds. Chickens were randomly assigned to one of six groups (Table 4.1), sex of the birds was not considered. Eight-day old chicks were inoculated (classified as primary vaccination) with 10^4 PFU of BeauR-M41(S) or the equivalent dose of 3 $\log_{10}$ CD_{50} BeauR-4/91(S) via the ocular-nasal route. Mock vaccinated chickens were inoculated with PBS (Chapter 4, Figure 4.1). Fourteen days after the primary vaccination, chickens received a second vaccination of either BeauR-M41(S), BeauR-4/91(S) or PBS, administered in the same dose and manner as the primary vaccination. Twenty three days after primary vaccination, a challenge dose of 3 $\log_{10}$ CD_{50} QX or PBS was administered in the same manner as the vaccinations to the appropriate groups. Clinical signs were observed from 3 – 7 days after each infection. The groups are detailed below:

- Group A: mock vaccinated/mock vaccinated/mock challenged
- Group B: BeauR-M41(S) vaccinated/BeauR-M41(S) vaccinated/QX challenged
- Group C: BeauR-4/91(S) vaccinated/BeauR-4/91(S) vaccinated/QX challenged
- Group D: BeauR-M41(S) vaccinated/BeauR-4/91(S) vaccinated/QX challenged
- Group E: BeauR-4/91(S) vaccinated/BeauR-M41(S) vaccinated/QX challenged
- Group F: mock vaccinated/mock vaccinated/QX challenged

On specific days post-primary vaccination (dppv) and post-challenge (dpc), 5 or 10 randomly selected chickens were humanely euthanized by cervical dislocation (Table 4.1). A sample size of five birds was used for the mock-infected group at all time points and all vaccinated groups on 4 dppv. This sample size of five young birds and 10 tracheal rings per bird is calculated to detect a significant difference in mean ciliary activity of 25% (95% certainty,

80% power, two-sided) between groups post IBV infection (de Wit *et al.,* 2013). The sample size was increased to 10 birds post heterologous challenge to increase the power to detect significant differences in protection between vaccinated groups.

2.5.1.4: Pathogenicity experiment: Beau-R and M41-CK.

SPF RIR chickens were housed in raised floor pens in separate positive pressure HEPA filtered rooms in groups of 24 birds. Chickens were randomly assigned to one of three groups (listed below), sex of the birds was not considered. At seven days of age chickens were inoculated with 10^4 PFU of rIBV Beau-R or IBV M41-CK or PBS for mock infection via the ocular-nasal route. The groups are detailed below. Clinical signs were observed from one to seven days post-infection (dpi). At specific points post infection, six randomly selected birds per group were humanly euthanised by cervical dislocation (Chapter 5, Figure 5.1). This sample size alongside 10 tracheal rings per bird was calculated to detect a significant difference in mean ciliary activity of 25% (95% certainty, 80% power, two-sided) between groups post IBV infection (de Witt *et al.,* 2013). All remaining birds were culled on the final day of the experiment, day 7.

- Group A: mock infected
- Group B: Beau-R infected
- Group E: M41-CK infected

2.5.1.5 Pathogencitiy experiment, M41-R.

This experiment was completed by Dr. Erica Bickerton and I before the start of this PhD course. All data from the experiment has been re-analysed with the aim of this PhD project in mind.

SPF RIR chickens were housed in raised floor pens in separate positive pressure HEPA filtered rooms in groups of 12 birds. Chickens were randomly assigned to one of three groups listed below with the sex of the birds not considered. At eight days of age chickens were inoculated with 10^5 PFU of rIBV Beau-R, M41-R 6, M41-R 12, IBV M41-CK or 1 x BES for mock infection (Figure 2.5). Clinical signs were observed from two to seven dpi. Three randomly selected birds per group were humanly euthanised by cervical dislocation on 4 and 6 dpi. All remaining birds were culled, also by cervical dislocation on the final day of the experiment. Ciliary activity was assessed at all sampling points.

- Group A: mock infected
- Group B: Beau-R infected
- Group C: M41-R 6 infected
- Group D: M41-R 12 infected
- Group E: M41-CK infected

2.5.2 Infection of chickens.

RIR SPF chickens were inoculated via the intraocular and intranasal route with a total volume of 0.1ml PBS or 0.1 ml 1 x BES medium containing a defined quantity of IBV or rIBV. Mock infected birds received 0.1 ml PBS or 1 x BES medium.

2.5.3 Assessment of clinical signs.

Clinical signs were assessed by a minimum of two persons. Chickens were observed for 2 min and the number of snicks counted by each person was recorded. The average number of snicks per bird per minute was calculated. Chickens were assessed individually for the presence of wheezing, rales, watery eyes and nasal discharge. The percentage of birds within each group exhibiting a particular symptom was calculated.

2.5.4 Post-mortem harvesting of tissues.

In each experiment a variety of tissues were collected, including trachea, eyelid, beak, Harderian gland (HG), lung, spleen, bursa and kidney. Sections of tissue were stored in PBS, RNAlater (ThermoFisher) or 20% sucrose depending on the downstream analysis

required. A set of sterile scissors and forceps were used per bird to avoid cross contamination of the samples.

2.5.5 Assessment of ciliary activity.

Tracheas were removed from chickens at specific time points in each study. Ten 1 mm sections (rings) were cut from three different regions of each trachea, 3 from the upper, 4 from the middle and 3 from the lower section. The level of ciliary activity of each tracheal section was determined using light microscopy and scored as follows 0 = complete ciliostasis, 1 = ~ 25% of cilia beating, 2 = ~ 50% of cilia beating, 3 = ~75% and 4 = no ciliostasis, 100% cilia beating. The average ciliary activity of ten rings was calculated. This method is an adaptation of methods previously described by Cook *et al.,* (1999) and Cavanagh *et al.,* (1997).

2.5.6 Blood sampling and serum collection.

In each vaccine-challenge experiment, one day pre-vaccination and two days prior to challenge, blood was sampled from each bird via a wing vein. During post-mortem, blood was collected from each bird. Blood was allowed to clot at room temperature and the serum was clarified via low speed centrifugation.

2.5.7 Tissue processing.

The tracheal rings used for the ciliary activity assay (section 2.6.5) were homogenised in 500 µl PBSa containing penicillin, 20 U/ml, streptomycin, 20 µg/ml and nystatin, 20 U/ml, using a Tissuelyser II (Qiagen) with 5mm beads (Qiagen). Sections were homogenised for up to six min at 27 Hz, producing a tissue derived supernatant that was subsequently clarified by low speed centrifugation. Tracheal rings not used for ciliary activity as well as eyelids, HGs and nasal turbinates that had been stored in PBS were also processed in the above manner. The resulting tissue derived supernatants were stored at – 80°C.

2.5.8 Viral Isolation in embryonated eggs.

Embryonated hens' eggs were inoculated with 100 µl of tissue-derived supernatant as detailed in section 2.6.1. Allantoic fluid was harvested 24 - 48 hours post infection (hpi) and assessed for viral presence by reverse transcription polymerase chain reaction (RT-PCR) using primers BG56 and 93/100 following methods detailed in section 2.7.4, 2.7.5 and 2.7.7.

2.5.9 Viral Isolation in *ex vivo* TOCs.

For the pathogenicity experiment described in section 2.5.1.5 virus re-isolation from trachea sections was performed in *ex vivo* TOCs prepared from 19 day old SPF RIR embryonated hens' eggs. This work was completed before the start of this PhD project but the data generated has been re-analysed. Briefly three tracheal rings from each bird in 120 µl PBS were freeze thawed three times using dry ice/ethanol and a 37°C water bath. Supernatant was clarified by low speed centrifugation. Tracheal suspensions were prepared by adding 100 µl of clarified supernatant to 400 µl TOC medium. TOCs were infected with 150 µl of the tracheal suspension in triplicate. After infection at 37°C for 1 h, an additional 1 ml of medium was added per TOC. TOCs were incubated at 37°C for up to 6 days. The supernatant harvested was screened for IBV RNA by RT-PCR using primers BG56 and 93/100 following methods detailed in section 2.7.4, 2.7.5 and 2.7.7.

Tissue-derived supernatant from tracheas collected post challenge during *in vivo* vaccine-challenge experiments (section 2.5.1.1 to 2.5.1.3) were titrated in *ex vivo* TOCS as described by Hodgson *et al.,* (2004) and in section 2.6.3.

2.5.10 Assessment of IBV derived RNA in harvested tissues by qRT-PCR.

2.5.10.1 Vaccine-challenge experiments.

Assessment of IBV derived RNA in the trachea, Conjunctival-associated lymphoid tissue (CALT) and HG harvested as part of the *in vivo* vaccine-challenge experiments detailed in section 2.5.1.1 to 2.5.1.3 was carried out by Dr. Samantha Ellis at The Roslin Institute.

Briefly total RNA was extracted from harvested tissues as detailed in section 2.7.1 and cDNA was subsequently synthesised from 1 µg of this extracted RNA using Superscript IV Reverse Transcriptase with a random oligo primer as detailed in section 2.7.4. For quantification of viral load, quantitative real time PCR (qRT-PCR) was performed using the Taqman Universal PCR Master Mix (Applied Biosystems) with primers and probes specific to the 5′ UTR region, as described by Callison *et al.,* 2009. Serial dilutions of M41 cDNA were included to generate a standard curve. The data, expressed in terms of the cycle threshold (CT) value, were normalized using the CT value of the 28S cDNA product for the same sample (Eldahayes *et al.,* 2006).

2.5.10.2 M41-R pathogenicity experiment.

Assessment of IBV derived RNA in the trachea and HG harvested as part of the M41-R pathogenicity experiment detailed in section 2.5.1.5 was carried out by Dr. Erica Bickerton. Total RNA was extracted from 30 µg of tissue as detailed in section 2.7.1, and 100 ng of the resulting RNA was used in each real-time RT-PCR reaction using a PrimerdesignTM genesig® Kit for Avian Infectious Bronchitis Virus, Advanced, per the manufacturer's protocol. This data was generated before the time period of this PhD, but has been re-analysed as part of this PhD project.

2.5.11 IBV ELISA.

Serum samples collected both pre-challenge and post-challenge, were assessed with the commercial IBV antibody test kit (BioChek BV). To determine the end-point titres, pre-challenge serum samples were diluted 1:80 and post-challenge samples were two-fold serially diluted in the range 1:80 – 1:2560 prior to incubation. After sample incubation, the remaining steps were followed directly according to the manufacturer's instructions. The sample/positive (S/P) ratio was determined by the following equation = (Mean sample – Mean Kit Negative)/(Mean Kit positive – Mean Kit Negative). S/P ratios above 0.2 were considered to be positive for IBV antibodies. Depending on the challenge virus, either anti-M41 or anti-QX polyclonal chicken serum was included on each independent test plate as a reference control (GD Animal Health). All ELISA assays were performed by Dr. Samantha Ellis at The Roslin Institute.

2.6 *In vitro* methods.

2.6.1 Growth of IBV/rIBV in embryonated hens' eggs.

IBV/rIBV was propagated in either 10 or 11-day old SPF RIR or Valo embroynated hens' eggs. Eggs were candled to ensure embryo viability before infection. The air sac was marked and a hole drilled using a Bosch Dremel Engraver approximately 0.5 cm above the allantoic membrane. Each egg was inoculated with up to 300 µl IBV/rIBV using a 1 ml syringe and a 25G needle. Once infected, the hole in each egg was sealed with nail varnish. Eggs were incubated at 37°C for up to 72 h, with embryo viability being monitored regularly through candling. After incubation eggs were culled by refrigeration for at least 4 h at 4^{o}C. The allanotic fluid from each egg was harvested and clarified by low speed centrifugation, 500 x *g* for 5 minutes (min). All harvested allanotic fluid was stored at -80^{o}C.

2.6.1.1 Stock viruses.

For the purpose of growing stock virus, IBV/rIBV was diluted 1:1000 in PBS prior to inoculation, and each egg received 100 µl. Typically 10 eggs were inoculated per stock. Eggs were incubated no longer than 24 h. The allantoic fluid from each egg was pooled into 50 ml Falcon tubes prior to clarification by centrifugation at 500 x *g* for 5 min. Once clarified, all supernatant was pooled, mixed and aliquoted into 2 ml cryovial tubes before being stored at -80ºC.

2.6.1.2 Rescue passaging.

For passaging cell lysate or allanotic fluid as part of the rescue of rIBV (section 2.9), each egg was typically inoculated with 300 µl and incubated for 48 to 72 h at 37°C.

2.6.2 Titration via plaque assays.

CK cells were seeded in 12 well plates, and incubated at 37°C, 5% CO_2. Once confluent, cells were washed once with PBSa and inoculated in triplicate with 250 µl of tenfold serially diluted rIBV/IBV in 1 x BES medium. After incubation for 1 hour at 37°C, 5% CO_2, the inoculum was removed and replaced with 2 ml of overlay media per well. Overlay media consisted of 1 x BES medium containing 1 % agar. After 72 hours incubation at 37°C, 5% CO_2 cells were fixed at room temperature for 1 hour using 10 % formaldehyde in PBSa. The agar plugs were removed and cells were stained at room temperature for 20 min using 0.1% crystal violet (w/v in water). Plaques were counted and the number of PFU per ml calculated.

2.6.3 Titration in *ex vivo* TOCs.

Prior to infection each TOC was assessed individually for the presence of at least 90% ciliary activity; those with less were discarded. Each TOC was washed once with PBSa and in replicates of five, each TOC was infected with 0.4 ml TOC medium containing tenfold serially diluted IBV or rIBV. Mock infected TOCs received 0.4 ml TOC medium. Inoculated TOCs were incubated for 6 days at 37°C, no CO_2, rotating at a rate of 7 – 8 rotations per h. The percentage of ciliary activity of each TOC was assessed using a light microscope and was recorded as either active (living) or not (dead). Those TOCs displaying less than 10% ciliary activity were marked as dead. The dose required to cause 50% ciliostasis (CD_{50}) was calculated using the method published by Reed and Muench (1938).

2.6.4 Growth kinetic assays.

2.6.3.1 In vitro growth kinetic assays.

DF1 or CK cells, were seeded in either six or 12 well plates depending on the experiment and the multiplicity of infection (MOI) to be achieved. Once confluent cells were washed with PBSa and subsequently infected with a defined quantity of rIBV or IBV in 0.5 ml 1 x BES medium. Mock infected cells were inoculated with 0.5 ml 1 x BES medium. Infected cells were incubated for 1 h at 37°C or 41°C after which the inoculum was removed, and cells were washed twice with PBSa to remove any unbound virus. Per well, 2 or 3 ml 1 x BES was added, depending on whether the assay was performed in 12 or six well plates respectively. Cells were incubated at either 37°C or 41°C for up to 96 h. Supernatant, containing viral progeny, was harvested at defined intervals post infection and titrated in CK cells as detailed in section 2.6.2.

2.6.3.2 Growth kinetic assays in ex vivo TOCs.

TOCs prepared from 2 – 3 week-old RIR SPF chickens were inoculated in triplicate with 10^4 PFU in 0.1 ml TOC medium of M41-CK, M41-R or M41-K. Inoculated TOCs were incubated upright for 1 h at 37°C, after which the inoculum was removed and each TOC washed twice with PBSa to remove residual virus. Per TOC, 1 ml TOC medium was added followed by incubation at 37°C rotating 7 – 8 revolutions per h. Supernatant was harvested 1, 24, 48, 72 and 96 h post infection, and the quantity of infectious progeny virus assessed through titration in CK cells as described in section 2.6.2.

2.6.4 Plaque reduction assays.

All serum used for plaque reduction assays was harvested from SPF RIR chickens 14 days post infection. Mock serum and anti-QX serum was harvested as part of the heterologous vaccine challenge experiment (section 2.5.1.3) from birds 14 dpc in group A (mock vaccinated and mock challenged) and group F (mock vaccinated/QX challenged). Anti-M41-CK serum was harvested from the homologous vaccine challenge study detailed in section 2.5.1.2. Serum was collected from birds 14 dpc in group B (mock vaccinated/M41-CK challenged). Anti- 4/91 serum was harvested previously from birds inoculated with 4/91. Serum was collected 14 dpc when the birds were 22 days of age.

Serum was diluted 1:10 using PBS, and a subsequent two-fold dilution series generated. In triplicate diluted serum was incubated for 30 min at room temperature with 100 PFU of either rIBV Beau-R, BeauR-M41(S), BeauR-M41(S1) or IBV M41-CK with gentle agitation. Each plaque reduction assay contained a viral control in which no serum was added; these

controls were done in triplicate. The serum/virus and viral control mixes were titrated in CK cells as described in section 2.6.2.

The difference between the PFU/ml generated in virus/serum mixes and the PFU/ml generated by virus incubated with mock serum was calculated. When a difference was identified this data was presented as percentage reduction in the number of PFU/ml in comparison to the relevant control samples.

2.6.5 Temperature swap assays.

CK cells were seeded in 6 well plates. Once confluent, cells were washed once with PBSa, and inoculated with 0.5 ml 1 x BES containing 10^5 PFU of rIBV or IBV. Infected cells were incubated at either 37°C or 41°C for 1 h (1st incubation), after which the inoculum was removed and the cells washed once with PBSa to remove unbound virus. Per well, 3 ml 1 x BES was added and infected cells were incubated for a further 23 h (2nd incubation) at either 37°C or 41°C. Supernatant was harvested, and the quantity of progeny infectious virus was determined by plaque assay as detailed in section 2.6.2. The list below details the group involved in each assay:

- 1st incubation at 37°C/ 2nd incubation 37°C
- 1st incubation at 37°C/ 2nd incubation 41°C
- 1st incubation at 41°C/ 2nd incubation 41°C
- 1st incubation at 41°C/ 2nd incubation 37°C

2.6.6 Growth of rFPV-T7 in CEF cells.

T150 flasks seeded with 2 x 10^7 CEF cells were inoculated with 2 ml serum free 1 x 199 media containing rFPV-T7 at a MOI of 0.01 to 0.1. The virus was allowed to attach for 1 h at 37°C, after which 20 ml 1 x 199 medium was added per flask. Infected cells were further incubated until extensive rFPV-T7 induced cytopathic effect (CPE) could be observed, typically 4 dpi. The cells and supernatant were harvested and in order to lyse the collected cells, all harvested material underwent 3 rounds of a -80°C freeze followed by a 37°C thaw. Cell debris was removed by low speed centrifugation, 500 *x g*, 15 min, 4°C. The clarified supernatant was aliquoted and stored at -80°C.

2.7 Molecular biology methods.

2.7.1 RNA extraction.

RNA was extracted from cell culture supernatant and allanotic fluid using an RNeasy mini kit (Qiagen, 74104) following the manufacturer's protocol for RNA clean-up. Intracellular RNA from cell lystate was extracted using the same Qiagen kit following the animal cells spin protocol with the accompanying DNase treatment step. RNA was extracted from tissues harvested as part of *in vivo* studies using the same Qiagen kit following the animal tissues spin protocol. RNA was typically eluted in 40 µl RNase free water (H_2O) and stored at -20˚C.

2.7.2 Small scale DNA extraction.

DNA was extracted from re-suspended cell pellets using the QIAamp DNA mini kit following the manufacturer's (Qiagen) blood or bodily fluids spin protocol. All DNA extracted by this method was stored at -20˚C.

2.7.3 Large scale DNA extraction.

An equal volume of proteinase K digestion buffer (section 2.5) was added per sample alongside 0.1 % proteinase K (section 2.5). For example, 5 ml sample was added to 5 ml proteinase K digestion buffer with 0.1 ml proteinase K. The reaction was incubated for 2.5 h at 50°C after which an equal volume of phenol-chloroform-isoamyl alcohol (25:24:1) containing 8-hydroxy-quioline was added, mixed through inversion 5-10 times and centrifuged for 15 min at 1,200 *x g*, 4°C. The upper phase was separated into a clean 50 ml tube and a second phenol-chloroform extraction carried out, followed by a final chloroform extraction. DNA was precipitated using 2.5 volumes of -20°C ethanol and 0.1 volumes of 3 M sodium acetate followed by centrifugation for 90 min at 2,300 *x g*, 4°C. The supernatant was removed and the pellet was washed with 10ml -20°C 70% ethanol. In order to dissolve the salts the sample was incubated on ice for 5 min before centrifugation for 1 h at 2,300 x g, 4°C. Once the ethanol had been removed the DNA pellet was re-suspended in 100µl water, molecular biology grade (Sigma) and incubated overnight at 4˚C. Once the DNA had fully dissolved, the quantity and purity was assessed using a Nanodrop 1000 (ThermoScientific). DNA extracted by this method was stored at 4˚C.

2.7.4 Reverse Transcription (RT).

IBV cDNA was generated from RNA isolated via section 2.7.1. To 5µl RNA (< 500ng) the following reagents were added. The final concentration of each reagent is highlighted in ().

- 1 µl 10mM dNTPs (Invitrogen by Life Technologies, 18427-013, 0.5 mM of each)
- 1 µl 50 µM random primer (GTTTCCCAGTCACGATCNNNNNNNNNNNNNN, Sigma; 2.5 µM)
- 6 µl molecular grade water

The sample was incubated at 65°C for 5 min before the reaction was cooled on ice for 2 min. Once cool the following reagents were then added:

- 4 µl Superscript IV (SSIV) buffer/ First strand buffer for superscript III (SIII; 1x)
- 1 µl 100 mM DTT (5mM)
- 1 µl Recombinant Ribonuclease Inhibitor (RNaseOut, Invitrogen by Life Technologies, 10777-019; 2U/µl)
- 1 µl SSIV (Invitrogen by Life Technologies, 108090010; 20 U/µl) or 1 µl Superscript III (Invitrogen by Life Technologies, 18080093; 20 U/µl)

The reaction was incubated in a thermo-cycler for either 10 min at 23°C, 10 min at 55°C and 10 min at 80°C if using SSIV or 5 min 25°C, 1 h at 50°C and 15 min at 70°C for SSIII. The resulting cDNA was either stored at -20°C or taken forward immediately for PCR analysis as detailed in section 2.7.5.

2.7.5 PCR analysis.

2.7.5.1 Non high fidelity PCR.

Each PCR reaction contained the following reagents made up to a final volume of 50 µl in Nuclease-free water (Sigma, W4502). The final concentration of each reagent is highlighted in ().

- 5 µl 10 x PCR buffer – Magnesium (Mg); (1x)
- 2 µl 50mM $MgCl_2$ (Magnesium Chloride); (2 mM)
- 1 µl 10mM dNTP mix (200 µM)
- 1 µl 10µM forward oligonucleotide (0.2 µM)
- 1 µl 10µM reverse oligonucleotide (0.2 µM)
- 5 µl template DNA/cDNA (< 500 ng) or 1 bacterial colony
- 0.5 µl Recombinant Taq polymerase (Invitrogen by Life Technologies, 10342, 2.5 U).

PCRs were performed using a thermal cycler (2720 Thermal Cycler, Applied Biosystems) with the following cycles: 95°C for 3 min followed by 25 cycles of 95°C for 30 seconds (s), X°C for 30 s and 72°C for 1 min per kb of DNA amplified and a final cycle of 72°C for 3 min. The annealing temperature, X, was dependent upon the melting temperatures of the oligonucleotide primers used and the extension times were dependant on the size of the PCR product amplified.

2.7.5.2 High fidelity PCR.

Each PCR reaction contained the following and was made up to a total reaction volume of 50 µl using Nuclease-free water. The final concentration of each reagent is shown in ().

- 2.5 µl 10 µM forward oligonucleotide (0.5 µM)
- 2.5 µl 10 µM reverse oligonucleotide (0.5 µM)
- 10 µl 5 x Q5 reaction buffer (1x)
- 1 µl 10mM dNTP mix (200 µM)
- Up to 5 µl Template DNA (< 1000 ng)
- 0.5 µl Q5 high fidelity DNA polymerase (New England Biolabs, M0491S, 0.02 U/µl)

PCRs were performed using a thermal cycler (2720 Thermal Cycler, Applied Biosystems) with the following cycles: 98°C for 1 min followed by 25 cycles of 98°C for 10 s, X°C for 30 s and 72°C for 30 s per kb of DNA amplified and a final cycle of 72°C for 2 min. The annealing temperature, X, was dependent upon the melting temperatures of the oligonucleotide primers used and the extension times were dependent on the size of the PCR product amplified.

2.7.5.3 PCR primer sets.

All primers were synthesised by Sigma, and re-suspended in molecular grade water to give a stock solution of 100 µM.

Table 2.8: Details of primer sets.

Forward primer	Reverse primer
BG56 CAACAGCGCCCAAAGAAG	93/100 AGGCTAGTATAGAGTTAGAGC
GPT forward ATGAGCGAAAAATACATCGTC	GPT reverse TTAGCGACCGGAGATTGGC
S-FOR AGTGTGGTAAGTTACTGG	3A-rev-SalI AATTGTCGACCCTCTAGCGACTT
SalI-M40 AATTGTCGACGTGACAGAGACAA	BG131 AGAGGTGTTACCAACATCTC
SalI-M40 AATTGTCGACGTGACAGAGACAA	3A-rev-SalI AATTGTCGACCCTCTAGCGACTT
S For* TGGTAAGTTACTGGTAAGAG	S Rev* TACGTGGGACTTTGGATCA

2.7.6 Restriction digest.

The following restriction endonuclease enzymes were used in this project including *Sal I* – HF® (NEB, R3138S), *Not I* (NEB, R0189S), *Kpn I* (NEB, R01425) and *Xhol I* (NEB, R0146S). All reactions were prepared following the manufacturers' protocol. Typically each 50 µl reaction contained 1 x the appropriate buffer, 1 unit (U) of restriction enzyme and up to 1 µg of DNA. Reactions were incubated for 1 h at 37˚C and heat inactivated for 20 min at 65°C.

2.7.7 Agarose gel electrophoresis.

PCR products were separated and visualised by agarose gel electrophoresis. Agarose gels contained 1 - 0.8% agarose in 50 ml 1 x Tris borate EDTA (TBE) buffer (Invitrogen by Life Technologies, CH5022) as well as 5 µl SYBR safe DNA gel stain (Invitrogen by Life Technologies, S33102). Each sample, 5 µl, was mixed with 2 µl DNA loading buffer. Gels were run in 1 x TBE buffer using a 9 x 11 horizontal submarine gel apparatus (Galileo Bioscience) at approximately 5 V/cm gel length. A 1kb+ DNA ladder (Invitrogen) was used to estimate DNA band sizes. The gel was visualised using a Bio-Rad Gel Doc EZ as per the manufacturer's protocol.

2.7.8 Pulsed field gel electrophoresis.

Large fragments of DNA were examined by pulsed field gel electrophoresis. Up to 1 µg of DNA was digested with restriction enzyme *Sal I* as described in section 2.7.6. Per sample, 5 µl of DNA loading buffer was added followed by incubation at 65˚C for 10 min. The digested

and denatured DNA was subsequently separated on 0.8% agarose gel (Pulsed Field Certified Agarose, Bio-Rad Laboratories, 1620137) prepared in 0.5 X TBE buffer. Gels were run in 0.5 x TBE buffer using pulsed field gel apparatus (BioRad) under the following conditions: initial pulse time of 0.1 s, final pulse time of 1.0 s, 6.0 V/cm for 12 h. To approximate size of fragments a CHEF DNA Size Standards 8-48 Kb marker was run alongside the samples (Bio-Rad Laboratories, 170-3707). Before visualization the gel was stained in sterile water containing 0.1g/mL ethidium bromide ($C_{21}H_{20}BrN_3$), at room temperature for 30 min with gentle agitation. To remove excess dye, and to provide a clear picture, gels were also partially de-stained in sterile water for 30 min with gentle agitation. The gel was visualised using a Bio-Rad Gel Doc EZ as per the manufacturer's protocol.

2.7.9 PCR purification.

PCR products or those products from restriction digest (section 2.7.6) that required less than 20 nucleotides removed were purified using the Monarch PCR and DNA clean up kit following the manufacturer's protocol (NEB, T1030S). Products were typically eluted in 10 µl and stored at -20˚C.

2.7.10 Gel purification.

Up to 5 µg of DNA was separated by agarose gel electrophoresis (section 2.7.7) using 1 x Tris-acetate-EDTA (TAE) buffer (Invitrogen by Life Technologies, 15558026) instead of 1 x TBE. Fragments were excised using a scalpel blade. The DNA was recovered from the excised fragment using a Monarch DNA gel extraction kit, (NEB, T1020S). Products were typically eluted in 10 µl and stored at -20˚C.

2.7.11 Ligation.

DNA fragments were ligated in a 3:1 vector/insert ratio using T4 DNA ligase (NEB, M0202). Each reaction contained the following reagents. The final concentration is highlighted ().

- 2 µl 10 x T4 DNA ligase buffer (1x)
- X µl Vector DNA
- Y µl Insert DNA
- 1 µl T4 DNA ligase (20 U/µl)
- Up to 20 µl molecular grade water

Reactions were incubated at RT for 10 - 30 min, after which the sample was used to transform bacterial cells (section 2.8.12).

2.7.12 Transformation of *E.coli.*

One Shot™ MAX Efficiency™ DH5αTM-T1^{R} chemically competent cells (Invitrogen by Life Technologies, 12297016) were transformed according to the manufacturer's protocol. Per reaction, up to 150 µl was subsequently spread onto Luria-Bertani broth (LB) agar plates containing ampicillin (100 µl/ml); plates were produced by the CSU department at The Pirbright Institute. Plates were incubated overnight at 37°C after which they were wrapped in cling film and stored, for up to 2 weeks, at 4°C.

2.7.13 Bacterial overnight cultures.

Transformed *E coli* generated from section 2.7.12 was amplified for mini or maxi preps of plasmid DNA. For mini preps, 1 bacterial colony was added to 5 ml LB broth (Sigma, L2542) plus ampicillin (100 µl/ml) and was incubated overnight at 37°C, 120 rpm. For maxi cultures 1 bacterial colony was added to 1 ml LB plus ampicillin and incubated for 8 h at 37°C, 120 rpm, after which the starter culture was added to 100 ml LB plus ampicillin. This large culture was incubated overnight at 37°C, 120 rpm.

2.7.14 Minipreps.

1 ml of the 5 ml overnight cultures resulting from section 2.7.13 were centrifuged for 5 min at 14,000 *x g*. Plasmid DNA in the resulting bacterial pellet was isolated using either a QIAprep Spin Miniprep Kit (Qiagen, 27106) or a Monarch Plasmid Miniprep Kit (NEB, T1010S) following the manufacturer's protocol. Samples were typically eluted in 30 – 50 µl and stored at -20˚C.

2.7.15 Maxipreps.

The large 100 ml cultures of transformed *E coli* resulting from section 2.7.13 were centrifuged for 15 min at x 500 x *g*. Plasmid DNA was isolated in the resulting pellet using the QIAfilter Plasmid Maxi Kit (Qiagen, 12263) following the manufacturer's protocol. The DNA pellet was typically suspended in 100 to 200 µl molecular grade water.

2.7.16 Sequencing.

All sequencing was outsourced. PCR products or plasmid DNA along with the relevant DNA primers were either sent to GATC (Germany) or Source Bioscience (UK). All samples were diluted to the quantities stated by the relevant company. The data generated from each

sequencing reaction was analysed by either Dr. Erica Bickerton or Michael Oade using Staden sequencing software, version 1.7.0.

2.8 Reverse genetic system utilising vaccinia virus for the generation of recombinant IBV.

An IBV reverse genetics system previously described by Britton *et al.* (2005), Casais *et al.* (2001) and Keep *et al.,* (2015) was used to modify the IBV genome allowing for the generation of novel rIBV. Briefly a complete cDNA copy of the Beaudette (Beau-R) or the M41-CK genome (M41-R, M41-K) has been assembled within the genome of a recombinant vaccinia virus (rVV) in place of the *Thymidine Kinase* (TK) gene (Figure 2.6). The 5′ UTR sequence of the IBV cDNA is preceded by a T7 polymerase promotor, and following the poly(A) tail is a hepatitis delta antigenome ribozyme site. The IBV cDNA can be modified through transient dominant selection (TDS, Figure 2.7), a method that takes advantage of recombination events between homologous sequences (Falkner and Moss, 1988, Falkner and Moss, 1990). The TDS method requires a plasmid containing the selective marker gene, *Escherichia coli guanine phosphoribosyltransferase* (GPT) gene, which confers resistance to MPA in the presence of xanthine and hypoxanthine, as well the IBV sequence to be inserted into the full length IBV cDNA. These plasmids are referred to as pGPT plasmids. Once the desired cDNA copy of IBV has been assembled within the rVV genome, the rescue of infectious rIBVs is carried out in primary CK cells (Casais *et al.,* 2001; section 2.9). The generation of a rIBV is therefore a multistep process that is summarised in Figure 2.8.

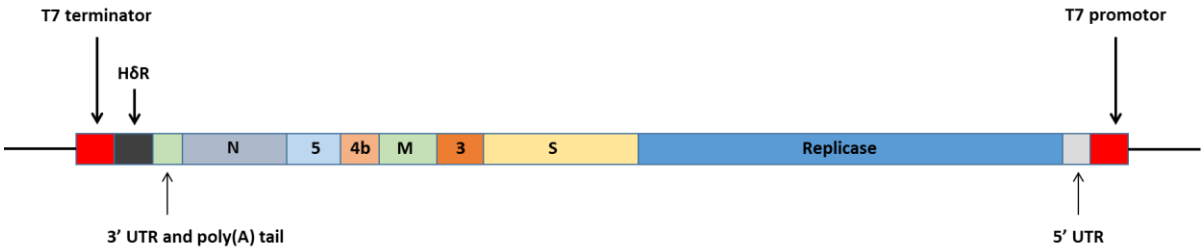

Figure 2.1: A full-length copy of the IBV genome is expressed by Vaccinia Virus. A cDNA copy of the IBV genome has been inserted within the TK gene of VV vNotI/tk via an introduced Not I restriction site (Casais *et al.,* 2003). The inserted sequence is flanked at either end by *Sal I* restriction sites. The IBV derived sequence is preceded by a T7 RNA polymerase promotor and is followed by hepatitis delta antigenome ribozyme (HδR) site and a T7 termination sequence. A full length mRNA can be produced by a T7 RNA polymerase which alongside the self-cleavage action of the incorporated ribozyme site produces an infectious full length authentic copy of the IBV genome.

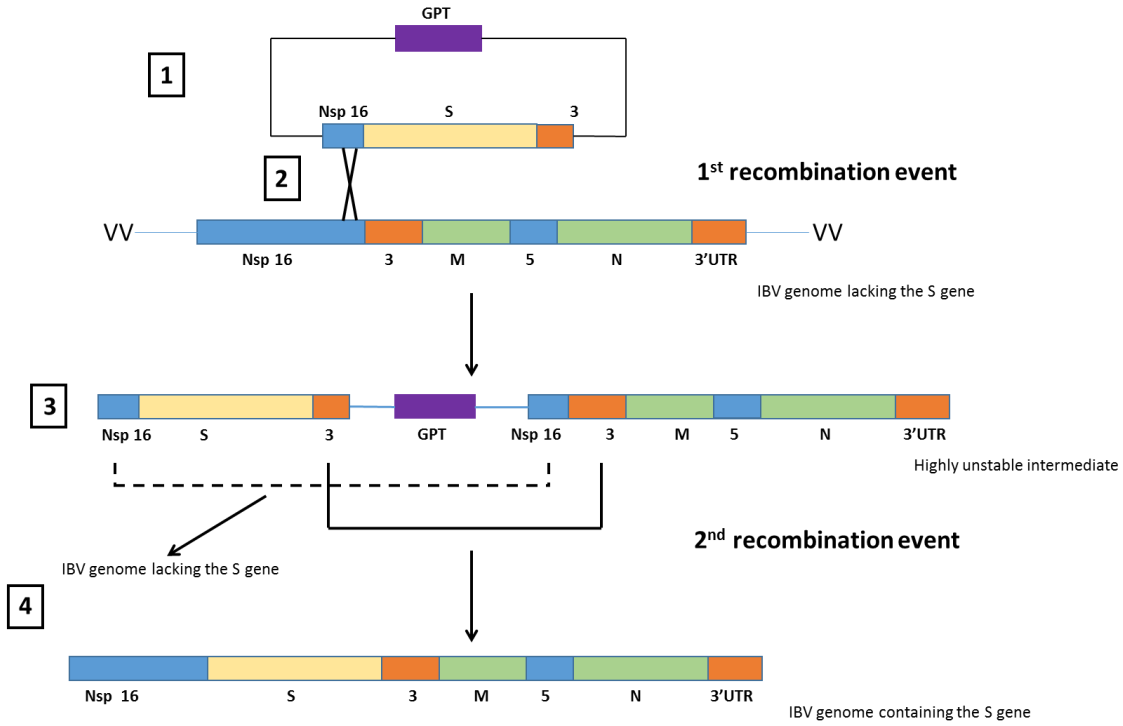

Figure 2.2: The incorporation of the IBV S gene using transient dominant selection. Transient Dominant selection is used to modify the cDNA copy of the IBV genome encoded by an rVV. (1) To modify the IBV genome, a plasmid is required that contains a GPT gene as well as the desired IBV derived sequence. For the insertion of the S gene into an IBV genome missing the S gene, the plasmid contains the S gene flanked by neighbouring sequence in nsp 16 and gene 3. (2) Recombination occurs between the homologous IBV sequences in the plasmid vector and the IBV cDNA, resulting in the complete plasmid sequence inserting into the rVV genome thereby creating, due to the presence of duplicate sequences, a highly unstable intermediate. (3) The presence of the GPT gene allows for the selection and isolation of this highly unstable intermediate through plaque purification in the presence of selection agents MPA, Xanthine and Hypoxanthine. (4) Once the selective pressure is removed a second homologous recombination event occurs that either results in the generation of an rVV containing the original unmodified IBV sequence or the generation of an IBV cDNA containing the desired modification; in this example the insertion of the S gene.

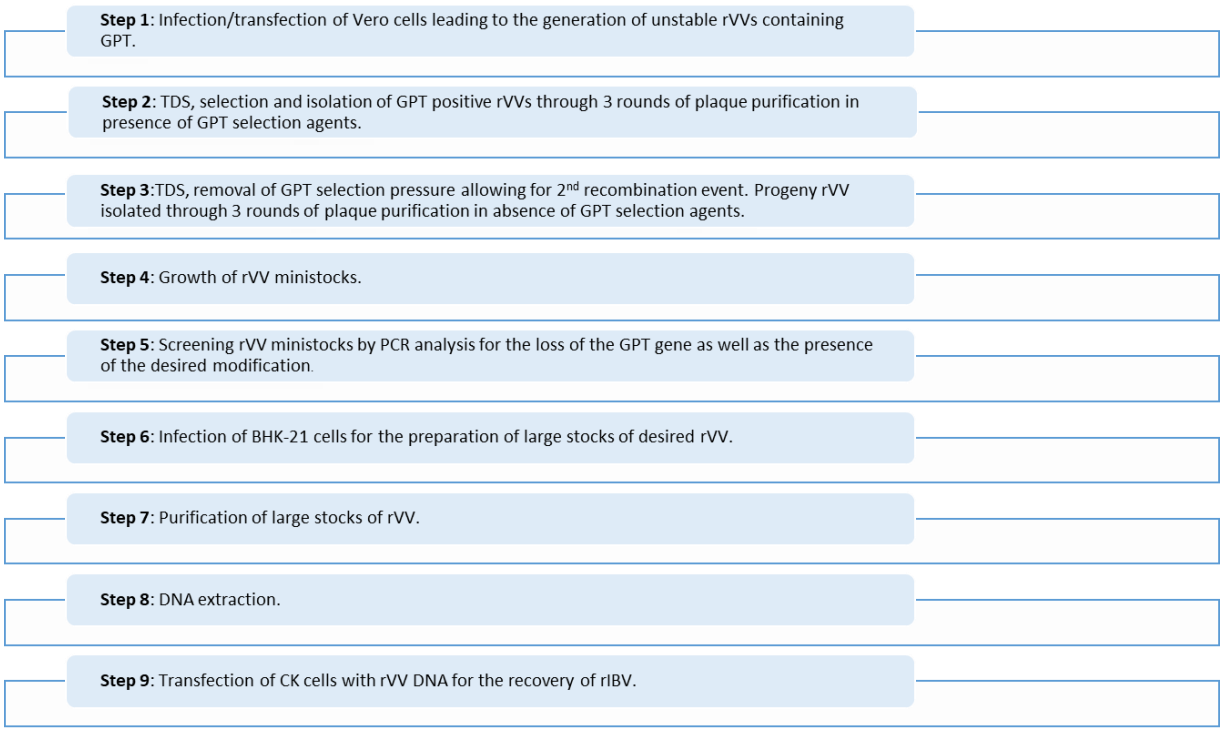

Figure 2.3: Flow chart detailing the multistep process used for the generation of rIBVs.

Since the reverse genetic system was first developed in 2001, many rIBVs have been successfully rescued. In addition there is a vast number of rVVs, not all of which served to directly produce rIBV but rather served as intermediate steps; once such rVV is M41R-del-S, which contains the M41-R genome but with the S gene deleted (Keep, 2013). These intermediate rVVs allow for targeted modification of the IBV genome in multiple stages.

The aim of this project was to construct two rIBVs, which required the construction of two rVVs. The first rVV was M41R-4/91(S1) which contained the M41-R genome with the S1 subunit of the S gene derived from the UK field strain 4/91. To construct an rVV containing this construct, a pGPT plasmid encoding the 4/91 S1 subunit flanked by M41-R derived nsp 16 and gene 3 sequence was used in a homologous recombination event alongside a receiver rVV encoding the full M41-R genome, rVV M41-R. In theory this approach could generate several rVVs with varying chimeric 4/91/M41 S1 subunits as well as the desired construct M41R-4/91(S1).

The second rVV, M41R-4/91(S), contained the M41-R genome with the ectodomain of the S gene derived from 4/91. The signal sequence and cytoplasmic tail of the S gene are derived from M41-R sequence, and these were maintained to conserve the nsp 16 sequence and the interaction of the S glycoprotein with the other M41-R derived structural proteins respectively. To construct rVV M41R-4/91(S) a pGPT plasmid encoding the 4/91(S) ectodomain flanked by M41-R nsp 16 and gene 3 sequence was used alongside the intermediate receiver rVV M41R-del-S.

The following sections will detail the construction of the plasmids used, and the methods used for constructing an rVV. Before use, each rVV was freeze-thawed up to three times using dry ice and a water bath set at 37°C. This was followed by sonication using a Branson Digital Cup Horn Sonifier 450, continuous pulse at 70 % output for 2 min. All rVV viruses were stored at -20°C unless otherwise stated.

2.8.1 Generation of pGPT vectors.

2.8.1.1 pGPT-M41-4/91(S1).

This generation of plasmid pGPT-M41-4/91(S1) was contracted to GeneArt® (Invitrogen by Thermo Fisher Scientific). The sequence of the desired insert (Appendix, Figure 8.1) was chemically synthesised and the resulting fragment cloned into pGPTNEB193. The plasmid DNA was provided at a concentration of 1 µg/ml.

2.8.1.2 pGPT-M41-R-4/91(S).

This vector was assembled in house using over lapping PCR methodology to generate the 4/91(S) sequence flanked by M41-R derived nsp 16 and 3a regions (Appendix, Figure 8.2). Once the fragment was complete this was cloned into pGPTNEB193 (Figure 2.9).

Briefly to generate the M41-R derived nsp 16 fragment primers Sal-M40 and BG131 (Table 2.8) were used to amplify rVV M41-R DNA. To generate the 4/91(S)-M41R-(3a) fragment, primers S-FOR and 3A-REV-SalI (Table 2.8) were used alongside the template pGPT-M41-4/91(S) (GeneArt). The plasmid used as a template was actually utilised in the reverse genetic system to successfully generate rIBV M41K-4/91(S) (Stevenson-Leggett, 2018) but due to the differences between M41-K and M41-R in nsp 16 it was not appropriate for the construction of M41R-4/91(S).

Once both fragments were generated, both acted as templates in an overlapping PCR utilising primers Sal-M40 and 3A-REV-SalI (Tbale 2.8). The reaction contained a 4:1 ratio of the smaller PCR fragment encoding nsp 16 to the larger fragment encoding the 4/91 S and M41-R 3a genes. The resulting PCR product was gel purified, digested with *Sal I* and subsequently ligated into the *Sal I* digested pGPTNEB193 vector. Figure 2.9 details the process of generating pGPT-M41R-4/91(S) and the relevant section numbers for the exact molecular biology methods used.

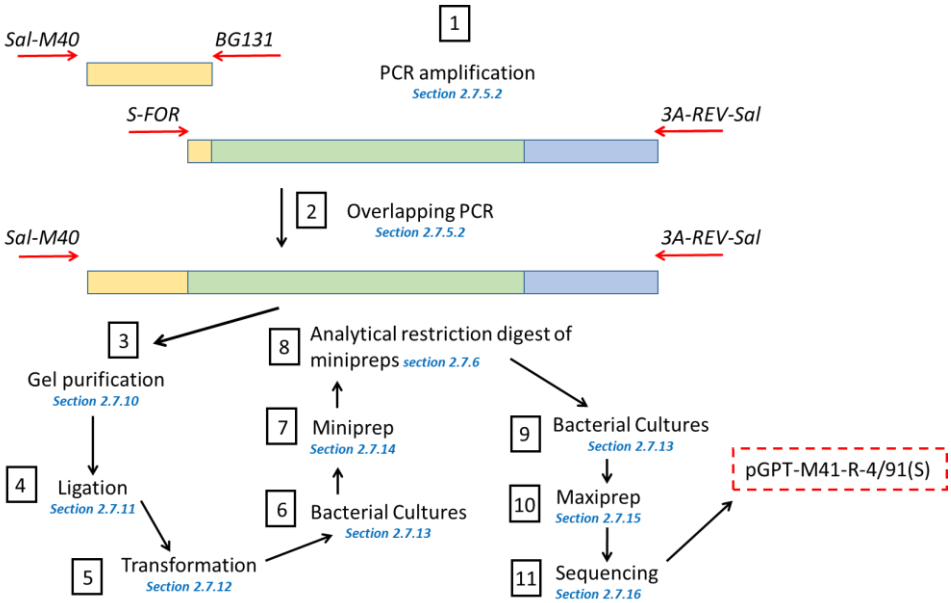

Figure 2.4: Schematic detailing the methods used to construct pGPT-M41-R-4/91(S) (1) To generate the M41-R derived nsp 16 fragment (yellow) primers (red arrows) Sal-M40 and BG131 were used to amplify rVV M41-R DNA. (2) To generate a fragment containing M41-R nsp 16, 4/91 S ectodomain (green) and the M41-R gene 3a (blue) primers S-FOR and 3A-REV-SalI were used to amplify the template pGPT-M41-4/91(S) (GeneArt). Once both fragments were generated, both acted as templates in an overlapping PCR (3) utilising primers Sal-M40 and 3A-REV-SalI. Steps 4 to 11 describe the order of methods used for cloning the overlapping PCR product. The section numbers highlighted in blue refer to the corresponding methods in this chapter.

2.8.2 Infection/transfection of Vero cells: the generation of rVVs containing GPT gene by homologous recombination.

Vero cells were seeded in 6 well plates, and once at approximately 60% confluency were washed once with PBSa. Cell were infected with rVV at an MOI of 0.2, and incubated for 2 h at 37°C. The inoculum was removed and the cells washed twice with Opti-MEM with Glutamax-1 (Gibco by Life Technologies, 51985026). Each well was transfected with a solution containing 3 ml Opti-MEM with Glutamax-1, 5 µg pGPT plasmid, and 12 µl lipofectin (Invitrogen by Life Technologies, 18292011). After 1 h at 37°C, 5% CO_2, the transfection solution was removed and replaced with 5 ml 1 X BES medium. Infected/transfected cells were incubated overnight before the addition of GPT selection agents. This prolonged incubation period allowed for the occurrence of recombination events between homologous sequences of the IBV cDNA within the rVV genome and the IBV sequence within the pGPT plasmid.

Following overnight incubation GPT selection agents in the following quantities were added per well: 12.5 µl MPA, 125 µl xanthine and 7.4 µl hypoxanthine. Cells were incubated at 37˚C until extensive CPE was observed, typically 2 to 3 days, after which both the cells and supernatant were harvested. The cells were pelleted by low speed centrifugation and re-suspended in 400 µl 1 x BES medium.

2.8.3 Transient dominant selection (TDS).

Vero cells were seeded in 6 well plates, and once confluent were washed once with PBSa. Each rVV was serially diluted in 1 x EMEM, 10^{-1} to 10^{-3}. Each well of cells was inoculated with 500µl serially diluted rVV and incubated for 1 - 2 h at 37˚C, 5% CO_2. The inoculum was removed and replaced with 3ml of overlay mixture; 1 x EMEM containing 1% agar. If GPT positive viruses were being plaque purified, GPT selection agents were added to the overlay mixture; 250 µl MPA, 2.5 ml xanthine and 149 µl hypoxanthine per 100 ml. Infected cells were incubated for 3 to 4 days at 37°C, 5% CO_2. Plaques were visualised using neutral red staining; 2 ml overlay mixture containing 0.01% (w/v) neutral red was added per well. Plaques could be visualised after a minimum of 6 to 7 h incubation at 37°C, 5% CO_2. Well isolated plaques, 2 to 10, were picked per rVV and re-suspended individually in 400µl 1 x EMEM.

2.8.4 Preparation of rVV mini-stocks.

Vero cells were seeded in 6 well plates, and once confluent were washed once with PBSa. Each well was inoculated with 500µl 1 x BES medium containing 150 µl rVV. After 1 hour incubation at 37°C, 2.5ml 1 x BES medium was added per well. The cells were incubated at 37°C, 5% CO_2 until extensive CPE was observed. The infected cells were pelleted by low speed centrifugation and re-suspended in 700 µl 1 x BES.

DNA was extracted from rVV mini-stocks as described in section 2.7.6. DNA was screened by PCR analysis (section 2.7.5.1) for the presence of GPT using primers GPT for and GPT rev, as well as the desired insert using primers S for* and S rev* (Table 2.8). The sequence of the latter PCR product was confirmed (section 2.7.16). Once the desired rVV ministocks had been identified, these ministocks were used to inoculate BHK-21 cells for the preparation of large rVV stocks (section 2.8.5).

2.8.5 Infection of BHK-21 cells for the preparation of large stocks of rVV.

BHK-21 cells were seeded in T150 flasks. Once confluent the growth media was removed from each flask and replaced with 18 ml 1 X GMEM. A further 2 ml 1 X GMEM containing 10 to 20 µl rVV was added. Infected cells were incubated at 37°C, until extensive VV-induced CPE was observed, typically 72 to 96 hpi. Both cells and supernatant were harvested into 50 ml Falcon tubes, and the infected cells pelleted by low speed centrifugation for 15 min, 4°C. Each pellet was re-suspended in TE buffer, pH 9 to produce a total of volume of 11 ml. Two 0.5 ml aliquots were kept for stock virus and stored at -80°C, whilst the remaining 10 ml was purified using ultracentrifugation (section 2.8.6).

2.8.6 Purification of large stocks of rVV.

Recombinant vaccinia virus, 10 ml, harvested as part of section 2.8.5 was centrifuged for 10 min at 500 *x g*, 4˚C, to pellet the nuclei. The cell pellet was discarded and the supernatant collected and made up to 13 ml using TE buffer pH 9. This was layered on top of 16 ml 30% sucrose solution in Beckman ultra-clear (25 x 89 mm) ultracentrifuge tubes. Using a Superspin 630 rotor and a Sorvall OTD65B ultracentrifuge, the sample was centrifuged at 4°C for 1 to 2 h at 14 k rpm (36,000 *x g).* The supernatant was carefully removed and the pellet re-suspended in 5 ml TE buffer pH 9. DNA was extracted as per section 2.7.3.

2.9 Recovery of recombinant IBV in CK cells.

The rescue of infectious rIBVs was carried out in primary CK cells (Figure 2.10) and has been described previously (Casais *et al.,* 2001, Britton *et al.,* 2005, Keep *et al.,* 2015). Briefly CK cells are infected with a rFPV-T7 that encodes a bacteriophage T7 RNA polymerase (Britton *et al.,* 1996). The cells are then transfected with rVV DNA containing a cDNA copy of the desired rIBV genome as well as a plasmid expressing the IBV N protein. The presence of the N protein has been found to be essential for efficient recovery of infectious virus (Casais *et al.,* 2001). The IBV N gene and the IBV cDNA are under the control of T7 promoters, and once transcribed in the cell cytoplasm by the T7 RNA polymerase encoded by rFPV-T7, an IBV replication cycle is initiated. Translation and genome replication follow and infectious virus is assembled and released.

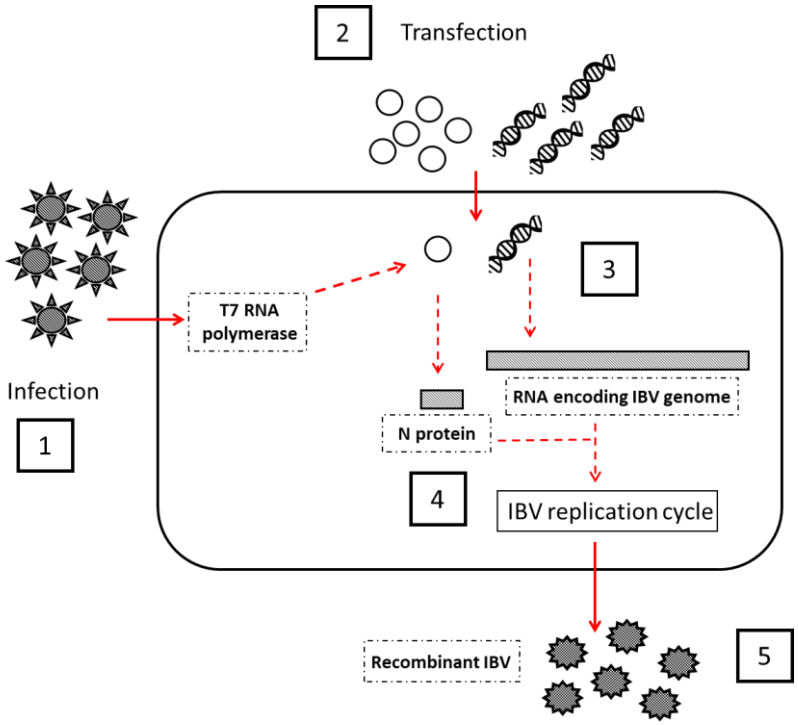

Figure 2.5: Schematic detailing the recovery of infectious rIBV in CK cells. (1) Primary CK cells are infected with a recombinant fowlpox virus which expresses a T7 RNA polymerase (rFPV-T7). (2) Cells are subsequently co-transfected with recombinant vaccinia DNA encoding the desired IBV cDNA under the control of a T7 RNA promotor, and a plasmid (pCI-Neo-N) expressing the IBV N protein under the control of both a cytomegalovirus (CMV) RNA polymerase II promoter and a T7 RNA promoter. (3) The rFPV-T7 derived RNA polymerase generates both the N protein from pCi-Neo-N, and infectious IBV RNA from the rVV DNA. This in turn (4) initiates an IBV replication cycle resulting (5) in the generation of recombinant IBV (rIBV).

2.9.1 Infection and transfection of CK cells.

CK cells were seeded in 6 well plates with the aim of achieving 40 – 50 % confluency. Prior to use the cells were washed twice in PBSa to ensure removal of unattached and/or dead cells. In replicates of 10, each well of CK cells were inoculated with 500 µl rFPV-T7 (MOI of 5 - 10) and incubated for 1 h at 37°C. Replicates of 10 are chosen as the successful recovery of rIBV is considered a low probability event. During the incubation period, transfection solutions A and B were prepared. Each solution was incubated at RT for 30 min before being combined to form solution AB. Solution AB was incubated for a further 15 min at RT before use.

Per well,

- Solution A: 1.5 ml Opti-MEM with Glutamax-1, 10 µg rVV DNA containing the modified IBV cDNA, 5 µg of plasmid expressing IBV N protein (pCi-Neo-N).
- Solution B: 1.5 ml Opti-MEM with Glutamax-1, 30 µl lipofectin.

After the 1 h incubation period, rFPV-T7 was removed from each well, and cells washed twice with Opti-MEM with Glutamax-1. Each well of cells was transfected with 3 ml solution AB, and incubated overnight at 37˚C after which solution AB was replaced with 5 ml 1 x BES medium. Cells were incubated at 37°C until extensive rFPV-T7 induced CPE was observed, typically 3 days.

The supernatant from each well was harvested and filtered (0.22µm filter) to remove rFPV-T7 and stored at -80°C. It was not expected that rIBV would be able to exit the cell so infected/transfected cells were frozen in 500 µl 1 x BES medium at -80˚C, and thawed at RT followed by turation 10 – 20 x using 1 ml syringes and needles. Once filtered (0.22µM), up to 300µl cell lysate was used to infect an embryonated hens' egg as detailed in section 2.6.1. Cell lysate was passaged twice in embryonated hens' eggs before the allantoic fluid was screened for the presence of rIBV by RT-PCR analysis using primers BG56 and 93/100 as detailed in section 2.7.1, 2.7.4, 2.7.5, 2.7.7.

2.10 Statistics.

Each figure in the results section of this PhD thesis details the statistical tests used to analysis the data set presented. Graphpad Prism, version 7.0, was used for all statistical analysis. Prior to each statistical test the normality of each data set was assessed using a Shapiro-Wilk test.

Chapter 3: Recombinant IBV Beau-R expressing either heterologous S1 or S2 subunits is unable to confer complete protection against homologous challenge.

3.1 Introduction.

Previous research has identified that vaccination with a Beau-R vector expressing either the M41 or 4/91 S ectodomain can induce a protective immune response against homologous challenge (Hodgson *et al.,* 2004; Armesto *et al.,* 2011). One of the drawbacks of expressing the complete S ectodomain is that its removes the unique ability of Beau-R to replicate in Vero cells; an ability conferred by the Beau-R S2 subunit (Bickerton *et al.,* 2018). Efficient replication in Vero cells is a desirable characteristic of vaccine viruses, as Vero cells are both licenced and routinely used by vaccine manufacturers (Montagnon *et al.,* 1981; Frazatti-Gallina *et al.,* 2004). As discussed in chapter 1 each individual S glycoprotein consists of two subunits, S1 and S2, of which the S1 forms the globular head and the S2 the stalk like structure (Doms *et al.,* 1993, Walls *et al.,* 2016; Kirchdoerfer *et al.,* 2016). Two rIBVs have been constructed that contain the S2 subunit from Beau-R and the S1 subunit from either M41 or QX; rIBV BeauR-M41(S1) and BeauR-QX(S1) respectively. Both rIBVs replicate to high titres in Vero cells (Bickerton *et al.,* 2018, Bickerton *et al.,* 2018B), consequently identifying both viruses as desirable vaccine candidates.

The role of the S glycoprotein in protective immunity is well documented (Cavanagh, 2007; de Wit and Cook, 2014; Jordan, 2017) and it is the S1 subunit that is reported to induce the majority of virus neutralising antibodies (Cavanagh and Davies, 1986; Cavanagh *et al.,* 1986, Ignjatovic and Galli, 1994; Johnson *et al.,* 2003; Song *et al.,* 1998; Mockett *et al.,* 1984). Previous research has reported varying degrees of success in both homologous and heterologous *in vivo* vaccine-challenge experiments that utilise a variety of expression systems for the S1 subunit (Johnson *et al.,* 2003; Yan *et al.,* 2013; Makadiya *et al.,* 2016; Song *et al.,* 1998).

Recombinant IBV vectors have the distinct advantage of mimicking the natural route of WT infection. Consequently local protective immune responses will be induced *in vivo* in areas that mirror the WT virus life cycle. The S glycoprotein is also a dynamic trimeric-protein structure that undergoes conformational changes during the replication cycle (Walls *et al.,* 2017). In WT infection epitopes will be presented to the immune system in both the pre-

fusion and post-fusion conformations. Non-IBV vectors such as recombinant fowl adenovirus (Johnson *et al.,* 2003), rNDV (Shirvani *et al.,* 2018) and recombinant baculovirus (Song *et al.,* 1998) that express the S1 subunit will not have the ability to present the S1 antigen as part of a trimeric structure nor in multiple forms thus limiting the induced immune response to a number of fixed epitopes. An IBV vector has capacity to allow both the pre-fusion and post-fusion forms of the S1 subunit to be presented, thereby allowing a variety of epitopes to be presented throughout the duration of the rIBV vaccine virus replication cycle.

To establish whether vaccination with a rIBV expressing heterologous S1 subunits, in which the S1 subunit is derived from a different genetic isolate and the S2 subunit is derived from the same genetic background as the vector IBV genome, could induce homologous protection against the donor S1 strain, an *in vivo* vaccine challenge experiment was carried out (Figure 3.1, Table 3.1). The results of this experiment are published in the research article (Ellis *et al.,* 2018) that forms the results section of this chapter. As an overview neither vaccination with the vaccine viruses, BeauR-M41(S1) or BeauR-QX(S1) protected birds against IB induced by challenge with IBV strains M41-CK or QX, respectively, as defined by the European Pharmacopoeia. This result lead to a second homologous vaccine-challenge experiment (Figure 3.2, Chapter 3 Table 3.2) utilising vaccine viruses, BeauR-M41(S1), BeauR-M41(S2) alongside a control rIBV vaccine BeauR-M41(S) which had previously been demonstrated to protect birds against challenge (Hodgson *et al.,* 2004). This experiment aimed to investigate the role of the individual subunits in vaccine induced immunity; the results of this are also presented in the enclosed research article (Ellis *et al.,* 2018). It was concluded that only BeauR-M41(S) induced a protective response, however this still fell short of the standards set by the European Pharmacopoeia.

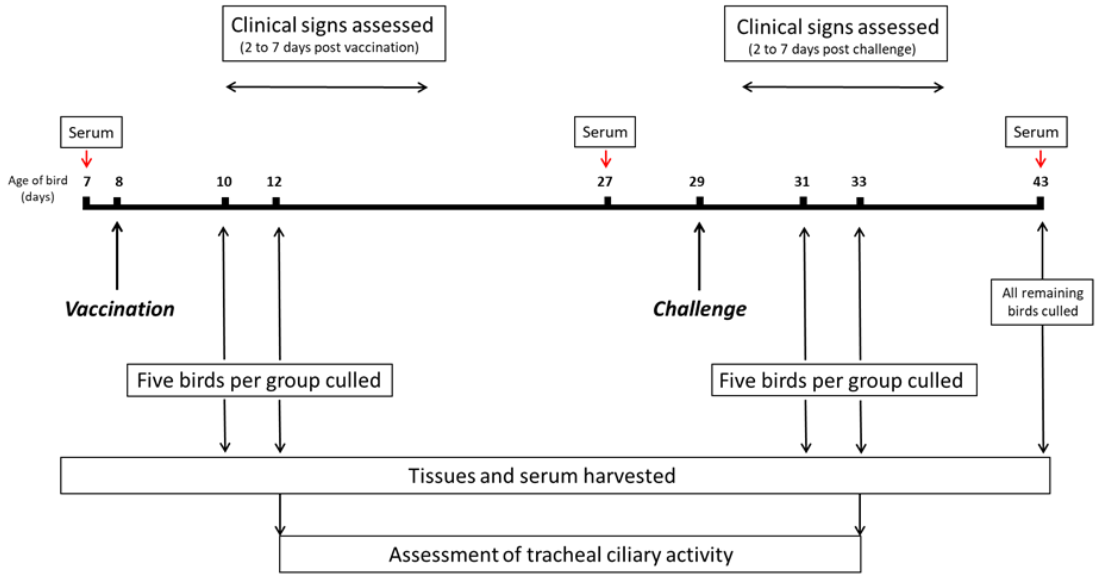

Figure 3.1: Schematic detailing protocol for *in vivo* homologous vaccine-challenge experiment – trial 1. Groups of eight day old SPF RIR chickens were vaccinated with BeauR-M41(S1), BeauR-QX(S1) or PBS. Three weeks (21 days) post vaccination birds were challenged with either M41-CK, QX or mock challenged with PBS. Clinical signs were assessed both post vaccination and post challenge. At defined intervals five randomly chosen birds were culled from each group and a variety of tissues harvested. Serum was collected pre-vaccination, post-vaccination (pre-challenge) and post-challenge. Tracheal ciliary activity was assessed on 4 dpv and 4 dpc. The experiment ended 14 dpc with all remaining birds culled.

Table 3.1: Groups, sampling points and numbers for the vaccine-challenge experiment assessing vaccine viruses BeauR-M41(S1) and BeauR-QX(S1) against homologous challenge.

Group	Vaccination	No. of birds sampled		Challenge	No. of birds sampled			Total no. of birds per group
		2 dpv	4 dpv		2 dpc	4 dpc	14 dpc	
A	PBS (mock)	5	5	PBS (mock)	5	5	10	30
B	PBS (mock)	5	5	M41-CK	5	5	10	30
C	PBS (mock)	5	5	QX	5	5	9*	29
D	BeauR-M41(S1)	5	5	M41-CK	5	5	10	30
E	BeauR-QX(S1)	5	5	QX	5	5	10	30

Note:* one bird was culled due to poor health unrelated to the IBV infection resulting in a lower number of birds in group C. This in turn resulted in a lower number of birds sampled 14 dpc.

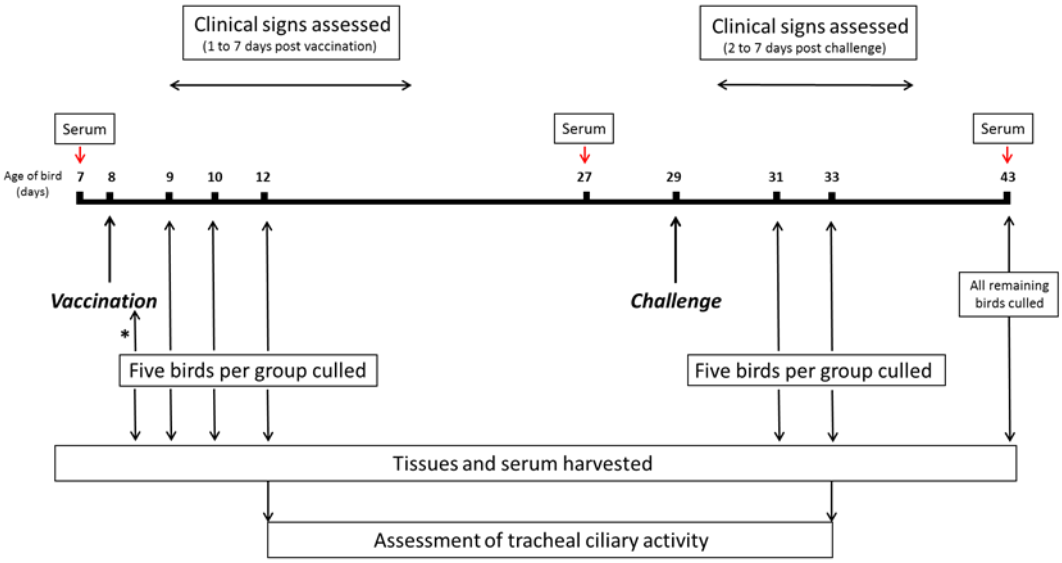

Figure 2.2: Schematic detailing protocol for *in vivo* homologous vaccine-challenge experiment – trial 2. Groups of eight-day old SPF RIR chickens were vaccinated with BeauR-M41(S1), BeauR-M41(S2), BeauR-M41(S) or PBS. Three weeks (21 days) post vaccination birds were challenged (homologous challenge) with M41-CK or mock challenged with PBS. Clinical signs were assessed both post vaccination and post challenge birds. At defined intervals, including 4 hpv, five randomly chosen birds were culled from each group and a variety of tissues harvested. Serum was collected pre-vaccination, post-vaccination (pre-challenge) and post-challenge. Tracheal ciliary activity was assessed 4 dpv and 4 dpc. The experiment ended 14 dpc with all remaining birds culled.

Table 3.2: Groups, sampling points and numbers for the vaccine-challenge experiment assessing vaccine viruses BeauR-M41(S1) and BeauR-M41(S2) and BeauR-M41(S) against homologous challenge.

Group	Vaccination	No. of birds sampled				Challenge	No. of birds sampled			Total no. of birds per group
		4 hpv	1 dpv	2 dpv	4 dpv		2 dpc	4 dpc	14 dpc	
A	PBS (mock)	5	5	5	5	PBS (mock)	5	5	10	40
B	PBS (mock)	5	5	5	5	M41-CK	5	5	10	40
C	BeauR-M41(S)	5	5	5	5	M41-CK	5	5	9*	39
D	BeauR-M41(S1)	5	5	5	5	M41-CK	5	5	10	40
E	BeauR-M41(S2)	5	5	5	5	M41-CK	5	5	10	40

Note: * one bird was culled due to poor health unrelated to the IBV infection resulting in a lower number of birds in group C. This in turn resulted in a lower number of birds sampled 14 dpc.

To clarify my contribution to the enclosed research article, I planned and organised both *in vivo* vaccine challenge experiments. I assessed clinical signs in both the experiments, Figure 2 and 6 in the enclosed article and took blood samples both pre-vaccination and pre-challenge that were used in ELISA assays, Figure 5 and 8. I also carried out post mortem examinations and generated the ciliary activity data presented in Table 1 and 2. I investigated viral load post-challenge through titrations of tracheal derived supernatant in *ex vivo* TOCs; this data is presented in Figure 4E and 7E. Tissues including eyelid, beak (nasal turbinates) and trachea were assessed for viral presence both post vaccination and post challenge; a selection of this data is presented in Table 3 of the enclosed article as well as Tables 3.3 and 3.4 of this chapter. Finally, I investigated the replication kinetics of the vaccine viruses, BeauR-M41(S1), BeauR-M41(S2) and BeauR-M41(S) *in vitro* (Figure 10).

3.2 Results.

The results section of this chapter consists of the following research article:

Recombinant Infectious Bronchitis Viruses expressing chimeric spike glycoproteins induce partial protective immunity against homologous challenge despite limited replication *in vivo.*

Authors: Samantha Ellis, Sarah Keep, Paul Britton, Sjaak de Wit, Erica Bickerton, Lonneke Vervelde.

Journal Details: Journal of Virology, December 2018, Volume 92, Issue 23, e01473-18.

Copyright Permission can be found in the Appendix (Figure 8.12).

AMERICAN SOCIETY FOR MICROBIOLOGY | Journal of Virology®

VACCINES AND ANTIVIRAL AGENTS

Recombinant Infectious Bronchitis Viruses Expressing Chimeric Spike Glycoproteins Induce Partial Protective Immunity against Homologous Challenge despite Limited Replication *In Vivo*

Samantha Ellis,[a] Sarah Keep,[b] Paul Britton,[b] Sjaak de Wit,[c] Erica Bickerton,[b] Lonneke Vervelde[a]

[a]Infection and Immunity, The Roslin Institute, University of Edinburgh, Penicuik, Midlothian, United Kingdom
[b]The Pirbright Institute, Pirbright, Surrey, United Kingdom
[c]GD Animal Health, Deventer, The Netherlands

ABSTRACT Vaccination regimes against *Infectious bronchitis virus* (IBV), which are based on a single virus serotype, often induce insufficient levels of cross-protection against serotypes and two or more antigenically diverse vaccines are used in attempt to provide broader protection. Amino acid differences in the surface protein, spike (S), in particular the S1 subunit, are associated with poor cross-protection. Here, homologous vaccination trials with recombinant IBVs (rIBVs), based on the apathogenic strain, BeauR, were conducted to elucidate the role of S1 in protection. A single vaccination of specific-pathogen-free chickens with rIBV expressing S1 of virulent strains M41 or QX, BeauR-M41(S1) and BeauR-QX(S1), gave incomplete protection against homologous challenge, based on ciliary activity and clinical signs. There could be conformational issues with the spike if heterologous S1 and S2 are linked, suggesting a homologous S2 might be essential. To address this, a homologous vaccination-challenge trial incorporating rIBVs expressing full spike from M41, BeauR-M41(S), and S2 subunit from M41, BeauR-M41(S2) was conducted. All chimeric viruses grew to similar titers *in vitro*, induced virus-specific partial protective immunity, evident by cellular infiltrations, reductions in viral RNA load in the trachea and conjunctiva and higher serum anti-IBV titers. Collectively, these findings show that vaccination with rIBVs primed the birds for challenge but the viruses were cleared rapidly from the mucosal tissues in the head. Chimeric S1 and S2 viruses did not protect as effectively as BeauR-M41(S) based on ciliary activity and clinical signs. Booster vaccinations and an rIBV with improved *in vivo* replication may improve the levels of protection.

IMPORTANCE Infectious bronchitis virus causes an acute, highly contagious respiratory disease, responsible for significant economic losses to the poultry industry. Amino acid differences in the surface protein, spike (S), in particular the S1 subunit, have been associated with poor cross-protection. Available vaccines give poor cross-protection and rationally designed live attenuated vaccines, based on apathogenic BeauR, could address these. Here, to determine the role of S1 in protection, a series of homologous vaccination trials with rIBVs were conducted. Single vaccinations with chimeric rIBVs induced virus-specific partial protective immunity, characterized by reduction in viral load and serum antibody titers. However, BeauR-M41(S) was the only vaccination to improve the level of protection against clinical signs and the loss of tracheal ciliary activity. Growth characteristics show that all of the rIBVs replicated *in vitro* to similar levels. Booster vaccinations and an rIBV with improved *in vivo* replication may improve the levels of protection.

KEYWORDS BeauR, S1, avian infectious bronchitis virus, coronavirus, partial protection, rIBV, recombinant vaccine, spike

Received 27 August 2018 **Accepted** 3 September 2018

Accepted manuscript posted online 12 September 2018

Citation Ellis S, Keep S, Britton P, de Wit S, Bickerton E, Vervelde L. 2018. Recombinant infectious bronchitis viruses expressing chimeric spike glycoproteins induce partial protective immunity against homologous challenge despite limited replication *in vivo*. J Virol 92:e01473-18. https://doi.org/10.1128/JVI.01473-18.

Editor Tom Gallagher, Loyola University Medical Center

Address correspondence to Samantha Ellis, samantha.ellis@roslin.ed.ac.uk, or Lonneke Vervelde, lonneke.vervelde@roslin.ed.ac.uk.

E.B. and L.V. contributed equally to this article.

Infectious bronchitis virus (IBV) is classified as a *Gammacoronavirus*, subfamily *Coronavirinae*, order *Nidovirales* (1). IBV is responsible for major economic losses to poultry industries worldwide as a result of poor weight gain, decreased egg production, and impaired egg quality. The effect of IBV on the ciliary activity in the trachea and the immune system may predispose infected chickens to secondary infections with opportunistic bacteria, which often increases the mortality rate associated with IBV (2–4).

IBV is an enveloped virus, with a single-stranded, positive-sense RNA genome (~28 kb) and encodes four structural proteins: nucleocapsid protein (N), spike glycoprotein (S), small membrane protein envelope (E), and integral membrane protein (M) (5, 6). The major surface protein of IBV, S, is a type 1 glycoprotein which oligomerizes to form trimers (7) and is thought to be the main inducer of protective immunity (8–12). The S protein is proteolytically cleaved into two subunits, the N-terminal subunit S1 (approximately 500 to 550 amino acids, 90 kDa) and the C-terminal subunit, S2 (630 amino acids, 84 kDa), which contains the transmembrane domain. The S1 subunit plays a critical role in binding to cellular receptors since it contains the receptor binding domain (13, 14), determines the virus serotype, and is responsible for the induction of neutralizing antibodies (14–16). Multiple studies have shown that recombinant S1 expressed in adenovirus and Newcastle disease virus vectors can induce a certain level of protection in specified-pathogen-free (SPF) chickens against challenge with wild-type virus (11, 17, 18).

Vaccine programs against IBV often include a combination of live or inactivated vaccines which are based on several dominant field serotypes of the virus. The current vaccines often induce insufficient cross-protection, and combinations of antigenically different vaccines are used in an effort to improve levels of protection (19). Alongside this, with the continual emergence of new field strains the control of IBV is persistently a significant problem to the poultry industry.

A reverse genetics system based on the avirulent strain of IBV Beaudette has been developed (20, 21). This system has many potential applications, such as to enhance our understanding of the role of individual genes in pathogenicity and to lead to a new generation of rationally designed live attenuated vaccines (20). Previous work using the reverse genetics approach demonstrated that replacement of the ectodomain of the S glycoprotein of the apathogenic IBV Beaudette strain with the same region from either of two pathogenic IBV strains, M41-CK or 4/91, resulted in two nonvirulent rIBVs, BeauR-M41(S) and BeauR-4/91(S), respectively. Notably, both rIBVs based on the BeauR backbone acquired the same cell tropism of that of the donor S, M41-CK or 4/91 (22, 23). Other work demonstrated that the Beaudette S2 subunit confers the unique ability of Beaudette to replicate in African green monkey kidney (Vero) cells, a continuous cell line licensed for vaccine production (24, 25). Vaccination with BeauR-M41(S) or BeauR-4/91(S) can confer protection against homologous challenge based on ciliary activity, reductions in clinical signs and viral load in the trachea at 5 days postchallenge (dpc), further demonstrating the dominant role of the S glycoprotein in inducing protective immunity (23, 26).

In this study, we investigated the protection conferred against homologous challenge by two rIBVs, BeauR-M41(S1) and BeauR-QX(S1), that contain S1 subunits from economically relevant strains, M41 and QX, respectively, with the S2 subunit derived from BeauR (Fig. 1). Notably both rIBVs have the advantageous ability to replicate in Vero cells (26; E. Bickerton et al., unpublished data) due to the presence of the Beaudette S2 subunit. We report here on the first application of rIBV with a chimeric S gene to be used in a vaccination trial. The rIBV BeauR-M41(S2) was also investigated in order to elucidate the relevant roles of both subunits in protective immunity. While the S1 subunit is considered to be immunodominant, the S2 subunit is highly conserved between strains and contains immunogenic regions (14, 27).

We have shown here that vaccination with a recombinant IBV expressing a chimeric S gene can induce a partially protective response against challenge, as assessed by viral load, cellular infiltration, clinical signs, and a boost in serum antibody titers postchallenge. Vaccination with rIBV expressing homologous S1 and S2 subunits (i.e., full S

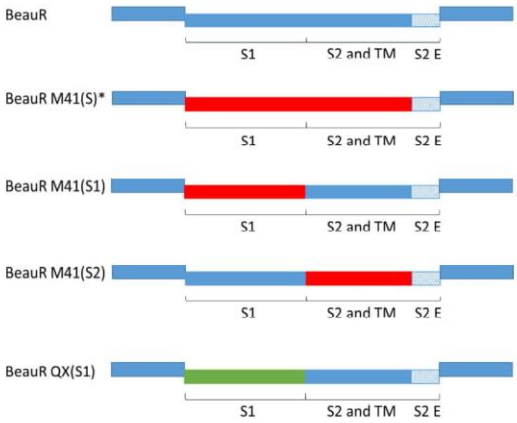

FIG 1 Design of rIBV constructs. Schematic of wild-type BeauR and rIBV genomes generated by reverse genetics to display homologous spike genes in Beaudette backbone. The rIBVs generated expressed either the S1 and/or S2 ectodomain and transmembrane domain (TM) from M41 and QX wild-type virus; with M41 derived genes represented by red boxes and QX derived genes represented by green boxes. In all rIBVs the Beaudette backbone is represented by solid blue boxes, and the endodomain (E) of S2 from Beaudette is represented by shaded blue boxes. *, BeauR-M41(S) displays the full ectodomain of M41 spike, as previously described (22).

gene) in the Beaudette backbone induced partial protection classified by the level of ciliary activity and presence of clinical signs following challenge with wild-type IBV. Comparison of *in vitro* growth characteristics shows that inclusion of a foreign S gene or a chimeric S gene in the rIBVs does not impede replication *in vitro*. However, our data show that despite the ability to induce a degree of virus-specific protective immunity, the rIBVs are hindered by limited *in vivo* replication and the attenuated BeauR backbone.

RESULTS

Characterization of rIBV BeauR-M41(S1) and BeauR-QX(S1) for homologous protection. To determine whether a single vaccination with rIBV expressing the S1 subunit of the S gene (with a Beaudette derived S2 subunit) was sufficient to induce protection against challenge with homologous pathogenic isolates of IBV, a vaccination/challenge trial was conducted with BeauR-M41(S1) and BeauR-QX(S1). No clinical signs nor loss of ciliary activity in the trachea were observed in either of the vaccinated groups after vaccination (data not shown). These results showed that replacement of the BeauR S1 gene with the S1 gene from pathogenic strains did not confer pathogenicity to the resulting BeauR-M41(S1) and BeauR-QX(S1) viruses.

Three weeks after the primary inoculation, chickens were challenged with a homologous wild-type virus strain, M41-CK or QX. Clinical signs were at the highest level in the challenge control groups, with QX more pathogenic than M41-CK (Fig. 2A and B). The rIBV vaccines expressing the S1 subunit did not confer full protection against clinical signs associated with IBV, although snicking and rales in the group vaccinated with QX(S1) resolved quicker than the QX challenge control (Fig. 2A and B). Vaccination with BeauR-M41(S1) or BeauR-QX(S1) did not prevent the loss of ciliary activity in the trachea following challenge with the homologous wild-type virus (Table 1).

To investigate the tissue tropism of the rIBVs, a range of tissues collected at 2 and 4 days postvaccination (dpv) were assessed by reverse transcription-PCR (RT-PCR). BeauR-M41(S1) and BeauR-QX(S1) RNA was not detected in the conjunctiva, Harderian gland, nasal mucosa-associated lymphoid tissue (NALT) or trachea at 2 and 4 dpv (data not shown). Histological analysis of the head-associated lymphoid tissues revealed

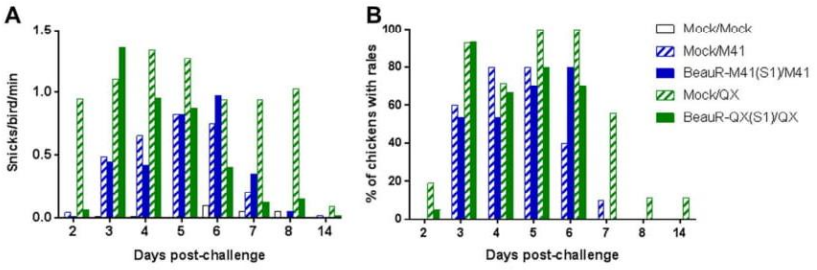

FIG 2 Assessment of clinical signs associated with BeauR-M41(S1) and BeauR-QX(S1) vaccination after challenge with M41-CK or QX. The findings for snicking (A) and rales (B) ($n = 10$ to 20 per group) are depicted.

cellular infiltrates in both the Harderian gland and the conjunctiva-associated lymphoid tissue (CALT) at 2 dpv (Fig. 3A to D), with areas of CALT more prominent in vaccinated tissues compared to mock-treated samples (Mock) (Fig. 3E). Collectively, these findings suggest that the recombinant vaccine viruses did infect these tissues but were no longer detectable by PCR at 2 dpv, suggesting rapid clearance from the sites of inoculation and mucosal tissues in the head-associated lymphoid tissues exerted by a virus-specific protective immune response.

To elucidate whether BeauR-M41(S1) and BeauR-QX(S1) were able to confer a degree of protection against homologous challenge, as evidenced by a reduction in viral load in infected tissues postchallenge, qPCR was conducted to assess the level of viral RNA in the trachea and CALT. At 2 dpc, the IBV viral RNA loads in both the trachea and the CALT were significantly lower in the BeauR-M41(S1)-vaccinated groups than in the challenge controls (Fig. 4A and C), but at 4 dpc the viral RNA load was only significantly lower in the CALT of the BeauR-QX(S1)-vaccinated group (Fig. 4B and D). The infectious viral load determined by titration of trachea tissue supernatant in tracheal organ cultures (TOCs) showed a reduction in infectious virions recovered from BeauR-M41(S1)- and BeauR-QX(S1)-vaccinated chickens, although this reduction was not significant compared to corresponding wild-type controls [BeauR-M41(S1), $P = 0.961$; BeauR-QX(S1), $P = 0.999$] (Fig. 4E). The wild-type control groups were the only groups to report significantly higher infectious viral loads recovered from the trachea compared to those of the Mock/Mock controls (Fig. 4E).

Serum IBV-specific antibodies were assessed postvaccination (prechallenge) at 21 dpv and at 2, 4, and 14 dpc. Compared to the challenge control group, titers were significantly higher in the BeauR-QX(S1)-vaccinated group at 2 and 4 dpc (Fig. 5A and B) ($P < 0.05$ and $P < 0.01$, respectively). At 14 dpc, serum titers were higher in both the BeauR-M41(S1)- and BeauR-QX(S1)-vaccinated groups compared to the challenge con-

TABLE 1 Assessment of protection against ciliostasis associated with BeauR-M41(S1) and BeauR-QX(S1) vaccination following challenge with M41-CK or QX

Vaccination/challenge	% ciliary activity (mean ± SD)[a]	No. of birds with 90% ciliary activity/total birds examined[b]	% of group protected[c]
Mock/Mock	92 ± 8.2	5/5	NA
Mock/M41	2 ± 1.4	0/5	0
BeauR-M41(S1)/M41	9 ± 16.3	0/5	0
Mock/QX	1 ± 0	0/5	0
BeauR-QX(S1)/QX	1 ± 1.4	0/5	0

[a]That is, the mean ciliary activity per group calculated from ciliostasis scores for 10 tracheal rings per individual bird using the following formula: [(total ciliostasis score of tracheal rings)/40] × 100.
[b]Ciliary activity was assessed according to European Pharmacopeia standards (27), wherein a bird is deemed protected against ciliostasis if no fewer than 9 of 10 tracheal rings per bird show normal ciliary activity (>50% ciliary activity retained).
[c]A vaccine is considered efficacious at conferring protection against ciliostasis when 80% or more of the birds in a group were protected. NA, not applicable.

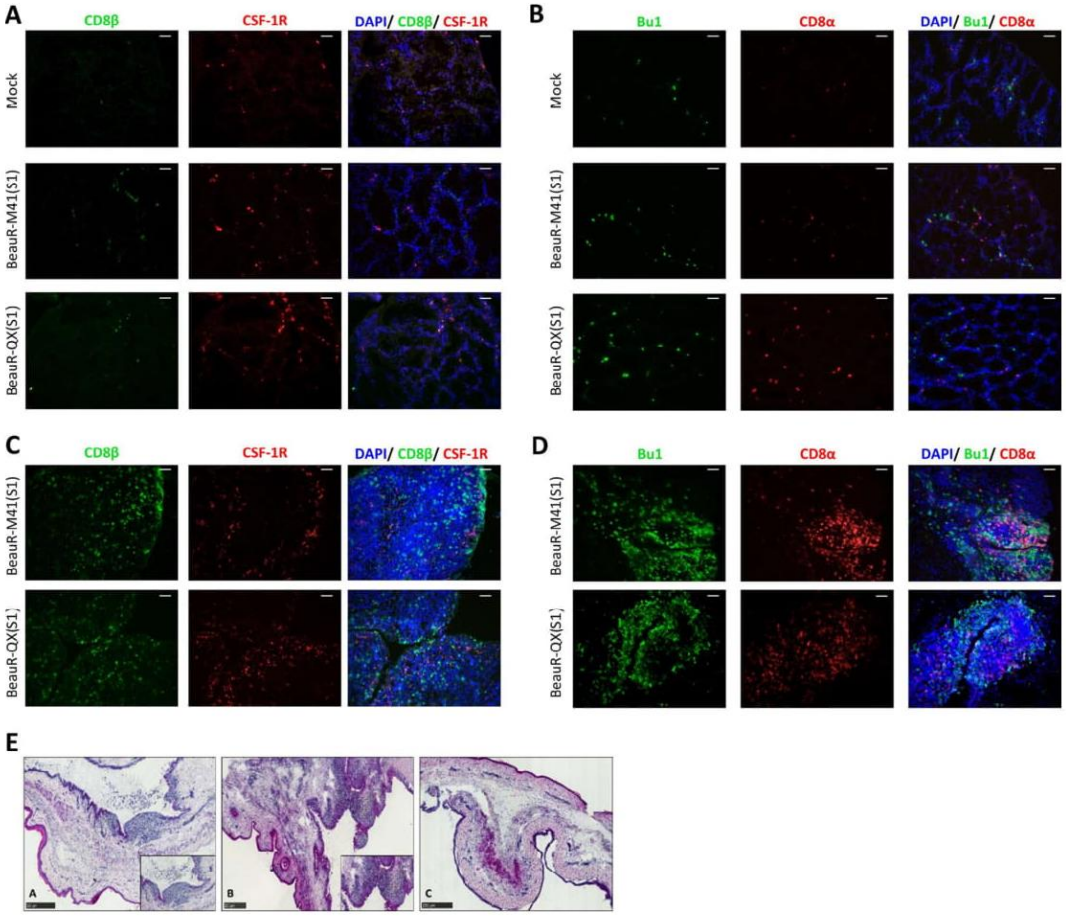

FIG 3 Cellular infiltrates of head-associated lymphoid tissues following vaccination with BeauR-M41(S1) and BeauR-QX(S1). (A and B) Harderian glands at 2 dpv. (C to E) CALT tissues at 2 dpv. Cryosections were stained with monoclonal antibodies to detect CSF-1R$^+$ (red) and CD8β^+ (green) cells (A and C) or to detect Bu-1$^+$ (green) and CD8α^+ (red) cells (B and D). Nuclei were labeled with DAPI (blue). Scale bars, 50 μm. (E) H&E-stained cryosections of the lower conjunctiva. Inset images depict the CALT regions detected in BeauR-M41(S) (see panel A) or BeauR-QX(S1) (see panel B) tissues which were not clearly evident in mock-treated lower conjunctiva (C). Scale bars, 250 μm. Representative images are shown in all panels.

trol groups, but only the QX-vaccinated group was significantly higher compared to the corresponding challenge control group (Fig. 5C and D) ($P < 0.05$). For both vaccinated groups, antibody titers at 21 dpv (prechallenge) could be classed as "borderline" positive due to being above the limits of the S/P cutoff (Fig. 5C and D).

In summary, results from trial 1 suggest that although vaccination of the chickens with BeauR-M41(S1) and BeauR-QX(S1) did not confer complete protection against homologous challenge based on clinical signs and ciliary activity, a single vaccination of young chickens induced a partially protective virus-specific immune response, as indicated by a significant reduction in the viral load in the trachea and the CALT. Higher IBV-specific serum antibody titers compared to challenge-only controls shows that vaccination with chimeric rIBVs was able to prime the birds for challenge. Whether the lack of full protection against the loss of ciliary activity and clinical signs was due to the absence of a homologous S2 subunit or an incorrect folding of M41/QX (S1) and BeauR

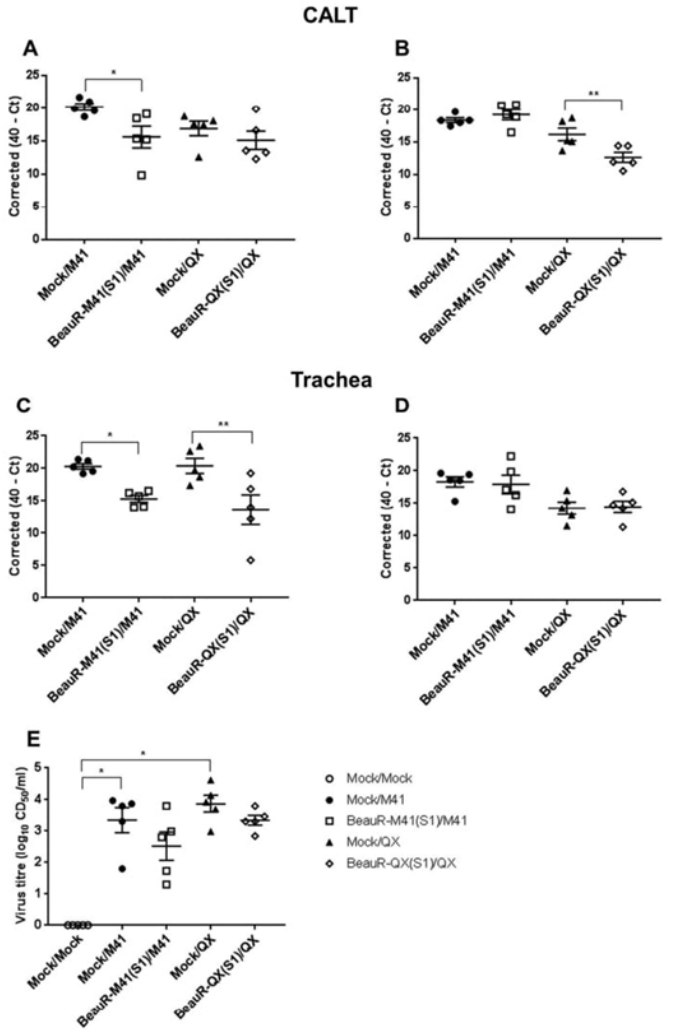

FIG 4 Viral load in the CALT and trachea in BeauR-M41(S1)- and BeauR-QX(S1)-vaccinated chickens after challenge with M41-CK or QX. (A to D) Relative viral RNA loads (expressed as corrected 40-C_T values) at specific time points: 2 dpc (A and C) and 4 dpc (B and D). (E) Infectious viral load titers in the trachea at 4 dpc. Data points are shown as individual animals, and lines represent means and standard errors of mean (SEM). Statistically significant differences between groups are highlighted. *, $P < 0.05$; **, $P < 0.01$.

(S2)—and therefore lower infectivity—could not be answered in this study. Therefore, a second trial addressing the issue of whether a homologous S2 is required for protection was conducted.

Relative contribution of S1 and S2 to homologous protection. In trial 2, the rIBVs used were BeauR-M41(S), BeauR-M41(S1), and BeauR-M41(S2) (described in Fig. 1), with an experimental design similar to that used for trial 1. No clinical signs were observed in any of the vaccinated groups after vaccination (data not shown). After vaccination, there was no loss of ciliary activity in the trachea, indicating the apathogenicity of the

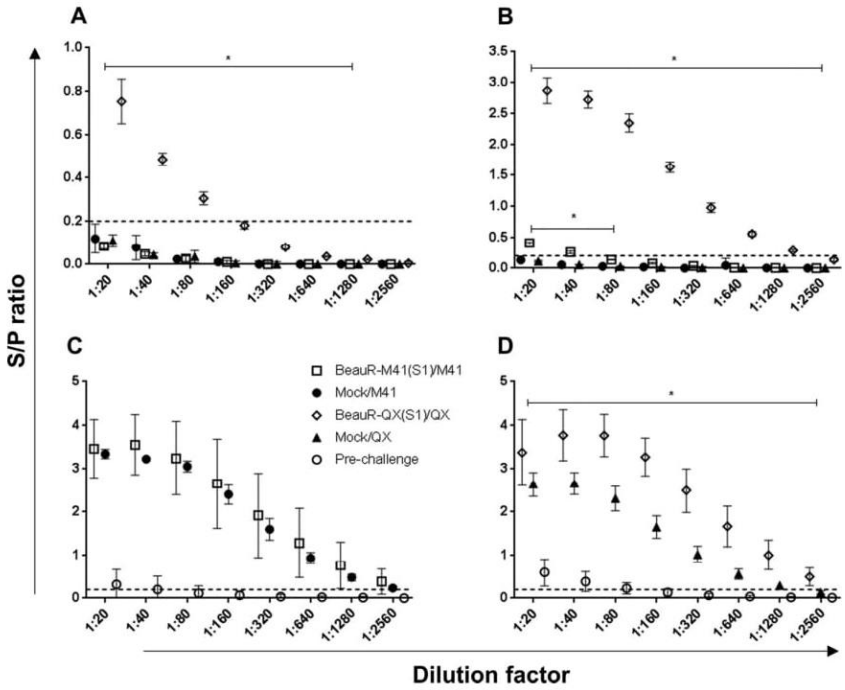

FIG 5 Measurement of serum anti-IBV titers of BeauR-M41(S1)- and BeauR-QX(S1)-vaccinated groups. Serum titers were assessed by commercial ELISA at 2 dpc (A) and 4 dpc (B) and in M41 groups at 14 dpc (C) and QX groups at 14 dpc (D). Prechallenge titers (i.e., 21 dpv) are included in panels C and D. The mean S/P ± the standard deviation from each group ($n = 5$ to 10) and includes four technical replicates/animal. Dashed line shows the cutoff for positive samples (S/P = 0.2). Solid bars denote a trend in statistical significance across dilutions in comparisons with the Mock/challenge-only group, e.g., BeauR-QX(S1)/QX compared to Mock/QX and BeauR-M41(S1)/M41 compared to Mock/M41. *, $P < 0.05$.

rIBVs (data not shown). Similar to trial 1, at 21 dpv the chickens were challenged with M41-CK. Clinical signs were observed until 7 dpc; BeauR-M41(S) was the only vaccinated group to show less prevalent clinical signs postchallenge compared to the M41-CK challenge control (Fig. 6A and B). There was little difference between the BeauR-M41(S1), BeauR-M41(S2), and M41-CK groups in terms of the presence and severity of clinical signs (Fig. 6A and B), but in the vaccinated groups clinical signs resolved more rapidly compared to the M41-CK controls. Ciliary activity was assessed at 4 dpc, and

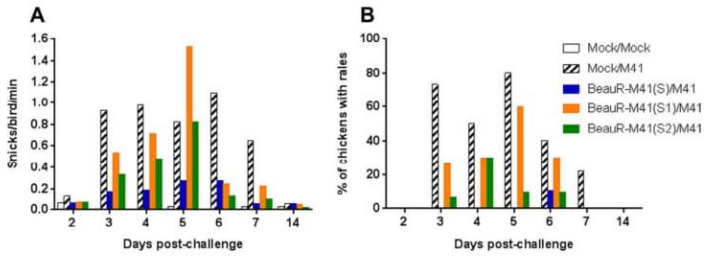

FIG 6 Assessment of clinical signs associated with BeauR-M41(S), BeauR-M41(S1), and BeauR-M41(S2) vaccination after challenge with M41-CK. The results for snicking (A) and rales (B) ($n = 10$ to 20 per group) are shown.

TABLE 2 Assessment of protection against ciliostasis associated with BeauR-M41(S), BeauR-M41(S1), and BeauR-M41(S2) vaccination following challenge with M41-CK

Vaccination/challenge	% ciliary activity (mean ± SD)[a]	No. of birds with 90% ciliary activity/total no. of birds examined[b]	% of group protected[c]
Mock/Mock	96 ± 5.2	5/5	NA
Mock/M41	0 ± 0	0/5	0
BeauR-M41(S)/M41	65 ± 36.2	3/5	60
BeauR-M41(S1)/M41	19 ± 33	1/5	20
BeauR-M41(S2)/M41	23 ± 43.4	1/5	20

[a]That is, the mean ciliary activity per group calculated from ciliostasis scores for 10 tracheal rings per individual bird using the following formula: [(total ciliostasis score of tracheal rings)/40] × 100.
[b]Ciliary activity assessed according to European Pharmacopeia standards (27), wherein bird is deemed protected against ciliostasis if no fewer than 9 of 10 tracheal rings per bird showed normal ciliary activity (>50% ciliary activity retained).
[c]The vaccine is considered to be efficacious at conferring protection against ciliostasis when 80% or more of the birds in a group were protected. NA, not applicable.

the level of protection afforded were assessed according to European Pharmacopeia standards (28). The BeauR-M41(S)-vaccinated group retained ~60% ciliary activity, showing an improved level of protection in comparison to groups vaccinated with BeauR-M41(S1) and BeauR-M41(S2), in which 20% protection in each group were evident (Table 2). Noteworthy, assessment on an individual bird level showed that three of five birds in the BeauR-M41(S) were classed as "protected against ciliostasis"; however, since the group average was 60%, this does not translate into protection on a group level (Table 2).

Viral RNA loads in the tracheas and CALTs isolated from challenged chickens were determined by qPCR to elucidate whether the S1 and S2 subunits played any further role in conferring protection. At 2 dpc only the CALT from BeauR-M41(S)- and BeauR-M41(S2)-vaccinated chickens showed any significant reduction ($P < 0.001$) in viral RNA load compared to the challenge control (Fig. 7A). However, at 4 dpc all groups had significantly lower viral RNA loads in the CALT (Fig. 7B) [$P < 0.001$, BeauR-M41(S); $P < 0.01$, BeauR-M41(S1) and BeauR-M41(S2)]. Viral RNA loads in the trachea were only significantly lower at 2 dpc in BeauR-M41(S)-vaccinated chickens [$P < 0.001$, BeauR-M41(S)] and significantly lower for all vaccinated groups at 4 dpc (Fig. 7C and D) [$P < 0.05$, BeauR-M41(S) and BeauR-M41(S2), $P < 0.01$, BeauR-M41(S1)]. Failure to locate the rIBVs in the head-associated lymphoid and respiratory tissues at 2 dpv in trial 1 led to the inclusion of the 1-dpv time point in trial 2. BeauR-M41(S), BeauR-M41(S1), and BeauR-M41(S2) were detected by RT-PCR in a number of the Harderian glands and tracheas isolated from chickens at 1 dpv; however, at 2 and 4 dpv the rIBVs were mainly detected in the nasal turbinates (Table 3), suggesting rapid clearance of rIBVs from the mucosal head tissues and sites of inoculation. Although the titers of infectious challenge virus recovered from tracheas at 4 dpc were not significantly reduced in BeauR-M41(S)-, BeauR-M41(S1)-, and BeauR-M41(S2)-vaccinated chickens compared to controls (because of the variation within each group), there was a general trend that vaccination resulted in a reduction in viral infectivity, with no detected infectious virus recovered in four of five birds in the S group, three of five birds in the S1 group, and one of five birds in the S2 group (Fig. 7E). Collectively, this shows that the chimeric rIBVs are able to induce a degree of local protection against the replication of IBV in the trachea.

To assess whether the rIBVs induced humoral antibody responses following vaccination with BeauR-M41(S), BeauR-M41(S1), and BeauR-M41(S2) viruses, IBV-specific serum titers were assessed at 2 and 4 dpc. At 2 dpc, there was clear evidence of a boost in antibody titers in the BeauR-M41(S)- and BeauR-M41(S2)-vaccinated groups (Fig. 8A), with significantly higher titers compared to Mock/M41 controls ($P < 0.001$). IBV induced antibody titers at 2 dpc in BeauR-M41(S)-vaccinated chickens were higher than those from BeauR-M41(S1)- and BeauR-M41(S2)-vaccinated chickens across the dilution series (Fig. 8A). At 4 dpc, serum antibody titers from all vaccinated groups were significantly

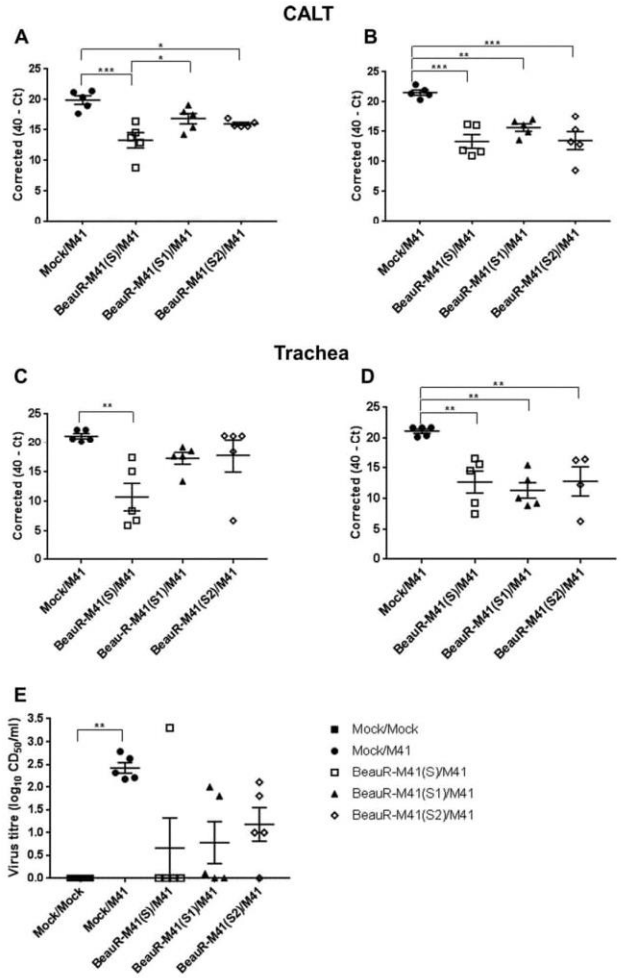

FIG 7 Viral load in the CALT and trachea in BeauR-M41(S)-, BeauR-M41(S1)-, and BeauR-M41(S2)-vaccinated chickens following challenge with M41-CK. (A to D) Relative viral RNA loads (expressed as corrected 40-C_T) at 2 dpc (A and C) and 4 dpc (B and D). (E) Infectious viral load titers in trachea (4 dpc). Data points are shown as individual animals, and lines represent means ± SEM. Statistically significant differences between groups are highlighted. *, $P < 0.05$; **, $P < 0.01$; ***, $P < 0.001$.

higher compared to the Mock/M41 titers (Fig. 8B), an observation suggestive of a primed antibody response in the vaccinated chickens. The serum antibody titers at 14 dpc indicated no significant differences between the vaccinated groups and the challenge-only controls (Fig. 8C), suggesting that a boosted response was lacking in response to challenge with wild-type virus.

The virus neutralization activity of the serum collected at 4 and 14 dpc were assessed, and at 4 dpc there was no neutralization of the virus detected (data not shown). At 14 dpc, only serum from BeauR-M41(S)- and BeauR-M41(S1)-vaccinated chickens had significantly higher neutralization activity of the virus compared to Mock/Mock controls ($P = 0.002$ and $P = 0.0066$, respectively; Fig. 9A). BeauR-M41(S) vaccination induced significantly higher virus neutralization titers compared to BeauR-

TABLE 3 Detection of IBV-derived RNA by RT-PCR in head-associated lymphoid tissues and tracheal samples following vaccination with BeauR-M41(S), BeauR-M41(S1), and BeauR-M41(S2)[a]

		No. of virus-positive tissues per group		
Vaccination	dpv	Harderian gland	Trachea	Nasal turbinates
Mock	1	0/5	0/5	NA
BeauR-M41(S)	1	3/5	0/5	NA
BeauR-M41(S1)	1	1/5	0/5	NA
BeauR-M41(S2)	1	1/5	2/5	NA
Mock	2	0/5	0/5	0/5
BeauR-M41(S)	2	1/5	0/5	3/5
BeauR-M41(S1)	2	0/5	0/5	3/5
BeauR-M41(S2)	2	0/5	0/5	2/5
Mock	4	0/5	0/5	0/5
BeauR-M41(S)	4	3/5	0/5	2/5
BeauR-M41(S1)	4	1/5	0/5	2/5
BeauR-M41(S2)	4	1/5	2/5	3/5

[a]The results are depicted as the number of positive samples/number of birds per group (total of five birds/group). All positive results were confirmed by sequencing of PCR products (data not shown). NA, not applicable.

M41(S2) vaccination ($P = 0.04$), whereas there was no significant difference in titers compared with serum from BeauR-M41(S1)-vaccinated chickens or the Mock/M41 challenge-only group (Fig. 9A). The levels of virus neutralization activity detected were moderately positively correlated to the anti-IBV serum titers ($r^2 = 0.5$, $P = 0.002$, Fig. 9B).

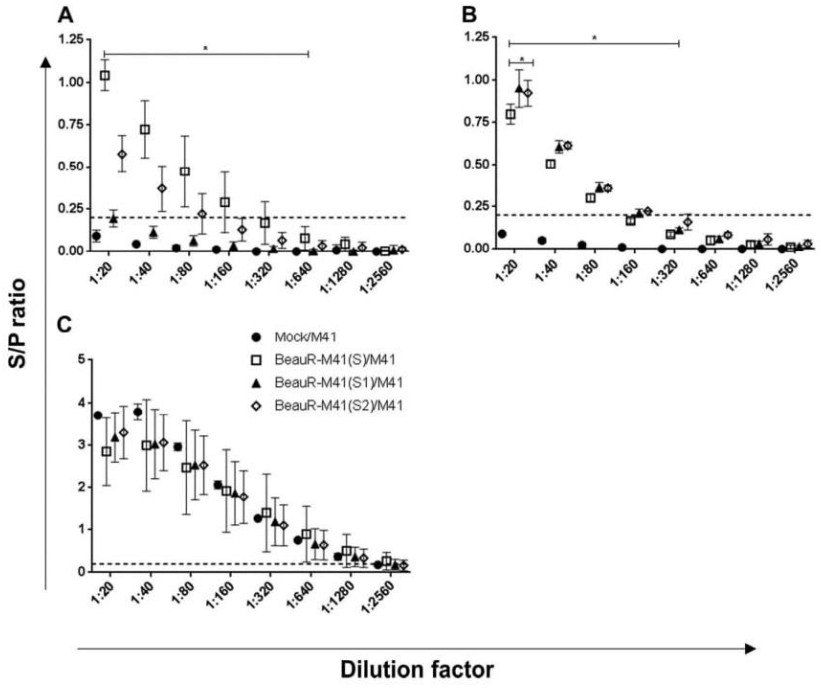

FIG 8 Measurement of serum anti-IBV titers of BeauR-M41(S)-, BeauR-M41(S1)-, and BeauR-M41(S2)-vaccinated groups. Serum titers were assessed by commercial ELISA at 2 dpc (A), 4 dpc (B), and 14 dpc (C). The mean S/P ratio ± SEM from each group ($n = 10$) includes four technical replicates/animal. Dashed line shows the cutoff for positive samples (S/P = 0.2). Solid bars denote a trend in statistical significance across dilutions in comparisons with the Mock/challenge-only group, e.g., BeauR-M41(S), BeauR-M41(S1), and BeauR-M41(S2) compared to Mock/M41. *, $P < 0.05$.

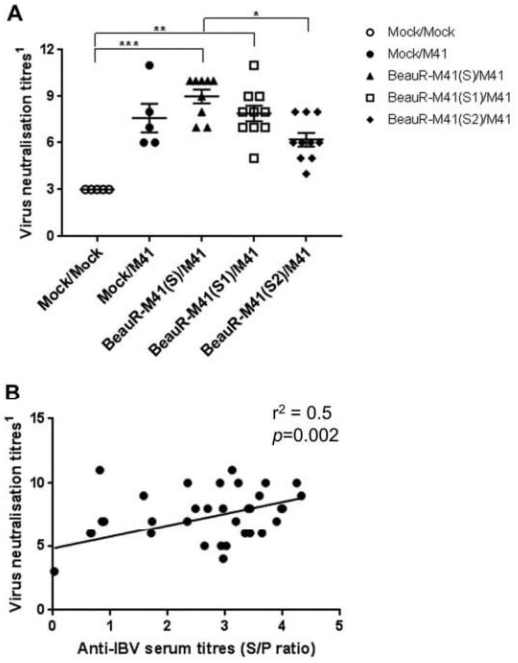

FIG 9 Measurement of virus neutralization antibody titers of BeauR-M41(S)-, BeauR-M41(S1)-, and BeauR-M41(S2)-vaccinated and Mock groups at 14 dpc. (A) Virus neutralization titers were determined by titration of serum in CK cells. Virus neutralization titers expressed as the $\log_2$ of the reciprocal of the highest serum dilution that showed complete inhibition of CPE ($n = 5$ or 10). Lines represent means ± SEM. Statistically significant differences between groups are highlighted. *, $P < 0.05$; **, $P < 0.01$; ***, $P < 0.001$. (B) Relationship between virus neutralization activity and anti-IBV serum titers at 14 dpc. Data points represent the S/P ratios from individual serum samples ($n = 39$) plotted against virus neutralization titers, compared by Spearman rank correlation analysis.

Characterisation of rIBVs *in vitro*. Following on from the observation of differences during the *in vivo* vaccination trials, to elucidate whether the inclusion of a chimeric S gene or a foreign S gene had an effect on viral replication, the replication kinetics of rIBV BeauR-M41(S), BeauR-M41(S1), and BeauR-M41(S2) viruses were investigated *in vitro*. At 12 h postinfection (hpi) all viruses had similar titers (Fig. 10A and B). This suggests that the inclusion of a foreign S gene or a chimeric S gene has not impeded replication *in vitro* in either chicken kidney cells (CKCs) derived from Valo chickens (Fig. 10A) or CKCs derived from Rhode Island Red (RIR) birds (Fig. 10B). Single-step growth curves performed in CKCs derived from RIR birds show that over the latent period (2 to 8 hpi), there were lower virus titers for BeauR-M41(S2) compared to the other viruses; however, when exponential growth was compared, there was no statistical difference between the viruses (Fig. 10C). The titers of BeauR-M41(S) and BeauR-M41(S1) were similar across all time points (Fig. 10C).

DISCUSSION

We have previously shown that rIBVs expressing the ectodomain of the Spike protein of a pathogenic strain in the context of an apathogenic strain BeauR could induce increased levels of protection against homologous and partially against heterologous challenge infection. Here, we extended this work and replaced only the S1 subunit of the ectodomain of BeauR with the S1 domain of M41 or QX, representing two strains that circulate in poultry flocks worldwide. These rIBVs have the advantage

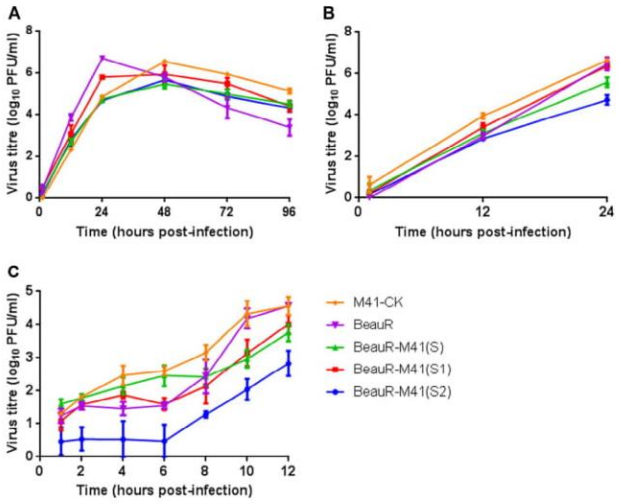

FIG 10 Comparison of the growth curves of BeauR-M41(S), BeauR-M41(S1), and BeauR-M41(S2). Multistep growth curves in CK cells derived from Valo chickens (A), 24-h growth curves (B), and single-step, 12-h growth curves (C) in CK cells derived from RIR chickens are depicted. Supernatant was harvested at various time points postinfection, and titers of progeny virus were determined by a plaque titration assay on CK cells. Data points represent the means of three independent experiments, and error bars represent the SEM.

of being able to replicate in Vero cells, potentially allowing large-scale vaccine production in cell culture rather than in embryonated eggs. In this first vaccination study, using a single dose of BeauR-M41(S1) or BeauR-QX(S1) in 1-week-old chicks, the birds were not protected against homologous challenge based on ciliary activity and clinical signs. Vaccination with BeauR-QX(S1) induced significantly higher serum titers postchallenge, and the clinical signs associated with challenge virus, although present, decreased rapidly compared to unvaccinated birds challenged with QX. Together, these data show that vaccination with chimeric rIBVs are able to induce a degree of virus-specific immunity with partial local protection in the mucosal head tissues and the primary site of replication, the trachea.

To address the questions of whether a full homologous S is required for optimal folding, virus replication, and protection using an apathogenic recombinant virus, a second vaccination experiment was performed. One-week-old birds were immunized once with BeauR-M41(S), BeauR-M41(S1), or BeauR-M41(S2). Replacement of the apathogenic BeauR-S1 or S2 subunits with a S1 or S2 from a pathogenic strain, allowed BeauR to remain apathogenic, suggesting that the S1 or S2 alone do not play a role in the pathogenicity of IBV. This further expands our previous work showing that spike switching of BeauR-S with M41-S had no effect on pathogenicity (23). Here, vaccination of chickens with a rIBV based on a BeauR backbone expressing a full S gene from the donor serotype enhanced the level of protection afforded against tracheal ciliostasis, with three of five birds classed as fully protected. However, when classified under European Pharmacopeia standards for assessment of IBV vaccines (28), at which 80% protection (at a group level) against ciliostasis is required, the BeauR-M41(S)-vaccinated group was only able to confer partial protection (~60%) and therefore is still not satisfactory for the criteria used for the assessment of IBV vaccines for industrial application. Consistent with previously published work, we show that collectively as a group the chickens vaccinated via ocular-nasal routes with BeauR-M41(S) had ~60% ciliary activity remaining, a reduction in clinical signs, and viral load postchallenge (26). The protection seen at the trachea may potentially be improved with assessment of

ciliostasis at a later time point, as Armesto et al. (23) reported that vaccination with BeauR-4/91(S) gave ~60% ciliary activity at 4 dpc, which then improved to 90 to 100% at 6 dpc. In trial 1 the viral RNA load in the trachea and CALT from the S1-vaccinated groups was reduced at 2 dpc, whereas in trial 2 all vaccinated groups had a clear significant reduction in viral RNA loads at 2 and 4 dpc in the trachea and CALT. The qPCR used here is designed to detect the 5′ untranslated region (5′ UTR) of the genome (29), and it therefore may be detecting incomplete virions or challenge virus captured in the lumen of the trachea. To further support the viral RNA load data, infectious viral load recovered from the trachea in both trials 1 and 2 were lower in rIBV-vaccinated chickens, indicating a degree of local protection at the site of infection, which was not robust enough to completely protect against viral replication *in vivo* and the loss of ciliary activity.

The major surface glycoprotein of coronaviruses, spike, is a type 1 glycoprotein and has two structurally distinct conformations: prefusion and postfusion (30–32). In the coronavirus replication cycle, the spike mediates the critical steps of receptor binding and membrane fusion. Upon binding of the S1 receptor binding domain to the host cell, an irreversible conformational switch to the postfusion state allows the S2 subunit to fuse viral and cellular membranes, facilitating entry of the viral genome and therefore downstream viral replication (32–34). Recently, the crystal structure of the prefusion spike from mouse hepatitis virus and human coronavirus (HKU1) were resolved, highlighting the critical role that the interaction between the trimers of S1 and S2 plays in stabilization of the prefusion conformation of spike (31, 32). Here, expression of a chimeric spike in a recombinant IBV backbone with the lack of a homologous S2 possibly resulted in conformational changes either within the S1 subunit or complete S protein, potentially affecting receptor binding and entry, but may have also altered immunogenic epitopes. The S2 subunits of BeauR shares 87 and 97% amino acid sequence similarities with QX and M41-CK, respectively, showing that there are only a few different amino acid residues between them. The interactions between S1 and S2 subunits are critical for the maintenance of conformation, recognition, and efficient fusion of the spike to host cells; it has been consistently shown that even a single amino acid change within the S2 subunit of coronavirus spikes may influence the secondary structure of the overall spike or the S1 subunit (35, 36).

The development of a cryo-electron microscopic structure of IBV M41 spike, highlighting the evolutionary difference between the prefusion spike structures of IBV compared to betacoronaviruses and alphacoronaviruses, nonetheless indicates a high degree of structurally similarity to porcine deltacoronavirus (37, 38). This structural model of prefusion IBV spike will significantly aid in addressing the challenges over whether (i) expression of a chimeric spike in a rIBV backbone causes conformational changes either within the S1 subunit or complete S or (ii) it is vital that homologous "matched" S1 and S2 and their interactions are required to maintain the correct prefusion conformation of spike, as suggested in other coronaviruses.

The Beaudette strain, used here in the reverse genetics system, has an extended *in vitro* tropism, ability to grow in cell cultures and an apathogenic nature, making it an excellent resource for the investigation of heterologous genes and growth characteristics of rIBV. During embryo passages, however, the Beaudette strain may have acquired mutations which are likely to contribute to its lack of pathogenicity and restrict its *in vivo* tropism and replication. Replacement of the BeauR S1 or S2 with corresponding subunits from a pathogenic strain did not indicate a significant impairment of *in vitro* growth of the viruses in comparison to the BeauR virus, showing no indication that BeauR-M41(S1) and BeauR-M41(S2) were unable to enter the cells, fuse with cell membranes, or fail to replicate *in vitro*. Nevertheless, the lack of full protection afforded by BeauR rIBVs against wild-type challenge and the limited *in vivo* replication strongly suggest that attenuations have occurred in genes playing an essential role in replication and that these are negatively impacting its suitability as a vaccine vector. Development of an alternative, less-attenuated backbone for the expression of heter-

ologous genes in rIBVs may promote the development of these live attenuated vaccines for the control of IBV.

Expression of the IBV S1 subunit alone has been shown to induce virus-neutralizing antibodies, albeit often requiring repeated vaccination (8, 10). Here, immunization of chickens with rIBVs based on the Beaudette backbone expressing either M41 S or chimeric S1/S2 induced virus-neutralizing antibodies; however, the Mock/M41 serum also had a degree of neutralizing activity. BeauR-M41(S) vaccinated chickens had significantly higher virus neutralizing titers than the BeauR-M41(S2) group, but there was no statistical difference with the BeauR-M41(S1) group, showing that neutralizing antibodies are induced following a single vaccination with rIBV expressing M41(S1).

Live attenuated vaccines against IBV need to induce a good level of mucosal immunity, with local tracheal and cell-mediated immunity also playing an important role in prevention of IBV infection (39–41). As discussed earlier, the BeauR backbone is impeded by poor *in vivo* replication, and the lack of protection shown against ciliostasis indicates that there is a poor level of local immunity induced in the trachea by vaccination with BeauR rIBVs. Cytotoxic responses can also play a key role in the early control of IBV, as indicated by previous studies showing NK cell activation (42), IBV-specific cytotoxic T-cell-lymphocyte (CTL) activity of splenocytes isolated from IBV-infected chickens (41), and higher CTL proportions in respiratory tissues following IBV infection (43). Cellular infiltrates in head-associated lymphoid tissues, as well as a reduction in viral load in the trachea and CALT, also imply that the rIBVs infected the chickens and suggests a possible role for the cell-mediated response. However, that we were unable to consistently detect the recombinant S1 viruses at 2 dpv raises possibilities that the viruses were either rapidly cleared from the tissues, replicate poorly at these sites of inoculation, or have limited replication in a few cells which are below detectable limits of the assays. In the BeauR-M41(S)-vaccinated group, more than 50% of the chickens were positive for vaccine virus, as assessed by RT-PCR, in the Harderian gland and nasal turbinates at 1 and 2 dpv, respectively. The primary site of IBV infection is thought to be the ciliated epithelium lining the trachea; however, following ocular-nasal vaccination, the virus has been detected in the nasal turbinates (44) and Harderian gland (45).

One possible explanation for the poor protection of ciliary activity afforded by the recombinant S1 viruses could be that we only administered a single vaccine dose to the SPF chicks. Previous studies using baculovirus expressed IBV recombinant proteins or IBV purified proteins have required multiple injections to achieve a degree of protection in SPF chickens (10, 17). There is also evidence of an impaired humoral response in young chicks with regard to IBV vaccination; vaccination of 1- and 7-day-old chicks showed a delay in both systemic and local IgA and IgG levels compared to vaccination of older chicks (14, 21, or 28 days old) (46). Here, in an attempt to improve the protection against respiratory signs and ciliostasis with the recombinant S1 viruses, a prime-boost approach may aid in overcoming these potential issues.

In summary, we have previously generated recombinant IBV based on a BeauR backbone expressing a heterologous S1 from M41 or QX, and in the present study we have shown that a single vaccination in young chicks with these rIBVs, although not adequate to completely prevent ciliostasis and clinical signs, can induce a degree of virus-specific protective immunity. This was characterized by a reduction in the viral load recovered from the trachea and CALT, cellular infiltrations at head mucosal and inoculation sites, higher serum antibody titers in vaccinated groups, and the induction of virus-neutralizing activity. Vaccination with BeauR-M41(S), despite expressing the homologous full S to attempt to overcome any issues with heterologous S1 and S2 subunits and suboptimal folding, only induce a partially protection against the loss of ciliary activity. Since the *in vitro* growth characteristics show that inclusion of a foreign S gene or a chimeric S gene in the rIBVs does not impede replication *in vitro*, perhaps the attenuated Beaudette backbone has hindered the *in vivo* replication of these rIBVs;

thus, to improve protection, multiple vaccinations, or an alternative backbone may be required.

MATERIALS AND METHODS

Ethics statement. All animal experimental protocols were carried out in strict accordance with the UK Home Office guidelines and under license granted for experiments involving regulated procedures on animals protected under the UK Animals (Scientific Procedures) Act 1986. The experiments were performed in The Pirbright Institute (TPI) Home Office licensed (X24684464) experimental animal house facilities and were approved by TPI's animal welfare and ethical review committee under the terms of reference HO-ERP-01-1. Trial 1 used SPF RIR chickens obtained from TPI Poultry Production Unit in Compton. Trial 2 used the same chicken breed but obtained from The National Avian Research Facility in Edinburgh.

Cells and viruses. Tracheal organ cultures (TOCs) were prepared from 19-day-old SPF RIR chicken embryos (47–49). Primary chicken kidney (CK) cells were prepared by The Central Services Unit, TPI, from kidneys extracted from either 2- to 3-week-old SPF RIR chickens or 2-week-old SPF derived Valo chickens (49). The pathogenic M41 strain (50) used in this study had previously been adapted in CK cells to produce M41-CK (accession number X04722) (26). The pathogenic strain, QX (QX L1148 strain, accession number KY933090) (51), was donated by Richard Jones, University of Liverpool. The rIBVs BeauR-M41(S), BeauR-M41(S1), BeauR-M41(S2), and BeauR-QX(S1) used here are described in a schematic illustration (Fig. 1) and constructed using the backbone of Beau-R, which is the molecular clone of Beau-CK (accession number AJ311317) (21, 25). All isolates of IBV and rIBV were propagated in 10-day-old RIR SPF embryonated eggs. Allantoic fluid was clarified by low-speed centrifugation at 24 to 48 hpi. Titrations to determine virus infectivity were either performed in TOCs as described previously (26) or in CK cells (49); titers are expressed as 50% (median) ciliostatic doses (CD_{50})/ml or PFU/ml, respectively.

Analysis of growth kinetics in CK cells. Confluent CK cells seeded in either 6-well or 12-well plates were inoculated with 10^4 PFU rIBV or IBV for multistep growth curves or 10^5 PFU rIBV or IBV for single-step growth curves in 0.5 ml of serum-free *N*,*N*-bis(2-hydroxyethyl)-2aminoethanesulphonic acid (BES) medium and incubated for 1 h at 37°C at 5% CO_2. Cells were washed with phosphate-buffered saline (PBS) to remove residual virus, and 2 ml of serum-free BES medium was added per well. Extracellular virus was harvested at defined intervals and assayed by titration in CK cells.

Experimental design of *in vivo* vaccination/challenge trials. SPF RIR chickens were housed in positive-pressure, HEPA-filtered isolation rooms in which each group was housed in a separate room. In two separate experiments, birds were randomly divided into 5 groups of 30 birds for trial 1 and 5 groups of 40 birds for trial 2. Eight-day-old chicks were inoculated (classified as primary inoculation) with 10^5 PFU of BeauR-M41(S1) or BeauR-QX(S1) (trial 1) or 10^4 PFU BeauR-M41(S), BeauR-M41(S1), or BeauR-M41(S2) (trial 2) in a total of 0.1 ml of PBS via conjunctival (eye drop) and intranasal routes. A challenge dose, equal to the primary inoculation, 10^5 PFU (trial 1) and 10^4 PFU (trial 2) of the corresponding wild-type viruses were administered in the same manner 21 days after the primary inoculation to the appropriate groups. Of note, the IBV QX strain used here could not be propagated in CK cells, so a CD_{50} dose of $10^{2.73}$ was used. Mock-infected controls were inoculated via the same route with 0.1 ml of PBS, and mock/challenge control groups were inoculated with 0.1 ml PBS and challenged with the same dose of wild-type virus. Birds were euthanized by cervical dislocation at specific times postinfection, and a panel of tissues was sampled to allow for downstream analysis. Blood samples were collected and processed for the collection of serum. The clinical signs used to determine pathogenicity were snicking, rales, and ciliary activity of the trachea (a bird was considered protected if 50% or more ciliary activity was retained in 9 of 10 tracheal rings; this must be in 80% of the group) (28, 52).

Isolation of tissues: virus isolation and ciliostasis assay. Tissues collected were divided into two parts; one part was stabilized in RNAlater (Ambion) for RNA extraction and the other in 20% sucrose–PBS (0.22-μm-pore size filtered) at 4°C overnight before snap freezing in OCT (Thermo Scientific) for histology. Tissues collected included: Harderian gland, CALT, NALT, and trachea. Tissues were removed at 2 and 4 days postvaccination (dpv) and at 2, 4, and 14 days postchallenge (dpc). Tracheas were removed from five randomly selected chickens from each group at 4 dpv and 4 dpc for assessment of ciliary activity as described previously (26). Part of the trachea and CALT tissues were stored in PBS for virus isolation.

Detection of viral RNA. For virus isolation and RNA extraction, tissues stored in PBS and RNAlater, respectively, were freeze-thawed and homogenized using a TissueLyser II (Qiagen), as described previously (23). Total RNA was isolated using an RNeasy Mini-Kit and DNase treated according to the manufacturer's instructions (Qiagen). cDNA was synthesized from 1 μg of tRNA using Superscript IV reverse transcriptase (Life Technologies) with a random oligonucleotide primer according to the manufacturer's instructions. To quantify infectious viral load in trachea, tissue-derived supernatant was titrated in TOCs. To determine whether infectious virus was present, 10-day-old SPF embryonated eggs were inoculated with 100 μl of allantoic fluid; then, at 24 to 48 hpi they were assessed for viral presence by RT-PCR using primers specific for the 3′ UTR, as described previously (53). For quantification of viral load, qPCR was performed using TaqMan Universal PCR Master Mix (Applied Biosystems) with primers and probes specific to the 5′-UTR region, as described previously (29). Serial dilutions of M41 cDNA (generated from 1 μg of tRNA) were included to generate a standard curve, and the data, expressed in terms of the cycle threshold (C_T) value, were normalized using the C_T value of the 28S cDNA product for the same sample (54).

Infectious bronchitis virus ELISA. Serum samples collected at 21 dpv (prechallenge) and at 2, 4, and 14 dpc were assayed with a commercial IDEXX IBV antibody test kit (IDEXX Laboratories). To determine the endpoint titer, the serum samples were twofold serially diluted in the range 1:20 to 1:2,560 prior to

incubation. After sample incubation, the remaining steps were followed directly according to the manufacturer's instructions. The sample/positive (S/P) ratio was calculated using by the following equation: [(mean sample – mean kit negative)/(mean kit positive – mean kit negative)]. S/P ratios greater than 0.2 were considered positive for IBV antibodies. Polyclonal chicken serum raised against M41 and QX serum were included on each independent test plate (GD Animal Health).

Immunocytochemistry. For fluorescent microscopy, cryostat sections (5 μm) were fixed in acetone, washed in PBS, and blocked for 1 h at room temperature with 10% normal goat serum and 0.5% bovine serum albumin in PBS (blocking buffer). Slides were washed and incubated for 1 h with optimally diluted primary antibodies (anti-Bu-1 [clone AV-20; AbD Serotec], anti-CD8α [clone 3-298, AbD Serotec], and anti-CD8β [clone EP42, AbD Serotec]) and anti-CSF1R (55) or isotype controls, all diluted in blocking buffer. Sections were washed, incubated with an Alexa Fluor 488-labeled goat anti-mouse IgG1/IgG2a or Alexa Fluor 568-labeled goat anti-mouse IgG1/IgG2b according to the appropriate isotype, and diluted in blocking buffer for 1 h. Nuclei were visualized using DAPI (4′,6′-diamidino-2-phenylindole (Invitrogen). Images were captured with a Leica DMLB fluorescence microscope with a coupled device digital camera and analyzed using ImageJ analysis software. For light microscopy, cryostat sections (5 μm) were fixed in acetone and stained with Harris' hematoxylin (Sigma-Aldrich) and 1% eosin (Sigma-Aldrich). Sections were dehydrated through graded ethanols and xylene and mounted in a xylene-based medium (DePex; Gurr-BDH Chemicals). Images were captured with a Hamamatsu Nano-zoomer-XR digital slide scanner.

Analysis of neutralizing antibody. Virus neutralization tests were performed by GD Animal Health (56). Briefly, twofold serial dilutions of serum were made in a 1:1 mixture of Medium-199 and Ham F10 in 96-well plates. To each well, an equal volume of CEK cells (in medium supplemented with 10% fetal calf serum) was added. After culture with M41 for 3 to 4 days at 37°C with 5% CO_2, cell monolayers were examined for cytopathic effect (CPE). All individual titers were expressed as the $\log_2$ value of the reciprocal of the highest serum dilution that showed complete inhibition of CPE.

Statistical analyses. Viral load qPCR data were tested for normality through residual plots, and the differences between the mean corrected 40-C_T values were statistically evaluated by a parametric one-way analysis of variance test adjusted for *post hoc* analysis using Tukey's pairwise comparison. Serum antibody levels, viral isolation titers, ciliary activity, and virus neutralization titers were tested for normality, and nonparametric analyses were performed. Differences between the groups were statistically evaluated by the nonparametric Kruskal-Wallis test adjusted for *post hoc* analysis and Mann-Whitney U pairwise comparison. The relationship between anti-IBV serum and virus neutralization titers were compared by Spearman rank correlation analysis. Analysis of the viral growth curves was conducted by fitting a polynomial curve to the exponential phase of viral growth (57); growth rates were then compared between groups by using the nonparametric Kruskal-Wallis test adjusted for *post hoc* analysis. For all statistical analyses, P values of <0.05 were considered significant. All statistical analyses were conducted using MiniTab v17 or GraphPad Prism 7.

ACKNOWLEDGMENTS

This project was funded by the BBSRC Animal Research Club with grants BB/M012794/1 and BB/M012069/1. This study was additionally supported by Institute Strategic Programme Grant funding from the BBSRC to The Roslin Institute under grant BB/J004324/1.

We thank all animal services staff at The Pirbright Institute (TPI) for their excellent assistance in running the animal experiments, and we thank all members of the coronavirus group at TPI and Dominika Borowska for their help with collecting and processing samples during the animal experiments.

REFERENCES

1. Carstens EB. 2010. Ratification vote on taxonomic proposals to the International Committee on Taxonomy of Viruses (2009). Arch Virol 155:133–146. https://doi.org/10.1007/s00705-009-0547-x.
2. Cavanagh D, Gleb J, Jr. 2008. Infectious bronchitis, p 117–135. *In* Saif YM, Barnes HJ, Glisson JR, Fadly AM, McDougald LR, Nolan LK, Swayne DE (ed), Diseases of poultry, 12th ed. Iowa State University Press, Ames, Iowa.
3. Matthijs MG, Ariaans MP, Dwars RM, van Eck JH, Bouma A, Stegeman A, Vervelde L. 2009. Course of infection and immune responses in the respiratory tract of IBV infected broilers after superinfection with *Escherichia coli*. Vet Immunol Immunopathol 127:77–84. https://doi.org/10.1016/j.vetimm.2008.09.016.
4. Vandekerchove D, De Herdt P, Laevens H, Pasmans F. 2004. Colibacillosis in caged layer hens: characteristics of the disease and the aetiological agent. Avian Pathol 33:117–125. https://doi.org/10.1080/03079450310001642149.
5. De Vries AAF, Horzinek MC, Rottier PJM, de Groot RJ. 1997. The genome organisation of the *Nidovirales*: similarities and differences between arteri-, toro- and coronaviruses. Semin Virol 8:33–47. https://doi.org/10.1006/smvy.1997.0104.
6. Perlman S, Netland J. 2009. Coronaviruses post-SARS: update on replication and pathogenesis. Nat Rev Microbiol 7:439–450. https://doi.org/10.1038/nrmicro2147.
7. Delmas B, Laude H. 1990. Assembly of coronavirus spike protein into trimers and its role in epitope expression. J Virol 64:5367–5375.
8. Cavanagh D, Davis PJ, Darbyshire JH, Peters RW. 1986. Coronavirus IBV: Virus retaining spike glycopolypeptide S2 but not S1 is unable to induce virus-neutralizing or haemagglutination-inhibiting antibody, or induce chicken tracheal protection. J Gen Virol 67:1435–1442. https://doi.org/10.1099/0022-1317-67-7-1435.
9. Cavanagh D, Davis DJ, Cook JK, Li D, Kant A, Koch G. 1992. Location of the amino acid differences in the S1 spike glycoprotein subunit of closely related serotypes of infectious bronchitis virus. Avian Pathol 21:33–43. https://doi.org/10.1080/03079459208418816.
10. Ignjatovic J, Galli L. 1994. The S1 glycoprotein but not the N or M proteins of avian infectious bronchitis virus induces protection in

vaccinated chickens. Arch Virol 138:117–134. https://doi.org/10.1007/BF01310043.
11. Johnson MA, Pooley C, Ignjatovic J, Tyack SG. 2003. A recombinant fowl adenovirus expressing the S1 gene of infectious bronchitis virus protects against challenged with infectious bronchitis virus. Vaccine 21:2730–2736. https://doi.org/10.1016/S0264-410X(03)00227-5.
12. Song CS, Lee YJ, Lee CW, Sung HW, Kim JH, Mo IP, Izumiya Y, Jang HK, Mikami T. 1998. Induction of protective immunity in chickens vaccinated with infectious bronchitis virus S1 glycoprotein expressed by a recombinant baculovirus. J Gen Virol 79:719–723. https://doi.org/10.1099/0022-1317-79-4-719.
13. Promkuntod N, van Eijndhoven REW, de Vrieze G, Gröne A, Verheije MH. 2014. Mapping of the receptor-binding domain and amino acids critical for attachment in the spike protein of avian coronavirus infectious bronchitis virus. Virology 448:26–32. https://doi.org/10.1016/j.virol.2013.09.018.
14. Koch G, Hartog L, Kant A, van Roozelaar DJ. 1990. Antigenic domains of the peplomer protein of avian infectious bronchitis virus: correlation with biological function. J Gen Virol 71:1929–1935. https://doi.org/10.1099/0022-1317-71-9-1929.
15. Cavanagh D, Davis PJ, Mockett APA. 1988. Amino acids within hypervariable region 1 of avian coronavirus IBV (Massachusetts serotype) spike glycoprotein are associated with neutralisation epitopes. Virus Res 11:141–150. https://doi.org/10.1016/0168-1702(88)90039-1.
16. Kant A, Koch G, van Roozelaar DJ, Kusters JG, Poelqijk FA, van der Zeijst BA. 1992. Location of antigenic sites defined by neutralising monoclonal antibodies on the S1 avian infectious bronchitis virus glycopolypeptide. J Gen Virol 73:591–596. https://doi.org/10.1099/0022-1317-73-3-591.
17. Toro H, Zhang JF, Gallardo RA, van Santen VL, van Ginkel FW, Joiner KS, Breedlove C. 2014. S1 of distinct IBV population expressed from recombinant adenovirus confers protection against challenge. Avian Dis 58:211–215. https://doi.org/10.1637/10670-091913.
18. Zhao R, Sun J, Qi T, Zhao W, Han Z, Yang X, Liu S. 2017. Recombinant Newcastle disease virus expressing the infectious bronchitis virus S1 gene protects chickens against Newcastle disease virus and infectious bronchitis virus challenge. Vaccine 35:2435–2442. https://doi.org/10.1016/j.vaccine.2017.03.045.
19. De Wit JJ, Cook JKA. 2014. Factors influencing the outcome of infectious bronchitis vaccination and challenge experiments. Avian Pathol 43:485–497. https://doi.org/10.1080/03079457.2014.974504.
20. Britton P, Evans S, Dove B, Davies M, Casais R, Cavanagh D. 2005. Generation of a recombinant avian coronavirus infectious bronchitis virus using transient dominant selection. J Virol Methods 123:203–211. https://doi.org/10.1016/j.jviromet.2004.09.017.
21. Casais R, Thiel V, Siddell SG, Cavanagh D, Britton P. 2001. Reverse genetics system for the avian coronavirus infectious bronchitis virus. J Virol 75:12359–12369. https://doi.org/10.1128/JVI.75.24.12359-12369.2001.
22. Casais R, Dove B, Cavanagh D, Britton P. 2003. Recombinant avian infectious bronchitis virus expressing a heterologous spike gene demonstrates that the spike protein is a determinant of cell tropism. J Virol 77:9084–9089. https://doi.org/10.1128/JVI.77.16.9084-9089.2003.
23. Armesto M, Evans S, Cavanagh D, Abu-Median A, Keep S, Britton P. 2011. A recombinant avian infectious bronchitis virus expressing a heterologous spike gene belonging to the 4/91 serotype. PLoS One 6:e24352. https://doi.org/10.1371/journal.pone.0024352.
24. Vidor E, Meschievitz C, Plotkin S. 1997. Fifteen years of experience with Vero-produced enhanced potency inactivated poliovirus vaccine. Pediatr Infect Dis J 16:312–322. https://doi.org/10.1097/00006454-199703000-00011.
25. Bickerton E, Maier HJ, Stevenson-Leggett P, Armesto M, Britton P. 2018. The S2 subunit of infectious bronchitis virus Beaudette is a determinant of cellular tropism. J Virol. https://doi.org/10.1128/JVI.01044-18.
26. Hodgson T, Casais R, Dove B, Britton P, Cavanagh D. 2004. Recombinant infectious bronchitis coronavirus Beaudette with the spike protein gene of the pathogenic M41 strain remains attenuated but induces protective immunity. J Virol 78:13804–13811. https://doi.org/10.1128/JVI.78.24.13804-13811.2004.
27. Kuster JG, Jager EJ, Lenstra JA, Koch G, Posthumus WP, Meloen RH, van der Zeijst BA. 1989. Analysis of an immunodominant region of infectious bronchitis virus. J Immunol 143:2692–2698.
28. European Pharmacoepia 6.1. 2010. Avian infectious bronchitis vaccine (live), p 3371–3373. European Directorate for the Quality of Medicines and HealthCare (EDQM), Council of Europe, Strasbourg, France.
29. Callison SA, Hilt DA, Boynton TO, Sample BF, Robison R, Swayne DE, Jackwood MW. 2006. Development and evaluation of a real-time Taq-Man RT-PCR assay for the detection of infectious bronchitis virus from infected chickens. J Virol Methods 138:60–65. https://doi.org/10.1016/j.jviromet.2006.07.018.
30. Kirchdoerfer RN, Cottrell CA, Wang N, Pallesen J, Yassine HM, Turner HL, Corbett KS, Graham BS, McLellan JS, Ward AB. 2016. Prefusion structure of a human coronavirus spike protein. Nature 531:118–121. https://doi.org/10.1038/nature17200.
31. Walls AC, Tortorici MA, Bosch BJ, Frenz B, Rottier PJM, DiMaio F, Rey FA, Veesler D. 2016. Cryo-electron microscopy structure of a coronavirus spike glycoprotein trimer. Nature 531:114–177. https://doi.org/10.1038/nature16988.
32. Walls AC, Tortorici MA, Snijder J, Xiong X, Bosch BJ, Rey FA, Veesler D. 2017. Tectonic conformational changes of a coronavirus spike glycoprotein promote membrane fusion. Proc Natl Acad Sci USA 114:11157–11162. https://doi.org/10.1073/pnas.1708727114.
33. Chu VC, McElroy LJ, Chu V, Bauman BE, Whittaker G. 2006. The avian coronavirus infectious bronchitis virus undergoes direct low-pH-dependent fusion activation during entry into host cells. J Virol 80:3180–3188. https://doi.org/10.1128/JVI.80.7.3180-3188.2006.
34. Li F, Berardi M, Li W, Farzan M, Dormitzer PR, Harrison SC. 2006. Conformational states of the severe acute respiratory syndrome coronavirus spike protein ectodomain. J Virol 80:6794–6800. https://doi.org/10.1128/JVI.02744-05.
35. Callison SA, Jackwood MW, Hilt DA. 1999. Infectious bronchitis virus S2 gene sequence variability may affect S1 subunit specific antibody binding. Virus Genes 19:143–151. https://doi.org/10.1023/A:1008179208217.
36. Grosse B, Siddell SG. 1994. Single amino acid changes in the S2 subunit of the MHV surface glycoprotein confer resistance to neutralization by S1 subunit-specific monoclonal antibody. Virol 202:814–824. https://doi.org/10.1006/viro.1994.1403.
37. Shang J, Zheng Y, Yang Y, Liu C, Geng Q, Luo C, Zhang W, Li F. 2018. Cryo-EM structure of infectious bronchitis coronavirus spike protein reveals structural and functional evolution of coronavirus spike proteins. PLOS Pathog 14:e1007009. https://doi.org/10.1371/journal.ppat.1007009.
38. Shang J, Zheng Y, Yang Y, Liu C, Geng Q, Tai W, Du L, Zhou Y, Zhang W, Li F. 2018. Cryo-EM structure of porcine delta coronavirus spike protein in the pre-fusion state. J Virol 92:4–14.
39. Dhinakar RG, Jones RC. 1996. Protectotypic differentiation of avian infectious bronchitis viruses using an in vitro challenge model. Vet Microbiol 53:239–252. https://doi.org/10.1016/S0378-1135(96)01258-8.
40. Kotani T, Wada S, Tsukamoto Y, Kuwamura M, Yamate J, Sakuma S. 2000. Kinetics of lymphocytic subsets in chicken tracheal lesions infected with infectious bronchitis virus. J Vet Med Sci 62:397–401. https://doi.org/10.1292/jvms.62.397.
41. Collisson EW, Pei J, Dzielawa J, Seo SH. 2000. Cytotoxic T lymphocytes are critical in the control of infectious bronchitis virus in poultry. Dev Comp Immunol 24:187–200. https://doi.org/10.1016/S0145-305X(99)00072-5.
42. Vervelde L, Matthijs MG, van Haarlem DA, de Wit JJ, Jansen CA. 2013. Rapid NK-cell activation in chickens after infection with infectious bronchitis virus M41. Vet Immunol Immunopathol 151:337–341. https://doi.org/10.1016/j.vetimm.2012.11.012.
43. Wattrang E, Dalgaard TS, Norup LR, Kjærup RB, Lundén A, Juul-Madsen HR. 2015. CD107a as a marker of activation in chicken cytotoxic T cells. J Immunol Methods 419:35–47. https://doi.org/10.1016/j.jim.2015.02.011.
44. Dolz R, Vergara-Alert J, Pérez M, Pujols J, Majó N. 2012. New insights on infectious bronchitis virus pathogenesis: characterization of Italy 02 serotype in chicks and adult hens. Vet Microbiol 156:256–264. https://doi.org/10.1016/j.vetmic.2011.11.001.
45. Toro H, Godoy V, Larenas J, Reyes E, Kaleta EF. 1996. Avian infectious bronchitis: viral persistence in the Harderian gland and histological changes after eyedrop vaccination. Avian Dis 40:114–120. https://doi.org/10.2307/1592380.
46. Van Ginkel FW, Padgett J, Martinez-Romero G, Miller MS, Joiner KS, Gulley SL. 2015. Age-dependent immune responses and immune protection after avian coronavirus vaccination. Vaccine 33:2655–2661. https://doi.org/10.1016/j.vaccine.2015.04.026.
47. Cook JKA, Darbyshire JH, Peters RW. 1976. The use of chicken tracheal organ cultures for the isolation and assay of avian infectious bronchitis virus. Arch Virol 50:109–118. https://doi.org/10.1007/BF01318005.
48. Jones BV, Hennion RM. 2008. The preparation of chicken tracheal organ

cultures for virus isolation, propagation and titration. Methods Mol Biol 454:103–107. https://doi.org/10.1007/978-1-59745-181-9_9.
49. Hennion RM, Hill G. 2015. The preparation of chicken kidney cell cultures for virus propagation. *In* Maier HJ, Bickerton E, Britton P (ed), Coronaviruses: methods and protocols, 1st ed. Humana Press, New York, NY.
50. Darbyshire JH, Rowell JG, Cook JKA, Peters RW. 1979. Taxonomic studies on strains of avian infectious bronchitis virus using neutralisation testes in tracheal organ cultures. Arch Virol 61:227–238. https://doi.org/10.1007/BF01318057.
51. Worthington KJ, Currie RJ, Jones RC. 2008. A reverse-transcriptase-polymerase chain reaction survey of infectious bronchitis virus genotypes in Western Europe from 2002 to 2006. Avian Pathol 37:247–257. https://doi.org/10.1080/03079450801986529.
52. Cook JKA, Orbell SJ, Woods MA, Huggins MB. 1999. Breadth of protection of the respiratory tract provided by different live-attenuated infectious bronchitis vaccines against challenge with infectious bronchitis viruses of heterologous serotypes. Avian Pathol 28:477–485. https://doi.org/10.1080/03079459994506.
53. Armesto M, Cavanagh D, Britton P. 2009. The replicase gene of avian coronavirus infectious bronchitis virus is a determinant of pathogenicity. PLoS One 4:e7384. https://doi.org/10.1371/journal.pone.0007384.
54. Eldaghayes I, Rothwell L, Williams A, Withers D, Balu S, Davison F, Kaiser P. 2006. Infectious bursal disease virus: strains that differ in virulence differentially modulate the innate immune response to infection in the chicken bursa. Viral Immunol 19:83–91. https://doi.org/10.1089/vim.2006.19.83.
55. Garcia-Morales C, Rothwell L, Moffat L, Garceau V, Balic A, Sang HM, Kaiser P, Hume DA. 2014. Production and characterisation of a monoclonal antibody that recognises the chicken CSF1 receptor and confirms that expression is restricted to macrophage-lineage cells. Dev Comp Immunol 42:278–285. https://doi.org/10.1016/j.dci.2013.09.011.
56. De Wit JJ, Mekkes DR, Kouwenhoven B, Verheijden JHM. 1997. Sensitivity and specificity of serological tests for infectious bronchitis virus antibodies in broilers. Avian Pathol 26:105–118. https://doi.org/10.1080/03079459708419198.
57. Wang GP, Bushman FD. 2006. A statistical method for comparing viral growth curves. J Virol Methods 135:118–123. https://doi.org/10.1016/j.jviromet.2006.02.008.

3.3 Discussion.

The inability of vaccination with either BeauR-M41(S1) or BeauR-QX(S1) to induce a fully protective immune response to homologous challenge with M41-CK or QX respectively, was unexpected. Both vaccine viruses are able to replicate in Vero cells to high titres (Bickerton *et al.,* 2018, Bickerton *et al.,* 2018b) which offers the ability to bulk manufacture without a dependency on embryonated hens' eggs. However, this advantage does not compensate for the lack of protection induced. The mean ciliary activity in both the BeauR-M41(S1) vaccinated/M41-CK challenged and BeauR-QX(S1) vaccinated/QX challenged chickens at 4 dpc was less than 10%; comparable to the mock vaccinated/M41-CK challenged and mock vaccinated/QX challenged control groups (Table 1 in the enclosed article). In addition, post challenge both rIBV vaccinated groups displayed IB related clinical signs (Figure 2 in the enclosed article), although birds vaccinated with BeauR-QX(S1) and challenged with IBV QX appeared to have recovered 1 day earlier. Previous research had eluded that the S1 subunit alone could induce a protective immune response (Cavanagh *et al.,* 1986, Ignjatovic and Galli, 1994; Johnson *et al.,* 2003; Song *et al.,* 1998; Yan *et al.,* 2013, Toro *et al.,* 2014).

Several research groups have vaccinated chickens with viral vectors expressing the IBV S1 subunits or with recombinant S1 (rS1) glycoprotein. Johnson *et al.,* (2003) investigated the use of a single dose of recombinant fowl adenovirus expressing the S1 gene from the IBV strain Vic S. The authors concluded that vaccination of commercial broiler chicks at one day of age protected four of eight birds against homologous challenge, and vaccination at six days of age protected six of thirteen birds. Unlike the studies presented in this chapter, Johnson *et al.* (2003) defined protection by the absence of challenge virus derived RNA in the trachea 6 dpc. Using this definition two of the five birds vaccinated with BeauR-M41(S1) would have been deemed protected against homologous challenge with M41-CK (Table 3.3). Unlike the study presented in this chapter, Johnson *et al.,* (2003) reported no ciliary activity data nor conclusive IB related clinical signs data therefore making it difficult to compare the level of protection induced. Johnson *et al.,* (2003) also concluded that the S1 subunit of Vic S could offer protection against heterologous challenge with the IBV strain N1/62, reporting a protection rate of 100% when using a vaccine dose of 10^6 $TCID_{50}$ compared to 80% with 10^3 $TCID_{50}$. The presence of challenge virus was however determined via virus isolation in embryonated hens' eggs with a read out of embryo dwarfing and IBV antigen ELISA on the harvested allanotic fluid. Similarly to the homologous vaccine-challenge study, there were neither conclusive clinical signs data presented nor ciliary activity post challenge.

Table 3.3: Number of birds positive for IBV derived RNA in the eyelid and trachea 4 dpc.

Group	Vaccine/challenge	No. of birds positive for IBV RNA/ no. of birds per group		No. of birds protected/ no. of birds in group
		Eyelid	Trachea	
A	Mock/Mock	0/5	0/5	N/A
B	Mock/M41	5/5	5/5	0/5
C	Mock/QX	5/5	5/5	0/5
D	BeauR-M41(S1)/M41	5/5	3/5	2/5*
E	BeauR-QX(S1)/QX	5/5	5/5	0/5

Note: IBV RNA was detected in the upper eyelids and trachea sections harvested 4 dpc using RT-PCR utilising primers BG56 and 93/100 that amplify the 3′ UTR. *Two birds in group D would be classified as protected according to the criteria set by Johnson *et al.,* (2003) due to the lack of challenge virus derived RNA present in the trachea.

The study by Johnson *et al.,* (2003) highlights the difference in techniques used and the differences in the definition of protection. These differences are not isolated to one study but are common throughout the IBV vaccination field (de Wit and Cook, 2014). Further studies, Song *et al.,* (1998), Chen *et al.,* (2010), Yan *et al.,* (2013) and Toro *et al.,* (2014) which are commonly cited as evidence that the S1 can induced a protective immune response, have notable technical differences to the study presented by Ellis *et al.,* (2018). These differences not only included the definition of protection but also include age of bird, the type of vaccination, whether it is live attenuated or a subunit vaccine, route of vaccine administration, vaccination dose and whether birds received a single vaccine dose or multiple.

Song *et al.,* (1998) vaccinated six week old chickens with rS1 derived from the nephrophathogenic IBV strain KM91 which had been expressed from a baculovirus vector. After three intramuscular (i.m.) vaccinations of the rS1 protein, 50% protection as defined by the absence of challenge virus derived RNA, was observed in the kidney and 25% in the trachea after homologous challenge. Similarly Yan *et al.,* (2013) used three doses of an i.m. vaccination of a plasmid encoding the S1 gene, reporting protection rate, also defined by the absence of IBV derived RNA, upon homologous challenge of 75%. These birds were i.m. vaccinated at 7, 21 and 35 days of age, and then challenged via the intra-ocular and intra-

nasal route 3 weeks later. Toro *et al.,* (2014) used a recombinant adenovirus expressing the S1 subunits of strains of the Ark IBV serotype; birds received an i.m vaccination at 3 days of age, and a booster, deliver via the intraocular route, at 20 days of age. A small reduction in viral load in tears as well as a reduction in tracheal mucosal damage was reported.

Chen *et al.,* (2010) vaccinated one day old SPF chickens with rFPV expressing either the S1 subunit from the nephropathogenic HN99 strain of IBV, rFPV-S1, or the S1 subunit alongside chicken interleukin 18 (Il18), rFPV-S1/Il18. Birds were vaccinated via wing prick and homologously challenged 43 days later via the ocular nasal route. Chen *et al.,* (2010) reported that 100% of those vaccinated with rFPV-S1/Il18 displayed no IB related clinical symptoms post challenge; 75% vaccinated with rFPV-S1 also presented no clinical symptoms. Kidney tissue extracted 14 dpc was assessed for viral presence with 100% and 75% of birds testing negative that had been vaccinated with rFPV-S1/Il 18 and rFPV-S1 respectively. Whilst the data presented does indicate the vaccines have induced protection against kidney infection and clinical disease it is unclear whether the respiratory tract is free of viral infection. Chen *et al.,* (2010) only sampled birds at 14 dpc and did not assess viral presence in tracheal tissue nor ciliary activity, and it is likely at this time point respiratory infection may have cleared. Whilst the results of this study are interesting, the difference in technical methodology and sampling points make it difficult to directly draw comparisons with the studies detailed in the chapter. Similarly the studies detailed by Song *et al.,* (1998), Yan *et al.,* (2013) and Toro *et al.,* (2014) are all very different to those presented in this chapter. It is very challenging therefore to conclusively assess whether the S1 subunit can induce a protective immune response, and whether the study presented in this chapter compares to previous research or is an anomaly.

As well as studies in which the authors suggest expression of the S1 subunit can induce protection, there have been studies published in which the authors conclude the S1 is insufficient. Zhao *et al.,* (2017) vaccinated 14 day old SPF birds with rNDV expressing the S1 subunit of IBV strain ck/CH/LDL/091022, rLaSota-S1. Vaccinated birds were homologlously challenged three weeks later. The presence of IBV in oral swabs collected 4, 8 and 12 dpc was determined via qRT-PCR, with those birds mock vaccinated reported to have a higher viral load in comparison to the vaccinated birds. Zhao *et al.,* (2017) concluded due to the presence of IBV RNA in oral swabs from vaccinated birds, that a single vaccine with rLaSota-S1 was insufficient to induce a fully protective immune response against homologous challenge. Despite the technical differences this is a similar conclusion to Ellis *et al.,* (2018). Zhao *et al.,* (2017) also investigated a prime-boost vaccination schedule with

birds receiving vaccinations at 14 and 28 days of age; birds were homologously challenged 7 dpsv. Tissues harvested 5 dpc showed a reduction in viral load in comparison to the unvaccinated control group. Despite this reduction however the tissues were positive for IBV indicating that similarly to a single vaccination, a prime-boost vaccination with rLaSota-S1 was insufficient to induce a fully protective immune response against homologous challenge. Similarly Shirvani *et al.,* (2018) also used an rNDV to express the IBV S1 subunit, rNDV-S1. Birds were vaccinated at one day of age and homologously challenged three weeks later. Viral load in tracheal swabs collected 5 dpc was assessed, with vaccinated birds demonstrated to have similar viral load as the unvaccinated control birds. This observation, alongside the presence of IB related clinical signs indicated that vaccination with rNDV-S1 was unable to induce a fully protective immune response.

The inability of Beau-R vaccines expressing heterologous S1 subunits to induce a fully protective immune response raised a number of questions regarding the role of the S2 subunit which has been shown in IBV, MHV and SARS-CoV to contain immunogenic regions (Kusters *et al.,* 1989; Koch *et al.,* 1990; Daniel *et al.,* 1993; Zhang *et al.,* 2004; Elshabrawy *et al.,* 2012). In comparison to the S1 subunit, the sequence of the S2 subunit is relatively conserved between IBV strains, with Toro *et al.,* (2014) reporting 74.4 – 99.7% amino acid identity of 251 complete sequences available in GenBank. To evaluate the role of the S2 subunit a second *in vivo* vaccine challenge experiment was carried out, which is also presented in the enclosed research article. Chickens were vaccinated at 8 days of age with BeauR-M41(S1), BeauR-M41(S2) or BeauR-M41(S) and challenged three weeks later with M41-CK. Only vaccination with BeauR-M41(S) offered protection against homologous challenge, however this protection fell short of the standards set by the European Pharmacopeia (Table 2 in the enclosed article). The conclusion that the expression of a full S ectodomain was required to elicit a protective immune response against homologous challenge raised a number of questions regarding the role of protective epitopes across both subunits, and also whether the chimeric S glycoproteins were folded in a comparable way to WT and therefore whether structural conformational epitopes had been affected.

Similar to Ellis *et al.,* (2018), research by Eldemery *et al.,* (2017) and Shirvani *et al.,* (2018) has also indicated a role for the S2 subunit in protective immunity. Eldemery *et al.,* (2017) vaccinated SPF chickens at 12 days of age with recombinant trimerised S (rS) or rS1 protein by subcutaneous injection, boosted three weeks later and challenged a further three weeks post boost. Viral load was assessed in tears and trachea at 5 dpc, with a reduction in tears observed in those birds vaccinated with rS and rS1 in comparison to the mock vaccinated

control group. Only those birds vaccinated with rS presented with reduced viral load in harvested tracheas and also reduced tracheal damage as determined by histopathology. Unfortunately no data is presented regarding clinical signs or ciliary activity so it cannot be stated for certain that vaccination with rS protected against clinical disease. The authors concluded that only rS could induce a protective immune response and hypothesised this was due to a number of reasons including epitopes present on the S2 subunit and a conformational stabilisation effect of the S2 subunit on the S1 subunit which could affect the structure of protective epitopes and/or receptor binding. Interestingly rS demonstrated higher affinity binding to chicken tissues including the trachea in comparison to rS1, with rS1 notably unable to bind to lung and kidney tissue.

Shirvani *et al.,* (2018) vaccinated one day old SPF chickens with rNDV expressing either S1 (rNDV-S1), S2 (rNDV-S2) or the S ectodomain (rNDV-S), and challenged three weeks later. Clinical signs were observed twice a day in the ten days after challenge with the average severity score presented; birds vaccinated with rNDV-S appear to have fewer clinical signs than those mock vaccinated and those vaccinated with rNDV-S1 and rNDV-S2. Tracheal swabs were collected 5 dpc and assessed by qRT-PCR for viral genome; the viral load appears similar in all vaccinated groups. Viral isolation from tracheal swabs in embryonated eggs however indicated that 93.3% of chickens vaccinated with rNDV-S were protected as no viable virus was re-isolated; 100% of chickens in all other vaccinated groups were positive for re-isolated challenge virus. The authors hypothesised that rNDV-S gave better protection due to the inclusion of the S2 subunit which may act as a chaperone, assisting folding of the S1 protein and therefore assisting presentation of conformational epitopes.

The S glycoprotein is a complex homo-trimeric structure that exists in both pre-fusion and post-fusion conformations. Until recently the structure of the IBV S glycoprotein could only be assumed using data generated from other coronaviruses such as MHV, PDCoV and HCoV-HKU1 (Kirchdoerfer *et al.,* 2016; Walls *et al.,* 2017; Shang *et al.,* 2018B); the pre-fusion conformation of the S glycoprotein of M41 was published in 2018 (Shang *et al.,* 2018). Similarly, to MHV and HKU1, the pre-fusion conformation of the IBV S exhibited on mature virions has a clove-like shape, with three S1 heads forming a crown-like structure that sits upon a trimeric S2 stalk structure (Shang *et al.,* 2018). As discussed in the Chapter 1 both the S1 and S2 subunits consist of several domains (Chapter 1, Figure 1.6). Shang *et al.,* (2018B) identified that the S1-CTD domains from three S protomers sit centrally on top of the spike trimer, with the three S1-NTD domains sitting lower on the outer edge, closer to the S2 subunit. The S2 contains three central helices, one from each protomer which form an

interface between the S1 and S2. The S1 located subdomains, SD1 and SD2, connect the S1 subunit to S2 and the S2 HR2 region is notably disordered.

To complicate the structure, the trimeric S1 exhibits quaternary packing (Figure 3.3); from one S protomer, the S1-CTD domain interacts with a S1-CTD domain located on another, as well as a S1-CTD domain and a S1-NTD domain located on a third protomer (Shang *et al.,* 2018). This quaternary packing of the S1 subunit partially conceals the RBD in the S1-NTD (Promkuntod *et al.,* 2014) as well as the putative RBD residing in the S1-CTD. It also locks the S2 into the pre-fusion state; the HR1 region and the FP of each S2 subunit is locked in place by a S1-CTD domain located on a different S protomer, as well as an S1-CTD domain and a SD1 subdomain located on the third S protomer (Shang *et al.,* 2018). Given the complexity of the structure it is not difficult to see why a chimeric S1/S2 glycoprotein may not be optimally folded.

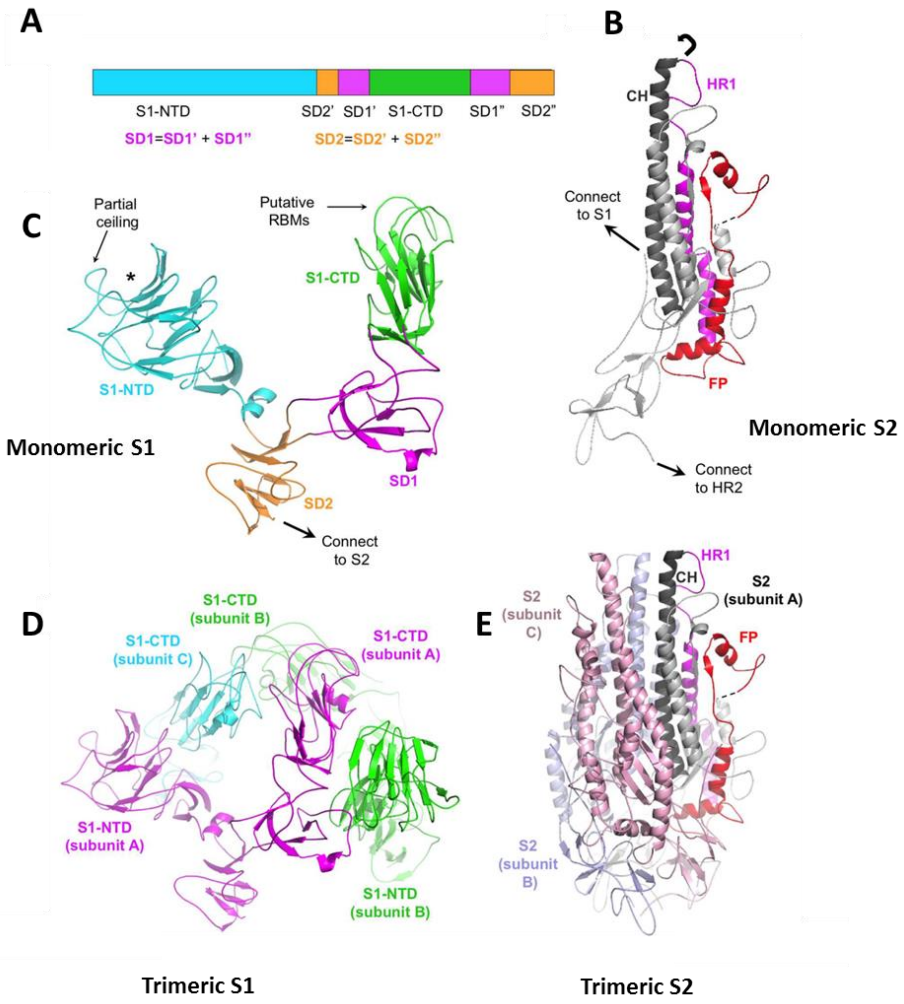

Figure 3.3: Quaternary packing of three S protomers into the trimeric S glycoprotein. (A) Schematic drawing of IBV S1 detailing the presence of two subdomains, SD1 and SD2. (B) Structure of monomeric S2 subunit. (C) Structure of the monomeric S1 subunit. (D) Structure of trimeric S1 subunit. The S1 subunit from each monomeric unit (protomer) are represented in green, blue or purple. (E) Structure of trimeric S2 subunit. The S2 subunit from each monomeric unit (protomer) are represented in grey, pink or purple. Figure adapted from Shang *et al.,* 2018.

There are a number of amino acid differences in S1-NTD domains of M41-CK, Beau-R and QX (Appendix, Figure 8.3), and notably this domain includes the HVR 1 and 2 identified by Cavanagh *et al.,* (1988). The S1-CTD domains also exhibit several amino acid differences most of which are concentrated in the HVR 3 region identified by Moore *et al.,* (1997). There is a difference of four amino acids between the SD1 subdomain of Beau-R and M41-CK and

18 between Beau-R and QX. There are 17 amino acid differences in the SD2 subdomain between Beau-R and QX and no differences between M41-CK and Beau-R. As discussed by Ellis *et al.,* (2018), the S2 subunits between Beau-R, QX and M41-CK are relatively conserved however there are a number of differences in the HR1 region, a region structurally restrained by the quaternary packing of the S1 subunits. Whilst it is unknown which residues play critical roles in the assembly of the trimeric S glycoprotein, the analysis of the amino acid sequences of the S protomers does indicate that there is potential for conformational changes with a chimeric S1/S2 glycoprotein. If, however, there are conformation changes these have not detrimentally affected the replication of the rIBV BeauR-M41(S1), BeauR-M41(S2) nor BeauR-QX(S1) *in vitro.* This indicates there have not been massive structural changes in the chimeric S glycoproteins, as these proteins are clearly functioning to allow virus entry and fusion. It is possible that small conformational changes have distorted/changed conformational epitopes accounting for the lack of protection induced by these rIBV vaccines.

The structure of the M41 S glycoprotein (Shang *et al.,* 2018) as well as the solved structures from other coronaviruses (Kirchdoerfer *et al.,* 2016; Walls *et al.,* 2016; Shang *et al.,* 2018B; Walls *et al.,* 2017; Shang *et al.,* 2018) raises questions about how the S1 subunit is presented to the immune system when delivered in vector vaccines, as a DNA vaccine or rS1 subunit vaccine (Johnson *et al.,* 2003; Song *et al.,* 1998; Toro *et al.,* 2014, Yan *et al.,* 2012). Given the complexity of the trimeric S glycoprotein structure it is unlikely an S1 subunit expressed on its own assembles comparably to an S1 expressed as part of WT infection. Furthermore the S2 subunit anchors the S1 to the viral membrane, therefore aiding in conformational presentation of the S1 subunit (Shang *et al.,* 2018). Neither Johnson *et al.,* (2003), Song *et al.,* (1998), Yan *et al.,* (2013) nor Toro *et al.,* (2014) address this issue and therefore it is unclear how the S1 subunit is assembled and what conformation is presented to the immune system. Using an IBV vector allows the S glycoprotein to be presented as in WT infection, and additionally allows for the structural changes of the S glycoprotein throughout the replication cycle.

The structure of S described by Shang *et al.,* (2018), discussed above is the pre-fusion conformation however the structure is remarkably different post-fusion, with the trimeric S exhibiting an elongated cone like shape (Walls *et al.,* 2016; Walls *et al.,* 2017; Shang *et al.,* 2018). Once the conformational restraint of the S1 is lifted through proteolytic processing, the three HR1 and HR2 regions in the trimeric S2 subunit refold into a 6-helix bundle structure exposing the FP (Walls *et al.,* 2016, Walls *et al.,* 2017; Shang *et al.,* 2018). These major conformational changes will result in the exposure of epitopes previously unseen in the pre-fusion structure (Walls *et al.,* 2017). The FP region is one such area that has been identified as an antigenic determinant in both MHV and SARS-CoV (Daniel *et al.,* 1993;

Zhang *et al.,* 2004). It is possible therefore that “hidden” epitopes in the S2, that become accessible after fusion, play a fundamental role in protective immunity. Subsequently it is therefore possible that epitopes in both the S1 and S2 subunit are required for the induction of a fully protective immune response, and this may account for why neither BeauR-M41(S1) nor BeauR-QX(S1) could induce such a robust response against homologous challenge.

The results of this chapter have raised questions regarding the possible mis-folding of a chimeric S glycoprotein, as well as the potential role of epitopes across both the S1 and S2 subunits in vaccine induced immunity. One other question that this chapter has raised regards the level of *in vivo* vaccine virus replication that is required to induce a protective immune response when utilising live attenuated vaccines. The rIBV Beau-R is a molecular clone of the apathogenic Beaudette-CK strain (Casais *et al.,* 2001). Whilst rIBV BeauR-M41(S) did induce protective immunity, as previously reported by Hodgson *et al.,* (2004), the response was not as robust as expected, with the vaccine virus inducing poor levels of local immunity within the trachea. In addition, ciliary activity post challenge fell short of the European Pharmacopeia standards, a finding comparable to Hodgson *et al.,* (2004). Armesto *et al.,* (2011) investigated rIBV BeauR-4/91(S) as a vaccine against homologous challenge; ciliary activity at ~65% 4 dpc also fell short of the European Pharmacopeia standards. One possible explanation for this, and also of the failure of BeauR-M41(S1) and BeauR-QX(S1) to elicit a protective immune response is the potentially limited *in vivo* replication of the vaccine viruses.

In the studies presented in this chapter neither rIBV BeauR-M41(S), BeauR-M41(S1), BeauR-M41(S2) nor BeauR-QX(S1) could be consistently detected at the sites of inoculation or in the trachea post vaccination (Table 3.4 and Table 3 in the enclosed article). It has long been established that the Beaudette strain cannot establish a long lasting productive infection *in vivo*, with the molecular clone Beau-R behaving similarly (Casais *et al.,* 2001). Interestingly chickens inoculated with Beaudette do produce virus neutralising antibodies, however these rapidly decrease over time (Geilhausen *et al.,* 1973), presumably due to the lack of or some limitation in viral replication. The lack of detectable *in vivo* replication of IBV Beaudette has been attributed to an unknown number of attenuating mutations accumulated during repeated passaging in both cell culture and embryonated hens’ eggs (Cavanagh *et al.,* 1988). These unknown mutations may play a significant role in the failure of the vaccine viruses to replicate efficiently *in vivo* and subsequently to induce a robust immune response. The replication of Beau-R *in vivo* is therefore important to investigate for the future of rationally designed vaccines and will be discussed further in Chapter 5 and 6. It remains a possibility therefore that both the S1 subunit and the S ectodomain could elicit a stronger protective immune response if delivered in a less attenuated IBV backbone.

Table 3.4: IBV derived RNA could not be detected after vaccination with BeauR-M41(S1) or BeauR-QX(S1).

Group	Vaccine	No. of dpv	No. of birds positive for IBV RNA	
			Eyelid	Trachea
A	Mock	2	0	0
B	Mock		0	0
C	Mock		0	0
D	BeauR-M41(S1)		0	0
E	BeauR-QX(S1)		0	0
A	Mock	4	0	0
B	Mock		0	0
C	Mock		0	0
D	BeauR-M41(S1)		0	0
E	BeauR-QX(S1)		0	0

Note: Upper eyelids and trachea sections harvested 2 and 4 dpv were assessed for the presence of IBV derived RNA by RT-PCR utilising primers BG56 and 93/100 which amplify the 3′ UTR.

The full length S glycoprotein has been used to vaccinate against SARS-CoV with reported success. Bukreyev *et al.,* (2004) vaccinated monkeys with a parainfluenza virus encoding the full length SARS-CoV S glycoprotein; vaccinated animals had reduced viral load in trachea swabs compared to unvaccinated animals. Buchholz *et al.,* (2004) also investigated the use of a parainfluenza virus expressing the SARS-CoV S glycoprotein; similarly to Bukreyev *et al.,* (2004) vaccinated hamsters exhibited a reduction in challenge viral load. Mouse models have also been used to demonstrate the protective ability of the SARS-CoV spike when expressed from a vaccinia virus vector, a baculovirus and also as a DNA vaccine (Bisht *et al.,* 2004, Yang *et al.,* 2004; He *et al.,* 2006). Whilst it is clear that the S glycoprotein is a very potent antigen, due to the use of animal models it is not conclusive whether the S glycoprotein alone can induce a fully protective immune response in the natural host. It is possible that other viral proteins are required. Interestingly whilst both BeauR-M41(S) and BeauR-4/91(S) can induce a protective immune response, as discussed above this response cannot be classified as fully protective against homologous challenge (Hodgson *et al.,* 2004; Armesto *et al.,* 2011); it may also be possible that other viral proteins are required to enable the rIBV to have closer resemblance to the challenge virus. The potential role of other viral proteins in vaccine induced immunity will be discussed further in Chapter 4.

In summary the results presented in this chapter demonstrate that neither rIBV BeauR-M41(S1), BeauR-QX(S1) nor BeauR-M41(S2) can induce a fully protective immune response against homologous challenge. This could be due to a number of reasons including the potential mis-folding of chimeric S glycoproteins, the need for protective epitopes across both subunits, and the inability of the vaccine viruses to establish a productive infection *in vivo*. A rIBV expressing the full length S ectodomain from M41-CK, BeauR-M41(S), can elicit a protective immune response against homologous challenge, however this response fell short of the European Pharmacopeia standards. This raises further questions regarding the level of replication of rIBV vaccines required to induce a protective immune response, and also whether additional viral proteins are required to enable the vaccine virus to appear more like the challenge virus.

Chapter 4: Investigating the role of the S glycoprotein in the induction of protective immunity against heterologous challenge.

4.1 Introduction.

The results discussed in Chapter 3 demonstrate the ability of the S glycoprotein, when expressed in a rIBV vector, to induce protective immune responses against homologous challenge. These results alongside those reported by Hodgson *et al.,* (2004) and Armesto *et al.,* (2011) demonstrate that it is possible to rationally design live attenuated rIBV vaccine viruses. Whilst results of homologous vaccine-challenge experiments are encouraging, the major challenge in the control of IBV is that vaccination against one serotype often offers limited cross protection towards another (reviewed by de Wit and Cook, 2014). Cavanagh *et al.,* (1997), concluded that there is a general a negative correlation between the level of protection afforded by a vaccine and the level of homology between the S genes of challenge and vaccine strain.

The mechanism of cross protection is not clear cut, with several studies demonstrating a degree of cross protection between unrelated vaccine and challenge strains (Cavanagh *et al.,* 1992; Cook *et al.,* 2001; Terregino *et al.,* 2008; Armesto *et al.,* 2011; Lim *et al.,* 2012; Bru *et al.,* 2017). Terregino *et al.,* (2008) evaluated the use of two commercial vaccines of different serotypes, Ma5 and 4/91, against challenge with a third serotype, QX. No challenge virus could be re-isolated from the tracheas of vaccinated birds indicating to the authors that a fully protected immune response against QX had been induced by vaccination with the two unrelated serotypes. Low sequence homologies between the hypervariable region of the S1 subunits were reported; 77.1% between Ma5 and QX and 81% between 4/91 and QX (Terregino *et al.,* 2008). Conversely, other studies have demonstrated limited cross protection between strains with high sequence homology (Cook *et al.,* 2001, Ladman *et al.,* 2006; Liu *et al.,* 2009). Vaccination with a Beaudette strain does not confer protection against a M41-CK challenge; despite the > 95% sequence homology between the S genes (Hodgson *et al.,* 2004); and the fact that both viruses belong to the Massachusetts serotype. Previous work has hypothesised that a small number of virus neutralising epitopes play a disproportionate role in cross-protection, which makes it difficult to predict effective vaccine strategies (Cavanagh *et al.,* 1997).

Effective vaccination against IBV is proving an increasing challenge to the global poultry industry due to the continuing emergence of novel strains, such as QX which was first isolated in China in 1995 (Wang *et al.,* 1998) and has subsequently spread worldwide (Beato *et al.,* 2005; Worthington *et al.,* 2008; Amin *et al.,* 2012; Valastro *et al.,* 2016). Commercial live IBV vaccines are generated through multiple passages, typically 80 – 100 times, of a pathogenic field isolate through embryonated hens' eggs with the aim of generating a virus that is attenuated but still retains immunogenicity (Geerligs *et al.,* 2011). Given the nature of this process, it is challenging to readily react to emerging strains in a time appropriate manner. The development of a reverse genetic system for IBV (Casais *et al.,* 2001), opened up the possibility of using rIBVs as vaccines that can be rationally designed and readily manufactured, removing the cumbersome trial and error prone method of attenuation by multiple passage through embryonated hens' eggs.

In this chapter, two rIBVs, BeauR-M41(S) and BeauR-4/91(S) were investigated as potential vaccines against heterologous challenge with a QX strain of IBV. Both rIBVs have been described previously and have been demonstrated to offer protection against homologous challenge (Hodgson *et al.,* 2004, Armesto *et al.,* 2011; Ellis *et al.,* 2018). The rIBV BeauR-4/91(S) has also been demonstrated to offer limited cross protection against a heterologous M41-CK challenge (Armesto *et al.,* 2011). Whilst cross protection studies are not novel, previous research has largely utilised traditional vaccine strains, such that the vaccine virus closely resembles the challenge virus and therefore it is difficult to assess just the role of the S glycoprotein. As discussed in the Chapter 3, those studies that utilised non IBV vectors as vaccines for the expression of the S glycoprotein or S1 subunit also come with limitations, making it difficult to fully assess the sole role of the S glycoprotein in the generation of a protective immune response against natural infection. In addition, rIBV vectors have the distinct advantage of mimicking the natural route of WT IBV infection.

The two rIBVs, BeauR-M41(S) and BeauR-4/91(S) used in this chapter as potential vaccine viruses are genetically based on the Beaudette genome with only the S gene derived from a different strain, either M41-CK or 4/91 (UK), respectively. The use of these rIBVs therefore allowed for the assessment of the M41-CK and 4/91 S glycoproteins alone, when delivered in a manner that mimics a WT virus infection, in vaccine induced immunity against a heterologous QX challenge. This chapter will detail the results of the *in vivo* vaccine-challenge study and the assessment of cross neutralising antibodies.

4.2 Results.

4.2.1 Confirmation that the S gene from a pathogenic strain does not confer virulence to a non-pathogenic strain.

To elucidate if rIBV expressing the S gene from either 4/91 or M41-CK could induce a level of cross protection against a heterologous challenge with the IBV strain QX, a vaccination challenge experiment in SPF RIR chicks was conducted (Figure 4.1). Briefly eight-day-old chicks received a primary vaccination of PBS (mock vaccination), BeauR-4/91(S) or BeauR-M41(S) as per grouping in Table 4.1. Fourteen days post primary vaccination (dppv) the birds received a secondary vaccination of either PBS (mock vaccination), BeauR-4/91(S) or BeauR-M41(S). Nine days post-secondary vaccination (dpsv) the birds were then challenged with either QX or mock challenged with PBS. Samples were harvested 4 dppv and 2, 4 and 14 days post challenge (dpc).

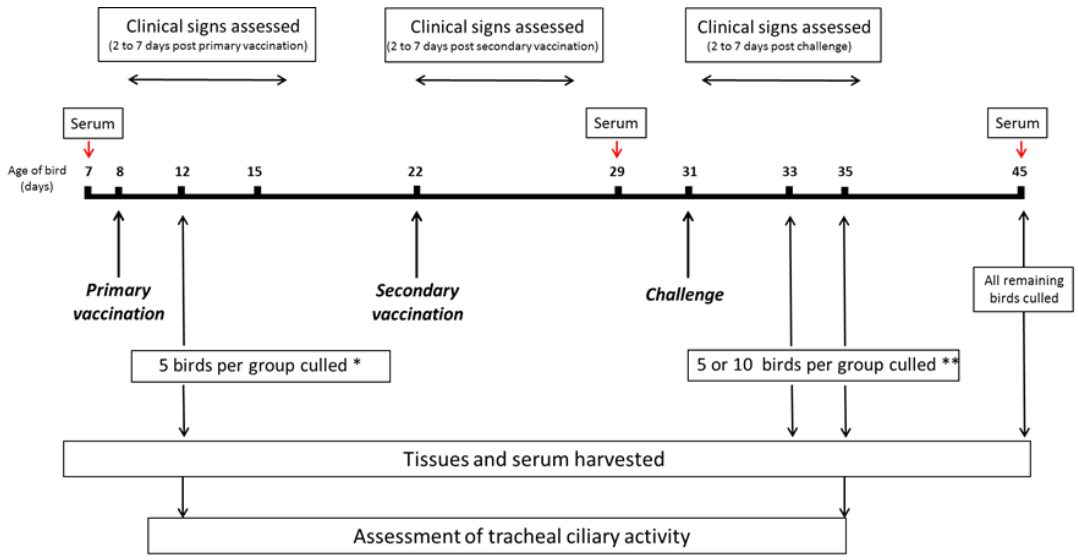

Figure 4.1: Schematic detailing protocol for *in vivo* heterologous vaccine-challenge experiment. Groups of eight day old SPF RIR chickens received a primary vaccination of BeauR-M41(S), BeauR-4/91(S), or PBS. Two weeks (14 days) later birds received a second vaccination of either BeauR-M41(S), BeauR-4/91(S) or PBS. Nine days post-secondary vaccination (dpsv) birds were challenged with QX or mock challenged with PBS. Clinical signs were assessed both post vaccination and post challenge birds. At defined intervals randomly chosen birds were culled from each group and a variety of tissues harvested. Serum was collected pre-vaccination, post-vaccination (pre-challenge) and post-challenge. Tracheal ciliary activity was assessed on 4 dpv and 4 dpc. The experiment ended 14 dpc with all remaining birds culled.

Table 4.1: Details of groups, vaccination schedule, sampling points and animal numbers.

Group	Primary vaccination	No. of birds sampled 4 dppv	Secondary vaccination	Challenge	No. of birds sampled			Total no. of birds per group
					2 dpc	4 dpc	14 dpc	
A	PBS (mock)	5	PBS (mock)	PBS (mock)	5	5	5	20
B	BeauR-M41(S)	5	BeauR-M41(S)	QX	10	10	9	34
C	BeauR-4/91(S)	5	BeauR-4/91(S)	QX	10	10	9	34
D	BeauR-M41(S)	0	BeauR-4/91(S)	QX	10	10	10	30
E	BeauR-4/91(S)	0	BeauR-M41(S)	QX	10	10	10	30
F	PBS (mock)	0	PBS (mock)	QX	10	10	12	32

Clinical signs were assessed 2 to 7 dppv, with no IBV related clinical signs observed. The levels of snicking were comparable between all vaccinated groups and the unvaccinated control groups, remaining below 0.05 snicks per bird per min (Figure 4.2). No rales were detected in any of the groups.

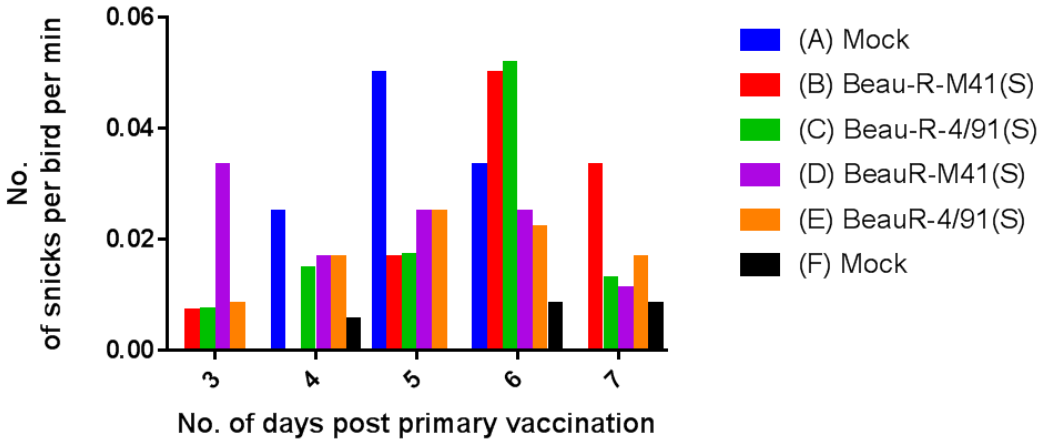

Figure 4.2: BeauR-4/91(S) and BeauR-M41(S) vaccinated chickens displayed rates of snicking comparable to mock vaccinated groups. SPF RIR chickens were vaccinated with either BeauR-M41(S), BeauR-4/91(S) or mock vaccinated with PBS at eight days of age. The number of snicks was assessed from day 3 to 7 dppv. Snicks were independently counted by two or three persons over a 2 min period with the average of these scores presented.

Tracheal ciliary activity was assessed in five randomly chosen birds in groups A (Mock), B (BeauR-M41(S)) and C (BeauR-4/91(S)) at 4 dppv. Ciliary activity in BeauR-4/91(S) and BeauR-M41(S) infected birds was comparable to those mock vaccinated; the group means were 87%, 95% and 87.5% respectively (Figure 4.3). The tracheal rings used for the ciliary activity assay were homogenised resulting in a tissue derived supernatant which was used to inoculate embryonated hen's eggs. Allanotic fluid was screened by RT-PCR utilising IBV specific primers BG56 and 93/100, which amplify the 3′ UTR. No PCR product was detected indicating that infectious vaccine virus could not be recovered from the trachea at 4 dppv (Figure 4.4).

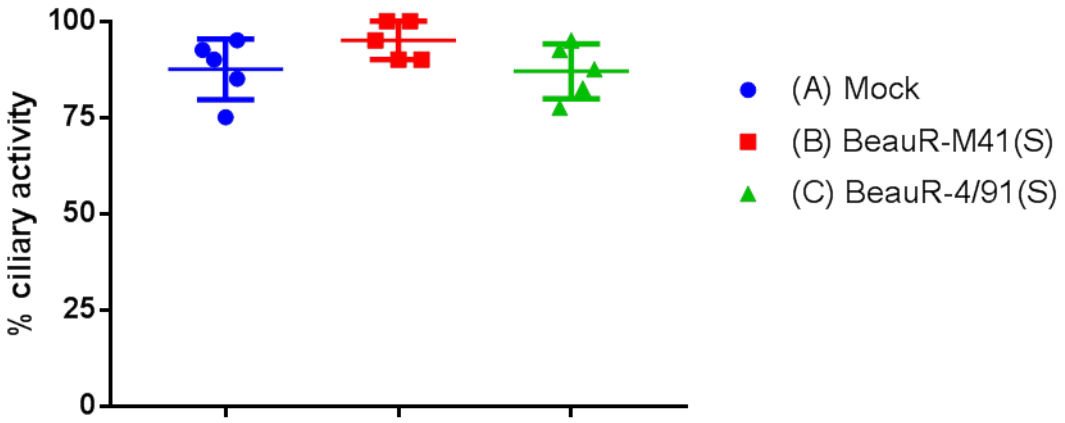

Figure 4.3 BeauR-4/91(S) and BeauR-M41(S) vaccinated chickens displayed tracheal ciliary activity comparable to mock vaccinated chickens. Tracheas were harvested from five randomly selected birds per group on four dppv. Each trachea was sectioned in 10 x 1mm rings and the ciliary activity of each ring was assessed by light microscopy and the percentage activity calculated. Plotted points represent individual animals and the mean activity of the 10 rings assessed. Error bars represent standard deviation (SD). Statistical differences between groups was evaluated using Kruskal-Wallis test followed by post Hoc Mann Whitney test corrected for multiple comparison.

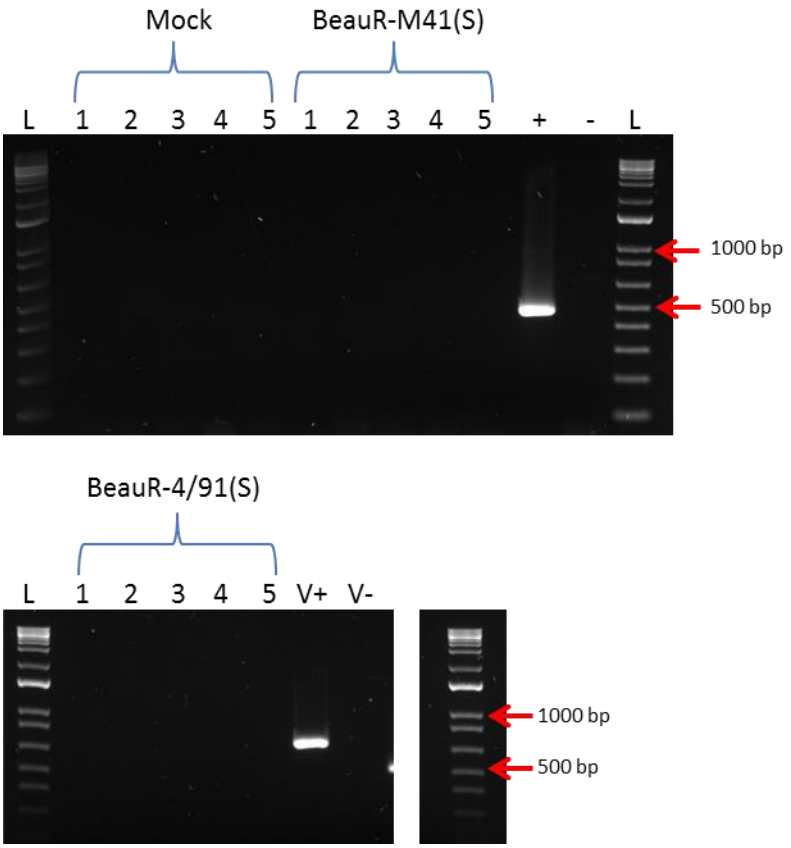

Figure 4.4: No infectious vaccine virus could be re-isolated from trachea sections harvested 4 dppv. SPF embryonated hen's eggs were inoculated with tissue derived supernatant generated from trachea harvested 4 dppv. A positive (V+) control of BeauR-M41(S) was included in the re-isolation experiment as was a PBS negative control (V-). Allantoic fluid harvested was screened for IBV related RNA by RT-PCR utilising primers BG56 and 93/100. A positive and negative RT-PCR control was included and denoted by + and – respectively. All samples were run on a 0.8% agarose gel alongside 1 KB+ ladder (L; Life Technologies).

The lack of infectious virus re-isolated from tracheas harvested 4 dppv alongside the lack of pathology as denoted by the comparative ciliary activities to mock infected birds, and the lack of IBV related clinical signs, demonstrates that both BeauR-M41(S) and BeauR-4/91(S) have an attenuated phenotype *in vivo*. These observations support previous reports that the S genes from the two pathogenic isolates do not confer virulence to the apathogenic rIBV

Beau-R therefore providing a strategy for the rational design of potential vaccine viruses (Hodgson *et al.,* 2004; Armesto *et al.,* 2011; Ellis *et al.,* 2018).

4.2.2 Neither the S glycoprotein from 4/91 nor M41-CK can induce a fully protective immune response against a QX challenge.

Fourteen days following primary vaccination each group received a second vaccination of BeauR-M41(S), BeauR-4/91(S) or PBS as per the groupings detailed in Table 4.1. The vaccination scheme included both homologous, e.g. BeauR-M41(S) followed by BeauR-M41(S) and heterologous vaccinations, e.g. BeauR-M41(S) followed by BeauR-4/91(S). The order in which the heterologous vaccination was administered was also investigated as previous research has suggested that vaccination order has an effect on the level of protection induced (Cook *et al.,* 1999). As with post primary vaccination, clinical signs were observed from 3 to 7 dpsv. No rales were observed in any of the groups. Levels of snicking (Figure 4.5) were largely comparable between vaccinated groups and unvaccinated control groups, remaining, bar two exceptions, below 0.1 snicks per bird per min. The two exceptions to this were observed 4 dpsv in those birds vaccinated with BeauR-4/91(S)/BeauR-4/91(S), 0.19 snicks per bird per min, and on day 7 in the BeauR-4/91(S)/BeauR-M41(S) vaccinated group, 0.14 snicks per bird per min.

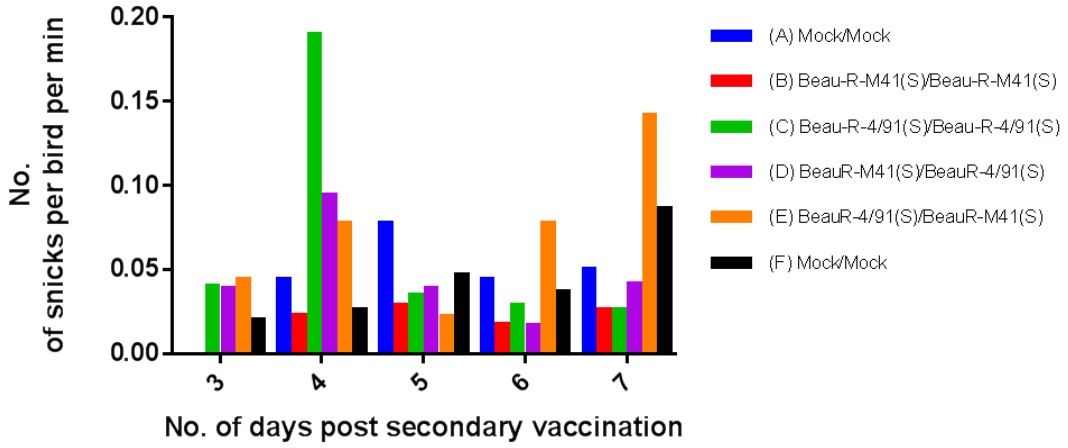

Figure 4.5: Vaccinated chickens displayed comparable rates of snicking to mock vaccinated chickens post-secondary vaccination. SPF RIR chickens received a secondary vaccination of BeauR-M41(S), BeauR-4/91(S) or PBS for mock vaccination. Vaccinated birds had 14 days prior received a primary vaccination of BeauR-M41(S), BeauR-4/91(S) or PBS for mock vaccination. The number of snicks was assessed from day 3 to 7 dspv. Snicks were independently counted by two or three persons over a 2 min period with the average of these scores presented.

Nine dpsv, birds were either challenged with QX, a different serotype to both M41-CK and 4/91, or mock challenged with PBS. From 2–7 dpc clinical signs were observed in all groups except the mock vaccinated/mock challenged control group (Mock/Mock/Mock). Up until 5 dpc there was no difference in the numbers of snicks between all vaccinated/challenged groups and the mock vaccinated/QX challenged group (Mock/Mock/QX) (Figure 4.6). On 6 dpc the snicks in the group vaccinated with BeauR-M41(S)/BeauR-M41(S) and the mock vaccinated/QX challenged control group increased whereas in all other vaccinated groups the number of snicks decreased. The peak of the number of snicks per bird per min in the mock vaccinated/QX challenged control bird group, 1 snick per bird per min, was at 7 dpc. At this time point all vaccinated/challenged groups except BeauR-4/91(S)/BeauR-4/91(S)/QX exhibited less than 0.25 snicks per bird per min, with the latter exhibiting 0.6 snick/bird/min. At 14 dpc snicking in all the vaccinated/QX challenges groups was comparable to the mock vaccinated/mock challenged control group indicating that all birds had recovered from the QX infection.

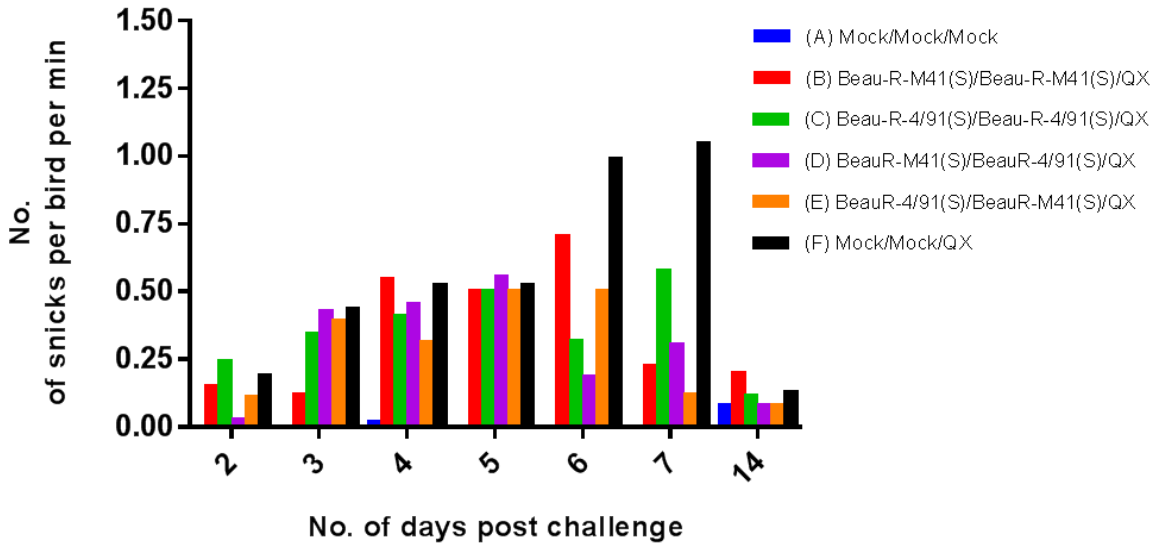

Figure 4.6: Assessment of snicking post challenge. SPF RIR chickens were vaccinated with either BeauR-M41(S), BeauR-4/91(S) or PBS for mock vaccination. Fourteen days later birds received a secondary vaccination of either BeauR-M41(S), BeauR-4/91(S) or PBS for mock. Nine days post-secondary vaccination birds were challenged with QX or mock challenged with PBS. The number of snicks was assessed from 2 to 7 dpc and the resulting number of snicks per bird per min calculated. Snicks were independently counted by two or three persons over a 2 min period with the average of these scores presented.

Rales were observed on days 3 to 5 dpc in all groups except unvaccinated/unchallenged (Figure 4.7) and followed a similar trend to the snicking in that the vaccinated birds appeared to recover more rapidly than the mock vaccinated/QX challenged control birds. On day 7 dpc only birds in the mock vaccinated/QX challenged group exhibited rales. Of the vaccinated groups, interestingly on 6 dpc only birds vaccinated with BeauR-4/91(S)/BeauR-4/91(S) and BeauR-M41(S)/BeauR-4/91(S) exhibited rales, although the numbers were reduced in comparison to the mock vaccinated/QX challenged control group; 22.2%, 20% and 41.7% respectively. Chickens that received vaccination BeauR-M41(S)/BeauR-M41(S) and BeauR-4/91(S)/BeauR-M41(S) did not display rales on 6 dpc.

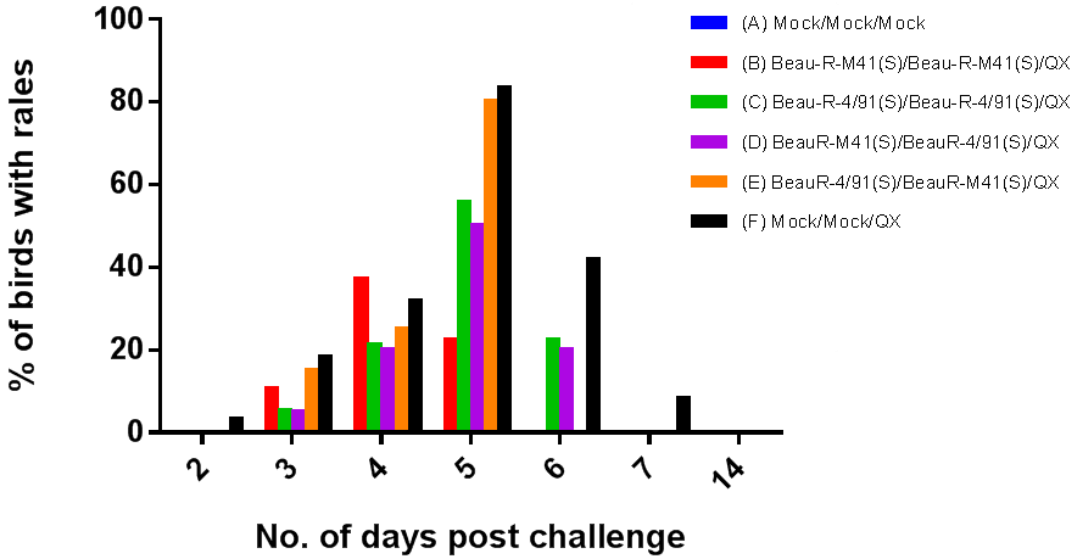

Figure 4.7: Vaccinated chickens exhibited in fewer rales post challenge in comparison to unvaccinated chickens. SPF RIR chickens were vaccinated with either BeauR-M41(S), BeauR-4/91(S) or PBS for mock vaccination. Fourteen days later birds received a secondary vaccination of either BeauR-M41(S), BeauR-4/91(S) or PBS for mock. Nine days post-secondary vaccination birds were challenged with QX or mock challenged with PBS. Chickens were checked individually for the presence of tracheal rales 2 – 7 dpc. The percentage of birds per group positive for rales was calculated.

Tracheal ciliary activity was assessed on 4 dpc in tracheas harvested from 10 randomly selected chickens in all groups except the mock vaccinated/mock challenged control group in which five birds were randomly sampled (Table 4.2, Figure 4.8). The industry standard for the assessment of IBV vaccines set by the European Pharmacopeia states that in order for a chicken to be protected at least 50% ciliary activity must be retained post challenge in nine out of ten rings sampled from a trachea (European Pharmacopeia, 2010). The mean ciliary activities for the vaccinated groups ranged from 2.25% to 18.75% (Table 4.2). The mock vaccinated/QX challenged control group displayed a mean activity of 1.0%, and the unvaccinated/unchallenged group a mean activity of 80.5%. Ciliary activities in the mock vaccinated/QX challenged control group as well as all vaccinated groups, except the BeauR-4/91(S)/BeauR-4/91(S) vaccinated group, were significantly different to the unvaccinated/unchallenged group ($p<0.05$, Figure 4.8). Interestingly, two birds vaccinated

with BeauR-4/91(S)/BeauR-4/91(S) retained ciliary activities comparable to unvaccinated/unchallenged birds, with one bird classified as fully protected with 10/10 tracheal rings retaining 50% or more ciliary activity (Table 4.2). The second bird displayed an average ciliary activity of 72.5%, with 7/10 rings retaining 50% or more activity.

Table 4.2 Percentage ciliary activities in tracheal samples harvested at 4 dpc.

Group	Ciliary activity (%)										No. of protected birds	Mean	Standard Deviation
A	Mock/Mock/Mock										N/A	80.50	11.65
	72.50	97.50	75.00	87.50	70.00								
B	BeauR-M41(S)/BeauR-M41(S)/QX										0	5.75	3.13
	5.00	7.50	10.00	2.50	0.00	7.50	5.00	5.00	10.00	5.00			
C	BeauR-4/91(S)/BeauR-4/91(S)/QX										1	18.75	34.73
	2.50	0.00	2.50	95.00	72.50	7.50	2.50	2.50	0.00	2.50			
D	BeauR-M41(S)/BeauR-4/91(S)/QX										0	6.25	10.22
	0.00	0.00	0.00	30.00	0.00	5.00	17.50	0.00	10.00	0.00			
E	BeauR-4/91(S)/BeauR-M41(S)/QX										0	2.25	4.78
	5.00	15.00	0.00	0.00	0.00	0.00	0.00	0.00	2.50	0.00			
F	Mock/Mock/QX										0	1.00	3.16
	0.00	0.00	0.00	0.00	0.00	0.00	0.00	0.00	0.00	10.00			

Notes: Birds considered protected if at least 50% ciliary activity is retained post challenge in nine out of ten rings sampled (European Pharmacopeia, 2010).

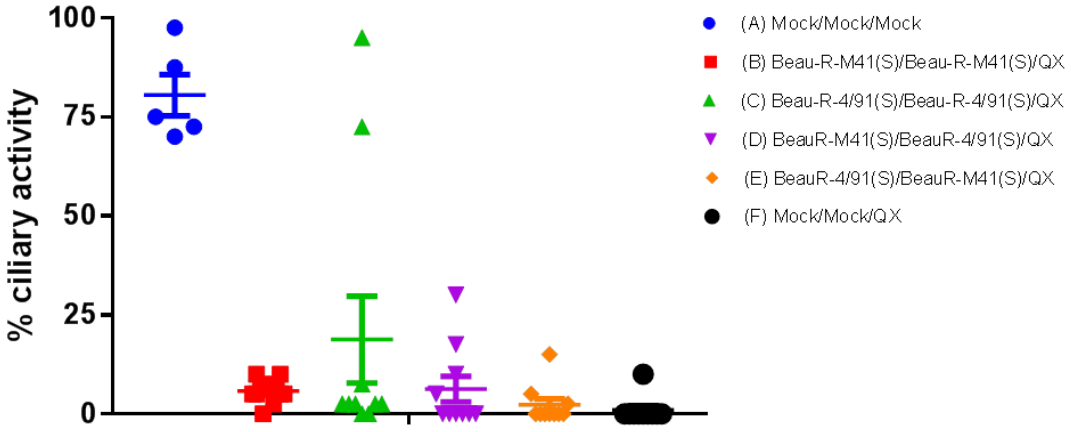

Figure 4.8: Vaccination strategies did not offer protection against the loss of ciliary activity post challenge. Ciliary activity was assessed in trachea extracted four days post challenge in five or ten randomly selected chickens as per post vaccination. Ciliary activity in all groups except BeauR-4/91(S)/BeauR-4/91(S)/QX was statistically reduced in comparison to the mock vaccinated/mock challenged control group. Ciliary activity in all vaccinated groups was comparable to the mock vaccinated/QX challenge control group. Statistical differences between groups were evaluated using Kruskal-Wallis test followed by post Hoc Mann Whitney test corrected for multiple comparisons. Error bars represent SD.

Whilst one vaccinated group, BeauR-4/91(S)/BeauR-4/91(S), did display some evidence of retained ciliary activity and it appears that the birds in all vaccinated groups recovered in terms of the clinical signs (rales and snicking) more rapidly than the mock vaccinated/QX challenged control birds, overall none of the vaccination strategies successfully offered full protection against heterologous challenge with QX.

4.2.3 Vaccination has resulted in a reduction of viral load post challenge.

To assess the implications of the vaccine strategies on viral load, tissue derived supernatants prepared from tracheas harvested 4 dpc, were titrated in *ex vivo* TOCs (Figure 4.9). Viral loads from all vaccinated/challenged groups were statistically higher than those from birds in the mock vaccinated/mock challenged control group, in which no virus was re-isolated. In birds vaccinated with BeauR-M41(S)/BeauR-M41(S) the viral loads were

statistically lower ($p<0.05$) than those observed from the mock vaccinated/QX challenged control group. Similarly, viral load in birds vaccinated with BeauR-4/91(S)/BeauR-4/91(S) was also lower ($p<0.05$). Overall, the results showed that birds which received homologous primary and secondary vaccinations had a lower viral load in comparison to mock vaccinated/QX challenged birds. However, there were no differences in viral loads between the mock vaccinated/QX challenged control group and those vaccinated with heterologous vaccines, BeauR-M41(S)/BeauR-4/91(S) or BeauR-4/91(S)/BeauR-M41(S). It therefore appears that a vaccination schedule with homologous primary and secondary vaccines had a greater effect on viral load than one involving heterologous primary and secondary vaccinations. In addition, interestingly the two birds vaccinated with BeauR-4/91(S)/BeauR-4/91(S) which retained ciliary activity post challenge comparable to mock vaccinated/mock challenged birds, had viral load comparable to the group average (mean), 3.5, 3.8 and 3.13 log_{10} CD_{50}/ml respectively, and to the group average of the unvaccinated/QX challenged control group, at 4.06 log_{10} CD_{50}/ml. This observation therefore indicates that viral load and ciliary activity may not necessarily correlate.

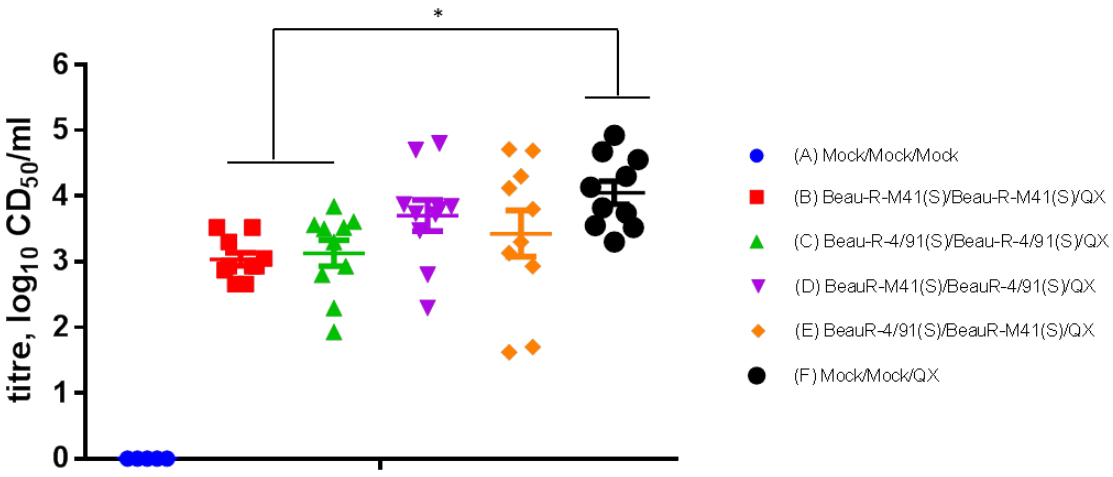

Figure 4.9: Infectious viral load in the trachea 4 days post challenge. Tissue derived supernatant prepared from trachea sections harvested four dpc was titrated in *ex vivo* TOCs. Data points represent individual animals, with lines representing the mean and standard error of the mean (SEM). Statistical differences in viral load were evaluated by a parametric one-way ANOVA with a Tukey test for multiple comparisons. Statistical differences are highlighted by * ($p< 0.05$).

Viral RNA loads in the head-associated lymphoid tissues at 2 and 4 dpc were also investigated and were determined by qPCR (Figure 4.10). This experiment was carried out by Dr. Samantha Ellis at The Roslin Institute. CALT extracted 4 dpc from chickens vaccinated with BeauR-M41(S)/BeauR-4/91(S) and BeauR-4/91(S)/BeauR-M41(S) showed a significant reduction ($p<0.05$) in viral RNA load compared to the mock vaccinated/QX challenged control group (Figure 4.10D). Interestingly, there was no significant reduction in viral load in the group vaccinated with BeauR-M41(S)/BeauR-M41(S) nor the group vaccinated with BeauR-4/91(S)/BeauR-4/91(S), both of which had lower infectious viral load in the trachea (Figure 4.9). There were no significant differences in viral RNA load between the vaccinated groups and the mock vaccinated/QX challenged control group in the head-associated lymphoid tissues (harderian gland) at any of the post-challenge time points (Figure 4.10A and C).

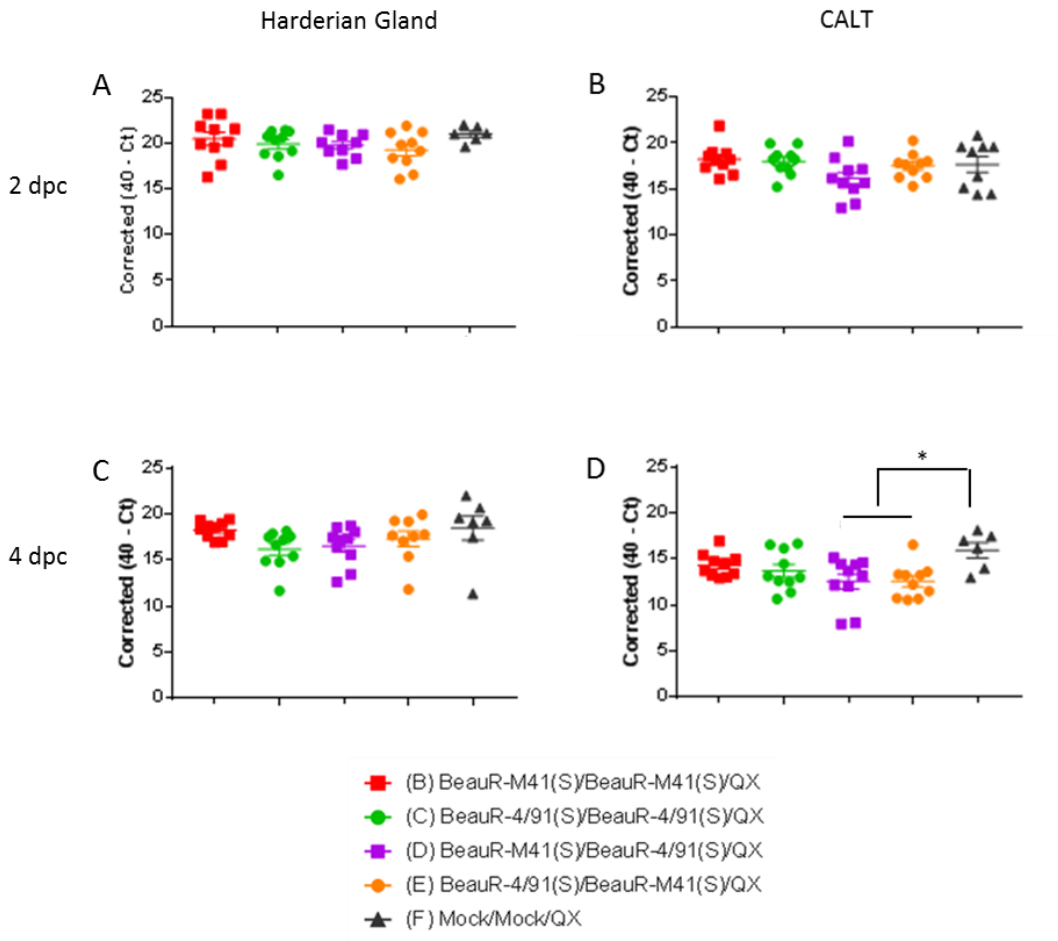

Figure 4.10: Viral load in the CALT and Harderian gland 2 and 4 days post challenge. Relative viral RNA load (expressed as corrected 40- cycle threshold, Ct) was assessed at specific time-points: (A) Harderian gland at 2 dpc, (B) CALT at 2 dpc, (C) Harderian gland at 4 dpc and (D) CALT at 4 dpc. Data points are shown as individual animals (three technical replicates per animal; n= 6 – 10 per group), lines represent the group mean and error bars represent the SEM. Statistical differences between groups were evaluated using one-way ANOVA with Tukey's multiple comparisons. Significant differences are highlighted by * (p<0.05). This work was completed by Dr. Samantha Ellis at The Roslin Institute.

4.2.4 Vaccination with a rIBV induces the production of IBV-specific antibodies.

Serum IBV-specific antibodies were assessed, using a commercial ELISA assay, 2 days pre-challenge (21 days post primary vaccination), by Dr. Samatha Ellis at The Roslin Institute. Antibody titres in the vaccinated groups were compared to the mock vaccinated control group (Figure 4.11). Mean titres were significantly higher in all the vaccinated groups in comparison to the mock vaccinated group (p<0.0001), indicating that vaccination had resulted in the generation of anti-IBV antibodies. There were no significant differences between the mean titres of each of the vaccination groups.

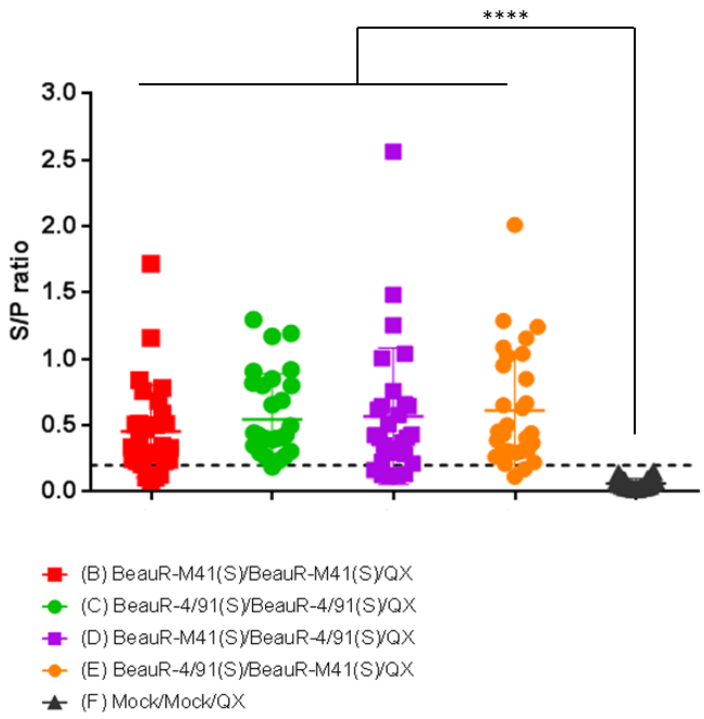

Figure 4.11: Vaccination with rIBV induced the production of anti-IBV antibodies. Serum anti-IBV titres were assessed by commercial ELISA (BioChek). Pre-challenge serum samples were diluted 1:80. The mean S/P from each group (n=20 or 30) is presented and this includes four technical replicates per sample. The dashed line indicates the cut-off threshold for positive samples (S/P ratio=0.2). The error bars represent the SD. Statistical differences between the group antibody titre means at pre-challenge were assessed using Kruskal Wallis and Dunn's multiple comparison tests. Significant differences are highlighted by **** (p<0.0001). This work was completed by Dr. Samantha Ellis at The Roslin Institute.

4.2.5 Vaccination with rIBV primed chickens for a boosted humoral response to challenge.

Using the same methodology anti-IBV serum antibody titres were also investigated at 4 dpc, also by Dr. Samantha Ellis at The Roslin Institute. At dilutions 1:80 through to and including 1:320, titres were significantly higher in all of the vaccinated groups compared to the mock vaccinated/QX challenge control group (Figure 4.12, $p<0.05$, Table 4.3). Serum dilution 1:640 displayed the same pattern except there were no significant differences between titres in the group vaccinated with BeauR-M41(S)/BeauR-M41(S) and the unvaccinated/QX challenged control group. At all dilutions the titres in the mock vaccinated/QX challenge control group remained below detection level. Overall the higher titres of anti-IBV antibody observed, indicates that vaccination with rIBV BeauR-M41(S) and/or BeauR-4/91(S) primed the birds for a boosted humoral response to challenge.

Further analysis highlighted significant differences observed between the vaccinated groups, indicating variations in the capability of the vaccine strategies to induce humoral responses. Serum anti-IBV titres were significantly higher in the BeauR-4/91(S)/BeauR-M41(S) vaccinated group compared to all the other vaccinated groups (Figure 4.12, Table 4.3, $p<0.05$). Interestingly, in comparison, when the birds were vaccinated in the reverse order, i.e. BeauR-M41(S)/BeauR-4/91(S), the titres were significantly lower. At all dilutions titres observed in the BeauR-M41(S)/BeauR-4/91(S) and the BeauR-4/91(S)/BeauR-4/91(S) group were similar suggesting the generation of a comparable humoral response to vaccination. At dilutions 1:80 through to and including 1:320, vaccination with BeauR-M41(S)/BeauR-M41(S) induced the lowest titres ($p<0.05$).

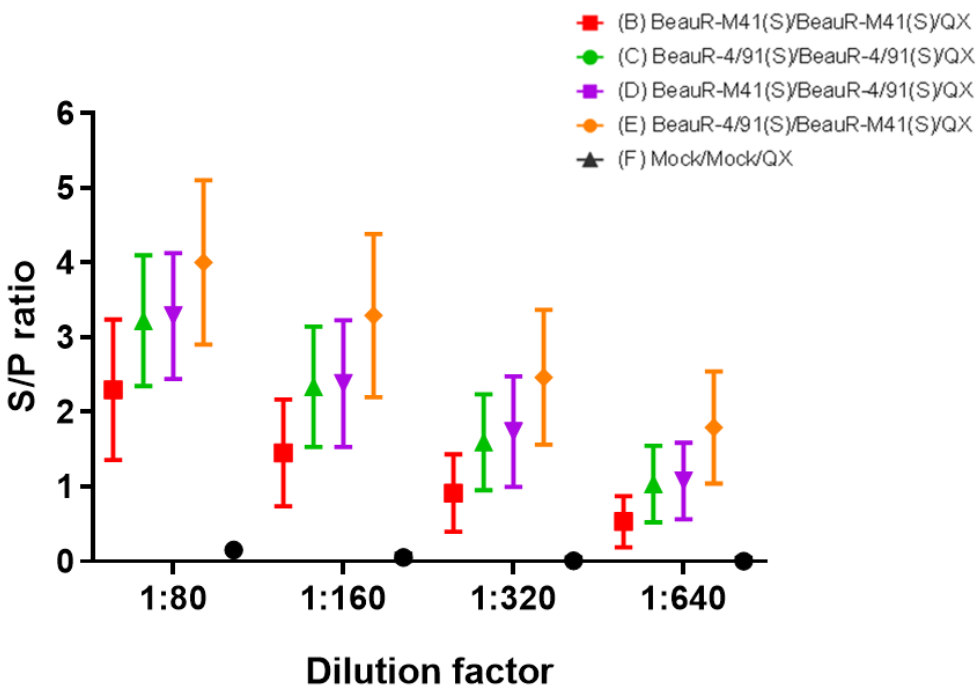

Figure 4.12: Vaccination with rIBV boosts the humoral response to heterologous QX challenge at 4pc. Serum anti-IBV titres were assessed by commercial ELISA (BioChek) at 4 dpc. Serum samples were diluted from 1:80 to 1:2560. The mean S/P of four technical replicates of each bird from each group is presented. The dashed line indicates the cut-off threshold for positive samples (S/P ratio=0.2). The error bars represent SD. Statistical differences between the groups were assessed two-way ANOVA with a Tukey multiple comparison test. Statistical differences are displayed Table 4.3. This work was completed by Dr. Samantha Ellis at The Roslin Institute.

Table 4.3: Statistical analysis of serum antibody titres at day 4 dpc.

Dilution	Groups	Significant	P Value
1:80	BeauR-M41(S)/BeauR-M41(S) vs. BeauR-4/91(S)/BeauR-4/91(S)	***	0.0008
	BeauR-M41(S)/BeauR-M41(S) vs. BeauR-M41(S)/BeauR-4/91(S)	***	0.0003
	BeauR-M41(S)/BeauR-M41(S) vs. BeauR-4/91(S)/BeauR-M41(S)	****	<0.0001
	BeauR-M41(S)/BeauR-M41(S) vs. Mock/QX	****	<0.0001
	BeauR-4/91(S)/BeauR-4/91(S) vs. BeauR-M41(S)/BeauR-4/91(S)	ns	0.9987
	BeauR-4/91(S)/BeauR-4/91(S) vs. BeauR-4/91(S)/BeauR-M41(S)	**	0.0074
	BeauR-4/91(S)/BeauR-4/91(S) vs. Mock/QX	****	<0.0001
	BeauR-M41(S)/BeauR-4/91(S) vs. BeauR-4/91(S)/BeauR-M41(S)	*	0.0181
	BeauR-M41(S)/BeauR-4/91(S) vs. Mock/QX	****	<0.0001
	BeauR-4/91(S)/BeauR-M41(S) vs. Mock/QX	****	<0.0001
1:160	BeauR-M41(S)/BeauR-M41(S) vs. BeauR-4/91(S)/BeauR-4/91(S)	**	0.0015
	BeauR-M41(S)/BeauR-M41(S) vs. BeauR-M41(S)/BeauR-4/91(S)	***	0.0007
	BeauR-M41(S)/BeauR-M41(S) vs. BeauR-4/91(S)/BeauR-M41(S)	****	<0.0001
	BeauR-M41(S)/BeauR-M41(S) vs. Mock/QX	****	<0.0001
	BeauR-4/91(S)/BeauR-4/91(S) vs. BeauR-M41(S)/BeauR-4/91(S)	ns	0.9997
	BeauR-4/91(S)/BeauR-4/91(S) vs. BeauR-4/91(S)/BeauR-M41(S)	***	0.0005
	BeauR-4/91(S)/BeauR-4/91(S) vs. Mock/QX	****	<0.0001
	BeauR-M41(S)/BeauR-4/91(S) vs. BeauR-4/91(S)/BeauR-M41(S)	**	0.001
	BeauR-M41(S)/BeauR-4/91(S) vs. Mock/QX	****	<0.0001
	BeauR-4/91(S)/BeauR-M41(S) vs. Mock/QX	****	<0.0001
1:320	BeauR-M41(S)/BeauR-M41(S) vs. BeauR-4/91(S)/BeauR-4/91(S)	*	0.0295
	BeauR-M41(S)/BeauR-M41(S) vs. BeauR-M41(S)/BeauR-4/91(S)	**	0.0042
	BeauR-M41(S)/BeauR-M41(S) vs. BeauR-4/91(S)/BeauR-M41(S)	****	<0.0001
	BeauR-M41(S)/BeauR-M41(S) vs. Mock/QX	*	0.0276
	BeauR-4/91(S)/BeauR-4/91(S) vs. BeauR-M41(S)/BeauR-4/91(S)	ns	0.9744
	BeauR-4/91(S)/BeauR-4/91(S) vs. BeauR-4/91(S)/BeauR-M41(S)	**	0.002
	BeauR-4/91(S)/BeauR-4/91(S) vs. Mock/QX	****	<0.0001
	BeauR-M41(S)/BeauR-4/91(S) vs. BeauR-4/91(S)/BeauR-M41(S)	*	0.0162
	BeauR-M41(S)/BeauR-4/91(S) vs. Mock/QX	****	<0.0001
	BeauR-4/91(S)/BeauR-M41(S) vs. Mock/QX	****	<0.0001
1:640	BeauR-M41(S)/BeauR-M41(S) vs. BeauR-4/91(S)/BeauR-4/91(S)	ns	0.1909
	BeauR-M41(S)/BeauR-M41(S) vs. BeauR-M41(S)/BeauR-4/91(S)	ns	0.134
	BeauR-M41(S)/BeauR-M41(S) vs. BeauR-4/91(S)/BeauR-M41(S)	****	<0.0001
	BeauR-M41(S)/BeauR-M41(S) vs. Mock/QX	ns	0.4115
	BeauR-4/91(S)/BeauR-4/91(S) vs. BeauR-M41(S)/BeauR-4/91(S)	ns	0.9998
	BeauR-4/91(S)/BeauR-4/91(S) vs. BeauR-4/91(S)/BeauR-M41(S)	*	0.0108
	BeauR-4/91(S)/BeauR-4/91(S) vs. Mock/QX	**	0.0071
	BeauR-M41(S)/BeauR-4/91(S) vs. BeauR-4/91(S)/BeauR-M41(S)	*	0.0182
	BeauR-M41(S)/BeauR-4/91(S) vs. Mock/QX	**	0.0046
	BeauR-4/91(S)/BeauR-M41(S) vs. Mock/QX	****	<0.0001

Notes: Serum anti-IBV titres were assessed by commercial ELISA (BioChek) at 4 dpc (Figure 4.12). Statistical differences between the groups were assessed two-way ANOVA with a Tukey multiple comparison test. This work was completed by Dr. Samantha Ellis at The Roslin Institute.

- Purple: Titres in vaccinated groups are higher than the unvaccinated/QX challenged control group.
- Orange: Titres observed in BeauR-4/91(S)/BeauR-M41(S) group are higher in comparison to all other vaccinated groups.
- Green: There is no difference in serum antibody titres between groups vaccinated with BeauR-M41(S)/BeauR-4/91(S) and BeauR-4/91(S)/BeauR-4/91(S).

Anti-IBV serum titres were assessed, also by Dr. Samantha Ellis at The Roslin Institute, at 14 dpc, the final day of the *in vivo* experiment (Figure 4.13). At this point birds were considered to have recovered from the QX challenge infection as no clinical signs were observed (Figure 4.6 and 4.7). Similarly to 4 dpc, serum antibody titres were significantly higher in all of the vaccinated groups in comparison to the unvaccinated/QX challenged control group (p<0.0001). This observation provides further evidence that the vaccination strategies have primed the birds for a boosted humoral antibody in response. Unlike serum titres at 4 dpc, however, there were no significant differences between the anti-IBV titres observed between the vaccinated groups, indicating at this stage of infection no one vaccination strategy was more effective than the others.

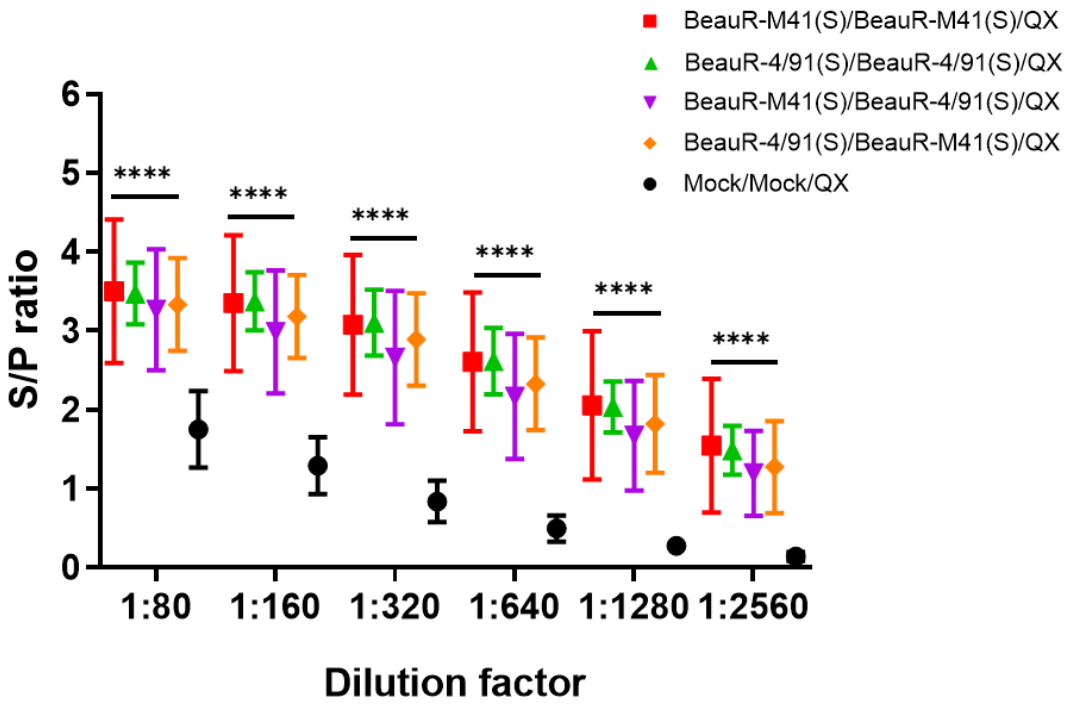

Figure 4.13: At 14 dpc all vaccinated groups displayed a boosted humoral response to challenge with QX. Serum anti-IBV titres were assessed by commercial ELISA (BioChek) at 14 dpc. Serum samples were diluted from 1:80 to 1:2560. The mean S/P of four technical replicates of each bird from each group is presented. The dashed line indicates the cut-off threshold for positive samples (S/P ratio=0.2). The error bars represent SD. Statistical differences between the groups were assessed one-way ANOVA with a Friedman test and Dunn's multiple comparison test. Statistical differences in comparison to the mock vaccinated/QX challenge control group (Mock/Mock/QX) are highlighted by **** (p<0.0001). This work was completed by Dr. Samantha Ellis at The Roslin Institute.

4.2.6 Shared epitopes between M41-CK and QX or 4/91 may not be neutralising to M41-CK infection.

Sequence alignment of the S glycoproteins of M41-CK, QX and 4/91 (Appendix, Figure 8.3) highlight shared regions of amino acid sequences and therefore the potential for shared epitopes, and in turn the potential for cross reactive antibodies. A series of plaque reduction assays was used to investigate the cross neutralising ability of specific anti-IBV sera. If sera raised against one strain of IBV were able to neutralise infection with a different strain of IBV, the sera would be considered to be cross neutralising, and therefore contain cross-reactive antibodies. In turn, this would indicate the presence of shared neutralising epitopes between the IBV strain in which the sera was raised against and the IBV strain used in the plaque reduction assay.

The IBV QX challenge strain used in the *in vivo* vaccine-challenge experiment is not able to be propagated *in vitro* (Bickerton *et al.,* 2018b) limiting the ability to assess whether neutralising antibody against QX is present in anti-M41, anti-4/91 and anti-QX sera. However, the neutralising ability of these sera against the IBV M41-CK and rIBVs BeauR-M41(S) and Beau-R is possible to assess *in vitro*. To investigate this, sera harvested from QX (anti-QX), 4/91 (anti-4/91), M41-CK (anti-M41-CK) and mock infected chickens was incubated with either Beau-R, BeauR-M41(S) or M41-CK. After a defined incubation period, the quantity of remaining infectious particles was determined through titration in CK cells. In this assay, if the sera contained antibodies capable of fully neutralising viral infection, no infectious particles would remain therefore resulting in a 100% plaque reduction.

The anti-M41-CK serum was neutralising to both M41-CK and BeauR-M41(S) with both viruses exhibiting comparable % plaque reduction profiles (Figure 4.14). At sera dilutions 1:20 to 1:80 both M41-CK and BeauR-M41(S) exhibited a greater than 50% reduction in PFU, indicating that at these dilutions anti-M41-CK sera was able to neutralise at least 50% of infectious particles. A less than 25% reduction in PFU was observed with both 1:160 and 1:320 dilutions. This would indicate that individual populations of neutralising antibody present in the un-diluted anti-M41-CK sera, and in the sera at dilutions 1:20 to 1:80, had possibly been diluted out thereby reducing the overall neutralising ability of that sera dilution. It is also possible that whilst no individual antibody population was missing from the sera at dilution 1:160 and 1:320 that populations of individual antibodies had instead been diluted to levels that were only partially effective, which would again reduce the overall neutralising ability of that sera dilution.

The similarity of the response of both M41-CK and BeauR-M41(S) to anti-M41-CK sera supports the notion that the majority of neutralising antibodies are directed against the S glycoprotein. If neutralising antibodies against other IBV proteins were present at detectable levels it would be expected that there would be a difference between the neutralisation profiles of M41-CK and BeauR-M41(S). Supporting this, Beau-R which contains a different S glycoprotein did not display a comparable neutralisation profile in response to anti-M41-CK sera (Figure 4.14). No plaques were observed after infection with Beau-R that had been incubated with 1:20, 1:40 and 1:80 dilutions of anti-M41-CK sera. At dilution 1:160 the mean reduction in PFU was 76% indicating that over 75% of infectious viral particles had been neutralised. The neutralisation observed at this dilution was greater than that exhibited for both M41-CK at 23% and BeauR-M41(S) at 16% ($p<0.001$). Interestingly, both M41-CK and Beau-R belong to the Massachusetts serotype and amino acid identity between the S glycoprotein is high at >95% (appendix). The difference in neutralisation profiles is therefore the result of the small, 5%, difference in amino acids.

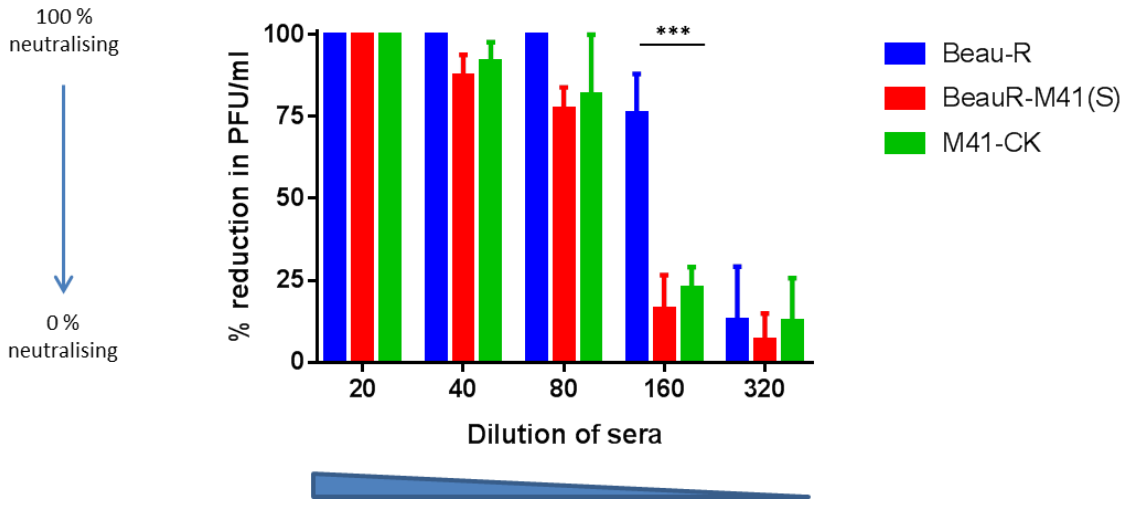

Figure 4.14: An Anti-M41-CK serum is able to neutralise M41-CK, BeauR-M41(S) and Beau-R infection *in vitro*. 100 PFU of M41-CK, BeauR-M41(S) or Beau-R was incubated with dilutions of either anti-M41-CK sera or mock sera. The quantity of infectious virus neutralised was assessed through titration in CK cells in triplicate. The percentage difference in the number of PFU/ml between the samples incubated with mock sera and those incubated with anti-M41-CK sera was calculated. Each point represents the mean of three independent replicates, with error bars representing the SEM. Differences were evaluated using a 2way ANOVA with a Tukey test for multiple comparisons. Significant differences ($p<0.005$) between neutralisation of Beau-R in comparison to both M41-CK and BeauR-M41(S) in response to anti-M41-CK sera are highlighted by ***.

The ability of anti-QX and anti-4/91 sera to neutralise M41-CK infection was also investigated. Beau-R, BeauR-M41(S) or M41-CK was incubated with decreasing quantities of either anti-QX, anti-4/91 or mock sera. Neutralisation was assessed through titration in CK cells. Decreasing quantities of sera had minimal effect on viral titre, indicating that antibodies present in the anti-QX and anti-4/91 serum were incapable of neutralising BeauR-M41(S), M41-CK or Beau-R infections at the dilutions assessed (Figure 4.15A to 4.15F). A small difference was observed between the response of Beau-R to anti-QX sera and to mock sera at dilution 1/20 ($p<0.005$). The titre of Beau-R at this dilution was approximately 0.5 $\log_{10}$ lower after incubation with anti-QX sera in comparison to after incubation with mock sera (Figure 4.15F). Similarly a small difference was observed at dilution 1/320 when comparing M41-CK infection in response to mock and anti-4/91 sera ($p<0.05$) (Figure 4.15A). In this case viral titre was higher in those samples incubated with anti-4/91 sera than those incubated with mock sera so whilst statistically different the biological relevance may be minimal.

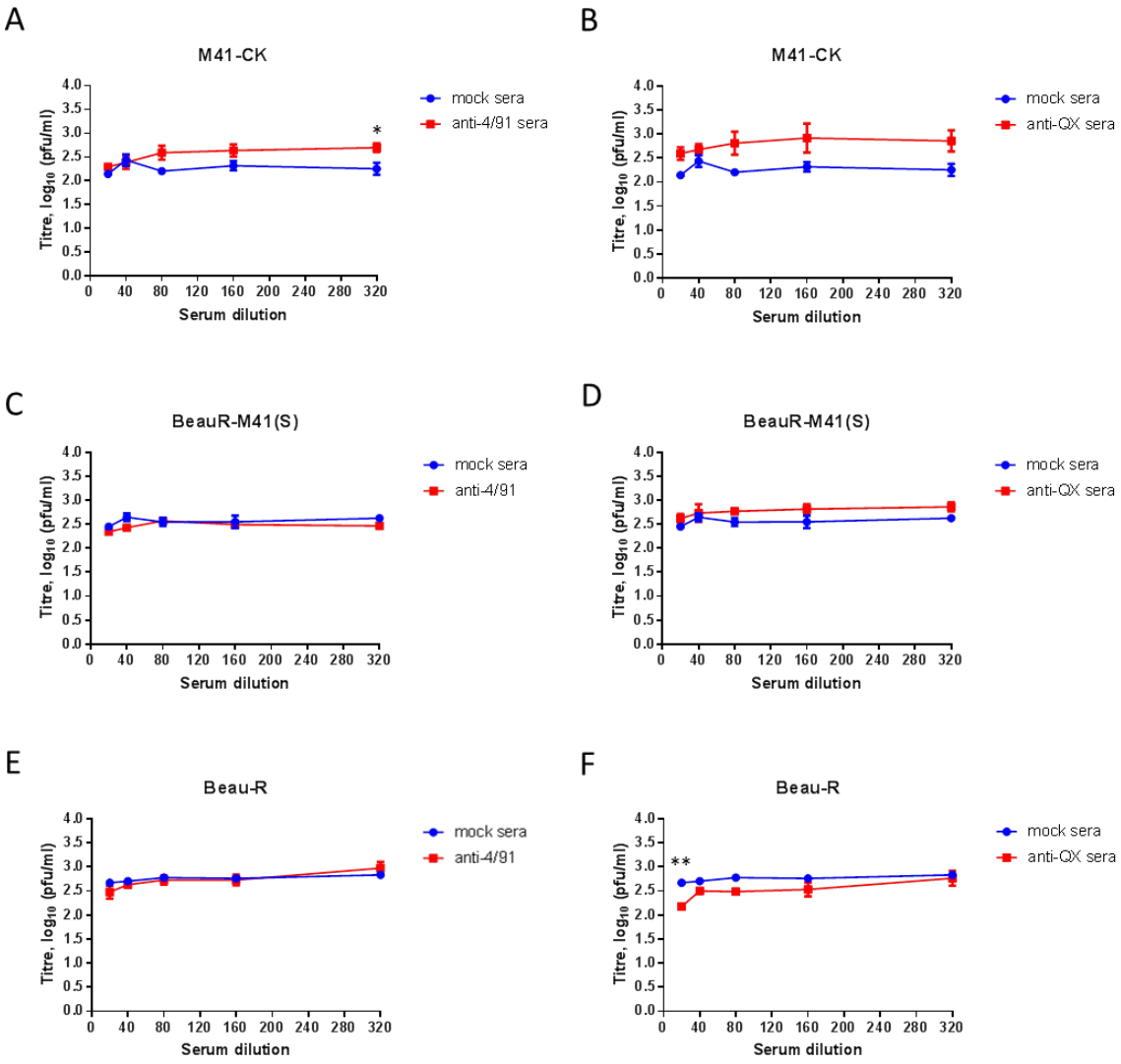

Figure 4.15: Anti-QX and anti-4/91 sera are not able to prevent M41-CK, BeauR-M41(S) nor Beau-R infection *in vitro*. 100 PFU of M41-CK, BeauR-M41(S) or Beau-R was incubated with 2 fold serial dilutions of either anti-QX, anti-4/91 sera or mock sera. The quantity of infectious virus neutralised was assessed through titration in CK cells in triplicate. The titre (PFU/ml) resulting from each dilution is shown. Each point represents the mean of three independent replicates, with error bars representing the SEM. Differences were evaluated using a Two-way ANOVA with a Tukey test for multiple comparisons. Significant differences are highlighted by * ($p<0.05$) and ** ($p<0.005$).

4.3 Discussion.

There have been numerous studies that have addressed the question of cross protective immunity against IBV reporting varying degrees of success (Wang *et al.,* 1996; Cavanagh *et al.,* 1997; Cook *et al.,* 1999; Terregino *et al.,* 2008; Lim *et al.,* 2012; Bru *et al.,* 2017). It is thought that the chances of a successful vaccination decrease as the amino acid homology between the S glycoprotein of the vaccine and challenge strain also decreases (Cavanagh *et al.,* 1997; Cook *et al.,* 1999). As homology decreases, the likelihood of differences in important neutralising epitopes increases. It is possible, however for vaccines to offer successful protection against heterologous challenge when sequence homology between the vaccine and challenge strain is deemed low (as reviewed in de Wit *et al.,* 2011), presumably due to conserved structural homology of important neutralising epitopes. It is likely therefore a small number of virus neutralising epitopes play a disproportionate role in cross-protection (Cavanagh *et al.,* 1997). Although the location of some neutralising monoclonal antibody epitopes are known (Mockett *et al.,* 1984, Mockett *et al.,* 1988; Kant *et al.,* 1992) it remains unknown which epitopes are required for the successful induction of cross-protective immunity. It therefore continues to be important to assess vaccine strategies against heterologous challenge.

Several previous studies have utilised commercial vaccines produced via the traditional method of passaging a field isolate through embryonated hens' eggs to produce an attenuated virus. As such, these commercial vaccines closely resemble the challenge strains, and it is therefore difficult to assess the individual contribution of each viral protein towards both homologous and heterologous immunity. As discussed in Chapter 3 the S glycoprotein or the S1 subunit has been expressed in a number of viral or bacterial vectors (Song *et al.,* 1998; Johnson *et al.,* 2003; Hodgson *et al.,* 2004; Chen *et al.,* 2010; Armesto *et al.,* 2011; Yan *et al.,* 2013; Zhoa *et al.,* 2017; Ellis *et al.,* 2018; Shirvani *et al.,* 2018) however there is no consensus in the field of the markers of protection and therefore it is difficult to compare levels of protection achieved against either homologous or heterologous challenge. It is also unclear how the expressed protein is presented, whether it assembles into trimers, whether it is anchored to a membrane thereby aiding conformation or whether the S1 is only expressed as a monomeric unit. The recombinant viruses used in this chapter and also used by Hodgson *et al.,* (2004), Armesto *et al.,* (2011) and Ellis *et al.,* (2018) express heterologous S glycoproteins from a rIBV vector. As such the S glycoproteins are expected to be trimeric and anchored into a viral membrane. Host processing of the S glycoprotein, such as glycosylation and palmitoylation, should also occur as in a natural WT IBV infection. The presentation of the expressed S glycoprotein to the host immune system should also be

comparable to WT infection. Alongside these benefits, vaccination with rIBV BeauR-M41(S) and BeauR-4/91(S) allowed for characterisation of the role of the 4/91 and M41-CK S glycoproteins in the induction of a protective immune response against a heterologous QX challenge as all other proteins in the vaccine viruses are Beaudette derived. Amino acid sequence identity of M, E and N between QX and Beau-R is 92%, 88% and 90% respectively (Appendix 8.4, 8.5, 8.6). In previous studies that have investigated vaccination with both Massachusetts and 4/91 serotypes against a QX challenge it is difficult to be as certain whether the protective response induced is solely the result of the presence of the S glycoprotein of either the Massachusetts strain or 4/91 strain (Terrenigo *et al.,* 2008; Awad *et al.,* 2016, de Wit *et al.,* 2011B).

Vaccination with BeauR-M41(S) or with BeauR-4/91(S) in any combination did not induce a fully protective immune response, as defined by the European Pharamacopeia (2010), against the QX challenge, as ciliary activity in all vaccinated groups was largely reduced to less than 25% by the QX infection (Figure 4.8). Two birds that were vaccinated with BeauR-4/91(S)/BeauR-491(S) were observed to retain more ciliary activity, however, only one sample would be deemed as protected by the European Pharamacopeia (2010) standards. To determine whether this vaccination combination offers protection to 10% of birds or whether this bird was an anomaly would require a much larger sample size. However, despite the overall reductions in ciliary activities observed, there are indications that each of the vaccination strategies induced an immune response that resulted in positive differences post challenge. All vaccinated groups appeared to recover more rapidly from clinical signs than the mock vaccinated/QX challenged control group (Figure 4.6 and 4.7). In groups which received the same primary and secondary vaccination, BeauR-M41(S)/BeauR-M41(S) or BeauR-4/91(S)/BeauR-4/91(S), less infectious challenge virus was present in the tracheas of the vaccinated birds at 4 dpc than in the mock vaccinated/QX challenged control group (Figure 4.9). Also in comparison to the mock vaccinated/QX challenge control group, lower viral RNA loads were detected in the CALT at 4 dpc (Figure 4.10) in birds vaccinated with different primary and secondary vaccinations, BeauR-M41 (S)/BeauR-4/91(S) or BeauR-4/91(S)/BeauR-M41(S). In addition all vaccinated groups at 4 dpc had higher titres of serum anti-IBV antibody than the mock vaccinated/mock challenged control group (Figure 4.12).

Previous research has suggested that the order in which live attenuated IBV vaccines are administered affects the outcome of heterologous challenge. Cook *et al.,* (1999) concluded that better cross protection was seen when a Ma5 (Massachusetts serotype) vaccine was administered before a 4/91 vaccine. It must be noted that both Beau-R and M41-CK are of

the Massachusetts serotype. Bourogaa *et al.,* (2014), Awad *et al.,* (2016) and Bru *et al.,* (2017) have all demonstrated a degree of cross protection using a Massachusetts vaccine followed by a secondary vaccine of a different serotype. These studies, however, did not directly compare the reverse order. In this study at 4 dpc whilst in terms of ciliary activity there was no difference between those birds vaccinated with BeauR-M41(S)/BeauR-4/91(S) and BeauR-4/91(S)/BeauR-M41(S), the order in which the BeauR-M41(S) (Massachusetts serotype) and BeauR-4/91(S) (4/91 serotype) were administered did appear to have affected serum antibody levels. Serum antibody titres were significantly higher in the group vaccinated with BeauR-4/91(S)/BeauR-M41(S) suggesting in this study, in terms of seropositivity, a 4/91 vaccine followed by an Massachusetts vaccine gave a better result. One possible explanation for this observation is that vaccination with BeauR-M41(S) may have induced an immune response that was partially neutralising toward BeauR-4/91(S).This in turn may have limited the replication of BeauR-4/91(S) and consequently impacted on the effectiveness of the second vaccination. Conversely BeauR-4/91(S) may not elicit a cross neutralising response toward BeauR-M41(S). Further work therefore could involve neutralisation assays investigating the response of BeauR-M41(S) and BeauR-4/91(S) to anti-BeauR-M41(S) and BeauR-4/91(S) sera.

Despite the indication that the vaccination strategies employed in this study have induced an immune response, ultimately the vaccines did not offer full protection against a QX challenge. This was unexpected as it contradicts previous work that has demonstrated that commercially available Massachusetts and 4/91 vaccines could offer protection against a QX challenge (Terregino *et al.,* 2008, de Wit *et al.,* 2011B, Awad *et al.,* 2016,). Awad *et al.,* (2016) investigated combinations of Ma5 (Massachusetts serotype) or H120, also of the Massachusetts serotype alongside 793B vaccines (4/91 serotype) against heterologous QX challenge; ciliary activity was reported at 68 and 92% respectively. Similarly de Wit *et al.,* (2011B) used a combination of Massachusetts vaccines or a mixture of Massachusetts combined with a D274 serotype, followed by a 793B vaccine reporting protection, as defined by ciliary activities, of 51% and 89% respectively. Terregino *et al.,* (2008) also evaluated vaccination with Ma5 and 4/91, against a QX challenge. Unlike this study in which challenge virus could be detected in the tracheas from all vaccinated/challenged chickens, Terregino *et al.,* (2008) detected no challenge virus in those SPF chickens that received vaccination. It is difficult to directly compare vaccine-challenge experiments due to differences in age of bird, breed, the SPF status of the birds, and the definition of protection, whether that be ciliary activity, viral load or seropositivity (reviewed by de Wit and Cook, 2014). Terregino *et al.,* (2008) did not assess ciliary activity and it is well documented that viral load and ciliary activity do not always correlate (Hodgson *et al.,* 2004; Armesto *et al.,* 2011; reviwed by de Wit and Cook, 2014; Ellis *et al.,* 2018). Similarly seropositivity and protection do not always

correlate (reviwed by de Wit and Cook, 2014). Whilst de Wit *et al.,* (2011B) did assess ciliary activity, the sampling points were 5, 8 and 11 dpc, and therefore not exactly comparable to the sampling point used in this study, 4 dpc. In addition, no clinical signs data was reported, and the age of the chickens, at both vaccination and challenge were also not comparable. It is also worth noting that both Terregino *et al.,* (2008) and Awad *et al.,* (2016) vaccinated birds that contained maternally derived antibody although this is thought to have a negative impact on vaccination (Klieve and Cumming, 1988). The inability of BeauR-M41(S) and BeauR-4/91(S) to induce a protective immune response against heterologous virus challenge, in terms of both ciliary activity and clinical disease (Figure 4.6 – 4.8) as well as challenge virus replication (Figure 4.9 – 4.10) is a notably different result to that published by Terregino *et al.,* (2008), de Wit *et al.,* (2011B) and Awad *et al.,* (2016). This raises some interesting questions, and may suggest that the S glycoprotein from either M41-CK and/or 4/91 alone may not be sufficient to elicit a protective immune response against a heterologous QX challenge.

Protective immunity against IBV is thought to largely involve the presence of antibodies capable of neutralising viral infection, and it has been demonstrated that the majority of these antibodies are directed against the S glycoprotein (Cavanagh *et al.,* 1986, Cavanagh and Davis, 1986; Ignjatovic and Galli, 1994). The comparative response of BeauR-M41(S) and M41-CK to anti-M41-CK sera supports this (Figure 4.14). The vaccine viruses used within this study did elicit an anti-IBV antibody response, with a boosted (memory) humoral response identified in response to the QX challenge in all vaccinated groups at 4 dpc (Figure 4.12). It remains to be determined whether the antibody response induced by BeauR-M41(S) and BeauR-4/91(S) elicited antibodies capable of neutralising the QX challenge virus. The restricted tropism of the QX strain used in this study (Bickerton *et al.,* 2018B) makes this question difficult to comprehensively answer. *In vitro* plaque reduction assays however identified that anti-QX and anti-4/91 sera could not fully neutralise M41-CK, BeauR-M41(S) nor Beau-R infection at dilutions 1:20 through to 1:320 (Figure 4.15). These assays, however, cannot definitely conclude that potential shared epitopes are not neutralising as it is possible that antibody directed against these epitopes has been diluted to a point where the effect is minimal. The small but significant difference between Beau-R infection after incubation with 1:20 mock sera and 1:20 anti-QX sera may support this. In a previous study, two-way cross neutralisation assays including a comparison between M41 and D388 as well as M41 and 4/91 have identified very low titres of neutralising antibody (de Wit *et al.,* 2011B). It is, unfortunately, not possible to assess less diluted sera largely due to limited quantity of sera paired with the relatively sizable quantities needed for plaque reduction based neutralisation assays.

Whether anti-M41-CK or anti-4/91 sera can neutralise QX infection *in vitro* remains an unanswered question. There are two possible alternatives to QX for the *in vitro* assessment of neutralising antibody presence in sera harvested as part of this *in vivo* vaccine-challenge experiment. One possible alternative is to utilise rIBV BeauR-QX(S1) as the majority of neutralising antibodies are thought to be directed against the S1 subunit (Mockett *et al.,* 1984; Cavanagh *et al.,* 1986, Cavanagh and Davis, 1986). This rIBV expresses the QX S1 subunit and the Beau-R S2 subunit which enables the virus to replicate in Vero cells (Bickerton *et al.,* 2018B). Vero cells would offer a number of advantages for use in neutralisation assays over the current protocol that uses primary CK cells, including a less limited supply and the ability to reliably seed in 96 well plates producing a clear monolayer. This would allow neutralisation to be defined by presence or absence of IBV induced CPE, rather than the more labour intensive and time consuming method of titration in CK cells to determine the PFU. BeauR-QX(S1) was however used as a vaccine virus in Chapter 3 and was unable to induce a protective immune response to a homologous QX challenge with possible misfolding of the chimeric S glycoprotein hypothesised as a potential reason. Further research is required to investigate this possibility which this could include neutralisation assays using monoclonal antibodies targeted toward the S1 and S2 subunits.

The second possible alternative to QX is the IBV strain D388 which was isolated in The Netherlands in 2004, and is deemed QX like. Sequencing results have reported that it is of the QX genotype with 98% sequence homology in the S1 subunit (de Wit *et al.,* 2011b; YuDong *et al.,* 1998; Liu and Kong, 2004). Virus neutralisation assays have yet to directly compare the original Chinese QX isolate to D388, and therefore as a result D388 cannot be defined as a QX serotype, and instead is referred to as D388 (QX) serotype. In house sequencing data identifies that D388 only has two amino acid differences in the S glycoprotein to the QX strain used in this study (unpublished data). In addition, across the whole genome there are only a further 41 nucleotide differences. This sequence similarity alongside the ability of D388 to replicate in CK cells (Chapter 5, Figure 5.8) identifies D388 as a possible suitable alternative to QX in the assessment of neutralising antibody generated through the vaccination strategies employed in this study. However, further research is required to demonstrate whether the sera raised against QX has the ability to neutralise D388 *in vitro* comparably to sera raised against D388.

Despite the limitations, the plaque reduction assays presented in this study alongside the inability of the vaccine viruses BeauR-M41(S) and BeauR-4/91(S) to elicit a protective immune response against a heterologous IBV could suggest that potential shared epitopes

on the S glycoprotein when expressed by a Beaudette vaccine vector do not generate cross protective antibodies, or do not do so in a quantity that positively affects the outcome after challenge. As stated, both Awad *et al.,* (2016) and Terregino *et al.,* (2008) did report a protective immune response using 4/91 serotype vaccines and Massachusetts vaccines, indicating the presence of shared neutralising epitopes. In both studies, however, the presence of neutralising antibody was not directly assessed. Amino acid sequence identity between the S glycoproteins of 4/91 and QX is 83.5% with M41-CK and QX sharing a similar percentage at 81.8%. The difference of 20% may therefore have removed neutralising epitopes. Further work utilising D388 as an alternative to QX in neutralisation assays is required to establish whether the vaccination with BeauR-M41(S) and/or BeauR-4/91(S) did elicit the generation of neutralising antibodies against QX. The results of these assays would therefore help to inform whether the 20% difference in sequence has in fact removed cross protective neutralising epitopes.

One important factor to note is that, there are many different strains within a serotype all with sequence differences across the genome, including within the S gene (Adzhar *et al.,* 1995; Adhzar and Gough, 1997; Cavanagh *et al.,* 1992; Cavanagh *et al.,* 2005). Using the Massachusetts serotype as an example, the S glycoprotein of Ma5, used by both Terregino *et al.,* (2008) and Awad *et al.,* (2016) has a 4% difference in amino acid sequence identity to M41-CK (Appendix, Figure 8.3). Similarly the sequence difference between the H120 and M41-CK S glycoproteins is also 4% as is the difference between Beau-CK and H120. There is an approximate 4% sequence difference between the 793B vaccine, also known as CR88 (4/91 serotype) and the S glycoprotein of 4/91. Plaque reduction assays in this chapter assessing the neutralisation profile of Beau-R and M41-CK in response to anti-M41-CK sera, have demonstrated that even small differences between S glycoproteins, approximately 4%, can have quite a noticeable effect on neutralisation.

The same logic also applies to the challenge virus; this study used an isolate of QX derived from The Netherlands in 2004 (Worthington *et al.,* 2008) whereas Terregino *et al.,* (2008) used an isolate of QX derived from Italy in 2005. Although both isolates are classified as QX-like, the sequence diversity between these two isolates is unknown and may, alongside the differences of the S glycoproteins of the vaccine strains discussed above, may have contributed to the differences observed in the level of cross-protection between the studies. In addition, de Wit *et al.,* (2011B) used D388 and not QX; as discussed in the results section there are differences across the genome. In addition, passaging, even one passage to produce a stock virus from a master seed vial, in cells or embryonated hen's eggs, is enough

to result in consensus level changes (Cavanagh *et al.,* 2005). One final thought to consider regarding sequence differences is that both BeauR-M41(S) and BeauR-4/91(S) are clonal therefore decreasing the variety of epitopes that exist on a sub consensus level; it is possible that sequence diversity has a role in successful vaccination. Questions therefore remain as to whether neutralising epitopes to QX do exist within BeauR-4/91(S) and BeauR-M41(S), and if they do, why these vaccine viruses did not elicit a stronger humoral response.

One interesting question that has arisen from this study is regarding the role of the other structural proteins in vaccine acquired immunity. As well as humoral responses, innate and cell mediated responses have been demonstrated to play a vital role in the clearance of IBV infection as well as in vaccine induced protection (Seo and Collisson 1997; Vervelde *et al.,* 2013; Collisson *et al.,* 2000; Gurjar *et al.,* 2013). Meir *et al.,* (2012) investigated vaccination with recombinant N (rN) protein and S1 (rS1) expressed in *E.coli.* 40% of birds vaccinated with rS1 were negative for IBV post challenge compared to 10% vaccinated with rN. Interestingly an increased cell mediated response was seen in those birds vaccinated with rN than rS1. Several other studies have linked the N protein to cell mediated immunity (Seo *et al.,* 1997B; Boots *et al.,* 1991; Ignjatovic and Sapats, 2005) as well as identifying B cell epitopes (Ignjatovic and Sapats, 2005). In addition, partial protection has been demonstrated using adoptive transfer of memory CD8+ T cells (Pei *et al.,* 2003). Analysis of the N protein identifies variation in sequence identity across IBV strains; Beau-R and QX share a 90% amino acid identity, QX and Ma5 share 92%, QX and CR88 (4/91 serotype vaccine) share 91% (Appendix, Figure 8.6). Although it has been demonstrated that the coronavirus M or N proteins alone cannot induce a protective immune response (Ignjatovic and Galli, 1994; Buchholz *et al.,* 2004; Meir *et al.,* 2012), it does not mean that neither protein has a role. Buchholz *et al.,* (2004) investigated the contributions of the structural proteins of SARS-CoV, through expression in a parainfluenza vector (Buchholz *et al.,* 2004). Vaccination with a vector expressing S, M and E resulted in a 2000 fold reduction of challenge virus, whilst S alone resulted in a 500 fold decrease. It is possible that the inclusion of M and E led to the formation of virus like particles and broader stimulation of the immune system. It is therefore plausible that immune responses to other structural proteins play a role in the induction of protective IBV immune responses, and without these responses neutralising antibodies induced by the S glycoprotein are either insufficient alone or not generated in sufficient quantities to offer a fully protective immune response against either homologous or heterologous challenge. Ultimately, it is also possible that as homology between S glycoproteins of vaccine and challenge viruses decreases, the collaborative role of shared epitopes within the other structural proteins may play a larger role in protective immunity.

Another question that this study raises, the same question raised in Chapter 3, is what level of vaccine virus *in vivo* replication is required to induce a protective immune response? As discussed in Chapter 3, the rIBV Beau-R is a molecular clone of the apathogenic Beaudette-CK strain (Casais *et al.,* 2001). Chapter 3 investigated the ability of Beau-R expressing heterologous S1 and/or S2 subunits to induce protective immune responses against homologous challenge (Ellis *et al.,* 2018). Whilst rIBV BeauR-M41(S) induced protective immunity, as also reported by Hodgson *et al.,* (2004), the response was not as robust as expected, with vaccine viruses inducing poor levels of local immunity within the trachea. In addition, ciliary activity post challenge at 65%, fell short of the European Pharmacopeia standard for vaccines, a finding comparable to both Hodgson *et al.,* (2004), and Armesto *et al.,* (2011) who investigated homologous and heterologous challenge using BeauR-4/91(S). As discussed in Chapter 3, one possible explanation for this is the limited *in vivo* replication of the Beau-R based vaccine viruses. In this study, as in previous studies (Hodgson *et al.,* 2004; Armesto *et al.,* 2011; Ellis *et al.,* 2018) neither rIBV BeauR-M41(S) nor BeauR-4/91(S) could be detected in the trachea post vaccination. The inability of Beau-R and subsequently the Beau-R based vaccine viruses to replicate *in vivo* is therefore important to investigate, and will be discussed further in Chapter 5.

In conclusion, this chapter has raised a number of interesting questions that will be important to answer to enable the design of the next generation of rationally attenuated vaccines. It is important to establish whether a less attenuated IBV vaccine backbone with improved replication *in vivo,* could potentially induce a more robust humoral response that includes the generation of long lasting neutralising antibodies. If this is achieved, it will be interesting to investigate whether the S glycoprotein from M41 and/or 4/91 could induce a more robust immune response to a heterologous QX challenge or whether the effects of improved *in vivo* replication would only be of benefit in response to homologous challenge. Alternatively, it is possible that improved *in vivo* replication will have minimal effect and that the inclusions of other IBV structural proteins resulting in the vaccine virus having a closer resemblance to the challenge virus, is required. Further work is required to investigate this. Of course, it is entirely possible that a mixture of improved *in vivo* replication as well as additional viral proteins derived from the challenge virus is ultimately required to optimise the protective immune responses induced by a rationally designed, rationally attenuated rIBV.

Chapter 5: Replication of the recombinant Infectious Bronchitis Virus, Beau-R is sensitive to temperature.

5.1 Introduction.

As discussed in Chapter 1, there is a large variety of IBV strains that all inflict varying degrees of disease severity *in vivo.* Infection of chickens with M41, a Massachusetts serotype results in classical IB symptoms including snicking, rales, watery eyes, nasal discharge, lethargy, and reduced weight gain. Viral replication is largely confined to the respiratory tract. Nephropathogenic strains, such as QX, are able to disseminate further and infect the enteric tract, oviducts and kidneys, often resulting in severe disease under field conditions (Cook *et al.,* 2001; Liu and Kong, 2004, Bayry *et al.,* 2005; de Wit *et al.,* 2011B). In contrast several strains, including vaccines such as H120 and the laboratory strain Beaudette, are considered apathogenic and infection of chickens does not result in IB (Bijlenga *et al.,* 2004). The Beaudette strain, first isolated in the 1937 (Beaudette and Hudson, 1937), has, in particular, been an enigma for several decades with the site of *in vivo* viral replication undetermined.

As discussed in the previous chapters, the advent of reverse genetics systems has opened the possibility for the development of rationally attenuated IBV that have the potential to be used as vaccines. In the two previous chapters the rIBV Beau-R, a molecular clone of the Beaudette strain, Beau-CK, has been investigated as a vaccine backbone. It has been demonstrated, under experimental conditions, that Beau-R expressing an S gene from a pathogenic isolate, can induce a protective immune response against the wild type IBV strain of which the “donor” S sequence was derived (Hodgson *et al.,* 2004, Armesto *et al.,* 2011, Ellis *et al.,* 2018). However, the protection level induced, around 65%, does not meet the European Pharmacopeia standard of 80%, and questions have been raised regarding the replication of these Beaudette-based vaccine viruses *in vivo*, and whether this accounts for the unexpectedly low protection rate.

In this chapter the *in vivo* dissemination pattern of the rIBV Beau-R in comparison to the pathogenic strain M41-CK is evaluated. The *in vivo* study confirms previous reports that infection with Beau-R does not result in clinical signs, and that replication *in vivo* is highly restricted. *In vitro* studies identify that whilst Beau-R can replicate at 37°C, replication is temperature sensitive and cannot be maintained at 41°C, the core body temperature of a

chicken. Further experiments utilising a panel of rIBVs, identified the replicase gene as a potential defining factor in the restriction of replication at non-permissive temperatures. The inability of rIBV Beau-R to replicate at 41°C likely has a contributory role in the attenuated phenotype observed *in vivo*, and has implications for the use of Beau-R as a backbone for the development of rationally designed recombinant vaccines.

5.2 Results.

5.2.1 The replication of rIBV Beau-R is restricted *in vivo*.

To establish the sites of viral replication and therefore the areas to which Beau-R based vaccines could deliver antigen, groups of seven-day old SPF RIR chickens were inoculated with either M41-CK, Beau-R or mock infected with PBS (Figure 5.1, Table 5.1). Samples from randomly chosen birds were harvested 1, 4, 6 and 7 days post infection (dpi), and assessed for viral presence. Birds were observed for IB related clinical signs, including snicking and rales 1 to 7 dpi, and ciliary activity was observed in extracted tracheal sections 4 and 6 dpi.

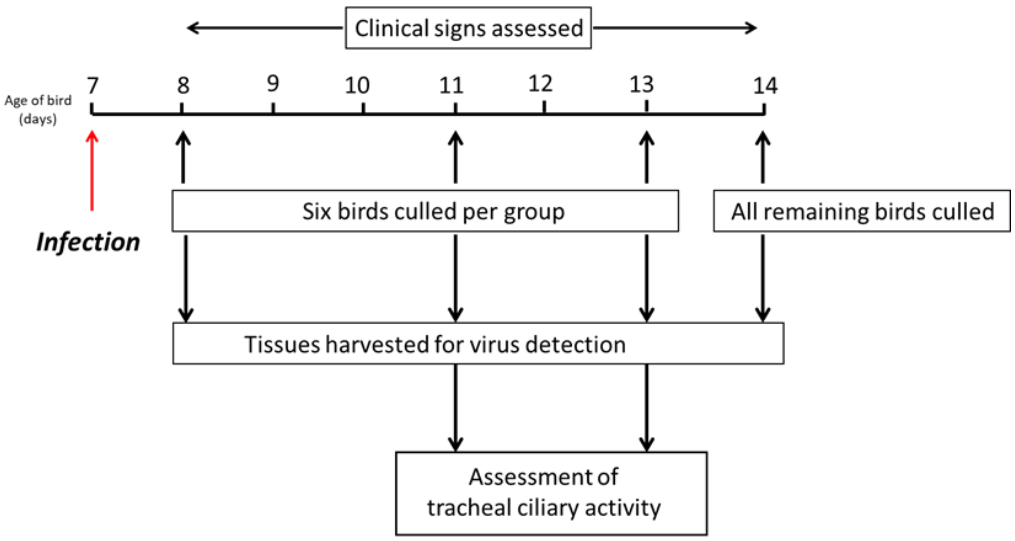

Figure 5.1: Schematic of experimental protocol: pathogenicity experiment Beau-R and M41-CK. Groups of seven-day old SPF RIR chickens were inoculated with Beau-R, M41-CK or PBS. The birds were assessed daily for the presence of clinical signs. At defined intervals randomly chosen birds were culled from each group and a variety of tissues harvested. Tracheal ciliary activity was assessed on 4 and 6 dpi. The experiment ended on 7 dpi with all remaining birds culled.

Table 5.1: Details of groups, sample days and numbers during the *in vivo* study assessing the dissemination pattern of rIBV Beau-R.

Group	Inoculation	Number of birds sampled				Total no. of birds per group
A	PBS (mock)	6	6	6	6	24
B	Beau-R	6	6	6	4*	24
E	M41-CK	6	6	6	6	24
No. of days post infection (dpi)	0	1	4	6	7	

Notes: *Two birds in group B were culled due to poor health unrelated to IBV resulting in a lower number of birds sampled 7 dpi.

IB related clinical signs including snicking and rales (Figure 5.2) were assessed from one to seven days post infection (dpi). Birds infected with Beau-R exhibited rates of snicking comparable to mock infected birds, both peaking on 7 dpi at 0.25 and 0.17 snicks per bird per min, respectively (Figure 5.2A). In contrast, on 7 dpi, M41-CK infected birds exhibited a snicking rate of 1.67 snicks per bird per min, and a maximal rate of 3.21 snicks per bird per min at 5 dpi. Rales were not observed in Beau-R or mock infected birds, but were observed in 94 and 100% of birds infected with M41-CK on 4 and 6 dpi, respectively (Figure 5.2B).

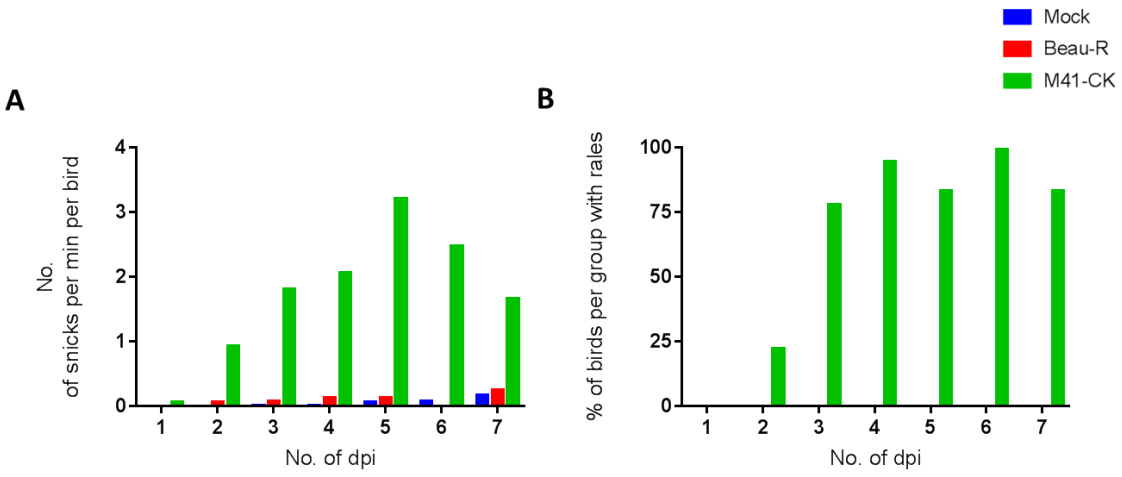

Figure 5.1 Beau-R infected chickens display clinical signs comparable to mock infected chickens. SPF chickens were inoculated at 7 days of age with 10^4 PFU of either Beau-R, M41-CK or PBS for mock infection. (A) Snicking was assessed from 1 to 7 dpi, with the number of snicks in a 2 min time period counted independently by 2 or 3 persons. The average of these scores are presented. (B) Chickens were assessed individually for the presence of tracheal rales 1 to 7 dpi. The percentage of birds exhibiting rales per group was calculated.

Tracheas were harvested from six randomly selected birds per group on 4 and 6 dpi and the ciliary activities were assessed (Figure 5.3). Mean ciliary activities were comparable between mock and Beau-R infected birds, 99% and 95%, respectively, at 4 dpi and of 95% and 96% at 6 dpi. In contrast, M41-CK infected birds exhibited lower scores of 1% and 0.4% at the same time points, respectively ($p<0.0001$). All birds within a group exhibited similar ciliary activity scores, with no outliers detected. Tracheal ciliary activity is used as a marker to determine whether a pathogenic isolate of IBV is present, with a ciliary activity score of less than 50% being deemed positive (European Pharmacopoeia, 2010; Cavanagh *et al.,* 1997). All birds infected with Beau-R retained over 85% ciliary activity, which alongside the absence of clinical signs (Figure 5.2) confirms previous reports that Beau-R has an attenuated phenotype *in vivo* (Hodgson *et al.,* 2004, Armesto *et al.,* 2011, Keep *et al.,* 2018). Birds infected with M41-CK exhibited less than 50% ciliary activity, and also presented IB related clinical signs (Figure 5.2), confirming previous reports that M41-CK exhibits a pathogenic phenotype *in vivo* (Hodgson *et al.,* 2004, Armesto *et al.,* 2011, Keep *et al.,* 2018).

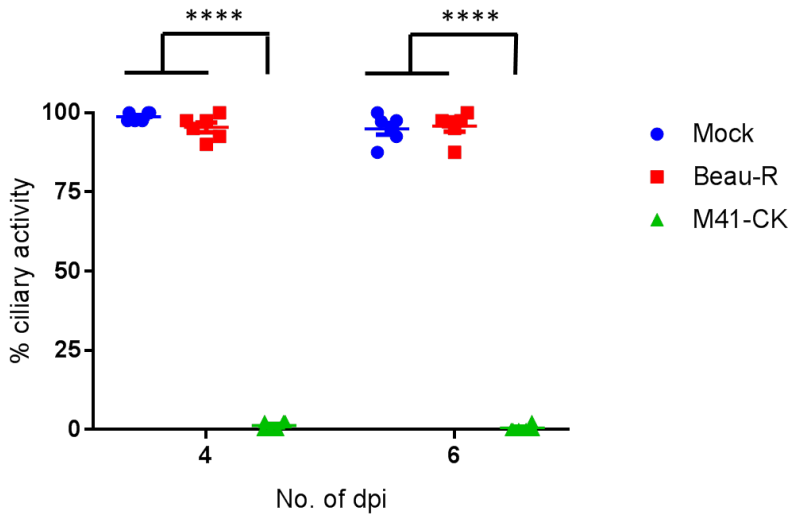

Figure 5.3: Tracheal ciliary activities in Beau-R infected birds were comparable to mock infected birds. SPF chickens were inoculated at 7 days of age with 10^4 PFU of either Beau-R, M41-CK or PBS for mock infection. Tracheas were removed from six randomly chosen birds per group at 4 and 6 dpi. Each trachea was sectioned in 10 x 1mm rings and the ciliary activities of each ring was assessed by light microscopy and the percentage activity calculated. Plotted points represent individual animals and the mean activity of the 10 rings assessed. Error bars represent SD. Statistical differences between groups were evaluated using a One-Way ANOVA followed by Tukey test for multiple comparisons, and are represented ****($p<0.0001$). There was no significant difference between the ciliary activities observed in mock and Beau-R infected birds on neither 4 nor 6 dpi.

5.2.2 Beau-R can be re-isolated from nasal turbinates.

To establish the sites of viral replication, a panel of tissues were harvested from six randomly selected chickens per group at 1, 4, 6 and 7 dpi. To establish whether the tissue contained IBV, each tissue was homogenised producing a tissue derived supernatant which was subsequently used to infect 9 or 10 day old embryonated hens' eggs. RNA was extracted from allantoic fluid and investigated by RT-PCR analysis using a random primer for the RT step and primers, BG56 and 93/100, specific for the IBV 3′UTR, for the PCR step. The genome of M41-CK contains a deletion in the 3′UTR (Casais *et al.,* 2003), allowing for differentiation of Beau-R derived PCR products (~650 bp) from M41-CK (~450 bp). Identification of IBV derived RNA in allantoic fluid indicates the presence of infectious virus in the tissue derived supernatant and therefore in the harvested tissue. Tissues harvested from mock infected birds were included in the experiment as negative controls.

Both infectious Beau-R and M41-CK were detected at 1 dpi, with both viruses re-isolated from nasal turbinates harvested from all sampled birds (Table 5.2). However, infectious Beau-R was not detected in tracheal tissue or in eyelids. In contrast, eyelids and tracheas from the M41-CK infected birds were virus positive; in four and six birds, respectively. Beau-R was sporadically detected in nasal turbinates, trachea and eyelid from 4 to 7 dpi. Interestingly, there was no consistency; one bird 6 dpi was positive for virus in the trachea but negative in eyelid and nasal turbinates and on 7 dpi two birds were positive in nasal turbinates and a third in the eyelid. In contrast to Beau-R, M41-CK was consistently detected in all sampled birds from 4 to 7 dpi, with all birds on 4 and 6 dpi positive for infectious virus in the eyelids. Additionally, nasal turbinates harvested from all M41-CK infected birds at 4 dpi were positive and five birds were positive in the trachea 4 and 6 dpi. No infectious virus was re-isolated from tissues extracted from mock infected birds. The virus isolation data suggests that productive replication of Beau-R, unlike M41-CK is largely restricted to early infection in the nasal turbinates.

Table 5.2: Virus re-isolation from tissues harvested from mock, Beau-R and M41-CK infected birds.

Group	Dpi	Nasal Turbinates	Eyelid	Trachea
Mock	1	0/6	0/6	0/6
Beau-R		6/6	0/6	0/6
M41-CK		6/6	4/6	6/6
Mock	4	0/6	0/6	0/6
Beau-R		2/6	0/6	0/6
M41-CK		6/6	6/6	5/6
Mock	6	0/6	0/6	0/6
Beau-R		0/6	0/6	1/6
M41-CK		0/6	6/6	5/6
Mock	7	0/6	0/6	0/6
Beau-R		2/4	1/4	0/4
M41-CK		2/4*	5/6	2/5*

Notes: Tissue derived supernatant was used to infect 9 or 10 day old embryonated hen's eggs. RNA was extracted from allantoic fluid and investigated by RT-PCR analysis using a random primer for the RT step and primers, BG56 and 93/100, specific for the IBV 3′UTR, for the PCR step. * Samples from trachea of one bird, and nasal turbinates from two birds were damaged and therefore were unable to be included in the experiment, resulting in a group of four or five samples assessed instead of six.

5.2.3 Replication of rIBV Beau-R *in vitro* is sensitive to temperature.

The finding of Beau-R in tissue harvested from nasal turbinates raised an interesting question regarding the potential for temperature to affect virus dissemination. The continuous movement of air in the upper respiratory tract will inevitably cool this area of the bird, and it has been demonstrated for several respiratory viruses including Influenza virus, Rhinoviruses and Respiratory Syncytial Virus (RSV) that replication can be confined to the upper respiratory tract as a consequence of viral replication being sensitive to the comparatively higher temperatures in the lower respiratory tract (Alford *et al.,* 1966; Maassah, 1967; Maassah, 1968; Juhasz *et al.,* 1999; Hatta *et al.,* 2007; Da Costal *et al.,* 2015; Foxman *et al.,* 2014). A growth kinetic experiment was therefore used to assess whether the replication of Beau-R was detrimentally affected by higher temperatures, specifically at 41°C, the core body temperature of a chicken. CK cells were infected with either Beau-R or M41-CK and incubated at either 41°C or 37°C, with supernatant harvested

at regular intervals. The quantity (titre) of viable infectious viral progeny in this harvested supernatant was assessed through titration in CK cells (Figure 5.4).

At all the time points assessed, except 1 hpi, the PFU/ml of Beau-R generated at 41°C was lower ($p<0.0001$) than at 37°C (Figure 5.4B), with very little viable infectious progeny virus detected at the higher temperature. In contrast, the PFU/ml of M41-CK was similar at both temperatures at 1, 12 and 24 hpi, after which at 48, 72 and 96 hpi, the titre was lower ($p<0.0001$) at 41°C (Figure 5.4C). Although both viruses exhibited reduced titres at 41°C, the difference between Beau-R and M41-CK is considerable (Figure 5.4D). At 41°C Beau-R generated significantly lower titres in comparison to M41-CK at all the time points except 1 hpi ($p<0.0001$). This is notably a different pattern to 37°C in which Beau-R generates higher titres of infectious progeny virus than M41-CK at 12 and 24 hpi ($p<0.005$). From 48 h titres of Beau-R are lower than M41-CK, with the difference at 72 and 96 h reaching statistical significance ($p<0.005$).

The reduction in PFU/ml observed during Beau-R infection at 41°C in comparison to 37°C identifies that Beau-R replication is sensitive to increased temperature, and specifically is detrimentally affected. The replication of M41-CK also seems to be negatively affected by the increased temperature, but only at later time points. Whilst titres of infectious progeny virus are statistically lower at 41°C, the replication of M41-CK is still sustained generating titres of approximately 10^4 PFU/ml. The results of this growth kinetics assay therefore indicate that unlike M41-CK, Beau-R is unable to establish a productive infection *in vitro* at 41°C, demonstrating that this temperature can be classified as non-permissive and that Beau-R is temperature sensitive.

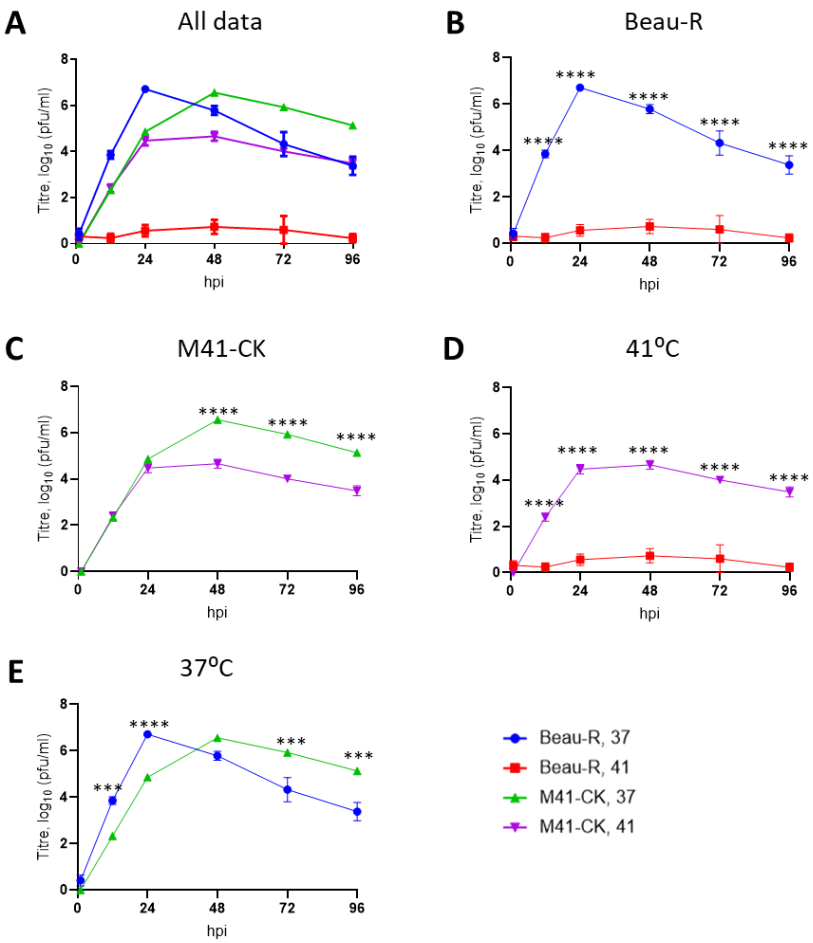

Figure 5.4: Assessment of M41-CK and Beau-R replication at 37°C and 41°C. CK cells seeded in 6 well plates were inoculated with 10^4 PFU of M41-CK or Beau-R, and incubated at either 37°C or 41°C. Supernatant was harvested at 24 h intervals and the quantity of infectious progeny was determined via titration in triplicate in CK cells. Each point represents the mean of three independent experiments with error bars representing SEM. Graph (A) represents all data gathered during the experiment, graph (B) displays the data generated from Beau-R infection, graph (C) the data generated from M41-CK infection, and graph (D) and (E) the data generated through incubation at 41°C and 37°C respectively. Statistical differences were assessed using a two-way ANOVA stating time and temperature as independent factors, followed by a Tukey test for multiple comparisons. Statistical differences between each time point are highlighted by *** ($p<0.0005$) and **** ($p<0.0001$).

To confirm that the temperature sensitive *in vitro* replication phenotype of Beau-R was not specific to CK cells, the growth of both Beau-R and M41-CK in DF1 cells, a continuous cell line derived from chicken embryo fibroblasts, was assessed. DF1 cells were infected with either Beau-R or M41-CK, and incubated at either 37°C or 41°C. The supernatant was harvested at 24h intervals, and the quantity of infectious progeny virus was assessed through titration in CK cells (Figure 5.5). A BSc placement student, Jamie Stuart, carried out this experiment under my supervision and direction.

The titres of M41-CK produced at 37°C and 41°C were below 10 PFU/ml indicating that extremely little infectious progeny, if any, had been produced. This strongly indicated that M41-CK was unable to establish a productive infection in DF1 cells at either temperature (Figure 5.4A), which was not unexpected as the M41-CK S glycoprotein restricts cell tropism (Casais *et al.,* 2003). Whilst it may seem counterintuitive, M41-CK was included in the experiment in case the higher temperature affected S mediated entry resulting in M41-CK being able to establish an infection in cells previously non-permissive.

Similarly, to M41-CK, the titres of Beau-R at 41°C were also below 10 PFU/ml suggesting that Beau-R was also unable to establish a productive infection. However, titres of Beau-R at 37°C reached approximately 10^5 PFU/ml at 24 through to 72 hpi only decreasing to 10^4 PFU/ml at 96 hpi. The difference between the PFU/ml generated at 41°C and 37°C was significant at all time points assessed ($p<0.0001$). The significantly lower titres of progeny virus produced from Beau-R infected DF1 cells at 41°C in comparison to 37°C demonstrates that the temperature sensitive replication phenotype is not restricted to CK cells, and may be a defining characteristic of Beau-R.

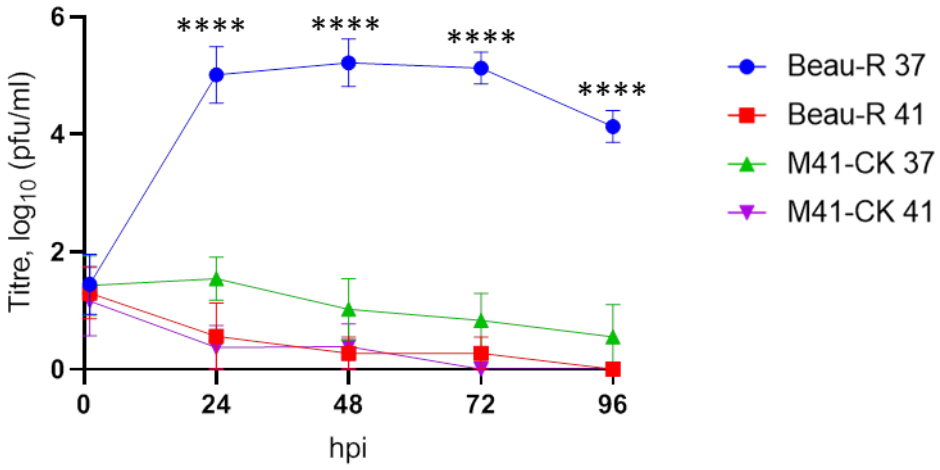

Figure 5.5: Beau-R replication is highly restricted at 41°C in DF1 cells in comparison to 37°C. DF1 cells seeded in six well plates were inoculated with 10^5 PFU of M41-CK or Beau-R, and incubated at either 37°C or 41°C. Supernatant was harvested at 24 h intervals and the quantity of infectious progeny was determined via titration in triplicate in CK cells. Each point represents the mean of three independent experiments with error bars representing SEM. Statistical differences at each time point were assessed using a two-way ANOVA followed by a Tukey test for multiple comparisons. Statistical differences at each time point between Beau-R at 37°C and Beau-R at 41°C as well as between Beau-R at 37°C and M41-CK at 37°C as well as at 41°C are highlighted by **** ($p<0.0001$). There were no statistical differences between M41-CK infection at 37°C and 41°C nor between M41-CK infection at either 37°C and 41°C with Beau-R infection at 41°C at any of the time points assessed. The experimental data was generated by Jamie Stuart under my supervision and I analysed the data.

5.2.4 Temperature sensitivity is not a shared characteristic of attenuated strains.

It was an interesting observation that the replication of the apathogenic rIBV Beau-R was limited at 41°C yet the pathogenic strain M41-CK could establish a sustained productive infection. To establish whether temperature sensitivity was a shared characteristic of attenuated strains the vaccine virus H120 was investigated. Alongside H120, the replication phenotype of serially passaged M41-CK isolates, M41-SK-106A, M41-SK-106A1, M41-SK-106C and M41-SK-106D that have been passaged 110 times through embryonated hen's eggs and are attenuated *in vivo* (Oade *et al.,* 2019), was also assessed. Passaging a pathogenic isolate through embryonated hens' eggs is a known method of attenuation, although the molecular mechanism remains unknown (Geerligs *et al.,* 2011; Oade *et al.,* 2019). The process of serially passaging in embryonated hens' eggs typically occurs at 37°C, and therefore it was possible that this process whilst attenuating the virus also rendered the replication of the virus temperature sensitive.

The growth of H120, M41-SK-106A, M41-SK-106A1, M41-SK-106C and M41-SK-106D was assessed in CK cells at both 37°C and 41°C and compared to both M41-CK and Beau-R. As in previous assays CK cells were infected and incubated at either 37°C or 41°C. The supernatants were harvested at 24 h intervals and titrated in CK cells to quantify the amount of viral progeny. This work was completed by Michael Oade, under my direction and the data generated has been analysed by me. The dataset is presented in Figures 5.6 and Figure 5.7 to allow clear representation of the findings.

The vaccine strain H120 was observed to initiate and maintain a productive infection at 37°C with the pattern of replication mirroring that of M41-CK (Figure 5.6B); both viruses reached peak titres at 48 h after which titres exhibited a steady gradual reduction to the lowest titres at 96 hpi. Despite this, the titres generated by H120 were lower than M41-CK at all time points except 1 h ($p<0.0005$). Overall, the replication patterns of both H120 and M41-CK were different to that of Beau-R which peaked at 24 h and then exhibited a more rapid decline. Beau-R infection generated lower PFU/ml than M41-CK at 48, 72 and 96 h ($p<0.05$), and also lower than H120 at 72 and 96 hpi, though only the latter reached statistical significance ($p<0.05$). Despite H120 maintaining a productive infection, the peak titres were lower than both Beau-R ($p<0.0001$) and M41-CK ($p<0.0005$). This was not the case, however, at 41°C in which the titres of M41-CK and H120 were comparable at all time points (Figure 5.5C). Additionally, the replication patterns were indistinguishable therefore demonstrating that similarly to M41-CK, and unlike Beau-R, H120 could both initiate and

sustain productive replication at 41°C. This replication however was sensitive to the higher temperatures at later time points during the experiment (Figure 5.6D) with lower titres of H120 generated at 41°C in comparison to 37°C at 48, 72 and 96 hpi; a comparable pattern to M41-CK (Figure 5.6E). The comparable replication, at 41°C, of H120 and M41-CK indicates that for H120 attenuation and temperature sensitivity do not correlate.

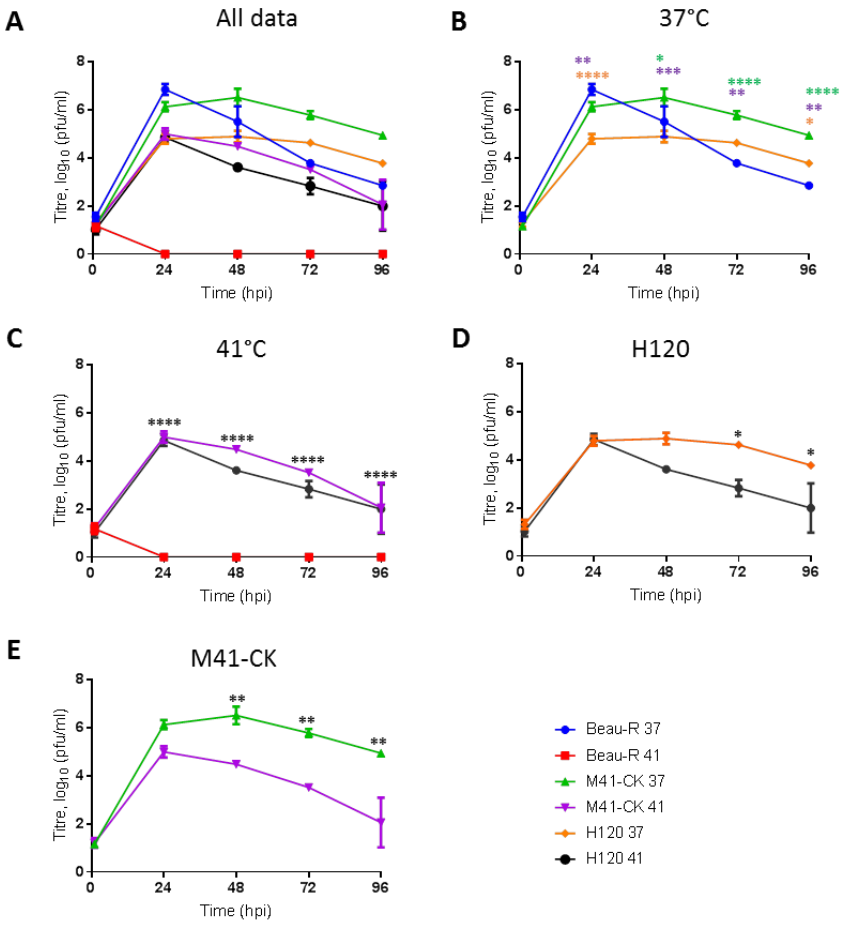

Figure 5.6: H120 shares the same replication phenotype as M41-CK at 41°C. CK cells seeded in six well plates were inoculated with 10^5 PFU of H120, M41-CK or Beau-R, and incubated at either 37°C or 41°C. Supernatant was harvested at 24 h intervals and the quantity of infectious progeny determined via titration in triplicate in CK cells. Each point represents the mean of three independent experiments with error bars representing SEM. Graph (A) represents all data gathered, (B) the data generated at 37°C, (C) at 41°C, (D) from H120 infection and (E) M41-CK. Statistical differences were assessed using a two-way ANOVA stating time and temperature as independent factors, followed by a Tukey test for multiple comparisons. Statistical differences at each time point are highlighted by * ($p<0.05$), ** ($p<0.005$), *** ($p<0.0005$) and **** ($p<0.0001$). (B) Statistical differences between Beau-R and H120 are highlighted by orange *, H120 and M41-CK by purple * and M41-CK and Beau-R green *. (C) Statistical differences, which are comparable between Beau-R and H120, and M41-CK and H120 are highlighted; there is no difference between M41-CK and H120 at any time point. The experimental data was generated by Michael Oade whilst I analysed the data.

Analysis of the replication patterns of the M41-CK serially egg passaged isolates, M41-SK-106A, M41-SK-106A1, M41-SK-106C and M41-SK-106D at both 41°C and 37°C were also compared (Figure 5.7). Viral titres produced by the attenuated M41-CK serially passaged isolates at 1, 72 and 96 h were comparable to each other at 37°C (Figure 5.7B). At 24 h both M41-SK-106A and A1 produced higher titres than M41-SK-106C and D ($p<0.05$). Each of the isolates produced lower titres of infectious progeny at all time points in comparison to M41-CK with statistical significance reached at 48 to 96 h ($p<0.005$, Table 5.3). At 41°C viral titres were comparable between M41-SK-106A, M41-SK-106A1 and M41-CK (Figure 5.7C). M41-SK-106D produced less infectious progeny virus than M41-CK at all time-points however this was not significant. There was a small significant difference between titres of both M41-SK-106A and M41-SK-106A1 in comparison to M41-SK-106D at 24 h ($p<0.05$) with the latter producing less infectious progeny. Despite some minor differences overall the replication kinetics of the serially passaged isolates M41-SK-106A, M41-SK-106A1, M41-SK-106C and M41-SK-106D are comparable to the parental virus M41-CK at both 37°C and 41°C.

Further analysis of the data set indicates that similarly to M41-CK, all the serially passaged isolates produced lower titres of infectious progeny at 41°C in comparison to 37°C from 48 to 96 h ($p<0.05$). Interestingly unlike M41-CK, there is no difference in viral titre between the two temperatures at 24 h for M41-SK-106A, A1 and D indicating at this time point viral replication in not sensitive to temperature. The isolate M41-SK-106C has a slightly different replication pattern with peak titres at 41°C significantly lower than at 37°C ($p<0.0005$). Overall, none of the isolates demonstrated a reduction in viral titres at 41°C as seen by the attenuated rIBV Beau-R. For these viruses therefore, similarly to H120, it does not appear that temperature sensitivity and the attenuated phenotype observed *in vivo* (Oade *et al.,* 2019) are directly linked.

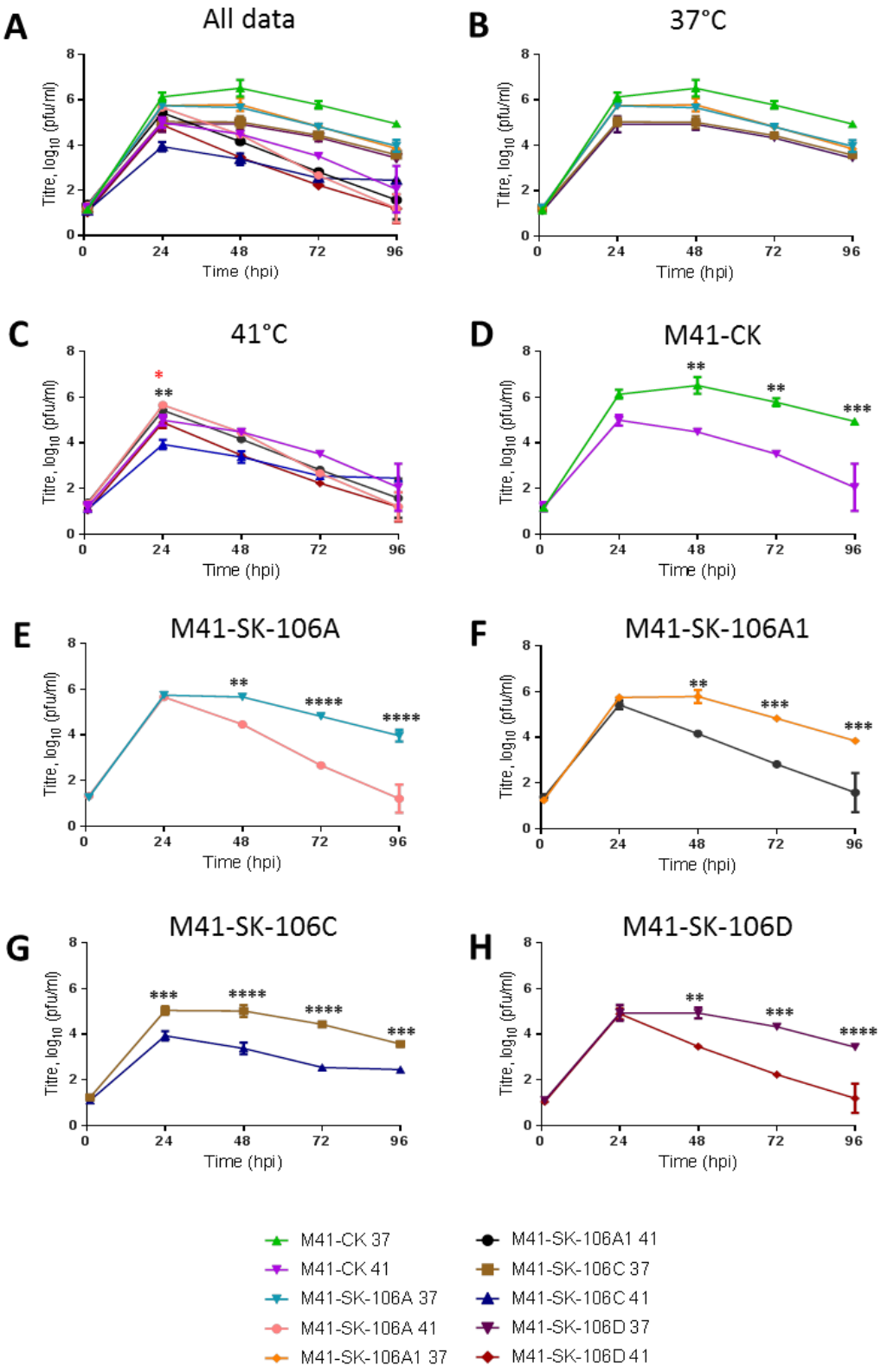
A
All data
B
37°C
C
41°C
D
M41-CK
E
M41-SK-106A
F
M41-SK-106A1
G
M41-SK-106C
H
M41-SK-106D
Titre, log10 (pfu/ml)
Time (hpi)
M41-CK 37
M41-CK 41
M41-SK-106A 37
M41-SK-106A 41
M41-SK-106A1 37
M41-SK-106A1 41
M41-SK-106C 37
M41-SK-106C 41
M41-SK-106D 37
M41-SK-106D 41

Figure 5.7: The replication of attenuated egg passaged isolates, M41-SK-106A, A1, C and D is comparable to the parent virus M41-CK at 41°C. CK cells seeded in six well plates were inoculated with 10^5 PFU of M41-CK, M41-SK-106A, M41-SK-106A1, M41-SK-106C and M41-SK-106D, and incubated at either 37°C or 41°C. Supernatant was harvested at 24 h intervals and the quantity of infectious progeny was determined via titration in triplicate in CK cells. Each point represents the mean of three independent experiments with error bars representing SEM. Graph (A) represents all data gathered, (B) displays only the data generated at 37°C, (C) at 41°C, (D) M41-CK, (E) M41-SK-106A, (F) M41-SK-106A1, (G) M41-SK-106C and (H) M41-SK-106D. Statistical differences were assessed using a two-way ANOVA stating time and temperature as independent factors followed by a Tukey test for multiple comparisons. Statistical differences at each time point on graph C between M41-SK-106A1 and M41-SK-106C are highlighted by * ($p<0.05$) and between M41-SK-106A and M41-SK-106C by ** ($p<0.005$). Statistical differences on graph (D) to (H) at each time point highlighted by * ($p<0.05$), ** ($p<0.005$), *** ($p<0.0005$) and **** ($p<0.0001$). Statistical differences between data presented on graph B are presented in Table 5.3.

Table 5.3: Statistical differences between viral titres produced from M41-CK and M41-SK-106A, A1, C and D infection of CK cells at 37°C

24	M41-CK vs. M41-SK-106A	ns
	M41-CK vs. M41-SK-106A1	ns
	M41-CK vs. M41-SK-106C	***
	M41-CK vs. M41-SK-106D	***
	M41-SK-106A vs. M41-SK-106A1	ns
	M41-SK-106A vs. M41-SK-106C	*
	M41-SK-106A vs. M41-SK-106D	*
	M41-SK-106A1 vs. M41-SK-106C	*
	M41-SK-106A1 vs. M41-SK-106D	*
	M41-SK-106C vs. M41-SK-106D	ns
48	M41-CK vs. M41-SK-106A	**
	M41-CK vs. M41-SK-106A1	*
	M41-CK vs. M41-SK-106C	****
	M41-CK vs. M41-SK-106D	****
	M41-SK-106A vs. M41-SK-106A1	ns
	M41-SK-106A vs. M41-SK-106C	ns
	M41-SK-106A vs. M41-SK-106D	*
	M41-SK-106A1 vs. M41-SK-106C	*
	M41-SK-106A1 vs. M41-SK-106D	**
	M41-SK-106C vs. M41-SK-106D	ns
72	M41-CK vs. M41-SK-106A	**
	M41-CK vs. M41-SK-106A1	**
	M41-CK vs. M41-SK-106C	****
	M41-CK vs. M41-SK-106D	****
	M41-SK-106A vs. M41-SK-106A1	ns
	M41-SK-106A vs. M41-SK-106C	ns
	M41-SK-106A vs. M41-SK-106D	ns
	M41-SK-106A1 vs. M41-SK-106C	ns
	M41-SK-106A1 vs. M41-SK-106D	ns
	M41-SK-106C vs. M41-SK-106D	ns
96	M41-CK vs. M41-SK-106A	**
	M41-CK vs. M41-SK-106A1	***
	M41-CK vs. M41-SK-106C	****
	M41-CK vs. M41-SK-106D	****
	M41-SK-106A vs. M41-SK-106A1	ns
	M41-SK-106A vs. M41-SK-106C	ns
	M41-SK-106A vs. M41-SK-106D	ns
	M41-SK-106A1 vs. M41-SK-106C	ns
	M41-SK-106A1 vs. M41-SK-106D	ns
	M41-SK-106C vs. M41-SK-106D	ns

Notes: Statistical differences were assessed using a two-way ANOVA stating time and virus as independent factors followed by a Tukey test for multiple comparisons. Differences between M41-CK and A, A1, C and D are highlighted in pink, purple, blue and green respectively. Differences between the attenuated egg passaged isolates are highlighted in orange. NS denotes not significant.

5.2.5 The ability to replicate at higher temperatures may be a shared characteristic of pathogenic isolates.

Whilst it appeared that temperature sensitivity was not a shared characteristic of apathogenic strains, it was possible that the ability to replicate at 41°C was a trait of pathogenic strains. It was hypothesised that the ability to replicate at higher temperatures aided the virus in initiating and sustaining productive replication in tissues other than the respiratory tract. To investigate this, the replication of the nephropathogenic strain D388 was assessed at 37°C and 41°C and compared to M41-CK. D388 was chosen as infection *in vivo* results in severe IB, with viral infection identified not only in the respiratory tract but also the kidneys and oviducts (de Wit *et al.,* 2014).

CK cells were infected with either M41-CK or D388 and incubated at either 37°C or 41°C (Figure 5.8). The supernatant was harvested at 24 h intervals and assessed for infectious viral progeny through titration in CK cells. The titres produced by both M41-CK and D388 were found to be comparable between both temperatures at all time points assessed (Figure 5.8B and C). Comparison of the titres of infectious progeny produced from D388 infection at 37°C and 41°C indicates that D388 replication is largely unaffected by temperature (Figure 5.8D). At both 24 and 48 h titres are comparable, with a small decrease in infectious progeny detected at 72 and 96 h with only the latter time point reaching statistical significance ($p<0.05$). M41-CK exhibited larger decreases in titres at 41°C in comparison to 37°C from 48 to 96 h (Figure 5.8E), however productive replication as seen previously is sustained. The ability of D388 to establish and maintain replication at 41°C suggests that whilst attenuation and temperature sensitivity may not be intrinsically linked, the ability to replicate at higher temperatures may be a shared characteristic of pathogenic isolates.

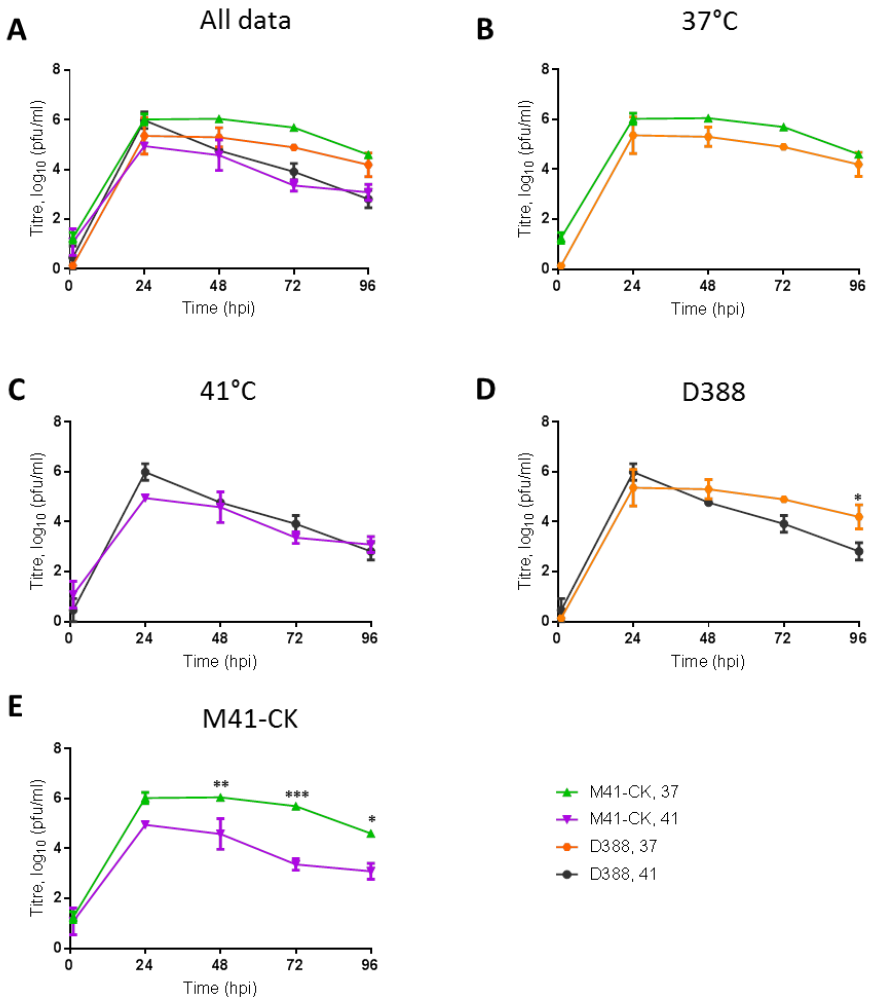

Figure 5.8: Productive replication of D388 at 41°C is comparable to 37°C. CK cells seeded in 12 well plates were inoculated with 1.5 $\log_{10}$ CD_{50} of M41-CK or D388 and incubated at either 37°C or 41°C. Supernatant was harvested at 24 h intervals and the quantity of infectious progeny was determined via titration in triplicate in CK cells. Each point represents the mean of three independent experiments with error bars representing SEM. Graph (A) represents all data gathered, (B) data generation at 37°C, (C) 41°C, (D) from D388 infection and (E) from M41-CK infection. Statistical differences were assessed using a two-way ANOVA stating time and temperature as independent factors, followed by a Tukey test for multiple comparisons. Statistical differences at each time point are highlighted by * ($p<0.05$), **($p<0.005$) and *** ($p<0.0005$).

5.2.6 Entry at permissive temperatures cannot recover replication at non-permissive temperatures.

To determine whether entry was the prohibitive step to establishing a productive infection of Beau-R at 41°C, a temperature swap experiment was carried out (Figure 5.9A). CK cells were infected with M41-CK, Beau-R, H120, or D388 and incubated at either 37°C or 41°C for 1 h allowing for viral attachment and entry. After 1 h the virus was removed and the cells were incubated at either the same temperature or were swapped to be incubated at the other. The resulting supernatant was assessed for infectious viral progeny in CK cells (Figure 5.9B to 5.9E).

The titre in PFU/ml of viable infectious progeny virus produced from CK cells infected with D388 and H120 was unaffected by changes in the incubation temperature. This was expected as the replication of D388 (Figure 5.8D) and H120 (Figure 5.6D) at 24 hpi, is not affected by a change in temperature between 37°C and 41°C. For both Beau-R (Figure 5.9D) and M41-CK (Figure 5.9E) a swap in incubation temperatures did affect the quantity of infectious viral progeny produced. The titres of viral progeny generated from both M41-CK and Beau-R infection was similar in those cells incubated at 37°C for binding and entry followed by incubation of 37°C for the remainder of the replication cycles (37-37), and those incubated at the first temperature of 41°C and then a second incubation temperature of 37°C (41-37). Titres were also similar when incubated at a first temperature of 37°C and then a second temperature of 41°C (37-41) and those at 41°C and then again at 41°C (41-41). A difference in the first incubation temperature therefore had no effect on the quantity of infectious viral progeny produced. This indicated that the temperature at which viral attachment and entry occurred was not the determining factor in whether a productive infection was established.

A significant difference in the titre of viral progeny of Beau-R and M41-CK was however identified between groups that had different second incubation temperatures. The titres generated when incubating at 41-41 were lower than 41-37 ($p<0.0001$), and similarly were lower when incubating at 37-41 when compared to 37-37 ($p<0.0001$). This therefore demonstrated that the second incubation temperature, in which the virus is undergoing active replication, assembly and egress, was the determining factor to whether a productive infection was established.

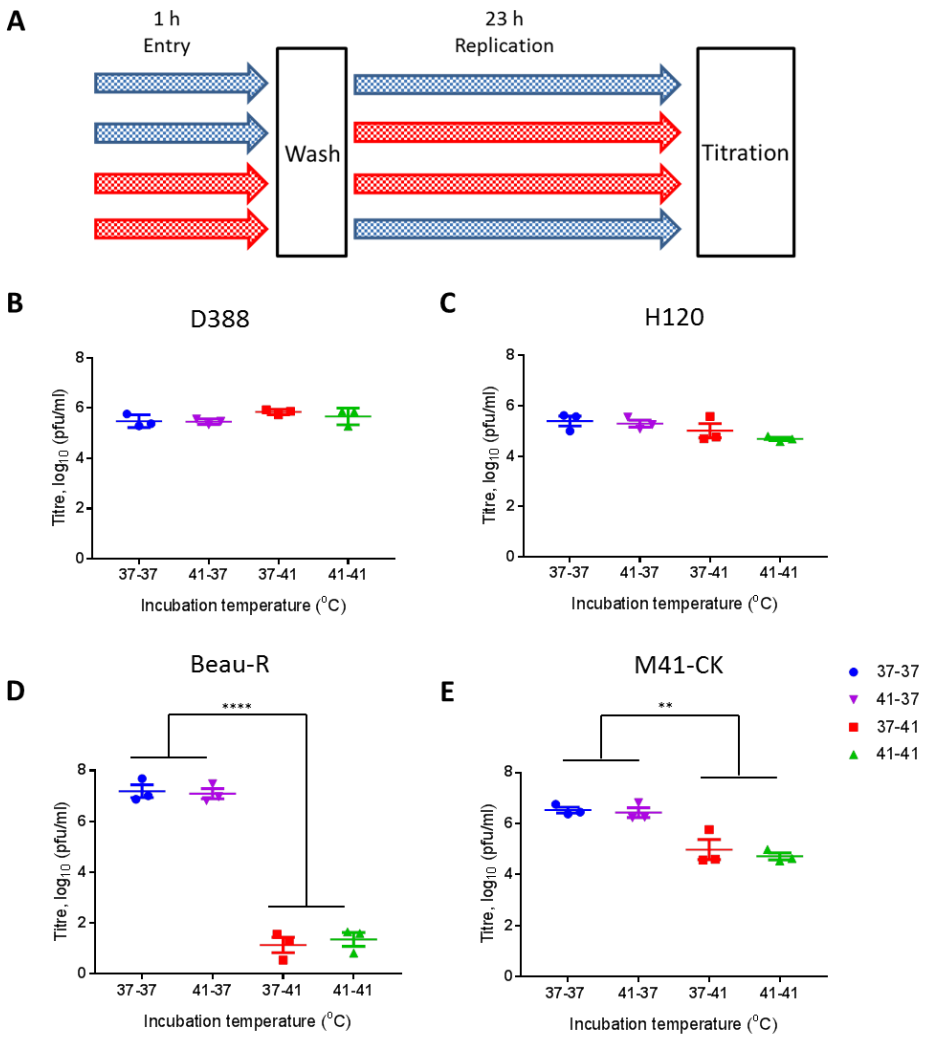

Figure 5.9: Entry does not restrict replication of Beau-R at 41°C. (A) Schematic detailing experimental protocol. CK cells seeded in six well plates were inoculated in triplicate with 10^5 PFU of either D388, H120, Beau-R or M41-CK. Cells were incubated for 1 h at either 37°C (blue) or 41°C (red), after which the viral inoculum was removed and the cells washed to remove any unbound virus. Cells were then incubated at either 37°C or 41°C for 23 h. The quantity of infectious viral progeny was assessed through titration in triplicate in CK cells. Graph (B) represents data generated from D388 infection, (C) H120, (D) Beau-R and (E), M41-CK. Each point represents the mean titre of infectious progeny virus generated from one independent experimental replicate. Error bars represent the SEM from three independent experimental replicates. Statistical differences were assessed using a one-way ANOVA with a Tukey test for multiple comparisons. Statistical differences are highlighted by ** ($p<0.005$) and **** ($p<0.0001$).

5.2.7 The spike glycoprotein from M41-CK cannot rescue Beau-R replication at non-permissive temperatures.

Temperature swap growth kinetic assays (Figure 5.9) suggested that viral entry was not the determining factor for replication at non-permissive temperatures. Coronavirus entry is mediated by the S glycoprotein (reviewed by Belouzard *et al.,* 2012). To investigate the role of the S protein in replication at non-permissive temperatures the rIBV BeauR-M41(S) containing the ectodomain of the S protein from M41-CK, in replacement of the Beau-R sequence (Casais *et al.,* 2003) was investigated (Figure 5.9). This experiment was completed by Phoebe Stevenson-Leggett.

CK cells were infected with either Beau-R or BeauR-M41(S) and incubated at either 37°C or 41°C (Figure 5.10). Supernatant was harvested every 24 h and the quantity of infectious viral progeny was determined by titration in CK cells. At both temperatures and at all time points the titres of Beau-R and BeauR-M41(S) were comparable to each other (Figure 5.10). The comparable replication of BeauR-M41(S) to Beau-R at 41°C demonstrated that the M41-CK derived S gene could not transfer the ability of M41-CK to replicate at 41°C to Beau-R and additionally supported the evidence that the S glycoprotein was not the determinant of temperature sensitivity observed for Beau-R.

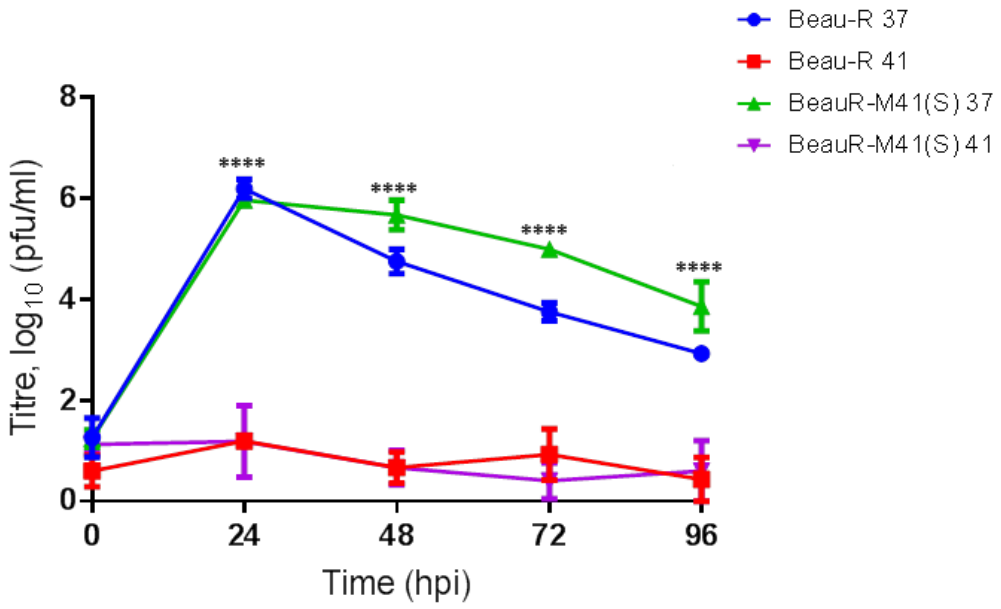

Figure 5.10: The S gene from M41-CK cannot rescue Beau-R infection at 41°C. CK cells seeded in six well plates were inoculated with 10^4 PFU of Beau-R or BeauR-M41(S) and incubated at either 37°C or 41°C. Supernatant was harvested at 24 h intervals and the quantity of infectious progeny was determined via titration in triplicate in CK cells. Each point represents the mean of three independent experiments with error bars representing SEM. Statistical differences at each time point were assessed using a two-way ANOVA stating virus and temperature as independent factors followed by a Tukey test for multiple comparisons. Statistical differences between the quantity of progeny virus produced by Beau-R at 37°C and Beau-R at 41°C, as well as BeauR-M41(S) at 37°C and 41°C at each time point are highlighted by **** ($p<0.0001$). There is no statistical difference between Beau-R and BeauR-M41(S) at either temperature.

5.2.8 The replicase gene is a determinant of temperature sensitivity.

The results of the temperature swap assays alongside the inability of BeauR-M41(S) to replicate at 41°C suggested that the temperature in which the virus was undergoing active replication and not entry, determined whether a productive infection was established. To rule out a role for the other structural genes, as well as the accessory proteins, the growth of rIBV BeauR-Rep-M41-Struct (Armesto *et al.,* 2009) was assessed at both permissive and non-permissive temperatures (Figure 5.10). BeauR-Rep-M41-Struct contains Beau-R derived sequence encoding the 5′ UTR and replicase gene, whilst the structural and accessory genes as well as the 3′ UTR derived from M41-CK sequence.

Similar to the previous assays, CK cells were infected with Beau-R or BeauR-Rep-M41-Struct, and incubated at either 37°C or 41°C (Figure 5.11). The supernatant was harvested at 24 intervals and assessed by plaque assay for infectious viral progeny. At 37°C titres of Beau-R and BeauR-Rep-M41-Struct were similar at 1, 48, 72 and 96 hpi with the titre of BeauR-Rep-M41-Struct at 24 hpi lower ($p<0.05$). At 41°C the titres of Beau-R and BeauR-Rep-M41-Struct were comparable to each other at all time points, demonstrating that similarly to Beau-R, BeauR-Rep-M41-Struct was unable to replicate and produce infectious progeny virus at 41°C (Figure 5.10). The M41-CK derived structural and accessory genes were therefore unable to transfer the ability of M41-CK to replicate at 41°C, suggesting the replicase gene is determining factor in temperature sensitivity.

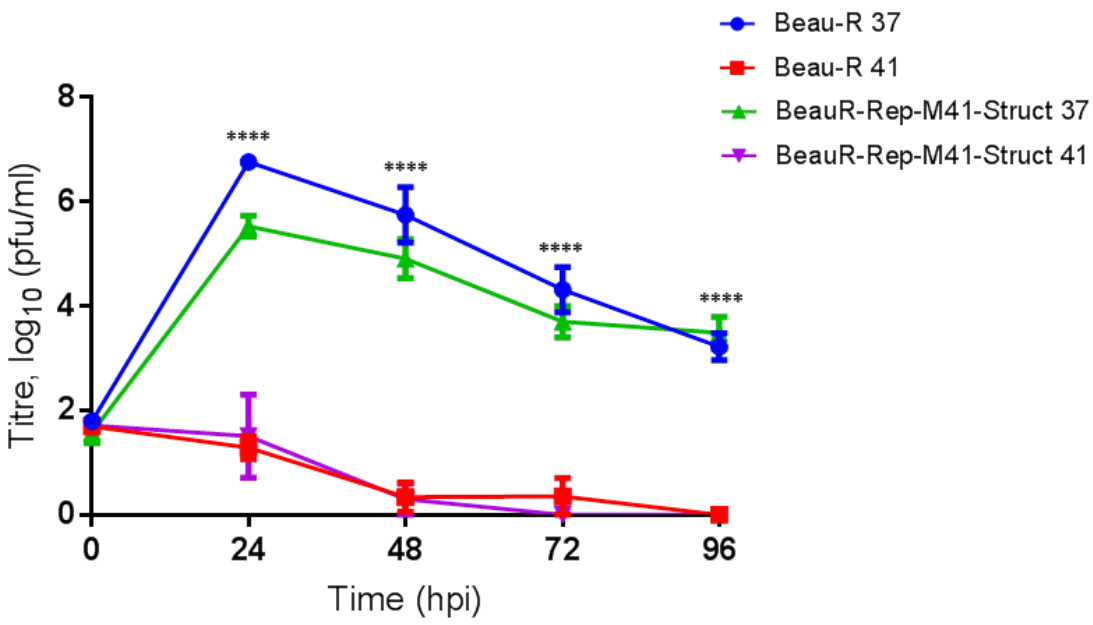

Figure 5.11: The structural and accessory genes from M41-CK cannot recover Beau-R replication at 41°C. CK cells seeded in 12 well plates were inoculated with 10^5 PFU of Beau-R or BeauR-Rep-M41-Struct and incubated at either 37°C or 41°C. Supernatant was harvested at 24 h intervals and the quantity of infectious progeny was determined via titration in triplicate in CK cells. Each point represents the mean of three independent experiments with error bars representing SEM. Statistical differences at each time point were assessed using a two-way ANOVA stating virus and temperature as independent factors followed by a Tukey test for multiple comparisons. Statistical differences between the quantity of progeny virus produced by Beau-R at 37°C and Beau-R at 41°C, as well as BeauR-Rep-M41-Struct at 37°C and 41°C at each time point are highlighted by **** ($p<0.0001$). There is no statistical difference between Beau-R and BeauR-Rep-M41-Struct at either temperature except for 24 hpi at 37°C ($p<0.05$).

5.3 Discussion.

The data presented in this chapter identifies that the attenuated rIBV Beau-R has a temperature sensitive replication phenotype with little or no infectious progeny virus produced during infection at 41°C in both CK and DF1 cells (Figure 5.4 and 5.5). The inability of Beau-R to establish a productive infection at 41°C may account for the restricted replication observed *in vivo*, in which viable virus could only be consistently detected in the nasal turbinates' (Table 5.2). In contrast, M41-CK was able to produce infectious progeny virus from CK cells incubated at 41°C and viable virus could be isolated from nasal turbinates, eyelids and trachea sections harvested from M41-CK infected birds. Additionally M41-CK infected birds, unlike Beau-R infected birds displayed clinical symptoms including a reduction in ciliary activity, associated with IB (Figures 5.2 and 5.3). These observations match previous reports that M41-CK displays a pathogenic phenotype *in vivo* and Beau-R an attenuated phenotype (Hodgson *et al.,* 2004; Armesto *et al.,* 2009; Ellis *et al.,* 2018; Keep *et al.,* 2018).

In birds as well as mammals the continuous movement of air through the respiratory tract will result in a temperature gradient in which the upper respiratory tract including the nasal cavities, mouth and throat is cooler than the trachea and lungs that constitute the lower respiratory tract (Alford *et al.,* 1966). For human pathogen research including influenza, rhinovirus and RSV, the upper respiratory tract is assumed to be 33-34^{o}C and the lower to be 37°C, commonly denoted as permissive and non-permissive temperatures respectively (Juhasz *et al.,* 1999; Bradel-Tretheway *et al.,* 2008; Foxman *et al.,* 2015; Nogales *et al.,* 2016). Unlike humans which have a core body temperature of 37°C, chickens exhibit a core temperature of 41°C, which means it is likely the temperature of upper respiratory tract is 37-38^{o}C, increasing to 41°C in the lower respiratory tract. The effect of this localised temperature change on the replication on several respiratory pathogens including influenza, rhinovirus and RSV is well documented and has been linked to viral dissemination through the host, viral pathogenicity and interspecies transmission (Juhasz *et al.,* 1999; Bradel-Trethway *et al.,* 2008; Massin *et al.,* 2010; Foxman *et al.,* 2015; Broadbent *et al.,* 2014; Nogales *et al.,* 2016; Deng *et al.,* 2019). It must be noted whilst Beau-R has been re-isolated from nasal turbinates (Table 5.2) indicating that replication may be temperature restricted *in vivo,* it has not been determined whether the virus is actively replicating in this tissue. The only way to establish whether active replication is occurring is to assess sgmRNA synthesis either through Northern blotting or via a leader-body junction RT-PCR as described by Bentley *et al.,* (2013).

Temperature sensitivity is not a novel topic in the field of virology and has been widely studied for influenza and RSV since the mid 1900's (Alford 1966; Maassah, 1967; Maassah 1968). The analysis of temperature sensitive mutants has been used in the identification of genes involved in viral replication and pathogenesis and the generation of vaccine viruses, notably against influenza (Hall *et al.,* 1992; Ray *et al.,* 1996; Belshe *et al.,* 1998; reviewed by Maassab and Bryant, 1999; Jin *et al.,* 2003; Sawicki *et al.,* 2005; Burke Schinkel *et al.,* 2017, Deng *et al.,* 2019). Whilst temperature sensitivity has not been a popular research subject for IBV with literature searches only identifying two publications (Yachida *et al.,* 1981; Gelb *et al.,* 1991), several temperature sensitive mutants of the betacoronavirus MHV have been generated (Sawicki *et al.,* 2005; Mielech *et al.,* 2015; Deng *et al.,* 2019). These mutants that all have mutations within the replicase gene, have proved useful tools for elucidating the specific role of individual replicase proteins (nsps) as well as protein-protein and protein-RNA interactions during the coronavirus replication cycle (Sawicki *et al.,* 2005; Clementz *et al.,* 2008; Mielech *et al.,* 20015; Deng *et al.,* 2019). Additionally, temperature sensitive mutants have identified pathogenic determinants within the MHV genome and have been demonstrated to protect mice against lethal challenge (Mielech *et al.,* 2015; Deng *et al.,* 2019).

Similarly to MHV, the data presented in this chapter suggests the temperature sensitive phenotype exhibited by Beau-R is conferred by the replicase gene. Neither the S gene from M41-CK nor the remainder of the structural, accessory genes and 3′ UTR could transfer the ability of M41-CK to replicate at 41°C to Beau-R (Figure 5.10 and 5.11). Additionally temperature swap experiments (Figure 5.9) also demonstrated that the temperature in which binding, attachment and entry occur is not the determinant to whether productive replication at 41°C is established. The data presented in this chapter however does not rule out a collaborative role of the 5′ UTR and 3′ UTR which interact during genome and sgmRNA synthesis (reviewed by Sola *et al.,* 2011). The rIBV BeauR-rep-M41-Struct contains Beau-R derived 5′UTR sequence and M41-CK derived 3′UTR sequence (Armesto *et al.,* 2009). It is possible that if the 5′UTR was replaced with M41-CK, that the resulting rIBV may be able to replicate at 41°C despite the replicase proteins being Beau-R derived. Swapping the 3′ UTR and 5′ UTR regions is a relatively straightforward modification to make using the reverse genetic systems described by Britton *et al.,* (2005). The development of a reverse genetics systems for the pathogenic lab strain M41-CK which is discussed in Chapter 6 also enables the investigation of whether the 5′ UTR and/or 3′ UTR as well as the replicase gene from Beau-R could remove the ability of M41-CK to replicate at 41°C.

Why the productive replication of Beau-R is highly restricted at 41°C remains an unanswered question. There are several possibilities which all require investigation. The most obvious hypothesis, given the restriction is likely the result of the replicase gene, is that RNA replication and/or sgmRNA transcription is affected by temperature. Defects in RNA synthesis and transcription at non-permissive temperatures have been reported for RSV, Influenza, Mumps virus, human parainfluenza virus type 3 (HPIV3) and Sendai virus L as well as MHV (Ray *et al.,* 1995; Juhasz *et al.,* 1999; Feller *et al.,* 2000; Sawicki *et al.,* 2005; Dalton *et al.,* 2006; Bradel-Thretheway *et al.,* 2008; Burke Schinkel *et al.,* 2017). There is a well-defined set of five mutations that impart temperature sensitivity on influenza virus; four of which are located on the polymerase subunits, PB1 and PB2 (Jin *et al.,* 2003). In addition, mutations in the L protein (the polymerase) of RSV and Mumps virus also induce a temperature sensitive phenotype (Juhasz *et al.,* 1999; Burke Schinkel *et al.,* 2017). Future research should therefore establish whether both Beau-R and M41-CK exhibit defects in viral RNA synthesis at non-permissive temperatures. Such experiments could utilise techniques such as Northern blotting and qRT-PCR analysis.

If defects in viral RNA synthesis are identified at non-permissive temperature, it is not necessarily indicative for a determining role of nsp 12, the RNA-dependant RNA polymerase (RdRp). As discussed in Chapter 1, the coronavirus replication cycle is complex and involves both positive and negative strand RNA synthesis (reviewed by Sola *et al.,* 2011; Fehr and Perlman 2015). Additionally, the structural and accessory genes are transcribed through a process of discontinuous transcription during negative strand synthesis (Sawicki and Sawicki, 1995). Viral RNA synthesis is therefore a complex activity, which requires the formation of replication-transcription complexes, which are formed by several nsps including, and not exclusively, nsp 10, 12, 13 and 14, as well as possibly a number of yet undefined viral proteins and cellular factors (reviewed by Sola *et al.,* 2011; Fehr and Perlman 2015). Research into temperature sensitive mutants of MHV have identified a mutation in nsp 10 (Gln65Glu) that affects negative strand synthesis, nsp 5 (Phe219Leu) that affects the conversion of negative strand to positive strand RNA, as well as a mutation in nsp 12 (His868Arg) that results in a reduction in elongation of both positive and negative strand (Swaicki *et al.,* 2005). Furthermore, it is possible that temperature sensitive phenotype inducing mutations do not directly affect the enzymatic function of an nsp but rather affects protein-protein interactions, which subsequently result in a downstream reduction in viral RNA synthesis.

An alternative hypothesis is that temperature has no effect on viral RNA synthesis, but rather affects proteolytic cleavage of the pp1a and pp1ab polyproteins, protein stability, protein-

protein interactions or virus-host interactions. Sparks *et al.,* (2008) identified a mutation in nsp 5 of MHV that resulted in reduced viral replication *in vitro* at non-permissive temperatures with hypothesis that the mutation had affected proteolytic cleavage. Similary Stobart *et al.,* (2012) also identified a mutation in MHV within nsp 5 that effected polyprotein processing and consequently viral replication. Research by Deng *et al.,* (2019) demonstrated that mutations in the ADRP and PLP2 domains of nsp 3 in MHV affect protein stability thereby affecting viral replication at non-permissive temperatures. Additionally, temperature sensitivity conferring mutations within the ubiquitin like domain preceding the PLP2 domain were found to affect thermal stability of PLP2 and as a consequence protease activity (Mielech *et al.,* 2015). It is of course possible that mutations affect the host response with both Deng *et al.,* (2019) and Mielech *et al.,* (2015) indicating an elevated innate immune response to infection with temperature sensitive mutant virus both *in vitro* and *in vivo*. Interestingly research utilising mouse adapted rhinovirus also demonstrated an elevated antiviral response at non permissive temperatures (Foxman *et al.,* 2015).

Despite the unknown mechanism of the temperature sensitive phenotype of Beau-R, the identification of the phenotype may have implications for the development of Beau-R as a vaccine viral vector. It is well established the Beaudette strain replicates poorly *in vivo*, with Beau-R behaving comparably (Hodgson *et al.,* 2004). Additionally, vaccination of birds with Beau-R cannot induce a protective immune response against an M41-CK challenge (Hodgson *et al.,* 2004) nor, as discussed in Chapter 3, can vaccination with Beau-R expressing heterologous S genes offer protection that meets the European Pharmacopoeia standards against homologous challenge (Hodgson *et al.,* 2004; Armesto *et al.,* 2011; Ellis *et al.,* 2018). It cannot be stated that the temperature sensitive replication phenotype of Beau-R observed *in vitro* (Figure 5.3 and 5.4) is the cause of the attenuated phenotype *in vivo* nor the poor replication or the inadequate protection induced by vaccine viruses BeauR-M41(S) and BeauR-4/91(S). Whilst it does seem logical that the restricted replication of Beau-R *in vivo* is a consequence of temperature sensitivity there may be several other attenuating mutations within the viral genome. As discussed in Chapter 3 and 4 there may be alternative reasons for the less than desired protection rate induced by Beau-R based vaccine viruses, which are independent of vaccine virus replication *in vivo*. In its current state however it does appear that the Beau-R backbone is too attenuated for further vaccine development.

The temperature sensitive phenotype is often associated with an attenuated *in vivo* phenotype which has led to vaccine development. Dual temperature sensitive and attenuated phenotypes have been reported for influenza virus, mumps, HIPV3, RSV and MHV (Hall *et al.,* 1992; Ray *et al.,* 1995; Juhasz *et al.,* 1999; Foxman *et al.,* 2014; Burke

Schinkel *et al.,* 2017; Mielech *et al.,* 2015; Deng *et al.,* 2019). It is not always clear how mutations that induce a temperature sensitive replication phenotype also attribute an attenuated phenotype. In some cases the *in vivo* temperature will simply not allow productive viral replication to be initiated or sustained at a level that will induce clinical disease. In other cases the non-permissive temperatures investigated *in vitro* are higher than that seen *in vivo*, leading to a false impression that the temperature sensitive and attenuated phenotypes are directly linked. In other cases temperature sensitive and attenuated mutations are simply independent of each other.

From the data presented in this chapter it remains unclear as to whether attenuation and temperature sensitivity for IBV are directly linked. Unlike Beau-R, the attenuated egg passaged viruses M41-SK-106A, M41-SK106A1, M41-SK-106C, M41-SK-106D and the vaccine virus H120 do not display a temperature sensitive phenotype in CK cells (Figure 5.6 and 5.7). However, it has not been assessed whether replication in *ex vivo* tracheal organ cultures (TOCs) would produce the same result. There is evidence from research into influenza virus that temperature sensitive phenotypes may be dependant of the cell type infected (Dalton *et al.,* 2006). It must be noted however that IBV RNA could be detected in trachea extracted from birds infected with the egg passaged M41 isolates, M41-SK-106A, M41-SK106A1, M41-SK-106C, M41-SK-106D, 4 dpi (Oade *et al.,* 2019) indicating that is it likely that a temperature sensitive phenotype would not be observed in *ex vivo* TOCs. Additionally, infectious H120 has been detected in the trachea extracted from infected birds 3 dpi, alongside a 40% drop in ciliary activity (Hodgson *et al.,* 2004). It seems likely therefore similarly to the M41 egg passaged isolates that H120 simply does not have a temperature sensitive phenotype and that the attenuated phenotypes observed *in vivo* are achieved by a different molecular mechanism.

Whether the ability to replicate at higher temperatures is a shared characteristic of all pathogenic strains is an interesting question. In this chapter both the nephropathogenic strain D388 and the pathogenic strain M41-CK were found to be able to establish a productive infection at 41°C (Figure 5.8). The titres produced in D388 infected CK cells incubated at 37°C and 41°C were comparable, indicating that there were no differences in productive replication at the two temperatures. This is not an unexpected result as it seems logical that all nephropathogenic strains would be able to replicate at 41°C as these strains infect the kidneys and oviducts, organs that are deep within the body of the bird, and which will certainly reside at a much higher temperature than that of the upper respiratory tract. However, to say with any conviction whether temperature sensitivity is a defining trait of all nephropathogenic strains further research is required to assess other nephropathogenic IBV

viruses. Further research could include the well characterised B1648 strain (Meulemans et al 1987; Lambrechts *et al.,* 1993; Cook *et al.,* 2001) which has been adapted for replication in CK cells (Britton, unpublished data).

The classical respiratory strains such as M41-CK may however present a more complex story, as unlike D388, M41-CK exhibits a consistent reduction in viral titres produced at 41°C in comparison to 37°C (Figure 5.4, 5.6, 5.7 and 5.8). It must be noted that in some assays productive replication is not affected by temperature at 24 hpi which could indicate a population effect in which some viruses within the population are not temperature sensitive and some are. It is not surprising that M41-CK can establish replication at temperatures higher than 37°C, since, as previously discussed it is likely that the temperature of the respiratory tract is in the region of 37- 41°C, and productive replication of M41-CK in tracheal tissue *in vivo* as demonstrated in this chapter (Table 5.2, Figure 5.3) is well documented (Hodgson *et al.,* 2004; Armesto *et al.,* 2011; Keep *et al.,* 2018; Ellis *et al.,* 2018). What is interesting is the drop in viral titres produced in cells infected at 41°C in comparison to 37°C (Figure 5.4, 5.6, 5.7, 5.8 and 5.9) which raises the question does such a drop in productive infection occur *in vivo*? Is less infectious M41-CK produced from cells located in the lower trachea in comparison to upper sections? Is increasing temperature prohibitive to dissemination of M41-CK from the primary sites of infection such as the upper trachea, eyelid and nasal turbinates to other tissues/organs within the bird? Is it possible that temperature may be a factor in why M41-CK has not been detected in kidney or lung tissue harvested from infected birds (Stevenson-Leggett, 2018)?

Whilst the M41-CK data presented in this chapter is interesting, one question that arises is the M41-CK temperature phenotype representative of all classical respiratory strains of IBV? The M41 strain, whilst pathogenic, is like Beaudette a lab adapted IBV. The M41 strain has been documented to induce kidney damage *in vivo* (Jones, 1974), however, M41 and M41-CK although related, are two distinct viruses with the latter produced through serially passage in TOCs and CK cells (Cook *et al.,* 1976; Darbyshire *et al.,* 1979). This passaging notably occurred at the lower temperature of 37°C and therefore may have imparted a degree of cold adaption onto M41-CK. The vaccine strain H120, although not pathogenic, also exhibits the same reduction in viral titre at 41°C in comparison to 37°C (Figure 5.6). This virus was also generated through serially passaging an IBV strain, H, first isolated in infected birds in The Netherlands in the 1950s (reviewed by Bijlenga *et al.,* 2004). It therefore remains to be determined whether non lab adapted classical respiratory strains of IBV do

exhibit reduced replication at 41°C or whether the reduction in viral titres observed for M41-CK is an artefact of its passaging history.

In summary, the data presented in this chapter identifies that the attenuated rIBV Beau-R exhibits restricted replication *in vivo* with infectious virus only consistently isolated from nasal turbinates harvested from infected birds. Replication *in vitro* in both primary CK cells and the continuous cell line DF1 was found to be temperature sensitive with productive infection highly restricted at 41°C. In contrast it has been identified that the pathogenic IBV M41-CK can be re-isolated from the nasal turbinates, eyelids and trachea harvested from infected birds and is able to produce infectious progeny virus at 41°C. Investigation into attenuated and pathogenic viruses indicates that whilst attenuation and temperature sensitivity may not be intrinsically linked, the ability to replicate at higher temperatures may be a characteristic of pathogenic isolates. Finally, the restricted replication of Beau-R is likely to be conferred by the replicase gene.

Chapter 6: Recombinant Infectious Bronchitis Virus, M41-R, as an alternative vector to Beau-R for antigen delivery.

6.1 Introduction.

The results of the *in vivo* vaccine-challenge experiments presented in chapter 3 and 4 indicate that rIBV Beau-R may not be an ideal vaccine vector. The observation in chapter 5 that the replication of Beau-R is temperature sensitive, and is highly restricted *in vivo*, further supports this.

Since the generation of the Beaudette based (Beau-R) reverse genetic system in the early 2000s (Casais *et al.,* 2001), a reverse genetics system based on the pathogenic IBV, M41-CK, has been developed. The M41-CK system was developed from the existing Beaudette-based system; briefly within the rVV vector, the Beaudette genome was sequentially deleted and replaced with the corresponding M41-CK sequence. This led to the generation of a full-length cDNA copy of the M41-CK genome encoded by an rVV vector, which was then "recovered" producing rIBV. The first full length clone of M41-CK, M41-R, was demonstrated to be apathogenic *in vivo*; a finding that was unexpected. The results of this *in vivo* study are presented in this chapter. Deep sequencing of a pathogenic M41-CK virus isolate highlighted a number of differences between the M41-R and M41-CK genome, notably four-point mutations within nsp 10, 14, 15 and 16. These mutations were repaired in M41-R cDNA within the rVV, to make the genome more M41-CK like, which lead to the generation of the second infectious clone. The second clone of M41-CK, M41-K, was determined to be pathogenic based on clinical signs and ciliary activity observed *in vivo* (Keep and Bickerton, unpublished data) identifying that the repair of the coding mutations in the replicase gene enabled the restoration of a pathogenic *in vivo* phenotype. The generation of the M41-CK reverse genetics system and the assessment of both M41-K and M41-R *in vivo* was research I conducted prior to the start of this PhD project.

In this chapter, the data generated as part of the *in vivo* pathogenicity experiment examining M41-R, that I carried out before the start of this PhD project, has been re-analysed and expanded in the context of using M41-R as a vaccine vector. The *in vivo* dissemination of M41-R was compared to both Beau-R and M41-CK. The results of these analyses highlighted that M41-R could be a favourable vaccine backbone so further investigations were carried out, including the ability of M41-R to replicate in *ex vivo* TOCs, and *in vitro* in

CK cells at 41°C. Finally this chapter also describes the design of two new rIBVs based on M41-R that have potential to act as vaccine viruses; M41R-4/91(S) and M41R-4/91(S1). These potential vaccine viruses are similar to the vaccine candidates assessed in chapter 3 and 4 that used rIBVs, based on the apathogenic Beaudette system, to express a heterologous S glycoprotein, or S1 subunit.

6.2 Results.

6.2.1 M41-R infection *in vivo* does not result in IB related clinical signs.

To establish whether M41-R infection *in vivo* resulted in IB, a pathogenicity experiment in chickens compared M41-R to the pathogenic parent virus M41-CK, and also to the apathogenic rIBV Beau-R. During the cloning of M41-CK, two isolates of M41-R were generated and independently recovered, M41-R 6 and M41-R 12; both isolates were included in the pathogenicity experiment.

In groups of 12, 8 day old SPF RIR chickens were infected with either Beau-R, M41-CK, one of two isolates of M41-R, or 1 X BES medium for mock infection (Figure 6.1, Table 6.1). Clinical signs including snicking and rales (Figure 6.2) were observed at regular intervals from 3 to 7 dpi. The rate of snicking (Figure 6.2A) peaked at 5 dpi with M41-CK infected birds exhibiting 1.56 snicks per bird per min. In contrast M41-R birds exhibited a snicking rate of 0.31 (M41-R 12) and 0.17 (M41-R 6), while Beau-R infected birds had a rate of 0.02 snicks per bird per min. No snicking was observed from mock infected birds on 5 dpi. Overall throughout the study the rate of snicking observed in the groups infected with both isolates of M41-R were lower than M41-CK but higher when compared to both the Beau-R and mock infected groups. Although the snicking rate displayed by M41-R infected birds remained below 0.5 snicks per bird per min, it could be concluded on the clinical sign of snicking alone that M41-R has retained some virulence characteristics.

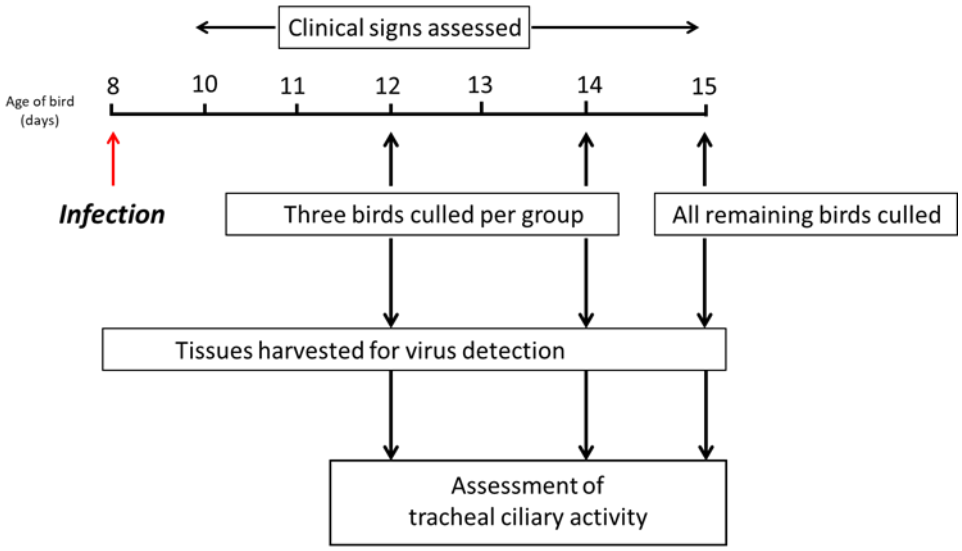

Figure 6.1: Schematic of experimental protocol: pathogenicity experiment M41-R. Groups of eight-day old SPF RIR chickens were inoculated with Beau-R, M41-R 6, M41-R 12, M41-CK or 1 x BES. The birds were assessed daily for the presence of clinical signs from two dpi; birds were 10 days old. On days 4 and 6 dpi randomly chosen birds were culled from each group and a variety of tissues harvested. The experiment ended on 7 dpi with all remaining birds culled. Tracheal ciliary activity was assessed on 4, 6 and 7 dpi.

Table 6.1: Groups and sampling numbers for M41-R pathogenicity experiment.

Group	Inoculation	Number of birds sampled			Total no. of birds per group
A	PBS (mock)	3	3	6	12
B	Beau-R	3	3	6	12
C	M41-R6	3	3	6	12
D	M41-R 12	3	3	6	12
E	M41-CK	6	6	6	12
No. of days post infection (dpi)	0	4	6	7	

As well as snicking, rales was also assessed from 3 to 7 dpi (Figure 6.1B). The percentage of birds infected with M41-CK exhibiting rales peaked on day 5 pi at 89%. Rales were not observed in those birds infected with Beau-R, M41-R 12 or those birds that were mock infected. Birds infected with M41-R 6 exhibited rales on 4 dpi, however at 9 % this was greatly reduced in comparison to M41-CK at 58 %.

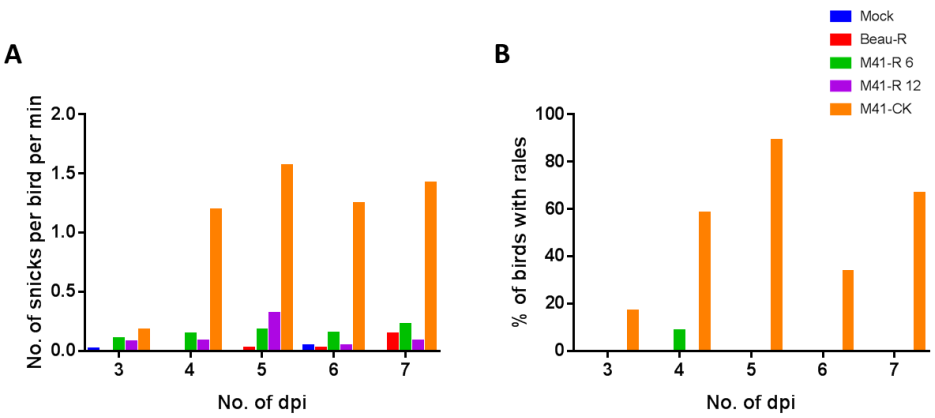

Figure 6.1: M41-R infected birds display rates of snicking and rales comparable to mock and Beau-R infected birds. SPF chickens were inoculated at 8 days of age with 10^5 PFU of either Beau-R, M41-R 6, M41-R 12, M41-CK or 1 X BES medium for mock infection. (A) Snicking was assessed from 3 to 7 dpi, with the number of snicks in a 2 min time period counted independently by 2 or 3 persons with the average of these scores presented. (B) Chickens were assessed individually for the presence of tracheal rales 3 to 7 dpi. The percentage of birds exhibiting rales per group was calculated.

In summary, the overall observed data indicated that neither infection with M41-R 6 nor M41-R 12 resulted in IB related clinical signs when compared to the pathogenic M41-CK control virus, and was more comparable to infection with the non-pathogenic rIBV Beau-R. The clinical signs data alone therefore suggests that M41-R is attenuated *in vivo.*

6.2.2: Ciliary activity 4 dpi in M41-R infected birds is comparable to mock infected birds.

One of the defining characteristics of an *in vivo* infection with a pathogenic IBV is ciliostasis in the trachea (Cavanagh *et al.,* 1997; Cook *et al.,* 1999). It is considered that a reduction of 50% (or greater) tracheal ciliary activity is indicative of the presence of a pathogenic isolate (Cavanagh *et al.,* 1997; Cook *et al.,* 1999; European Pharmacopoeia, 2010). To assess whether M41-R infection affected tracheal ciliary activity, tracheas were removed from three randomly selected birds per group on 4, 6 and 7 dpi. The percentage ciliary activities in ten 1 mm sections from three different regions per extracted trachea were assessed and the mean activities calculated (Figure 6.3). The tracheal ciliary activities observed at 4 dpi in birds

infected with M41-R 6 and M41-R 12 were comparable to both Beau-R and mock infected birds, with the group means of 84%, 74%, 87% and 92%, respectively. In contrast the ciliary activities in tracheas harvested from the M41-CK infected birds were 0% ($p<0.0001$).

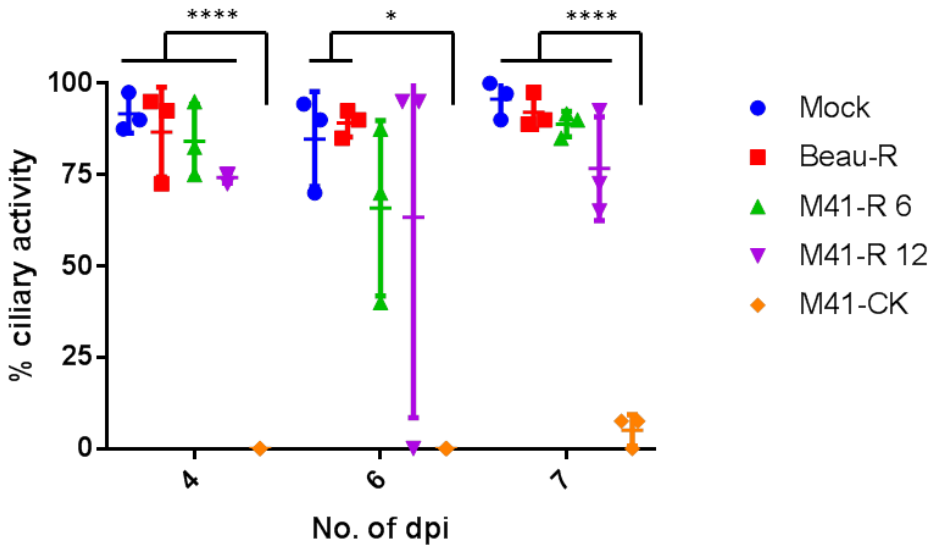

Figure 6.2: Tracheal ciliary activity in M41-R infected birds was higher than in M41-CK infected birds 4 and 7 dpi. SPF chickens were inoculated at 8 days of age with Beau-R, M41-R 6, M41-R 12, M41-CK or 1 X BES medium for mock infection. Tracheas were removed from 3 randomly chosen birds per group at 4, 6 and 7 dpi. Each trachea was sectioned into 10 x 1mm rings and the ciliary activity of each ring was assessed by light microscopy and the percentage activity calculated. Plotted points represent individual animals and the mean activity of the 10 rings assessed. Error bars represent SD. Statistical differences between groups were evaluated using a One-Way ANOVA followed by Tukey test for multiple comparisons, and are represented by * ($p<0.05$) and ****($p<0.0001$). Both isolates of M41-R exhibited higher ciliary activity than the M41-CK control group at 4 and 7 dpi. Higher ciliary activities in the Mock and Beau-R infected group compared to the M41-CK infected group were observed 4, 6 and 7 dpi.

On day 6 pi ciliary activities were comparable between the mock and the Beau-R infected groups at 85% and 89%, respectively. Ciliary activities in birds infected with M41-CK were again 0% ($p <0.05$). However, birds infected with either M41-R isolate displayed variable tracheal ciliary activities, ranging from 40% to 88% (M41-R 6) and 0% to 95% (M41-R 12)

with overall mean activities still above 50%, at 66% and 63%, respectively. This variability in the ciliary activities observed has meant there are no significant differences between the mean ciliary activities observed in the M41-R infected groups in comparison to both the M41-CK infected and mock infected group. There was much more consistency in the ciliary activities observed in tracheas harvested from birds at 7 dpi with values ranging from 85% to 92% for M41-R 6 and 65% to 93 % for M41-R 12. The observed ciliary activities at this time point were comparable to both mock infected and Beau-R infected birds, but significantly different to those observed in tracheas from M41-CK infected birds ($p<0.0001$).

In summary, the *in vivo* observations demonstrated that the two M41-R isolates showed significantly reduced pathogenicity when compared to the parental M41-CK virus but retained some virulence in terms of snicking when compared to the apathogenic Beau-R. The IBV Beaudette strain is not accepted as a potential vaccine candidate due to it lacking any retained virulence that may have resulted in its inability to induce a protective immune response. It is generally accepted that a vaccine candidate needs to retain some virulence in order to stimulate an effective protective immune response but not sufficient to induce disease or harmful pathology (reviewed by Bijlenga *et al.,* 2004). The *in vivo* observations therefore indicate that M41-R may have potential as a vaccine candidate.

6.2.3 M41-R derived RNA could not be detected in the trachea 4 dpi but was detected in harderian glands.

Trachea and Harderian glands (HG) were removed from randomly selected birds from all groups on 4 dpi and assessed by qRT-PCR for the presence of IBV RNA. No IBV RNA was detected in the tracheas from Beau-R, M41-R 6 or M41-R 12 infected birds indicating that neither virus had established a productive infection, or had been cleared by 4 dpi. All sampled birds infected with M41-CK were positive for the presence of IBV RNA (Table 6.2). In addition, RNA extracted from the HGs removed from the birds at 4 dpi was also assessed for the presence of IBV, as published work using an Arkansas strain of IBV had identified the virus in the HG as well as in tears (van Ginkel *et al.,* 2008). No IBV RNA was detected in HGs extracted from birds infected with Beau-R or mock infected with PBS (Table 6.2). However, the HGs sampled from all birds infected with M41-R 6 were positive for IBV RNA and one of the three birds infected with M41-R 12 was also positive for IBV RNA. The HGs extracted from two of three birds infected with M41-CK were also positive for IBV derived RNA.

Table 6.2: The presence of IBV RNA in the trachea and Harderian gland harvested 4 dpi as assessed by qRT-PCR.

Group	No. of birds positive for IBV RNA/total no. of birds per group	
	Trachea	Harderian Gland
Mock	0/3	0/3
Beau-R	0/3	0/3
M41-R 6	0/3	3/3
M41-R 12	0/3	1/3
M41-CK	3/3	2/3

Notes: Total RNA was extracted from 30 µg of tracheal sections and 30 µg of one harderian gland harvested per bird at 4 dpi. The presence of IBV derived RNA was assessed using qRT-PCR using a Primerdesign$_{TM}$ genesig® Kit for Avian Infectious Bronchitis Virus, Advanced. This work was completed by Dr. Erica Bickerton.

6.2.4 M41-R derived RNA could be detected in the trachea 6 and 7 dpi.

Tracheal sections harvested on 6 and 7 dpi were also assessed by qRT-PCR for the presence of IBV derived RNA. IBV RNA was only detected in two of the three birds sampled at 6 dpi that had been infected with M41-CK; all other tracheal samples were negative for IBV RNA. Similarly, two of three birds in the M41-CK group samples at 7 dpi were also positive for IBV RNA. No IBV derived RNA could be detected in tracheas harvested from Beau-R and mock infected birds. Interestingly, tracheal samples at 7 dpi from three birds infected with isolates of M41-R, one with M41-R 6 and 2 with M41-R 12, were positive for IBV (Table 6.3).

Table 6.3: The presence of IBV RNA in the trachea harvested 6 and 7 dpi as assessed by qRT-PCR.

Group	No. of birds positive for IBV RNA/total no. of birds sampled	
	6 dpi	7 dpi
Mock	0/3	0/3
Beau-R	0/3	0/3
M41-R 6	0/3	1/6
M41-R 12	0/3	2/6
M41-CK	2/3	2/3

Notes: Total RNA was extracted from 30 µg of tracheal sections harvested per bird at 6 and 7 dpi. The presence of IBV derived RNA was assessed using qRT-PCR using a PrimerdesignTM genesig® Kit for Avian Infectious Bronchitis Virus, Advanced. This work was completed by Dr. Erica Bickerton.

6.2.5 Investigation as to whether infectious M41-R could be recovered from trachea harvested 4 and 6 dpi.

Supernatants derived from homogenised tracheas harvested 4 and 6 dpi, were used to infect *ex vivo* tracheal organ cultures (TOCs). The supernatants harvested from the TOCs were subsequently assessed for the presence of IBV derived RNA by RT-PCR analysis utilising a random primer for the RT step and primers BG56 and 93/100 for the PCR step which are specific for the IBV 3′ UTR. Infectious IBV could not be recovered from tracheas harvested from either mock, Beau-R or M41-R 6 infected birds on either 4 or 6 dpi (Table 6.4). This was expected as trachea sections from these birds were negative for the presence of IBV derived RNA when screened by qRT-PCR (Table 6.2 and 6.3). Similarly to M41-R 6 no infectious virus was re-isolated from the trachea of the M41-R 12 birds sampled 6 dpi, however virus could be re-isolated from one M41-R 12 infected bird on 4 dpi (Table 6.4). This was unexpected as all the tracheas extracted from M41-R infected birds had previously been screened negative for the presence of IBV derived RNA (Table 6.2).

Infectious virus could be re-isolated from all birds infected with M41-CK on both 4 and 6 dpi (Table 6.4). The latter time point is interesting as only two of the three birds were positive for

IBV RNA in the trachea as examined by qRT-PCR (Table 6.3). Further investigation highlighted that the bird in which infectious virus could be re-isolated from trachea that had been screened negative for IBV RNA in the trachea was positive for IBV RNA in the HG. This therefore raised a question to whether active viral replication in this bird was occurring in the HG and infectious particles had been caught in the mucous that lines the trachea, which were then subsequently re-isolated. Unlike the M41-CK bird discussed here, the M41-R bird 4 dpi in which infectious virus was re-isolated was also negative for IBV RNA in the HG.

Table 6.4: The presence of infectious IBV in the trachea 4 and 6 dpi.

Group	No. of birds positive for infectious IBV/total no. of birds per group	
	4 dpi	6 dpi
Mock	0/3	0/3
Beau-R	0/3	0/3
M41-R 6	0/3	0/3
M41-R 12	1/3	0/3
M41-CK	3/3	3/3

Notes: *Ex vivo* TOCs prepared from 19 day old SPF RIR hen's eggs were inoculated in triplicate with tissue derived supernatant prepared from trachea harvested at 4 and 6 dpi. Supernatant harvested from the TOCs was screened for the presence of IBV RNA by RT-PCR utilising a random primer for the RT step and IBV specific primers BG56 and 93/100 for the PCR step.

6.2.6 Infectious M41-R could not be re-isolated from Harderian glands harvested 4 dpi.

The results of the qRT-PCR data suggested that M41-R may be replicating in the HG. To investigate whether infectious M41-R, Beau-R and M41-CK could be re-isolated, supernatant derived from homogenised HGs harvested 4 dpi was used to inoculate SPF Valo embryonated hens' eggs. Allantoic fluid from each inoculated egg was harvested 24 hpi and the RNA extracted. The presence of IBV derived RNA was assessed by RT-PCR analysis utilising primers BG56 and 93/100 (Figure 6.4). IBV RNA could be detected in all samples

from the M41-CK group, indicating that HGs from M41-CK infected birds did contain infectious IBV. No IBV derived RNA could be detected in eggs inoculated with M41-R 6 or M41-R 12 HG derived supernatant. Interestingly Beau-R derived RNA could be detected in one egg, indicating that 1 HG was positive for the presence of infectious Beau-R.

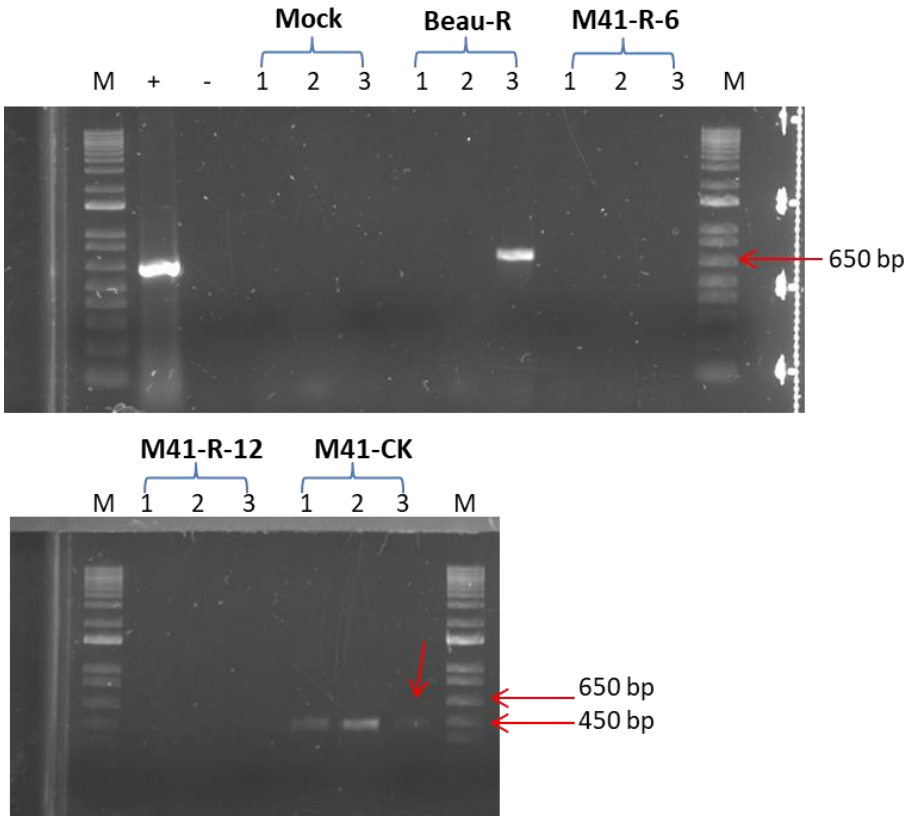

Figure 6.4: Viral isolation from Harderian glands harvested 4 dpi. SPF embryonated hens' eggs were inoculated with tissue derived supernatant prepared from 1 HG per bird harvested 4 dpi; one egg was inoculated with supernatant derived from 1 HG. Allantoic fluid was screened for the presence of IBV related RNA by RT-PCR utilising a random primer for the RT step and IBV specific primers BG56 and 93/100 for the PCR step. A positive Beau-R RNA control as well as a negative no template control was included in the RT-PCR reaction and are denoted by + and – respectively. All samples were run on a 0.8 % agarose gel alongside a 1 KB+ ladder (Life Technologies). The expected PCR product size for M41-R and M41-CK derived RNA is ~450 bp and Beau-R is 650 bp.

6.2.7 The attenuated in vivo phenotype of M41-R is the result of 4 point mutations with the replicase gene.

The retention of ciliary activity, comparable to the attenuated rIBV Beau-R at both 4 and 7 dpi demonstrated that both rIBV M41-R 6 and M41-R 12 displayed an attenuated phenotype *in vivo* (Figure 6.3). The lack of clinical signs in M41-R infected birds in comparison to M41-CK (Figure 6.2), and the lack of M41-R RNA in extracted trachea (Table 6.2 and 6.3) further demonstrated that M41-R displayed *in vivo* characteristics associated with the attenuated rIBV Beau-R rather than the pathogenic strain M41-CK. This was unexpected since M41-R is the molecular clone of M41-CK. As part of another project, the M41-CK genome was investigated by high throughput sequencing; this identified a number of differences between the previous M41-CK genome data that had been generated by Sanger consensus sequencing. The sequence of M41-R was based on the latter dataset and sequencing of the M41-R genome within the vaccinia virus vector confirmed this. Comparison of the M41-R genome sequence to the newly generated M41-CK genome sequence identified a number of differences which are summarised in Table 6.5. Interestingly, all the sequence differences are located in the replicase gene, a previously identified pathogenic determinant (Armesto *et al.,* 2009). Most of the sequence changes do not result in amino acid changes however there are four coding point mutations located in nsp 10 (C12139T), 14 (G18119C), 15 (T19052A) and 16 (G20144A). It was therefore reasonable to hypothesise that the difference in the *in vivo* phenotypes between the parent strain M41-CK and M41-R was the result of these point mutations.

Table 6.5: Sequence differences between M41-CK and M41-R.

Region of Replicase	Nucleotide position	Nucleotide change	Amino Acid Change
Nsp2	1048	T → C	Silent
	1434	T → C	Silent
Nsp4	7578	C → T	Silent
Nsp9	11682	C → T	Silent
	11709	C → T	Silent
Nsp10	12137	C → T	Pro → Leu
Nsp13	15404	G → T	Silent
Nsp14	17945	A → T	Silent
	18114	G → C	Val → Leu
Nsp15	19047	T → A	Leu → Ile
	19064	C → A	Silent
Nsp16	20139	G → A	Val → Ile
	20294	A → G	Silent

Notes: The nucleotide position corresponding to M41-CK is highlighted in red and M41-R in black. The sections in green highlight coding point mutations.

Prior to this PhD project I repaired the coding point mutations in M41-R which generated rIBV M41-K (Figure 6.4). Analysis of M41-K *in vivo* demonstrated a pathogenic phenotype confirming the role of the point mutations C12139T, G18119C, T19052A and G20144A in attenuation. The generation of neither M41-K nor the *in vivo* data will be discussed further in this chapter. M41-K however will be discussed as part of experiments that aimed to characterize M41-R *in vitro* and its potential to act as a vaccine vector. From this point onward, including the data presented in Figure 6.5, all experiments were performed during the course of this PhD project.

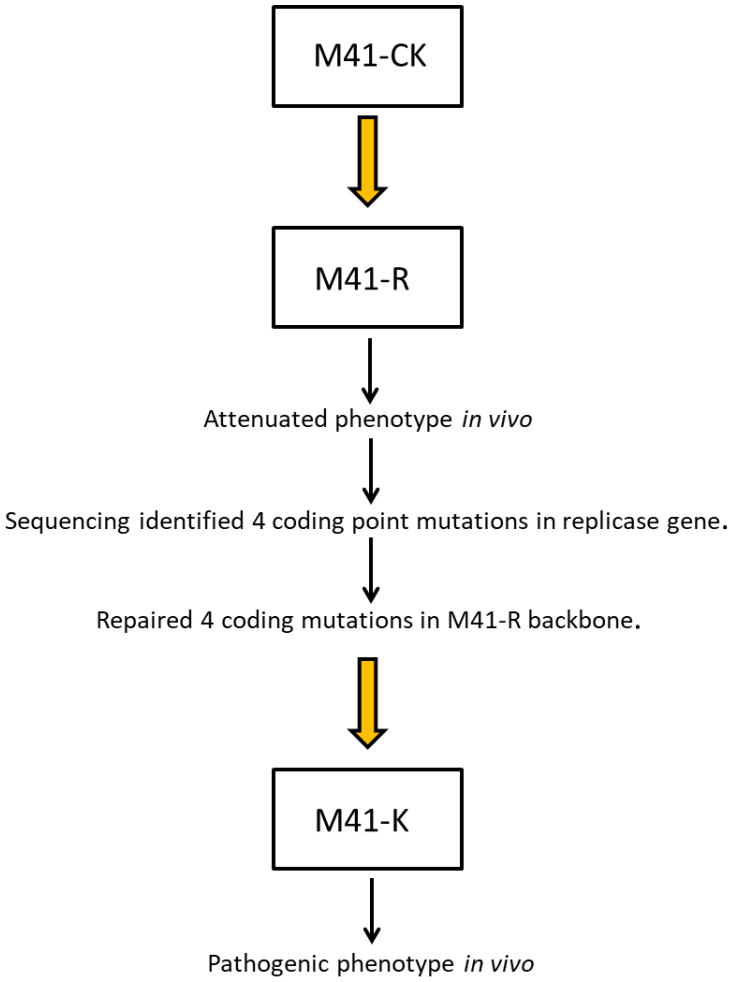

Figure 6.5: Flow chart describing the relationship between M41-CK, M41-R and M41-K, and the order in which M41-K and M41-R were generated.

6.2.8 M41-R is able to replicate in *ex vivo* tracheal organ cultures.

The attenuated *in vivo* phenotype of M41-R, together with the retention of some virulence characteristics in comparison to Beau-R, highlighted the possibility of utilising M41-R as a vaccine virus. To ensure that M41-R was capable of replicating in trachea tissue, and therefore had the potential to induce local immune responses, *ex vivo* TOCs prepared from three week old SPF RIR chickens were infected with either M41-R, M41-K or M41-CK. As both isolates of M41-R behaved similarly *in vivo*, one isolate, M41-R 12, was selected for the *in vitro* experiments. Supernatants were harvested at regular intervals over a 96 h time period and assessed for virus progeny (Figure 6.6). Titres of both M41-K and M41-R were comparable throughout the duration of the experiment. The titres of both M41-R and M41-K were lower in comparison to M41-CK throughout the experiment, with statistical significance reached at 48 and 72 h ($p<0.005$ and $p<0.05$ respectively). Despite this, the replication pattern of both M41-R and M41-K were similar to the parent virus M41-CK, demonstrating that M41-R has the ability to replicate in tracheal tissue and therefore is likely to induce local immune responses *in vivo*. The ability of M41-R to replicate in *ex vivo* TOCs does however raise the question regarding why neither isolate of M41-R was consistently detected in trachea harvested from infected birds.

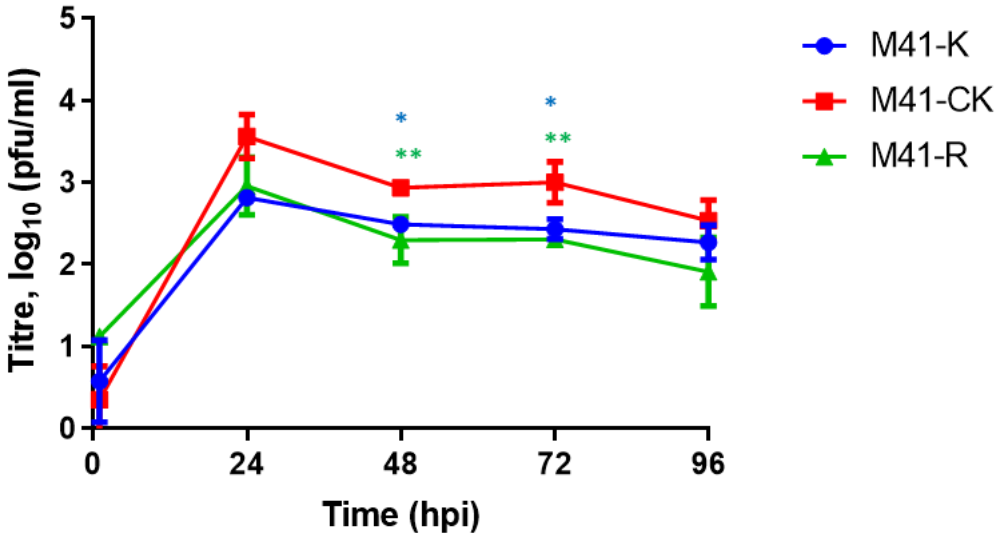

Figure 6.6: M41-R is able to replicate in *ex vivo* TOCs. *Ex vivo* TOCs were prepared from three week old SPF chickens. TOCs were inoculated in triplicate with 10^4 PFU of M41-K, M41-R or M41-CK. Supernatant was harvested at 24 h intervals and the quantity of infectious progeny assessed through titration, in triplicate, in CK cells. Each point plotted represents the mean of three independent replicates, with error bars representing SEM. Statistical differences at each time point were assessed using a One-Way ANOVA with Tukey analysis for multiple comparisons. Statistical differences between M41-CK and M41-R are highlighted by ** ($p<0.005$) and M41-CK and M41-K by * ($p<0.05$). There were no statistical differences between M41-K and M41-R at any time point assessed.

6.2.9 M41-R replication is sensitive to temperature *in vitro*.

As discussed in chapter 5 rIBV Beau-R is able to establish a productive infection in *ex vivo* TOCs but cannot establish a productive infection in tracheal tissue *in vivo* when delivered by the ocular/nasal route. This is possibly the consequence of the replication of Beau-R being sensitive to temperature and in particular, highly restricted at 41°C. To investigate whether the replication of rIBV M41-R was also temperature sensitive, which would help inform about its suitability as a vaccine vector, CK cells were infected with M41-R, M41-K or M41-CK and incubated at either 37°C or 41°C. The quantity of the resulting viral progeny harvested over a 96 h time period was assessed via titration in CK cells (Figure 6.7 and 6.8). The complete dataset generated is displayed in Figures 6.7 and 6.8, and split apart for clarity to allow visualisation of different comparisons for analysis.

The titres of infectious progeny virus generated by M41-CK and M41-R infection at 37°C were comparable from 1 to 96 h (Figure 6.7B) indicating at these time points and temperature the replication kinetics of the pathogenic M41-CK and the non-pathogenic M41-R were similar. The titres of M41-K at 24 and 48 h were lower than M41-CK ($p<0.05$) and also lower than M41-R at 24 h ($p<0.0001$). Despite the slightly lower titres however the replication pattern at 37°C of the pathogenic rIBV M41-K was similar to both the non-pathogenic rIBV M41-R and the pathogenic parental virus, M41-CK.

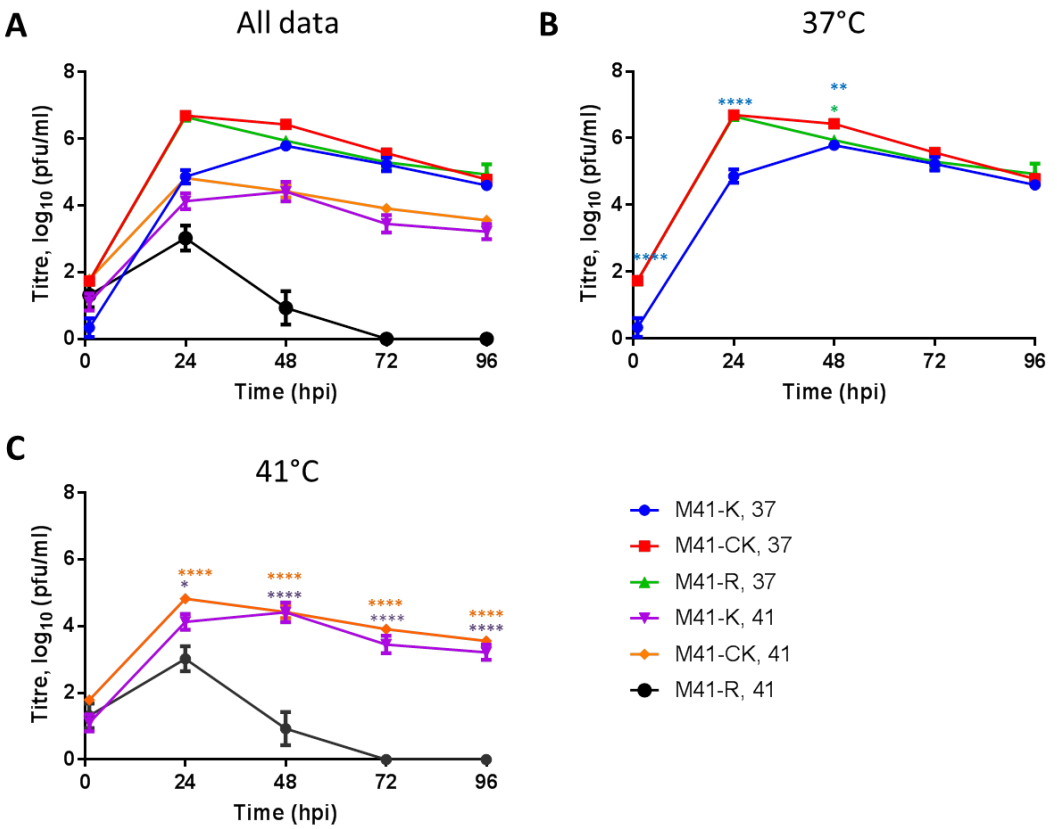

Figure 6.7: Assessment of M41-R replication at 37°C and 41°C. CK cells seeded in 6 well plates were inoculated with 10^5 PFU M41-K, M41-CK or M41-R, and incubated at either 37°C or 41°C. Supernatant was harvested at 24 h intervals and the quantity of infectious progeny was determined via titration in triplicate in CK cells. Each point represents the mean of three independent experiments with error bars representing SEM. (A) represents all data gathered during the experiment, and (B) displays only the data generated through incubation at 37°C and (C) at 41°C. Statistical differences were assessed using a Two-way ANOVA stating time and virus as independent factors, followed by a Tukey test for multiple comparisons. (B) Statistical differences between M41-CK and M41-K are highlighted by **** ($p<0.0001$) and ** ($p<0.005$). Differences between M41-R and M41-CK are highlight by * ($p<0.05$). (C) Statistical differences between M41-CK and M41-R are highlighted by **** ($p<0.0001$) and differences between M41-K and M41-R are highlighted by **** ($p<0.0001$) and * ($p<0.05$).

At 41°C differences in the replication kinetics were observed between M41-CK, M41-K and M41-R. The replication patterns of M41-K and M41-CK were similar with the titres of infectious progeny virus comparable at all time points assessed (Figure 6.7C). In contrast the titres of M41-R were lower than both M41-K and M41-CK at 48 to 96 h ($p<0.005$). At 24 h M41-R exhibited lower titres than both M41-K and M41-CK however only the latter reached statistical significance ($p<0.005$). The pattern of replication of M41-R was different to both M41-K and M41-CK. Similarly to M41-CK, titres of M41-R peaked at 24 h, albeit at a lower level whereas titres of M41-K peaked at 48 h. After the peak titre, both M41-K and M41-CK displayed a gradual and steady decline in infectious progeny virus from 24 or 48 to 96 h; M41-R on the other hand exhibited a sharp decline between 24 – 48 h. This difference in replication kinetics could therefore indicate that the point mutations differentiating M41-CK and M41-K from M41-R, nsp 10 (C12139T), 14 (G18119C), 15 (T19052A) and 16 (G20144A), may have a determining role in the restricted *in vitro* replication phenotype observed at 41°C.

Further analysis of the growth curve data highlights that overall replication at 41°C of both M41-K and M41-R produces lower titres of infectious progeny virus than replication at 37°C (Figure 6.8B and 6.8D). This was comparable to the parent virus, M41-CK, which also generally produces lower quantities of infectious progeny at 41°C (Figure 6.8C); an observation also noted in Chapter 5. This pattern of lower titres produced at 41°C compared to 37°C is largely comparable between M41-K and M41-CK. There is one interesting exception; at 24 hpi the titres produced by M41-K infection at 37°C and 41°C are similar, indicating that at this time point replication is either not affected by temperature, or not affected to a level that reduces the quantity of infectious progeny virus produced.

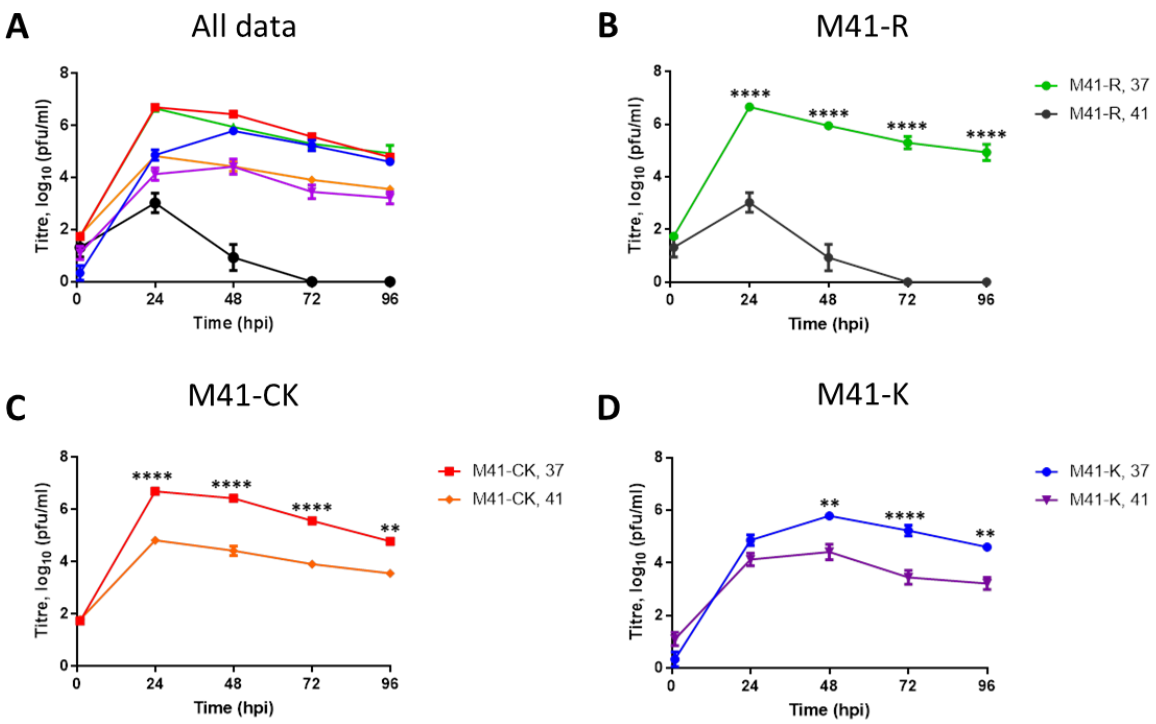

Figure 6.8: Replication kinetics of M41-CK, M41-K and M41-R at 37°C and 41°C. CK cells seeded in 6 well plates were inoculated with 10^5 PFU M41-K, M41-CK or M41-R, and incubated at either 37°C or 41°C. Supernatant was harvested at 24 h intervals and the quantity of infectious progeny was determined via titration in triplicate in CK cells. Each point represents the mean of three independent experiments with error bars representing SEM. Graph A represents all data gathered during the experiment, and graph B, C and D only displays data generated by M41-R, M41-CK and M41-K respectively. Statistical differences were assessed using a Two-way ANOVA stating time and temperature as independent factors, followed by a Tukey test for multiple comparisons. Statistical differences at each time point are highlighted by ** ($p<0.005$) and **** ($p<0.0001$).

The difference in the replication patterns of M41-R at 37°C and 41°C is not comparable to the replication patterns observed for M41-K or M41-CK. The differences in the amounts of infectious progeny produced by M41-R at 37°C and 41°C at 24 hpi are much greater than those for M41-CK and M41-K, which do not exhibit a difference (Figure 6.8). The titre, (PFU/ml), produced by M41-CK infection at 41°C is lower than the titre observed at 37°C by approximately a magnitude of 1.5 – 2 log_{10}, whereas the titre of M41-R is reduced by 3.5 – 4 log_{10}. The differences exhibited between M41-R infection at 37°C and 41°C become more prominent as the infection proceeds with no detectable progeny produced at 72 and 96 h. This is in contrast to both M41-CK and M41-K which produced a seemingly steady quantity of infectious virus at both incubation temperatures at 48 to 96 hpi. At these time points for both viruses the difference in PFU/ml between 37°C and 41°C is approximately 1.5 – 2 log_{10}. This growth kinetic experiment therefore demonstrates that the replication of M41-R is restricted at 41°C identifying that M41-R replication can be classified as temperature sensitive.

6.2.10 Entry of M41-R *in vitro* is not sensitive to temperature.

To determine whether entry was the prohibitive step to establishing a productive infection at 41°C, a temperature swap experiment was carried out (Figure 6.9A). CK cells were infected with M41-K or M41-R and incubated at either 37°C or 41°C for 1 h allowing for viral attachment and entry. After 1 h the virus was removed and the cells washed in PBSa to remove any residual virus, after which the cells were incubated at either the same temperature or were swapped to be incubated at the other. The resulting supernatant was assessed for infectious viable progeny virus (Figure 6.9B and 6.9C).

Titres of M41-K in all treatment groups were comparable to each other (Figure 6.9B) indicating that productive replication of M41-K is unaffected by the swap in incubation temperatures. This was expected as the replication of M41-K, in terms of the generation of infectious viable progeny virus, is not sensitive to temperature at 24 h (Figure 6.8D). In contrast, the swap in incubation temperatures did have an effect on the replication of M41-R (Figure 6.9C). The titres of M41-R were comparable between those groups in which inoculated cells were incubated at a first temperature of 37°C for virus entry and then a second temperature of 37°C for viral replication (37-37) and for those that were initially incubated at a temperature of 41°C and then incubated at a temperature of 37°C (41-37). Similarly titres were comparable between groups in which infected cells were initially incubated at 37°C and then incubated at 41°C (37-41), and those incubated at 41°C and

then continued at 41°C (41-41). A difference in the first incubation temperature therefore had no effect of the quantity of infectious viable progeny virus produced indicating the temperature at which viral attachment and entry occurred was not the determining factor.

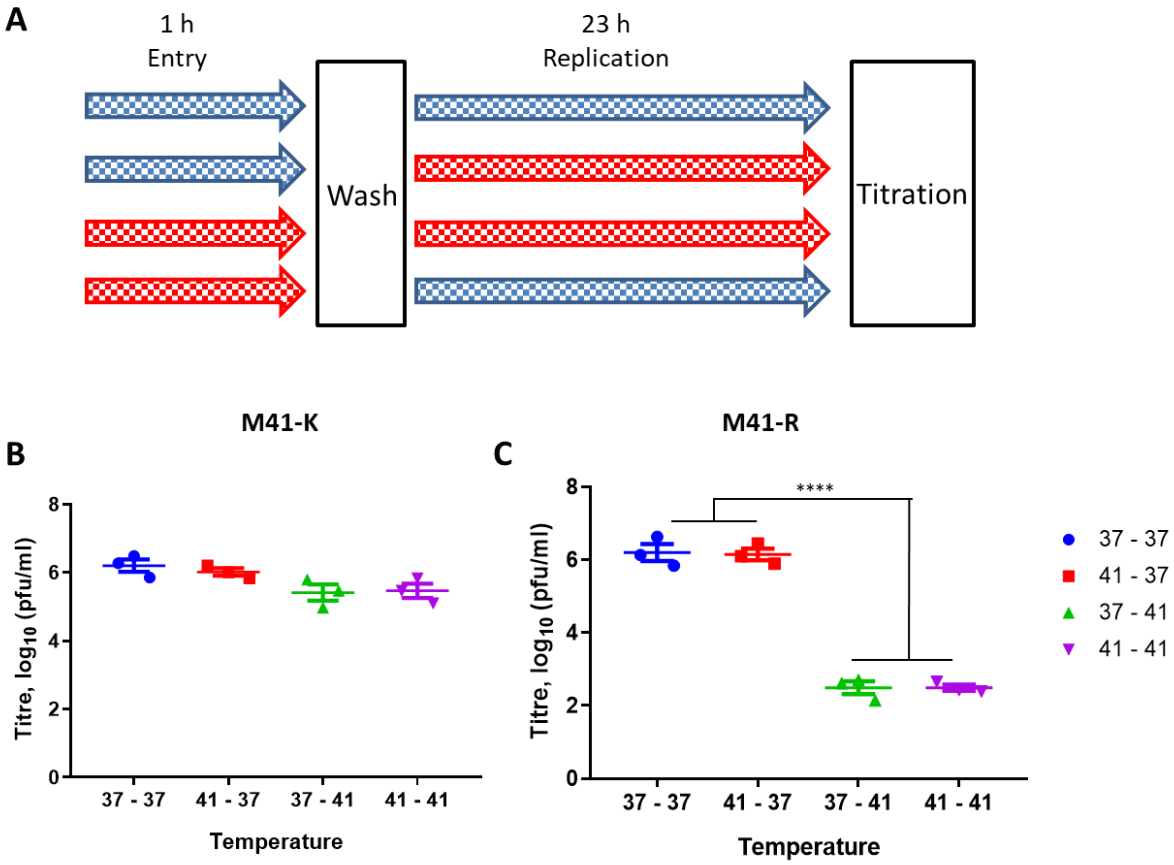

Figure 6.8: Entry does not restrict replication of M41-R at 41°C. (A) Schematic detailing experimental protocol. CK cells seeded in 6 well plates were inoculated in triplicate with 10^5 PFU of either M41-K or M41-R. Cells were incubated for 1 h at either 37°C (blue) or 41°C (red), after which the viral inoculum was removed and the cells washed to remove any unbound virus. Cells were then incubated at either 37°C or 41°C for 23 h. The quantity of infectious viral progeny was assessed through titration in triplicate in CK cells. Graph (B) represents data generated from M41-K infection and graph (C), M41-R. Each point represents the mean titre of infectious progeny virus generated from one independent experimental replicate. Error bars represented the SEM from three independent experimental replicates. Statistical differences were assessed using a one-way ANOVA with a Tukey test for multiple comparisons. Statistical differences are highlighted by **** ($p<0.0001$).

Differences in the titres of M41-R were observed in groups that had different secondary incubation temperatures. The titres produced from infections incubated at 37-41 were lower than those incubated at 37-37 ($p<0.0001$), similarly infections at 41-41 produced much lower titres than those incubated at 41-37 ($p<0.0001$). It is therefore the second incubation temperature in which the virus was expected to undergo active replication, assembly and egress that affects the production of viable progeny viruses and is therefore the determining factor. Coronavirus entry is mediated by the S glycoprotein and therefore the results of the temperature swap experiment, which tend to rule out entry, also rule out a potential determinant role for the S glycoprotein. This in turn further indicates the role of the replicase located mutations C12139T, G18119C, T19052A and G20144A in the restricted replication phenotype of M41-R observed at 41°C. In addition, the results of the temperature swap experiments also indicate the potential to generate rIBVs based on the M41-R genome that express heterologous S glycoproteins without affecting the temperature sensitive phenotype; this would be an important benefit for the development of M41-R as a vaccine vector.

6.2.11 The replication of M41-R is not comparable to Beau-R at 41˚C.

The finding that M41-R was temperature sensitive raised some concerns regarding its potential role as a vaccine vector. Whilst it appeared that M41-R could establish a limited infection at 41°C, in terms of both time and quantity of infectious viral progeny, there was a concern that M41-R may not offer much improvement in terms of *in vivo* replication compared to that of Beau-R. A growth kinetic assay was performed to directly compare productive viral replication of both Beau-R and M41-R (Figure 6.10). CK cells were inoculated with Beau-R or M41-R and incubated at either 37°C or 41°C. The quantity of viable infectious virus progeny over a 48 h time period was assessed. The pathogenic clone, M41-K, was also included in the experiment as a positive control to confirm that the CK cells incubated at 41°C were capable of supporting a productive infection.

The titres of viable infectious progeny virus were comparable between cells incubated at 37°C infected for both Beau-R and M41-R at all-time points (Figure 6.10). M41-K infected cells produced lower titres of progeny virus in comparison to Beau-R at 24 hpi ($p<0.005$), but titres were comparable at both 1 and 48 hpi. However, at 41°C, at 24 and 48 hpi, titres of virus produced from both Beau-R and M41-R infected cells were lower than those observed for M41-K ($p<0.005$). Interestingly, at 41°C, the titres of infectious progeny virus were higher from cells infected with M41-R at both 24 and 48 hpi when compared to cells infected with Beau-R ($p<0.05$), indicating that M41-R and Beau-R do not share the same replication

phenotype at 41°C. The observation that M41-R is able to produce infectious progeny virus at 41°C, unlike Beau-R, alongside the identification that M41-R exhibits an attenuated phenotype *in vivo* supports the development of M41-R as a vaccine vector. In addition, the growth kinetic assays (Figure 6.7, 6.8 and 6.10) highlight the possibility that M41-R may be able to replicate *in vivo* for a defined period of time, for up to 48 h.

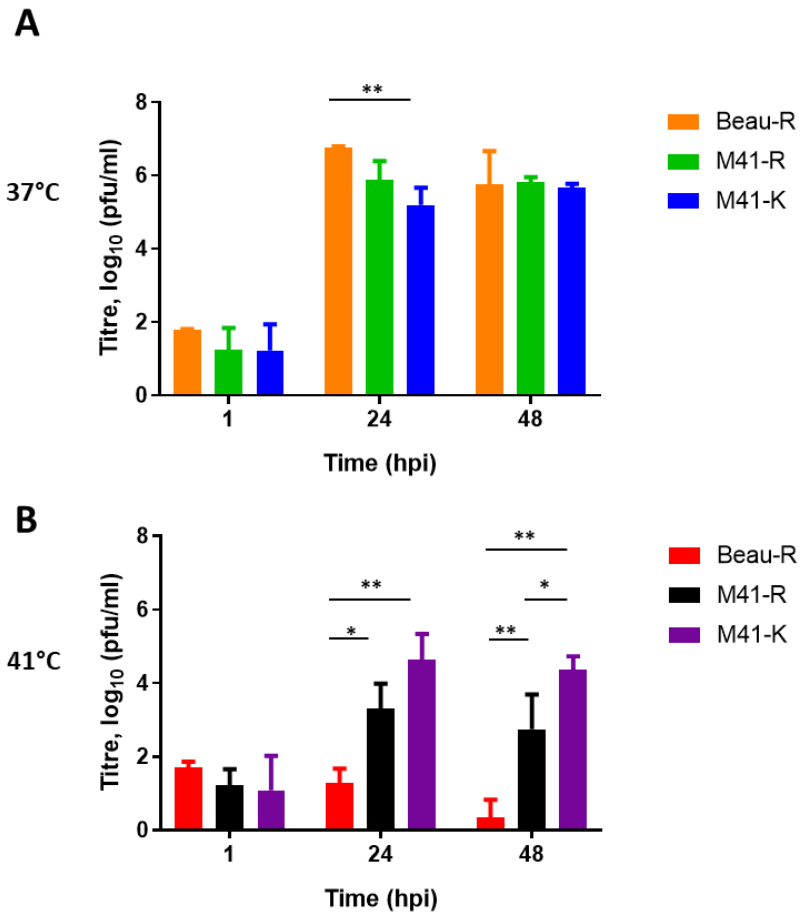

Figure 6.10: Productive M41-R replication is higher than Beau-R replication at 41°C. CK cells seeded in 12 well plates were inoculated with 10^4 PFU Beau-R, M41-R or M41-K and incubated at either (A) 37°C or (B) 41°C. Supernatant was harvested at 1, 24, and 48 hpi and the quantity of infectious progeny virus assessed through titration, in triplicate, in CK cells. Error bars represent the SEM of three independent experiments. Statistical differences at each time point were assessed using a one way ANOVA with Tukey analysis for multiple comparisons and are highlighted by * ($p<0.05$) and ** ($p<0.005$).

6.2.12 M41-R as a vaccine vector; the generation of rIBV M41R-4/91(S1) and M41R-4/91(S).

To investigate whether M41-R would be a suitable vaccine vector, two rIBVs were designed based on the M41-R genome with modifications to the S glycoproteins. The UK field isolate 4/91 was chosen as the "donor S" strain, primarily due to the previous construction of rIBV BeauR-4/91(S) which demonstrated that it was possible to construct a rIBV expressing a heterologous 4/91 S glycoprotein. In addition, as discussed in chapters 3 and 4, BeauR-4/91(S) can, under experimental conditions, induce a protective immune response against homologous 4/91 challenge *in vivo* (Armesto *et al.,* 2011). This response is not as robust as was expected with a protection level, as defined by ciliary activity, of 65%; comparable to the protection induced by BeauR-M41(S) (Hodgson *et al.,* 2004; Ellis *et al.,* 2018). Similar to BeauR-M41(S) it is theorised that the protection level would be improved if the 4/91(S) was expressed in a less attenuated IBV vector, that is not based on the Beaudette genome.

One of the rIBVs designed as a potential vaccine candidate based on the M41-R genome was M41R-4/91(S), containing the ectodomain of the S glycoprotein from the virulent IBV field strain 4/91 (UK). Similarly to BeauR-4/91(S) the S glycoprotein signal sequence and cytoplasmic tail are derived from the vector backbone sequence, in this case M41-R, with the rest of the S glycoprotein from 4/91 (UK). The generation of rIBV M41R-4/91(S) would allow a direct comparison to BeauR-4/91(S) in an *in vivo* homologous vaccine challenge experiment thereby answering the question of whether protection levels are improved utilising a less attenuated IBV vector for antigen delivery. The second rIBV designed and based on the M41-R genome was M41R-4/91(S1); this contains a chimeric S gene with the sequence of the S1 subunit derived from the UK field strain 4/91, and the remainder of the S gene from M41-R. Whilst results presented in Chapter 3 indicated that a homologous S1 and S2 glycoprotein was required for the induction of a robust protective immune response using Beau-R as the vector backbone, it was theorised that a heterologous S1 subunit alone could be used for protection if delivered by a less attenuated IBV vector backbone. Therefore, rIBV M41R-4/91(S1) would be included in the same homologous *in vivo* vaccine challenge experiment as both rIBV M41R-4/91(S) and rIBV BeauR-4/91(S). This would allow the investigation to determine whether the S1 subunit is sufficient to induce a protective immune response when expressed in a less attenuated IBV vector, or whether a spike glycoprotein composed of homologous S1 and S2 subunits is required.

6.2.12.1 Generation of recombinant vaccinia viruses.

The first stage to making a rIBV is to construct an rVV containing a full-length cDNA copy of the IBV genome containing the desired modification (Keep *et al.,* 2015). The process of constructing an rVV is described in Chapter 2, and will not be discussed in detail here.

Briefly, to construct a rVV containing the M41R-4/91(S1) genome sequence, the rVV M41-R containing the full-length genome sequence of M41-R was used in the reverse genetic system alongside plasmid pGPT-M41-4/91(S1) (see appendix for sequence of the insert, Figure 8.1). This generated four isolates of rVV M41R-4/91(S1) as well as generating several rVVs with varying chimeric 4/91/M41 S1 subunits. The rVVs containing chimeric S1 sequences were not fully investigated as part of this PhD project. Similarly, four isolates of M41R-4/91(S) were generated using the reverse genetic system utilising rVV M41R-del-S, which encodes the M41-R genome but with the S gene deleted, alongside the plasmid pGPT-M41R-4/91(S) (see appendix for sequence of the insert, Figure 8.2). This was a more targeted approach than that used for the construction of M41R-4/91(S1) as chimeric sequences were not desired. In all the rVV isolates generated, eight in total, the presence of correct S gene sequence in the correct position was confirmed by Sanger sequence analysis.

6.2.12.2 The recovery of infectious rIBV

The four isolates of rVV M41R-4/91(S1) and four isolates of rVV M41R-4/91(S) were taken forward for the recovery of infectious rIBV in CK cells. The detailed method used for the recovery process is described in Chapter 2. Despite several attempts none of the four isolates of rVV M41R-4/91(S1) generated infectious rIBV M41R-4/91(S1), which could indicate the 4/91 S1 subunit is not compatible with an M41 S2 subunit. Similarly, the four isolates of rVV M41R-4/91(S) also failed to generate rIBV, which could indicate an overall incompatibility of the 4/91 S glycoprotein with an M41-R vector, although I personally think this is unlikely and will discuss further in the next section.

6.3 Discussion.

The results of the *in vivo* vaccine-challenge experiments presented in Chapter 3 and 4 indicated that rIBV Beau-R may not be an ideal vaccine vector. The identification in Chapter 5 that the replication of Beau-R is temperature sensitive, and is highly restricted at 41°C, the core body temperature of a chicken, further supported the idea that a new vaccine vector should be considered. This chapter details results indicating that rIBV M41-R is a possible and more suitable alternative to Beau-R as a vaccine vector.

The *in vivo* pathogenicity experiment confirmed that similar to Beau-R, *in vivo* infection with M41-R does not induce IB related clinical signs (Figure 6.2). Also, similarly to Beau-R, infection with M41-R does not reduce tracheal ciliary activity at 4 or 7 dpi (Figure 6.3). This is in contrast to the pathogenic IBV M41-CK in which infection did result in IB-related clinical signs and a reduction in ciliary activity at 4, 6 and 7 dpi (Figure 6.2 and 6.3). It is unclear at this stage whether the reduced ciliary activity observed at 6 dpi in the M41-R infected groups is a true representation of an M41-R infection. In the groups infected with M41-R 6 and M41-R 12, one bird in each group exhibited less than 50% ciliary activity at 6 dpi. Interestingly both these birds were negative for IBV RNA in the trachea, and no infectious progeny virus could be re-isolated. All birds infected with M41-CK exhibited a 100% reduction in ciliary activity on both 4 and 6 dpi, and on 4 dpi were positive for IBV RNA and for presence of infectious progeny virus. A larger sample size is required to establish whether it is a pattern with M41-R infection that one third of birds will exhibit a reduction in tracheal ciliary activity at 6 dpi or whether these birds discussed above could be classified as outliers, and another factor in these individual birds played a role in the reduced ciliary activity observed. Overall, the lack of IB related clinical signs alongside the retention of ciliary activity comparable to both mock and Beau-R infected birds at 4 dpi demonstrated that M41-R displays an attenuated phenotype *in vivo* when compared to the parental M41-CK virus.

A comparison of the dataset generated from sequencing the M41-R full genome within the vaccinia virus vector with the dataset of the M41-CK genome generated by high throughput sequencing methods, identified four coding mutations as well as a number of non-coding mutations within the replicase gene (Table 6.5). The coding mutations that differentiate M41-R from the pathogenic parent M41-CK are C12139T (nsp 10), G18119C (nsp 14), T19052A (nsp 15) and G20144A (nsp 16). The replicase gene has previously been reported as a pathogenic determinant of IBV (Armesto *et al.,* 2009, Ammayappan *et al.,* 2009, Huo *et al.,* 2016). In addition, there have been several publications that have linked nsp 10, 14, 15 and

16 to pathogenicity in other coronaviruses including SARS-CoV and MHV (Zust *et al.,* 2011; Menachery *et al.,* 2014; Deng *et al.,* 2017; Kindler *et al.,* 2017; Graham *et al.,* 2012; Sperry *et al.,* 2005).

The point mutations located in nsp 15, T19052A, and 16, G20144A, have resulted in conservative amino acid changes within the respective proteins, Leu183Ile and Val209Ile. In both cases, a non-polar amino acid has been replaced by another non-polar amino acid likely reducing the possibility of the mutations having induced major conformational changes to the respective protein structure. In addition, the amino acid changes are also found amongst other coronaviruses; amino acid residue 209 in nsp 16 is also an Ile in TCoV, SARS-CoV, MHV and HKU1 and amino acid residue 183 in nsp 15 is also an Ile in HKU1 and MHV (Appendix, Figure 8.8). Furthermore the mutation in nsp 15, Leu183Ile is not within the proposed NendU core domain (Deng and Baker, 2018). Similarly, the mutation in nsp 16, Val209Ile is not part of the essential KDKE motif required for 2'O-methyltransferase activity, and it is not one of the residues reported to be essential for effective interaction with the stimulatory co-factor, nsp 10 (Chen *et al.,* 2011, Decroly *et al.,* 2011; Lugari *et al.,* 2010). It therefore seems unlikely that the point mutations in nsp 15 and 16 have played a major contributory role in the attenuated phenotype observed during M41-R *in vivo* infection.

Quick inspection suggests the point mutation in nsp 10 (C12139T) has also resulted in conservative amino acid change, both non-polar to non-polar. However, in nsp 10 the point mutation has resulted in a change at residue 85 from Pro to Leu; the structure of the two amino acids is quite different as proline contains a cyclic structure raising the possibility that the mutation has resulted in conformational changes. In addition, unlike the nsp 15 and 16 mutations, the Pro85Leu mutation has occurred at a highly conserved residue (Appendix, Figure 8.10). Furthermore nsp 10 consists of two zinc fingers that are co-ordinated by a number of Cys and His residues (Joseph *et al.,* 2006), one of which is located at residue 84, neighbouring the Pro85Leu mutation. It is also interesting that an Ala substitution at position 82 in MHV, equivalent to residue 83 in IBV, was lethal in that no viable virus could be recovered (Donaldson *et al.,* 2007). Alanine mutagenesis studies utilising SARS-CoV have also identified several residues near to the Pro85Leu mutation that have reduced the binding of nsp 10 to 14 (Bouvet *et al.,* 2014). Further work is therefore required to establish whether this mutation has played a major role the attenuated *in vivo* phenotype of M41-R, and if so, whether this is the result of reduced binding capacity with nsp 14.

The mutation in nsp 14 is also a conservative change, Val to Leu at residue 393. Similar to the nsp 10 mutation, Val393Leu has occurred at a position conserved amongst other coronaviruses, and in addition has occurred in a conserved area (Appendix, Figure 8.11). Nsp 14 is a bifunctional enzyme with both ExoN activity (Minskaia *et al.,* 2006, Ma *et al.,* 2015) and N7-MTase activity (Chen *et al.,* 2009; Ma *et al.,* 2015). The mutation Val393Leu has occurred within the N7-MTase domain (Appendix, Figure 8.11), however it is not one of the critical residues for catalytic activity or for methyl donor substrate binding (Chen *et al.,* 2013; Jin *et al.,* 2013). It is also not within the nsp 10 binding area which is located in the ExoN I domain (Ma *et al.,* 2015). The residue is however located amongst a number of residues that have been identified to support the methyl donor substrate binding pocket (Chen *et al.,* 2013). In addition, residue Phe401 has been identified as being involved in purine binding in SARS-CoV (Ma *et al.,* 2015); the equivalent residue in IBV is Tyr396, located only three amino acids from the Val393Leu mutation. It is therefore plausible that the Val393Leu mutation has affected N7-MTase capping activity which in turn due to the presence of uncapped RNA molecules may affect the ability of the virus to evade host RNA sensors *in vivo* (Zust *et al.,* 2011), and/or have effects on RNA degradation and viral translation, both of which could result in lower viral load and consequently less disease burden (reviewed by Savajol *et al.,* 2014).

The mutations in both nsp 10 and nsp 14 are of interest, and it is possible an interaction between the two also plays a role in the attenuated *in vivo* phenotype of M41-R. Whilst nsp 10 has not been demonstrated to be a stimulatory factor to the nsp 14 N7-MTase activities (Bouvet *et al.,* 2010), it does bind to the EXoN domain which is theorised to result in a stabilisation effect (Ma *et al.,* 2015). The two domains of nsp 14 do not exist independently and a number of residues are involved (Ma *et al.,* 2015); it therefore seems reasonable to hypothesise that nsp 10 binding stabilises the entire nsp 14 protein structure. Further research is required to identify the effect that all the mutations present in M41-R are having, including whether nsp 10 can efficiently bind to nsp 14, and also whether the N7-MTase activity of nsp 14 has been detrimentally affected. One important point to note is that the addition of a cap-1 structure to viral mRNA is a sequential process (Bouvet *et al.,* 2010; Ma *et al.,* 2015), with nsp 14 N7-MTase activity preceding nsp 16 2'O-methyltransferase capping activity (Chapter 1, Figure 1.6). It therefore remains a possibility that the attenuation of M41-R is the result of the collaborative effect of mutations in nsp 10, 14 and 16.

Despite the unknown molecular mechanism, the attenuated *in vivo* phenotype observed highlighted that M41-R had the potential to act as a vaccine vector. The *in vivo* dissemination

pattern in trachea and HG harvested from M41-R infected birds was compared to Beau-R infected and M41-CK infected birds. Whilst M41-CK could consistently be detected in harvested tracheal tissue at all time points assessed, similarly to Beau-R, M41-R could not (Table 6.2 and 6.3). Whilst this is a concern for IBV vaccine vectors as they need to induce robust local immune responses (reviewed by Bijlenga *et al.,* 2004), it must be noted that it is possible M41-R can replicate in the trachea earlier in infection, particularly as growth kinetic assays in *ex vivo* TOCs (Figure 6.6) highlight that M41-R can replicate in tracheal tissue. Future studies should assess earlier time points during *in vivo* infection, including at both 1 and 2 dpi and should additionally include assessment of nasal turbinates, eyelids and lung tissue. A kinetic study in *ex vivo* TOCs using a lower PFU should also be carried out as it is possible that M41-R may not be able to initiate and sustain a productive infection at lower titre than the 10^4 PFU used to generate the data in Figure 6.6. In the bird, infectious virus will be caught in mucous produced in the trachea, making it very unlikely that tracheal tissue is infected with large quantities of virus.

In HGs examined at 4 dpi, both M41-R and M41-CK derived RNA could be detected whereas Beau-R was not (Table 6.2). Interestingly, also at 4 dpi, infectious Beau-R could be re-isolated from the HG of one bird whereas HGs extracted from M41-R infected birds yielded no infectious virus (Figure 6.4). All three HGs extracted at 4 dpi from the M41-CK infected birds yielded infectious virus, yet only two were positive for IBV derived RNA (Table 6.2, Figure 6.4). It must be noted that whilst both HGs from each sampled bird were harvested, one was taken forward for RNA extraction and subsequent qRT-PCR analysis and the other for viral isolation. Discrepancies between the qRT-PCR and the viral isolation data may be a reflection of this process as it is possible that the virus replication was localised to one HG only. The same phenomenon is seen in trachea harvested from one bird infected with M41-R 12 at 4 dpi; no IBV RNA was detected, but infectious virus was recovered. This discrepancy may again be the reflection of the process of using one section of trachea for RNA extraction and one for virus isolation. It could also however be a reflection of the sensitivity of the two techniques. Virus isolation is a very sensitive method, and is considered the “gold standard” technique at determining viral presence (reviewed by de Wit and Cook 2014) however qRT-PCR is thought to be up to one hundred times more sensitive (Jackwood *et al.,* 2012) although can give false negatives if the samples contain substances that inhibit the reaction (Jackwood *et al.,* 1997). One final possibility for the discrepancies is contamination of samples, however this seem extremely unlikely as all the relevant negative controls, as well samples harvested from the mock infected birds, are all identified as negative for IBV RNA by qRT-PCR and infectious IBV by virus isolation.

IBV specific humoral immune responses have been identified in HGs extracted from experimentally infected SPF chickens (van Ginkel *et al.,* 2008). The detection of M41-R derived RNA in HGs supports the development of M41-R as a vaccine vector as this finding highlights the possibility that this rIBV can induce local responses in immune active tissues. It remains to be determined how efficiently M41-R is replicating in the HG, and the dynamics of replication from 1 to 7 dpi. This *in vivo* experiment was completed before the start of this PhD project and not with the objective of using M41-R as a vaccine vector; as such the optimal time points for antigen delivery were not necessarily included. Further research is required to establish the *in vivo* dissemination pattern of M41-R through early infection to the point of viral clearance in the trachea and HG as well as in a variety of tissues not harvested during this experiment. It is likely given the results of the Beau-R/M41-CK pathogenicity study presented in Chapter 5 in which Beau-R was re-isolated from nasal tissue harvested 1 and 4 dpi, that M41-R would also be detected in this tissue at these time points. It will also be important to identify if M41-R can spread from infected birds to naïve birds thus indicating how an M41-R vaccine virus may disseminate through a poultry flock, and if there is a risk of recombination with either field or other vaccine isolates.

The data gathered from the *in vivo* experiment identified that M41-R exhibited an attenuated phenotype which subsequently highlighted the potential for M41-R to act as a vaccine vector. Further investigation demonstrated that like M41-CK and the pathogenic clone, M41-K, M41-R has the ability to productively replicate in *ex vivo* TOCs and therefore in tracheal tissue (Figure 6.6). *In vitro* assays however identified that M41-R replication is temperature sensitive and is limited in terms of both time and quantity of infectious viral progeny production at 41°C (Figure 6.7 and 6.8). In comparison to both M41-K and M41-CK, peak titres of M41-R are reduced and the period of productive replication is much shorter, with no M41-R detected at 96 h (4 dpi). It is plausible that this temperature sensitivity accounts for the lack of M41-R detected in tracheal tissue harvested during the *in vivo* experiment. If M41-R did establish an infection in the trachea, it is likely that the productive infection had run its course before the first time point, at 4 dpi, when trachea was harvested from infected birds. Whilst the temperature sensitive phenotype identified in this chapter may initially appear to be a disadvantage in terms of using M41-R as a vaccine, it may actually provide several benefits which will be discussed later in this section.

The restricted replication of M41-R at 41°C is likely to be the result of one or more or some combination of the four coding mutations that differentiate M41-R from M41-CK and M41-K; C12139T (nsp 10), G18119C (nsp 14), T19052A (nsp 15) and G20144A (nsp 16). The role

of the non-coding mutations at this stage cannot be completely ruled out, as there may be potential functions in the maintenance of secondary RNA structure and the regulation of viral transcription. As discussed the proteins in which the coding mutations are present, nsp 10, 14, 15 and 16, have several roles in the virus life cycle including capping of the viral RNA and proofreading. It cannot be stated with certainty that the same mechanism by which M41-R has been attenuated by these point mutations is also the same mechanism which has resulted in a temperature sensitive phenotype or vice versa. Temperature sensitivity and the replication of IBV as well as other coronaviruses, has been discussed in detail in Chapter 5. With regards to M41-R further research is required to assess the function of the relevant nsps at both 37°C and 41°C, and also whether interactions between the nsps is affected at the different temperatures. It is interesting to note that temperature sensitive MHV mutants have been identified with mutations in Gln65Glu in nsp 10, Cys376Tyr and Cys408Arg in nsp 14 and Pro12Ser and Leu153Pro in nsp 16 (Sawicki *et al.,* 2005). Expression in yeast of SARS-CoV derived nsp 14 containing mutations equivalent to the MHV mutations Cys376Tyr and Cys408Arg, also led to a temperature sensitive phenotype, with the authors indicating that the higher temperatures had destabilised the structure of the N7-MTase domain (Chen *et al.,* 2013). There is precedent therefore for nsp 10, 14 and 16 to have a role in temperature sensitivity of viral replication.

The identification that M41-R replication was temperature sensitive raised concerns that M41-R may not offer much improvement over Beau-R as a vaccine vector. It has been theorised that the inability of the Beau-R based vaccine virus, BeauR-M41(S), to induce a fully protective immune response against homologous challenge is due to the inability of the vaccine virus to establish a sufficiently prolonged infection *in vivo*, which is the result of replication being temperature sensitive and highly restricted at 41°C; this has been discussed in more detail in Chapter 5. Growth kinetic assays, however highlighted that whereas Beau-R cannot establish a productive infection at 41°C, M41-R can, albeit limited (Figure 6.7 and 6.10) therefore suggesting that M41-R will not exhibit that same restrictions as Beau-R in delivering antigen *in vivo*. Recent research has in fact demonstrated that birds inoculated with M41-R are protected against homolgous M41-CK challenge to standards set the by European Pharmacopoeia (2010; unpublished date), indicating therefore that M41-R can deliver sufficient antigen *in vivo*. Further more, research has demonstrated successful *in ovo* vaccination that also offers homologous protection (unpublished data). The limited replication kinetics observed at higher temperatures may actually therefore be advantageous for continued vaccine development as it suggests that it may be possible that M41-R based vaccines could replicate *in vivo* for a small period of time, and in a restricted number of tissues. The growth curve data presented in this chapter indicate that replication of the M41-R vaccine viruses would likely diminish over a 72 h period thus limiting spread to naïve birds,

limting vaccine re-infection, reducing the window of possibility for recombination with other IBV strains, and also reducing opournunities for potential reversion to virulence. In addition, temperature swap assays indicated that the restricted *in vitro* replication phenotype at 41°C is not the result of temperature prohibiting viral entry (Figure 6.8). This relates to findings in Chapter 5, and advantagously enables the modification of the S glycoprotein without impacting replication at 41°C.

To further investigate M41-R as a vaccine vector, two rIBVs were designed; one expressing a chimeric 4/91(S1)/M41(S2) glycoprotein and the second expressing the 4/91 S ectodomain. Unfortunately, neither rIBV M41R-4/91(S1) nor rIBV M41R-4/91(S) could be successfully recovered from the respective rVV vectors in the time frame available during this PhD project. The latter was unexpected as rIBV BeauR-4/91(S) has previously been successfully rescued (Armesto *et al.,* 2011) and was found to replicate well in *ex vivo* TOCS. It is possible that the M41-R background cannot support expression of heterologous genes, however, this seem unlikely considering it has been possible to generate an rIBV M41-R expressing a H120(S1)/Beau-R(S2) glycoprotein (Keep, 2013) and a rIBV M41-R expressing the Beau-R S glycoprotein (Stevenson-Leggett, unpublished data). It has also been possible to generate M41-K expressing the 4/91(S) (Stevenson-Leggett, 2018), however it must be noted that this virus was rescued after multiple failed attempts. It seems likely that the failure of M41R-4/91(S) to be successfully recovered from the rVV vector is simply the result of the low probabilities of rescuing rIBV in CK cells (Chapter 2, Figure 2.10). Despite the many successful recoveries of rIBV by our group (Casais *et al.,* 2001; Casais *et al.,* 2003; Casais *et al.,* 2005; Hodgson *et al.,* 2006; Armesto *et al.,* 2009; Armesto *et al.,* 2011; Bentley *et al.,* 2013; Bentley *et al.,* 2013B; Bickerton *et al.,* 2018; Bickerton *et al.,* 2018B; Keep *et al.,* 2018), the rescue of rIBV is always considered a low probability event, as the process involves infecting primary CK cells, and then transfecting the same cells with both rVV DNA and a plasmid expressing the N protein. CK cells are a mixed population and not all the cells in the dish will support IBV replication. There will also be many cells in the dish which are either transfected or infected, and some neither. In addition CK cells, being a primary cell line, are not easily transfected, and in my experience transfection efficiency is generally lower in cells previously infected. Typically each rescue involves replicates of ten in an effort to increase the probability of a successful rescue.

The probability of successfully recovering rIBV from the respective rVV vector is further compounded when the rIBV is not able to be propagated in CK cells. The S glycoprotein is a determinant of tropism (Casais *et al.,* 2003), and rIBVs take on the tropism of the donor S

strain (Casais *et al.,* 2003; Armesto *et al.,* 2011; Bickerton *et al.,* 2018). The 4/91 strain of IBV is unable to be propagated in CK cells, and as such neither is BeauR-4/91(S) or M41K-4/91(S), and nor will M41R-4/91(S). In the rescue process, S mediated entry is not a restriction as the rVV DNA encoding the IBV genome of interest is transfected into the cell. Progeny rIBV expressing the 4/91 S glycoprotein however, will not be able to exit the cells so infected/transfected cells are lysed through freeze-thaw and titration. This treatment as well as lysing the cells can damage the small quantities of rIBV that may be present, thereby reducing the overall probability of a successful rescue attempt. Future work will continue to attempt to successfully recover M41R-4/91(S) from its rVV vector.

The failure of M41R-4/91(S1) to be recovered from the corresponding rVV vector may also be the result of the issue above, or may be the result of an incompatibility of the 4/91(S1) with a M41 S2 subunit. Although rIBVs have been successfully rescued containing chimeric S glycoproteins, the S2 subunit has always been derived from Beau-R (Bickerton *et al.,* 2018; Bickerton *et al.,* 2018b, Keep, 2013). The S2 subunit from Beau-R is unusual as it contains a second cleavage site and confers Beaudette's unique ability to replicate in Vero cells (Bickerton *et al.,* 2018) and may also confer the ability to replicate in CK cells (Bickerton *et al.,* 2018b). It therefore may be the case that it is not possible to generate chimeric S glycoproteins containing the M41 S2 subunit. As discussed in Chapter 3 and Chapter 4 is possible there are conformational changes in a chimeric S1/S2 glycoprotein in comparison to the WT counterpart. It is subsequently possible that the functions of the M41 S2 subunit may be more sensitive to such conformational changes than the Beau-R S2 subunit, thereby restricting the ability of any rIBV to productively replicate. However, before any further research investigating this possibility is undertaken, further attempts at recovering M41R-4/91(S1) from its vaccinia vector should be carried out.

Whilst there are several other alternative reverse genetic technologies as discussed in Chapter 1, the M41R-491(S) and M41R-4/91(S1) cDNA is already assembled; it is the recovery stage that is posing the problem. It is possible during the TDS process even with the proofreading capability of the vaccinia virus vector that errors have been introduced into the IBV cDNA which are preventing rescue; sequencing the full IBV genome would enable any mutations to be identified. One option for the recovery of rIBV that could be investigated would be to perform *in vitro* transcription on the rVV DNA containing M41R-4/91(S) and M41R-4/91(S1) which then could then be transfected into CK cells (Thiel *et al.,* 2001). This may increase the possibility of a successful rescue as it circumvents the need to successfully transfect cells that have already been infected with rFPV-T7.

In summary, despite the inability to rescue rIBV M41-R expressing modified spike glycoproteins, the data presented in this chapter supports the continual development of M41-R as a vaccine vector. Mutations in nsp 10, 14, 15 and 16 have resulted in an attenuated phenotype *in vivo* indicating the role of these nsps as pathogenicity factors. The same mutations have also resulted in a restricted replication phenotype at 41°C. Notably this replication phenotype offers improvement when compared to the highly restricted replication of Beau-R at 41°C and may in fact offer benefits for vaccine development in terms of limiting vaccine dissemination within the bird, as well as from one bird to another. Further research is required to investigate the role of each of the mutations and each of the nsps in both pathogenicity and temperature sensitivity and to establish whether there is a direct link between temperature sensitivity and attenuation.

Chapter 7: Final discussion.

The overall aim of this PhD project was to evaluate the protection offered by live attenuated vaccine candidates that had been rationally designed and generated through reverse genetics. All the vaccine candidates assessed through *in* vivo vaccine challenge studies were based on the attenuated rIBV Beau-R and expressed either a heterologous S glycoprotein or a heterologous S1 or S2 subunit, and consequently therefore a chimeric S glycoprotein. Protection was assessed *in vivo* and was defined by the standards set by the European Pharmacopeia (2010). According to these standards none of the vaccine candidates offered full protection against a virulent IBV challenge. Partial protection at ~65% was however observed with rIBV Beau-R expressing a heterologous S glycoprotein derived from the pathogenic M41-CK strain, BeauR-M41(S), against homologous challenge; this result has been published by Ellis *et al.,* (2018). The demonstration that the S glycoprotein expressed in a rIBV vector can induce a partially protective immune response confirms previous findings by Hodgson *et al.,* (2004) and Armesto *et al.,* (2011).

The inability of rIBV expressing heterologous S1 subunits to protect against homolgous challenge was an unexpected result as previous literature had indicated that the immunodominant S1 subunit alone could induce protective immunity (Song *et al.,* 1998; Johnson *et al.,* 2003; Yan *et al.,* 2013; Toro *et al.,* 2014). On closer inspection of this literature however it is difficult to compare previous *in vivo* studies with those detailed in this PhD thesis due to technical and methodical differences including age and breed of bird, route of vaccination and sampling points post challenge. The inability of the vaccine candidates to offer complete protection has raised questions regarding the possible mis-folding of a chimeric S glycoprotein in comparison to WT and the presence of important protective epitopes in S2 subunit. These are questions that are important to answer and are questions that have also been raised by Eldemery *et al.,* (2017) and Shirvani *et al.,* (2018). Future research should therefore investigate whether neutralising epitopes presented by a chimeric S glycoprotein are comparable to WT. Neutralisation assays utilising monoclonal antibodies or polyclonal sera against a panel of rIBVs expressing heterologous S1 or S2 subunits would provide an indication as to whether conformational neutralising epitopes have been altered.

The protection induced by rIBVs expressing heterologous S glycoproteins, rIBV BeauR-M41(S) and BeauR-4/91(S), against a heterologous QX challenge was also assessed. Birds received either the same primary and secondary vaccination or a different secondary

vaccination to the primary. None of the combinations offered full protection against the QX challenge which was unexpected as groups have reported success in using 4/91 and M41 based vaccines against a QX challenge (Terregino *et al.,* 2008; Awad *et al.,* 2016, de Wit *et al.,* (2011). One notable difference is that rIBVs used in this thesis are only expressing the 4/91 and M41 S glycoproteins and not any of the other structural proteins. The inability of the vaccine candidates to offer protection against loss of ciliary activity after a QX challenge as well as the incomplete protection against homologous challenge raised a question regarding the potential role of the other structural proteins in the induction of a completely protective immune response. It will be important to assess in the future if a rIBV expressing both a heterologous S and N protein for example gives improved protection in comparison to a rIBV expressing a heterologous S glycoprotein alone. An interesting rIBV to assess in a vaccine-challenge experiment would be BeauR-Rep-M41-Struct generated by Armesto *et al.,* (2009). This rIBV contains the replicase gene from Beau-R and the structural and accessory genes from M41-CK.

One other question that this thesis has raised is the level of *in vivo* replication required for a live attenuated vaccine candidate to induce a fully protective immune response. Investigation of the rIBVs expressing heterologous S glycoproteins and rIBVs expressing chimeric S glycoproteins *in vitro* have indicated that the modifications have not impacted productive viral replication, however replication was not detected *in vivo* in tissues harvested pv. The *in vitro* research was completed in primary CK cells but should be repeated in *ex vivo* TOCs, a more biologically relevant tissue. It is possible that rIBVs expressing chimeric S glycoproteins cannot bind to tracheal tissue as effectively as a WT glycoprotein due to possible conformational changes. The research investigating *in vitro* replication of the vaccine candidates in Chapter 3 was completed at 37°C, however it has been demonstrated in Chapter 5 that productive replication of the Beau-R backbone is temperature sensitive and is highly restricted at 41°C, the core body temperature of a chicken. Further research identified the replicase gene as the likely restricting factor. Whether replication is highly restricted at 38°C or 39°C, a temperature more relatable to the respiratory tract, remains to be determined. It is however likely that temperature sensitivity does play a role in the restricted replication of the vaccine candidates *in vivo*.

Temperature sensitivity has been used in vaccine development for several other viruses including influenza (Jin *et al.,* 2003; Juhasz *et al.,* 1999). Whilst this thesis has identified that productive replication of Beau-R is temperature sensitive, it has not determined the mechanism. There are a number of possibilities including RNA synthesis, protein production, viral assembly and cellular responses, all of which will require further investigation. Western

blots and confocal microscopy could be used to assess viral protein production and Northern blot to assess sgmRNA synthesis. Reverse genetics could be utilised to look at the role of individual nsps or combinations of nsps or the role of the 3' and 5' UTR that may have resulted in the temperature sensitive replication phenotype of Beau-R. Although it does appear that temperature sensitivity is not a shared characteristic of attenuated strains it is important to identify mechanisms of temperature sensitivity as this may be beneficial to the design of rationally attenuated rIBVs that could be used as vaccine candidates. Future work should also assess whether the ability to replicate at higher temperatures is a shared characteristic of pathogenic strains and particularly those that are classified as nephropathogenic. It is possible that temperature is a factor that effects viral dissemination through the host enabling virulent isolates to sustain replication in secondary sites of infection including the lungs, kidneys and oviducts.

Finally the research detailed in this thesis identifies a potential alternative rIBV for the design of rationally designed vaccine candidates. This backbone, rIBV M41-R, is a molecular clone of the pathogenic lab strain M41-CK that has been attenuated by four point mutations in the replicase gene. These point mutations, located in nsp 10, 14, 15 and 16, have also imparted a replication temperature sensitive phenotype. Whether temperature sensitivity is a direct cause of the attenuated *in vivo* phenotype is not known, and it is possible the mechanism of attenuation and temperature sensitivity are unrelated. Further research should investigate the role of nsp 10, 14, 15 and 16 in both attenuation and temperature sensitivity. However, regardless of the mechnism, recent research has demonstrated that M41-R can be used as an *in ovo* and *in vivo* vaccine against homologous challenge with M41-CK (unpublished research). This is of significant interest to poultry industries as *in ovo* vaccination in particular offers an effective means of vaccination that is highly controlled with every embroyo receiving the correct dose. Not only does this mean that the chicks are protected from the point of hatch, it is also advantageous over spray and drinking water administered vaccines where it is impossible to know that every chick has received the correct vaccine dosage. Additionally, the temperature sensitive replication phenotype of M41-R offers a number of possible advantages offer current live attenuated vaccines such as H120, including limited replication *in vivo*, restricted dissemination through the host and limited oppurnunity to spread to naiive chicks, and potentially more limited opportunities to revert to a pathogenic phenotype. Further research should therefore also continue to assess M41-R as a vaccine virus, as well as the ability to modify the M41-R genome, particularly the ability to generate M41-R expressing heterologous S glycoproteins.

In summary this thesis has provided research that will impact the design of the next generation of rationally designed rationally attenuated rIBVs be used as live attenuated vaccine candidates. This thesis has also raised questions that provide avenues for future research in both vaccine development and molecular virology, not only for IBV but also for other coronaviruses.

Chapter 8: Appendix.

AATTGTCGACTAGTTTTGCTGTAAAAGTGACAGAGACAAGTTGGCACGAAGTTTTATATGACATTGCA
CAGGATTGTGCATGGTGGACAATGTTTTGTACAGCAGTGAATGCCTCTTCTTCAGAAGCATTCTTGAT
TGGTGTTAATTATTTGGGTGCAAGTGAAAAGGTTAAGGTTAGTGGAAAAACGCTGCACGCAAATTATA
TATTTTGGAGGAATTGTAATTATTTACAAACCTCTGCTTATAGTATATTTGACGTTGCTAAGTTTGAT
TTGAGATTGAAAGCAACGCCAGTTGTTAATTTGAAAACTGAACAAAAGACAGACTTAGTCTTTAATTT
AATTAAGTGTGGTAAGTTACTGGTAAGAGATGTTGGTAACACCTCTTTTACTAGTGACTCTTTTGTGT
GTACTATGTAGTGCTTTGCTTTATGATAAAAATACTTACGTTTACTACTACCAAAGTGCCTTTAGGCC
TGGTCAAGGTTGGCATCTACATGGGGGTGCTTATGCAGTAGATAAGGTTTTTAATGGAACCAACAATG
CAGTCAGTGTATCTGATTGCACTGCTGGTACTTTTTATGAAAGCTATAATATTTCTGCTGCTTCTGTA
GCCATGACAGTACCACCTGCTGGTATGTCTTGGTCAGTTTCACAGTTTTGTACAGCTCATTGTAACTT
CTCAGACTTTACAGTGTTTGTTACGCATTGTTTTAAAAGTCAACAAGGTAGTTGTCCATTGACAGGTA
TGATTCCTCAGAATCATATTCGTATTTCTGCTATGAGATCTGGATTTTTGTTTTATAATTTAACAGTT
AGCGTATCTAAATACCCTAAATTTAAATCGCTTCAATGTGTTGGCAATTCTACATCTGTCTATTTAAA
TGGTGATCTTGTTTTCACTTCTAATGAAACAACTCACGTTACGGGTGCAGGCGTTTATTTTAAAAGTG
GTGGGCCTGTAACTTATAAAGTTATGAAAGAAGTTAAAGCCCTAGCCTACTTTATTAATGGTACCGCA
CAAGAGGTTATTTTATGTGATAACTCACCTAGAGGTTTGCTTGCATGTCAGTATAACACTGGTAATTT
TTCAGATGGATTCTACCCTTTTACTAATTCTTCTTTAGTTAAGGATAGGTTTATTGTATATCGAGAAA
GTAGCACTAACACTACTTTAGAGTTAACTAATTTCACTTTTACTAATGTAAGTAATGCTTCTCCTAAT
TCAGGTGGCGTTGATACTTTCCAATTATATCAAACACATACTGCTCAGGATGGTTATTATAATTTTAA
TTTATCATTTCTGAGTAGTTTTGTGTATAAACCATCTGATTTTATGTATGGGTCATACCACCCAAATT
GTAATTTTAGACCAGAGAATATTAATAATGGCTTATGGTTTAATTCATTATCTGTGTCACTTACTTAC
GGACCCATTCAAGGTGGTTGTAAGCAATCTGTTTTTAGTAATAAAGCAACTTGTTGCTATGCTTATTC
TTACCGAGGTCCTACTAGATGTAAGGGTGTTTATAGAGGGGAGCTAACGCAATACTTTGAATGTGGAC
TTCTAGTTTATGTAACTAAGAGTGATGGCTCTCGTATACAAACTAGAAGTGAACCACTGGTGTTAACT
CAATATAATTATAACAACATTACTTTAAATAAGTGTGTTGAGTATAATATATATGGTAGAGTTGGTCA
AGGTTTTATTACTAATGTAACTGAAGCAACTGCTAATTATAGTTATCTAGCAGATGGTGGTTTAGCTA
TTTTAGATACTTCAGGAGCCATAGACATATTTGTTGTTCGAGGTGCATATGGTCTTAATTATTATAAG
GTTAATCCCTGTGAAGATGTTAACCAACAGTTTGTAGTGTCTGGTGGCAATTTAGTTGGCATTCTTAC
ATCTCATAATGAAACAGATTCTGAATTTATTGAGAACCAGTTTTACATCAAACTCACTAACGGAACAC
GTCGTTTTAGACGTTCTATTACTGAAAATGTTGCAAATTGCCCTTATGTTAGTTATGGTAAGTTTTGT
ATAAAACCTGATGGTTCAATTGCCACAATAGTACCAAAACAATTGGAACAGTTTGTGGCACCTTTACT
TAATGTTACTGAAAATGTGCTCATACCTAACAGTTTTAATTTAACTGTTACAGATGAGTACATACAAA
CGCGTATGGATAAGGTCCAAATTAATTGTCTGCAGTATGTTTGTGGCAATTCTCTGGATTGTAGAGAT
TTGTTTCAACAATATGGGCCTGTTTGTGACAACATATTGTCTGTAGTAAATAGTATTGGTCAAAAAGA
AGATATGGAACTTTTGAATTTCTATTCTTCTACTAAACCGGCTGGTTTTAATACACCATGTCGACAAT
T

Figure 8.1: Nucleotide sequence cloned into pGPT-Neb-193 generating pGPT-4/91(S1). Sequence encoding *Sal I* restriction sites are underlined. Red indicates M41-CK derived nsp 16 sequence, green 4/91(UK) S1 sequence and purple M41-CK derived S2.

AATTGTCGACGTGACAGAGACAAGTTGGCACGAAGTTTTATATGACATTGCACAGGATTGTGCATGGT
GGACAATGTTTTGTACAGCAGTGAATGCCTCTTCTTCAGAAGCATTCTTGATTGGTGTTAATTATTTG
GGTGCAAGTGAAAAGGTTAAGGTTAGTGGAAAAACGCTGCACGCAAATTATATATTTTGGAGGAATTG
TAATTATTTACAAACCTCTGCTTATAGTATATTTGACGTTGCTAAGTTTGATTTGAGATTGAAAGCAA
CGCCAGTTGTTAATTTGAAAACTGAACAAAAGACAGACTTAGTCTTTAATTTAATTAAGTGTGGTAAG
TTACTGGTAAGAGATGTTGGTAACACCTCTTTTACTAGTGACTCTTTTGTGTGTACTATGTAGTGCTT
TGCTTTATGATAAAAATACTTACGTTTACTACTACCAAAGTGCCTTTAGGCCTGGTCAAGGTTGGCAT
CTACATGGGGGTGCTTATGCAGTAGATAAGGTTTTTAATGGAACCAACAATGCAGTCAGTGTATCTGA
TTGCACTGCTGGTACTTTTTATGAAAGCTATAATATTTCTGCTGCTTCTGTAGCCATGACAGTACCAC
CTGCTGGTATGTCTTGGTCAGTTTCACAGTTTTGTACAGCTCATTGTAACTTCTCAGACTTTACAGTG
TTTGTTACGCATTGTTTTAAAAGTCAACAAGGTAGTTGTCCATTGACAGGTATGATTCCTCAGAATCA
TATTCGTATTTCTGCTATGAGATCTGGATTTTTGTTTTATAATTTAACAGTTAGCGTATCTAAATACC
CTAAATTTAAATCGCTTCAATGTGTTGGCAATTCTACATCTGTCTATTTAAATGGTGATCTTGTTTTC
ACTTCTAATGAAACAACTCACGTTACGGGTGCAGGCGTTTATTTTAAAAGTGGTGGGCCTGTAACTTA
TAAAGTTATGAAAGAAGTTAAAGCCCTAGCCTACTTTATTAATGGTACCGCACAAGAGGTTATTTTAT
GTGATAACTCACCTAGAGGTTTGCTTGCATGTCAGTATAACACTGGTAATTTTTCAGATGGATTCTAC
CCTTTTACTAATTCTTCTTTAGTTAAGGATAGGTTTATTGTATATCGAGAAAGTAGCACTAACACTAC
TTTAGAGTTAACTAATTTCACTTTTACTAATGTAAGTAATGCTTCTCCTAATTCAGGTGGCGTTGATC
TTTCCAATTATATCAAACACATACTGCTCAGGATGGTTATTATAATTTTAATTTATCATTTCTGAGTA
GTTTTGTGTATAAACCATCTGATTTTATGTATGGGTCATACCACCCAAATTGTAATTTTAGACCAGAG
AATATTAATAATGGCTTATGGTTTAATTCATTATCTGTGTCACTTACTTACGGACCCATTCAAGGTGG
TTGTAAGCAATCTGTTTTTAGTAATAAAGCAACTTGTTGCTATGCTTATTCTTACCGAGGTCCTACTA
GATGTAAGGGTGTTTATAGAGGGGAGCTAACGCAATACTTTGAATGTGGACTTCTAGTTTATGTAACT
AAGAGTGATGGCTCTCGTATACAAACTAGAAGTGAACCACTGGTGTTAACTCAATATAATTATAACAA
CATTACTTTAAATAAGTGTGTTGAGTATAATATATATGGTAGAGTTGGTCAAGGTTTTATTACTAATG
TAACTGAAGCAACTGCTAATTATAGTTATCTAGCAGATGGTGGTTTAGCTATTTTAGATACTTCAGGA
GCCATAGACATATTTGTTGTTCGAGGTGCATATGGTCTTAATTATTATAAGGTTAATCCCTGTGAAGA
TGTTAACCAACAGTTTGTAGTGTCTGGTGGCAATTTAGTTGGCATTCTTACATCTCATAATGAAACAG
ATTCTGAATTTATTGAGAACCAGTTTTACATCAAACTCACTAACGGAACACGTCGCTCTAGACGTTCT
GTTACTGGGAATGTTACAAATTGCCCTTATGTTAGTTATGGCAAGTTTTGTATAAAACCAGATGGTTC
TTTATTTATAATAGTACCACAAGAGTTAGAACAGTTTGTGGCGCCTTTACTCAATGTTACTGAGCATG
TGCTCATACCTGATAGTTTTAATTTAACTGTCACAGATGAGTACATACAAACTCGTATGGATAAGGTT
CAAATTAATTGCCTTCAGTATGTTTGTGGTAATTCTATTGAATGCAGAAAGTTGTTTCAGCAGTATGG
ACCTGTTTGTGATAATATATTGTCTGTTGTAAATGGTGTAGGTCAAAGAGAGGATATGGAACTTTTAA
GTTTCTATTCGTCTACTAAACCTAGTGGTTACAATACACCAATTTTTAATAATGTTAGCACTGGTGAC
TTTAATATTTCTCTCTTACTAACACCACCTAATAGTCCTACTGGGCGCTCTTTTATTGAAGATCTTCT
TTTTACAAGTGTAGAATCTGTTGGATTACCAACTGATGAAGAGTATAAAAAGTGTACAGCAGGACCTT
TAGGTTTTGTTAAGGACCTTGTTTGTGCTAGAGAGTATAATGGCTTGCTTGTGTTGCCTCCTATTATT
ACTGCAGACATGCAAACTATGTATACTAGCTCTTTAGTAGCCTCTATGGCTTTAGGTGGCATTACTGC
AGCTGGTGCTATACCTTTTGCTACACAACTGCAGGCCAGAATTAACCATTTGGGTATTACTAATTCTC
TTTTGTTGAAAAATCAAGAAAAAATTGCTGCTTCCTTTAATAAGGCCATCGGTCATATGCAGGGAGGG
TTTAAAAGTACTTCTCTAGCATTACAACAGATTCAAGATGTTGTTAATAAACAGAGTTCTATTCTTAC
AGAGACTATGCAATCACTTAATAAAAATTTTGGTGCTATTTCCTCCGTACTTCAAGACATTTACCAGC
AACTTGATGCTATTCAGGCAGATGCTCAGGTTGATCGTCTTATTACAGGTAGACTTTCTTCACTATCT
GTTTTAGCTTCTGCTAAACAGGCAGAGTATCATAGAGTGTCACAACAGCGTGAGTTGGCCACTCAGAA
AATTAATGAGTGTGTTAAGTCTCAGTCTAATAGGTATTCATTTTGTGGTAATGGAAGACATGTTTTAA
CCATACCACAAAATGCACCTAATGGTATAGTGTTTATACACTTTACTTATACTCCAGAGAGTTTTGTT
AATGTTACTGCAATAGTGGGTTTTTGTGTAAATCCAGCTAATGCCAGTCAGTATGCAATAGTGCCCGT
TAATAACAGAGGTATTTTTATTCAAGTTAATGGTAGTTACTACATCACTGCACGTGATATGTATATGC
CAAGAGACATTACAGCAGGAGACATAGTTACGCTTACTTCTTGTCAAGCAAATTATGTAAGTGTAAAT
AAGACTGTCATTACTACATTTGTAGATAATGATGACTTTGATTTTGATGACGAATTGTCAAAATGGTG

GAATGATACTAAGCATGAGCTACCAGATTTCGACGAATTCAATTATACAGTACCAGTATTAAATATTA
GTAATGAAATTGACAGAATTCAAGAAGTTATTCAGGGATTAAATGACTCCCTAATAGATCTTGAAACA
CTCTCAATTCTTAAAACTTATATTAAGTGGCCTTGGTATGTGTGGCTTGCCATAGCTTTTGCCATTAT
TATCTTCATCCTAATCTTAGGATGGGTTTTCTTCATGACTGGATGTTGTGGTTGTTGTTGTGGATGCT
TTGGCATTATGCCTCTAATGAGTAAGTGTGGTAAGAAATCTTCTTATTACACGACTTTTGATAACGAT
GTGGTAACTTAACAATACAGACCTAAAAAGTCTGTTTAATGATTCAAAGTCCCACGTCCTTCCTAATA
GTATTAATTTTTCTTTGGTGTAAACTTGTACTAAGTTGTTTTAGAGAGTTTATTATAGCGCTCCAACA
ACTAATACAAGTTTTACTCCAAATTATCAATAGTAACTTACAGCCTAGACTGACCCTTTGTCACAGTC
TAGACTAATGTTAAACTTAGAAGCAATTATTGAAACTGGTGAGCAAGTGATTCAAAAAATCAGTTTCA
ATTTACAGCATATTTCAAGTGTATTAAACACAGAAGTATTTGACCCCTTTGACTATTGTTATTACAGA
GGAGGTAATTTTTGGGAAATAGAGTCAGCTGAAGATTGTTCAGGTGATGATGAATTTATTGAATAAGT
CGCTAGAGGGTCGACAATT

Figure 8.2: Nucleotide sequence cloned into pGPT-Neb-193 generating pGPT-4/91(S). Sequence encoding *Sal I* restriction sites are underlined. Red indicates M41-CK derived nsp 16 sequence, green 4/91(UK) S sequence and purple M41-CK derived gene 3 sequence.

```
Beau        MLVTPLLLVTLLCALCSAVLYDS-SSYVYYYQSAFRPPSGWHLQGGAYAV 49
M41         MLVTPLLLVTLLCVLCSAALYDS-SSYVYYYQSAFRPPNGWHLHGGAYAV 49
4/91(UK)    MLGKPLLLVTLWYALCSALLYDK-NTYVYYYQSAFRPGQGWHLHGGAYAV 49
QX          MLVKSLFLVTILCALCSANLFDSDNNYVYYYQSAFRPPNGWHLQGGAYAV 50

Beau        VNISSEFNNAGSSSGCTVGIIHGGRVVNASSIAMTAPSSGMAWSSSQFCT 99
M41         VNISSESNNAGSSPGCIVGTIHGGRVVNASSIAMTAPSSGMAWSSSQFCT 99
4/91(UK)    DKVFNGTNNAVSVSDCTAGTFYESYNISAASVAMTVPPAGMSWSVSQFCT 99
QX          VNSTNYTNNAGSAHECTVGVIKDVYNQSVASIAMTAPLQGMAWSKSQFCS 100

Beau        AHCNFSDTTVFVTHCYKHGG--CPLTGMLQQNLIRVSAMKNGQLFYNLTV 147
M41         AHCNFSDTTVFVTHCYKYDG--CPITGMLQKNFLRVSAMKNGQLFYNLTV 147
4/91(UK)    AHCNFSDFTVFVTHCFKSQQGSCPLTGMIPQNHIRISAMRSGFLFYNLTV 149
QX          AHCNFSEITVFVTHCYSSGSGSCPITGMIPRDHIRISAMKNGSLFYNLTV 150

Beau        SVAKYPTFRSFQCVNNLTSVYLNGDLVYTSNETIDVTSAGVYFKAGGPIT 197
M41         SVAKYPTFKSFQCVNNLTSVYLNGDLVYTSNETTDVTSAGVYFKAGGPIT 197
4/91(UK)    SVSKYPKFKSLQCVGNSTSVYLNGDLVFTSNETTHVTGAGVYFKSGGPVT 199
QX          SVSKYPNFKSFQCVNNFTSVYLNGDLVFTSNKTTDVTSAGVYFKAGGPVN 200

Beau        YKVMREVKALAYFVNGTAQDVILCDGSPRGLLACQYNTGNFSDGFYPFTN 247
M41         YKVMREVKALAYFVNGTAQDVILCDGSPRGLLACQYNTGNFSDGFYPFIN 247
4/91(UK)    YKVMKEVKALAYFINGTAQEVILCDNSPRGLLACQYNTGNFSDGFYPFTN 249
QX          YSIMKEFKVLAYFVNGTAQDVVLCDNSPKGLLACQYNTGNFSDGFYPFTN 250

Beau        SSLVKQKFIVYRENSVNTTCTLHNFIFHNETGANPNPSGVQNIQTYQTKT 297
M41         SSLVKQKFIVYRENSVNTTFTLHNFTFHNETGANPNPSGVQNIQTYQTQT 297
4/91(UK)    SSLVKDRFIVYRESSTNTTLELTNFTFTNVSNASPNSGGVDTFQLYQTHT 299
QX          STLVREKFIVYRESSVNTTLALTNFTFTNVSNAQPNSGGVNTFHLYQTQT 300

Beau        AQSGYYNFNFSFLSSFVYKESNFMYGSYHPSCKFRLETINNGLWFNSLSV 347
M41         AQSGYYNFNFSFLSSFVYKESNFMYGSYHPSCNFRLETINNGLWFNSLSV 347
4/91(UK)    AQDGYYNFNLSFLSSFVYKPSDFMYGSYHPNCNFRPENINNGLWFNSLSV 349
QX          AQSGYYNFNLSFLSQFVYKASDFMYGSYHPSCSFRPETINSGLWFNSLSV 350

Beau        SIAYGPLQGGCKQSVFKGRATCCYAYSYGGPSLCKGVYSGELDHNFECGL 397
M41         SIAYGPLQGGCKQSVFSGRATCCYAYSYGGPSLCKGVYSGELDLNFECGL 397
4/91(UK)    SLTYGPIQGGCKQSVFSNKATCCYAYSYRGPTRCKGVYRGELTQYFECGL 399
QX          SLTYGPLQGGCKQSVFSGKATCCYAYSYKGPMACKGVYSGELSTNFECGL 400

Beau        LVYVTKSGGSRIQTATEPPVITQNNYNNITLNTCVDYNIYGRTGQGFITN 447
M41         LVYVTKSGGSRIQTATEPPVITRHNYNNITLNTCVDYNIYGRTGQGFITN 447
4/91(UK)    LVYVTKSDGSRIQTRSEPLVLTQYNYNNITLNKCVEYNIYGRVGQGFITN 449
QX          LVYVTKSDGSRIQTRTEPLVLTQYNYNNITLDKCVAYNIYGRVGQGFITN 450

Beau        VTDSAVSYNYLADAGLAILDTSGSIDIFVVQGEYGLNYYKVNPCEDVNQQ 497
M41         VTDSAVSYNYLADAGLAILDTSGSIDIFVVQGEYGLTYYKVYPCEDVNQQ 497
4/91(UK)    VTEATANYSYLADGGLAILDTSGAIDIFVVRGAYGLNYYKVNPCEDVNQQ 499
QX          VTDSAANFSYLADGGLAILDTSGAIDVFVVQGIYGLNYYKVNPCEDVNQQ 500

Beau        FVVSGGKLVGILTSRNETGSQLLENQFYIKITNGTRRFRRSITENVANCP 547
M41         FVVSGGKLVGILTSRNETGSQLLENQFYIKITNGTRRFRRSITENVANCP 547
4/91(UK)    FVVSGGNLVGILTSHNETDSEFIENQFYIKLTNGTRRSRRSVTGNVTNCP 549
QX          FVVSGGNIVGILTSRNETGSEQVENQFYVKLTNSSHRRRRSIGQNVTSCP 550

Beau        YVSYGKFCIKPDGSIATIVPKQLEQFVAPLFNVTENVLIPNSFNLTVTDE 597
M41         YVSYGKFCIKPDGSIATIVPKQLEQFVAPLLNVTENVLIPNSFNLTVTDE 597
4/91(UK)    YVSYGKFCIKPDGSLFIIVPQELEQFVAPLLNVTEHVLIPDSFNLTVTDE 599
QX          YVSYGRFCIEPDGSLKMIVPEELKQFVAPLLNITESVLIPNSFNLTVTDE 600
```

```
Beau        YIQTRMDKVQINCLQYVCGSSLDCRKLFQQYGPVCDNILSVVNSVGQKED 647
M41         YIQTRMDKVQINCLQYVCGKSLDCRDLFQQYGPVCDNILSVVNSIGQKED 647
4/91(UK)    YIQTRMDKVQINCLQYVCGNSIECRKLFQQYGPVCDNILSVVNGVGQRED 649
QX          YIQTRMDKVQINCLQYVCGNSLECRKLFQQYGPVCDNILSVVNSVSQKED 650

Beau        MELLNFYSSTKPAGFNTPVLSNVSTGEFNISLLLTNPSSRRKRSLIEDLL 697
M41         MELLNFYSSTKPAGFNTPFLSNVSTGEFNISLLLTTPSSPRRRSFIEDLL 697
4/91(UK)    MELLSFYSSTKPSGYNTPIFNNVSTGDFNISLLLTPPNSPTGRSFIEDLL 699
QX          MELLSFYSSTKPKGYDTPVLSNVSTGEFNISLLLKPPSSPSGRSFIEDLL 700

Beau        FTSVESVGLPTNDAYKNCTAGPLGFFKDLACAREYNGLLVLPPIITAEMQ 747
M41         FTSVESVGLPTDDAYKNCTAGPLGFLKDLACAREYNGLLVLPPIITAEMQ 747
4/91(UK)    FTSVESVGLPTDEEYKKCTAGPLGFVKDLVCAREYNGLLVLPPIITADMQ 749
QX          FTSVETVGLPTDAEYKKCTAGPLGTLKDLICAREYNGLLVLPPIITADMQ 750

Beau        ALYTSSLVASMAFGGITAAGAIPFATQLQARINHLGITQSLLLKNQEKIA 797
M41         ILYTSSLVASMAFGGITAAGAIPFATQLQARINHLGITQSLLLKNQEKIA 797
4/91(UK)    TMYTSSLVASMALGGITAAGAIPFATQLQARINHLGITNSLLLKNQEKIA 799
QX          TMYTASLVGAMAFGGITSAAAIPFATQIQARINHLGITQSLLMKNQEKIA 800

Beau        ASFNKAIGHMQEGFRSTSLALQQIQDVVSKQSAILTETMASLNKNFGAIS 847
M41         ASFNKAIGRMQEGFRSTSLALQQIQDVVNKQSAILTETMASLNKNFGAIS 847
4/91(UK)    ASFNKAIGHMQGGFKSTSLALQQIQDVVNKQSSILTETMQSLNKNFGAIS 849
QX          ASFNKAIGHMQEGFRSTSLALQQIQDVVNKQSAILTETMNSLNKNFGAIT 850

Beau        SVIQEIYQQFDAIQANAQVDRLITGRLSSLSVLASAKQAEYIRVSQQREL 897
M41         SMIQEIYQQLDAIQANAQVDRLITGRLSSLSVLASAKQAEHIRVSQQREL 897
4/91(UK)    SVLQDIYQQLDAIQADAQVDRLITGRLSSLSVLASAKQAEYHRVSQQREL 899
QX          SVIQDIYAQLDAIQADAQVDRLITGRLSSLSVLASAKQSEYIRVSQQREL 900

Beau        ATQKINECVKSQSIRYSFCGNGRHVLTIPQNAPNGIVFIHFSYTPDSFVN 947
M41         ATQKINECVKSQSIRYSFCGNGRHVLTIPQNAPNGIVFIHFSYTPDSFVN 947
4/91(UK)    ATQKINECVKSQSNRYSFCGNGRHVLTIPQNAPNGIVFIHFTYTPESFVN 949
QX          ATQKINECVKSQSNRYGFCGSGRHVLSIPQNAPNGIVFIHFTYTPESFVN 950

Beau        VTAIVGFCVKPANASQYAIVPANGRGIFIQVNGSYYITARDMYMPRAITA 997
M41         VTAIVGFCVKPANASQYAIVPANGRGIFIQVNGSYYITARDMYMPRAITA 997
4/91(UK)    VTAIVGFCVNPANASQYAIVPVNNRGIFIQVNGSYYITARDMYMPRDITA 999
QX          VTAIVGFCVNPANASQYAIVPANGRGIFIQVNGTYYITARDMYMPRDITA 1000

Beau        GDVVTLTSCQANYVSVNKTVITTFVDNDDFDFNDELSKWWNDTKHELPDF 1047
M41         GDIVTLTSCQANYVSVNKTVITTFVDNDDFDFNDELSKWWNDTKHELPDF 1047
4/91(UK)    GDIVTLTSCQANYVSVNKTVITTFVDNDDFDFDDELSKWWNDTKHELPDF 1049
QX          GDIVTLTSCQANYVNVNKTVITTFVEDDDFDFDDELSKWWNDTKHQLPDF 1050

Beau        DKFNYTVPILDIDSEIDRIQGVIQGLNDSLIDLEKLSILKTYIKWPWYVW 1097
M41         DKFNYTVPILDIDSEIDRIQGVIQGLNDSLIDLEKLSILKTYIKWPWYVW 1097
4/91(UK)    DEFNYTVPVLNISNEIDRIQEVIQGLNDSLIDLETLSILKTYIKWPWYVW 1099
QX          DDFNYTVPILNISGEIDYIQGVIQGLNDSLINLEELSIIKTYIKWPWYVW 1100

Beau        LAIAFATIIFILILGWVFFMTGCCGCCCGCFGIMPLMSKCGKKSSYYTTF 1147
M41         LAIAFATIIFILILGWVFFMTGCCGCCCGCFGIMPLMSKCGKKSSYYTTF 1147
4/91(UK)    LAIAFAIIIFILILGWVFFMTGCCGCCCGCFGIMPLMSKCGKKSSYYTTF 1149
QX          LAIGFAIIIFILILGWVFFMTGCCGCCCGCFGIIPLMSKCGKKSSYYTTF 1150

Beau        DNDVVTEQYRPKKSV 1162
M41         DNDVVT--------- 1153
4/91(UK)    DNDVVTEQYRPKKSV 1164
```

QX DNDVVTEQYRPKKSV 1165

Figure 8.3: Amino acid alignment of the Spike (S) glycoprotein from a variety of strains. Sequences were aligned using BioEdit, version 7.2.5. Sequences were downloaded from GenBank, accession numbers KY933089.1 (QX), MK728875.1 (M41), AJ311317.1 (Beaudette), JN192154.1 (4/91). This was completed by Dr. Erica Bickerton.

Beau-CK	100%						
CR88	92.03%	100%					
H120	97.34%	91.59%	100%				
M41-CK	97.78%	92.03%	99.55%	100%			
4/91	92.92%	92.47%	92.92%	93.36%	100%		
Ma5	97.78%	92.03%	99.55%	100%	93.36%	100%	
QX	92.03%	90.26%	92.47%	92.92%	91.59%	92.92%	100%
	Beau-CK	**CR88**	**H120**	**M41-CK**	**4/91**	**Ma5**	**QX**

IDENTITY STATS

```
min     = 90.26
max     = 100
mean    = 94.1380952380953
stddev  = 2.99388999869117
```

Figure 8.4. Amino acid identidy between the Membrane (M) proteins of different IBV strains.

Amino acid sequences were aligned using mafft (version 7.31; Katoh and Standley, 2013) using default parameters. Pairwise sequence identity and similar were calculated using SIAS – sequence identity and similarity tool (http://imed.med.ucm.es/Tools/sias.html), setting sequence length as the length of the multiple sequence alignment (MSA) and selecting BLOSUM62 similarity matrix. All other parameters were set to default. This work was completed by Michael Oade using in house sequences for Beau-CK, CR88, H120, M41-CK, 4/91 and QX. Seqeunce relating to Ma5 was downloaded from NCBI, accession number KY626045.1.

H120	100%						
Ma5	100%	100%					
Beau-CK	92.72%	92.72%	100%				
M41-CK	94.54%	94.54%	98.18%	100%			
QX	85.45%	85.45%	88.18%	90%	100%		
CR88	67.27%	67.27%	70.9%	71.81%	70%	100%	
4/91	80%	80%	83.63%	84.54%	87.27%	76.36%	100%
	H120	**Ma5**	**Beau-CK**	**M41-CK**	**QX**	**CR88**	**4/91**

IDENTITY STATS

```
min     = 67.27
max     = 100
mean    = 83.8490476190476
stddev  = 9.91875131578563
```

Figure 8.5: Amino acid identity between the Envelope (E) proteins of different IBV strains. Amino acid sequences were aligned using mafft (version 7.31; Katoh and Standley, 2013) using default parameters. Pairwise sequence identity and similar were calculated using SIAS – sequence identity and similarity tool (http://imed.med.ucm.es/Tools/sias.html), setting sequence length as the length of the multiple sequence alignment (MSA) and selecting BLOSUM62 similarity matrix. All other parameters were set to default. This work was completed by Michael Oade using in house sequences for Beau-CK, CR88, H120, M41-CK, 4/91 and QX. Seqeunce relating to Ma5 was downloaded from NCBI, accession number KY626045.1.

Ma5	100%						
H120	99.26%	100%					
4/91	95.59%	94.86%	100%				
CR88	94.37%	93.88%	95.84%	100%			
QX	91.93%	91.19%	91.93%	90.95%	100%		
M41-CK	93.64%	92.9%	93.88%	93.39%	91.19%	100%	
Beau-CK	92.42%	91.68%	93.15%	92.42%	90.22%	94.13%	100%
	Ma5	**H120**	**4/91**	**CR88**	**QX**	**M41-CK**	**Beau-CK**

IDENTITY STATS

```
min      = 90.22
max      = 99.26
mean     = 93.2771428571429
stddev   = 2.00348302156197
```

Figure 8.6: Amino acid identity between the Nucleocapsid (N) proteins of different IBV strains. Amino acid sequences were aligned using mafft (version 7.31; Katoh and Standley, 2013) using default parameters. Pairwise sequence identity and similar were calculated using SIAS – sequence identity and similarity tool (http://imed.med.ucm.es/Tools/sias.html), setting sequence length as the length of the multiple sequence alignment (MSA) and selecting BLOSUM62 similarity matrix. All other parameters were set to default. This work was completed by Michael Oade using in house sequences for Beau-CK, CR88, H120, M41-CK, 4/91 and QX. Seqeunce relating to Ma5 was downloaded from NCBI, accession number KY626045.1.

Beau-CK	100%						
M41-CK	95.36%	100%					
Ma5	96.73%	96.39%	100%				
H120	96.48%	96.13%	99.48%	100%			
CR88	81.8%	81.8%	81.54%	81.54%	100%		
4/91	82.4%	81.45%	82.83%	82.83%	94.33%	100%	
QX	81.97%	81.2%	82.66%	82.48%	82.74%	84.29%	100%
	Beau-CK	**M41-CK**	**Ma5**	**H120**	**CR88**	**4/91**	**QX**

IDENTITY STATS

```
min      = 81.2
max      = 99.48
mean     = 86.9728571428572
stddev   = 6.75971198516985
```

Figure 8.7: Amino acid identity between the Spike (S) proteins of different IBV strains. Amino acid sequences were aligned using mafft (version 7.31; Katoh and Standley, 2013) using default parameters. Pairwise sequence identity and similar were calculated using SIAS – sequence identity and similarity tool (http://imed.med.ucm.es/Tools/sias.html), setting sequence length as the length of the multiple sequence alignment (MSA) and selecting BLOSUM62 similarity matrix. All other parameters were set to default. This work was completed by Michael Oade using in house sequences for Beau-CK, CR88, H120, M41-CK, 4/91 and QX. Seqeunce relating to Ma5 was downloaded from NCBI, accession number KY626045.1.

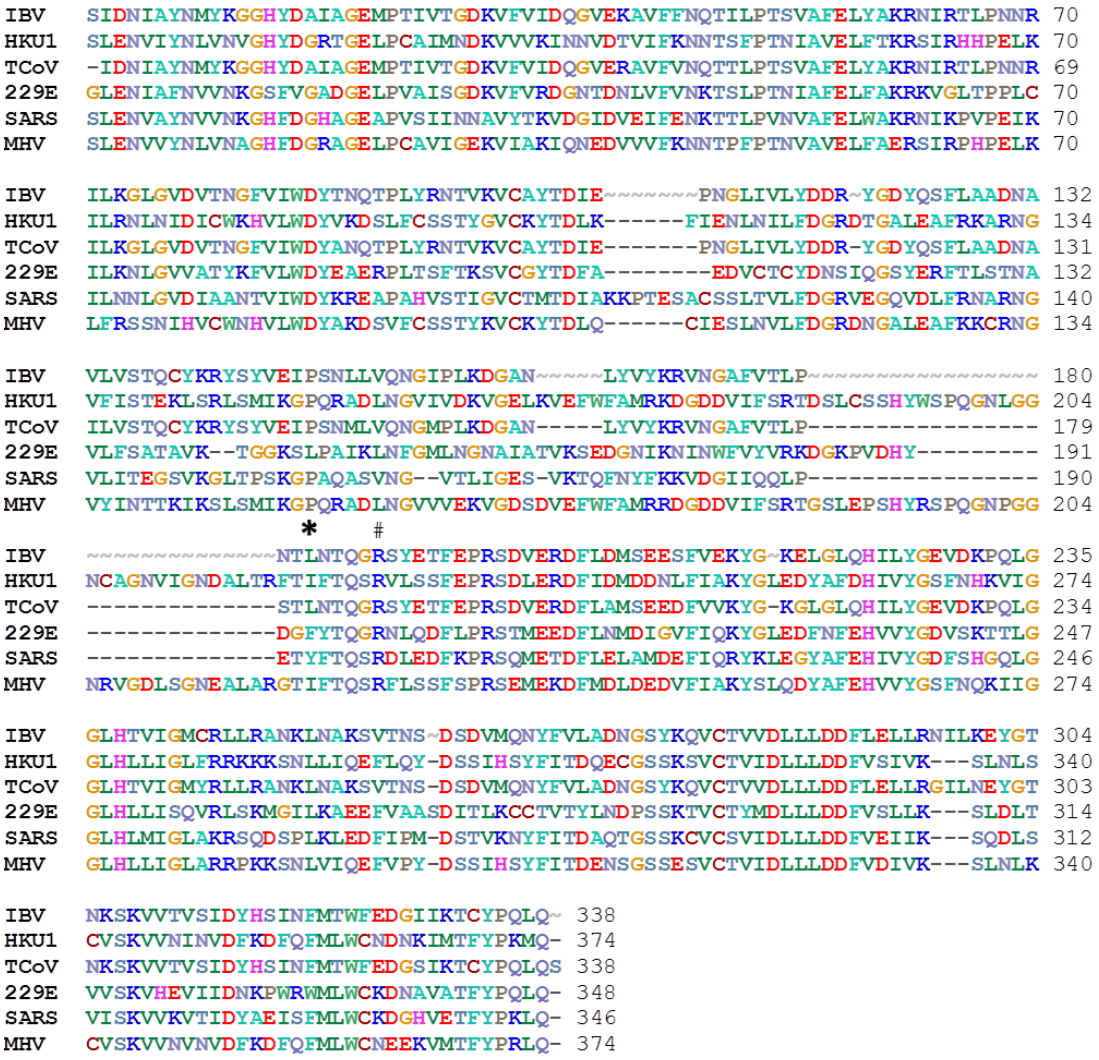

Figure 8.8: Nsp 15 amino acid sequence alignment. * Denotes location of the coding mutation, leucine to isoleucine, within the M41-R genome sequence. # indicates silent marker mutation. The accession numbers of the strains compared are as follows: HCoV-229E, KF514433.1; HCoV-HKU1, NC_006577.2; MHV, KF268339.1; SARS-CoV, KF514395; TCoV: NC_010800.1. The IBV sequence used was M41 sequence generated "in house." Seqeunces were aligned by Dr. Erica Bickerton using BioEdit, version 7.2.5.

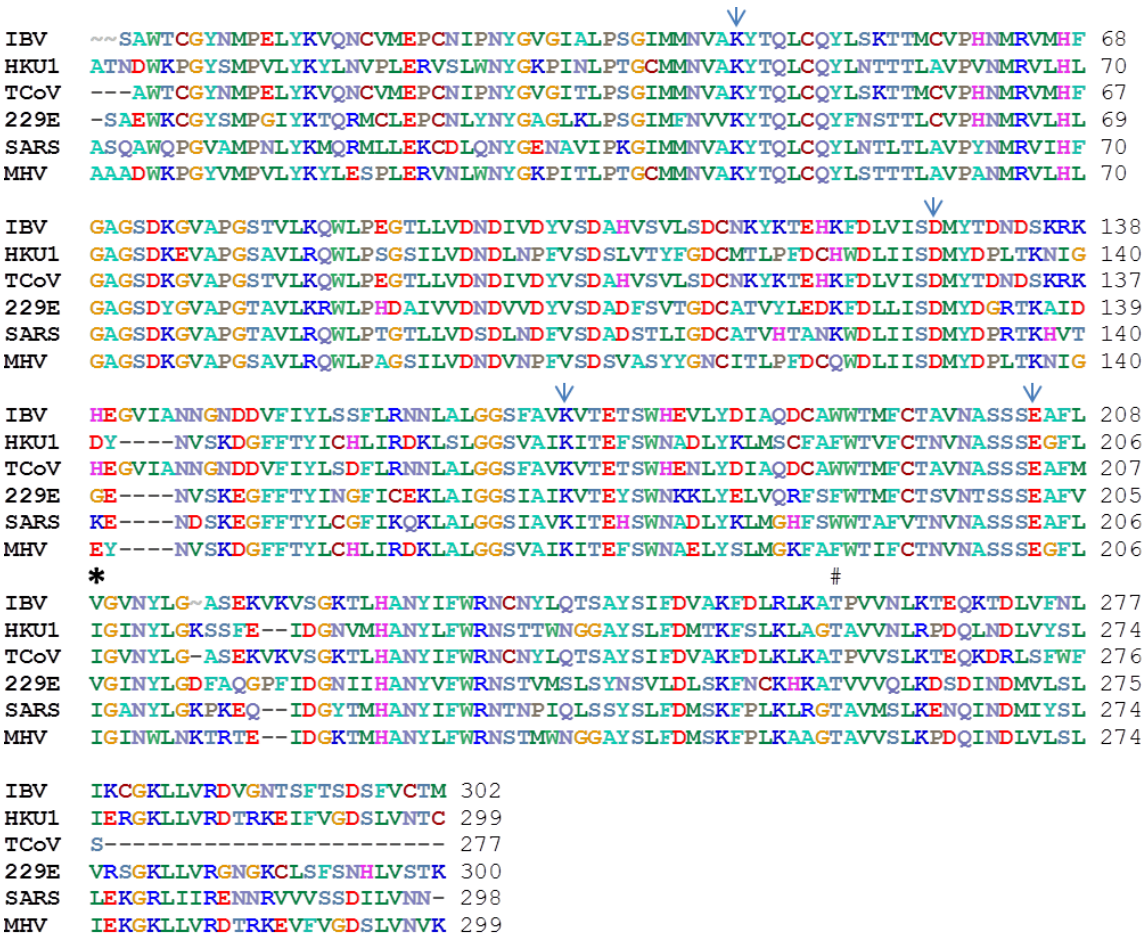

Figure 8.9: Nsp 16 amino acid sequence alignment. * Denotes location of the coding mutation, valine to isoleucine , within the M41-R genome sequence. # indicates silent marker mutation. Arrows indicate the catalytic KDKE motif. The accession numbers of the strains compared are as follows: HCoV-229E, KF514433.1; HCoV-HKU1, NC_006577.2; MHV, KF268339.1; SARS-CoV, KF514395; TCoV: NC_010800.1. The IBV sequence used was M41 sequence generated “in house.” Sequences were aligned by Dr. Erica Bickerton using BioEdit, version 7.2.5.

Figure 8.10: Nsp 10 amino acid sequence alignment. * Denotes location of the coding mutation, proline to leucine , within the M41-R genome sequence. The accession numbers of the strains compared are as follows: HCoV-229E, KF514433.1; HCoV-HKU1, NC_006577.2; MHV, KF268339.1; SARS-CoV, KF514395; TCoV: NC_010800.1. The IBV sequence used was M41 sequence generated “in house.” Sequences were aligned by Dr. Erica Bickerton using BioEdit, version 7.2.5.

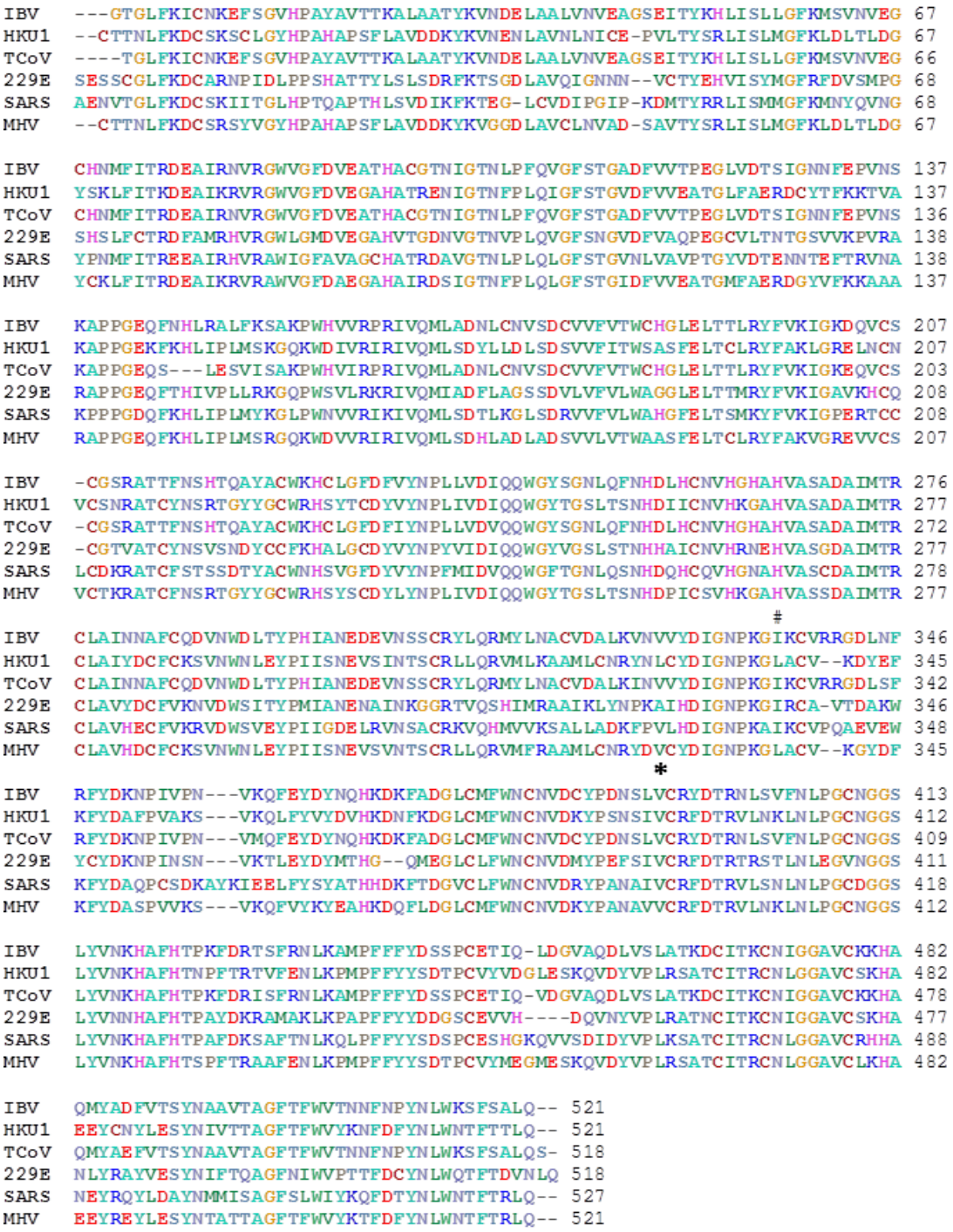

Figure 8.11: Nsp 14 amino acid sequence alignment. * Denotes location of the coding mutation, valine to leucine , within the M41-R genome sequence. # indicates silent marker mutation. The accession numbers of the strains compared are as follows: HCoV-229E, KF514433.1; HCoV-HKU1, NC_006577.2; MHV, KF268339.1; SARS-CoV, KF514395; TCoV: NC_010800.1. The IBV sequence used was M41 sequence generated “in house.” Sequences were aligned using by Dr. Erica Bickerton BioEdit, version 7.2.5.

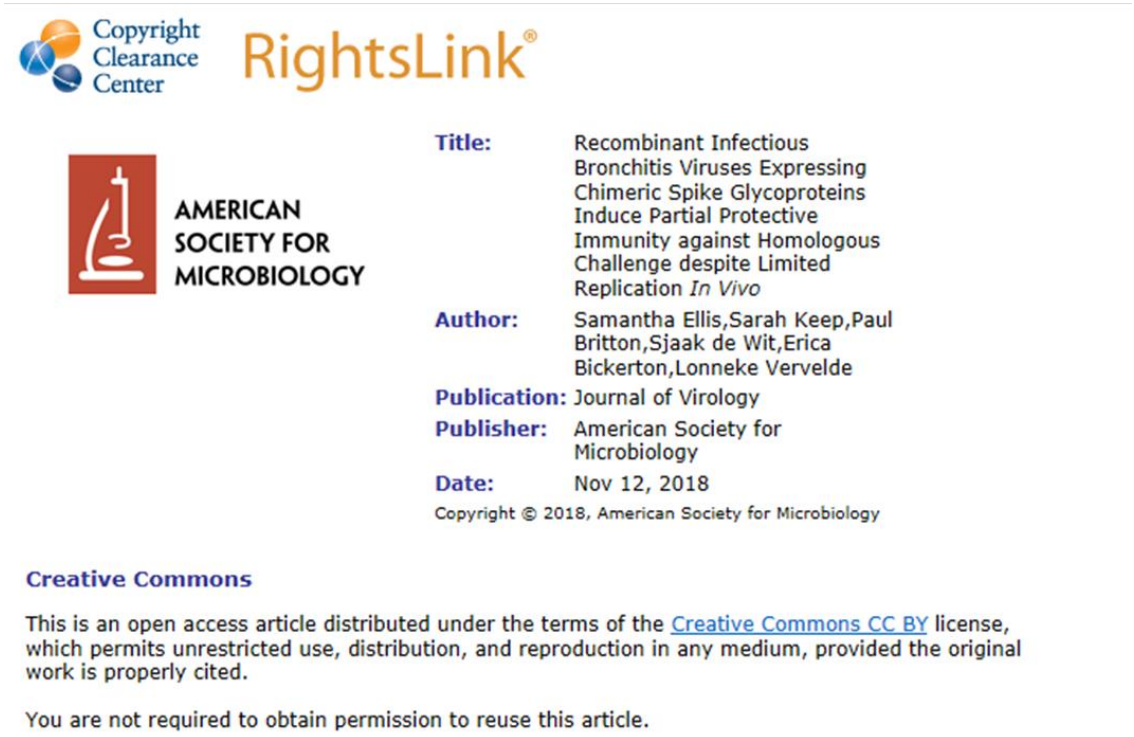

Figure 8.12: Copyright permission for Ellis *et al.*, (2018).

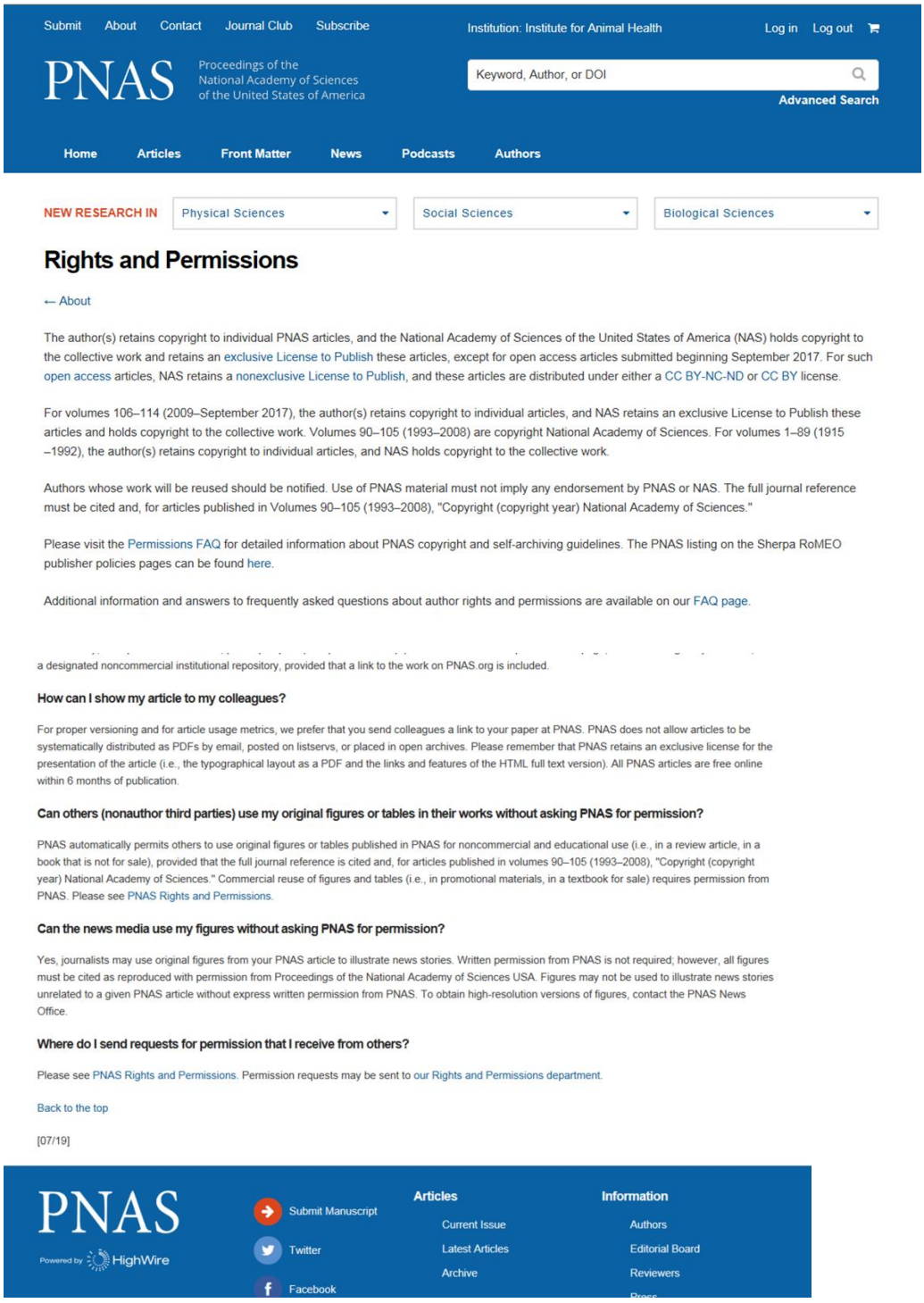

Figure 8.13 Copyright perimission to use a figure published by Ma *et al.*, (2015). Taken from https://www.pnas.org/page/about/rights-permissions , accessed 19th June 2019.

Chapter 9: References

Abdel-Moneim, A., El-Kady, M., Ladman, B. and Gelb Jr, J. (2006). S1 gene sequence analysis of a nephropathogenic strain of avian infectious bronchitis virus in Egypt. *Virology Journal* 10.1186/1743-422X-3-78.

Adzhar, A., Gough, R., Haydon, D., Shaw, K., Britton, P., Cavanagh, D. (1997). Molecular analysis of the 793/B serotype of infectious bronchitis virus in Great Britain. *Avian Pathology* **26**: 625 – 40.

Adzhar, A., Shaw, K., Britton, P. and Cavanagh, D. (1995). Avian infectious bronchitis virus: differences between 793/B and other strains. *Veterinary Record* **136**: 548.

Alford, R., Kasel, J., Gerone, P. and Knight, V. (1966). Human Influenza resulting from aerosol inhalation. *Experimental Biology and Medicine* **122**: 800 – 804.

Almazan, F., Dediego, M., Galan, C. Escors, D., Alverez, E., Ortego, J., Sola, I., Zuniga, S., Alonso, S., Moreno, J., Noglaes, A., Capiscol, C. and Enjuanes, L. (2006). Construction of a severe acute respiratory syndrome coronavirus infectious cDNA clone and a replicon to study coronavirus RNA synthesis. *Journal of Virology* **80**: 10900 – 10906.

Almazan, F., DeDiego, M., Sola, I., Zuniga, S., Nieto-Torres, J., Marquez-Jurado, S., Andres, G. and Enjuanes, L. (2013). Engineering a replication-competent, propagation-defective Middle East respiratory syndrome coronavirus as a vaccine candidate. *mBio* **4**: e00650-13.

Almazan, F., Galan, C. and Enjuanes, L. (2004). The nucleoprotein is required for efficient coronavirus genome replication. *Journal of Virology* **78**: 12683 – 12688.

Almazan, F., Gonzalez, J., Penzes, Z., Izeta, A., Calvo, E., Plana-Duran, J. and Enjuanes, L., (2000). Engineering the largest RNA virus genome as an infectious bacterial artificial chromosome. *Proceedings of the National Academy of Science USA* **97**: 5516 – 5521.

Andrade, L., Villegas, P. and Fletcher, O. (1983). Vaccination of day-old broilers against infectious bronchitis: effect of vaccine strain and route of administration. *Avian Diseases* **27**: 178 – 187.

Ambali, A. and Jones, R. (1990). Early pathogenesis in chicks of infection with an enterotropic strain of infectious bronchitis virus. *Avian Diseases* **34:** 809 – 817.

Amin, O., Valastro, V., Salviato, A., Drago, A., Cattoli, G. and Monne, I. (2012). Circulation of QX-like infectious bronchitis virus in the Middle East. *Veterinary Record* doi:10.1136/vr.100896.

Armesto, M., Bentley, K., Bickerton, E., Keep, S. and Britton, P. (2013). Coronavirus reverse genetics. Reverse Genetics of RNA Viruses: Applications and Perspectives. Chichester, Wiley-Blackwell.

Armesto, M., D. Cavanagh, and P. Britton. (2009). The replicase gene of avian coronavirus infectious bronchitis virus is a determinant of pathogenicity. *PLoS ONE* **4**: e7384.

Armesto, M., Evans, S., Cavanagh, D., Abu-Median, A., Keep, S. and Britton, P. (2011). A recombinant avian infectious bronchitis virus expressing a heterologous spike gene belonging to the 4/91 serotype. *Plos One* 6: e24352

Ammayappan, A., Upadhyay, C., Gelb, J. and Vakharia, V. (2009). Identification of sequence changes responsible for the attenuation of avian infectious bronchitis virus strain Arkansas DPI. *Archives of Virology* **154**: 495 – 499.

Athmer, J., Fehr, A., Grunewald, M., Clinton-Smith, E., Denision, M. and Perlman, S. (2017). In situ tagged nsp15 reveals interactions with coronavirus replication/transcription complex-associated proteins. *MBio* **8**: e02320-16.

Awad, F., Hutton, S., Forrester, A., Baylis, M. and Kannan, G. (2016). Heterologous live infectious bronchitis virus vaccination in day-old commercial broiler chicks: clinical signs, ciliary health, immune responses and protection against variant infectious bronchitis viruses. *Avian Pathology* **45**: 169 – 177.

Babcock, G., Esshaki, D., Thomas, W. and Ambrosino, D. (2004). Amino acids 270 to 510 of the severe acute respiratory syndrome coronavirus spike protein are required for interaction with receptor. *Journal of Virology* **78:** 4552 – 4560.

Balint, A., Farsang, A., Zadori, Z., Hornyak, A., Dencso, L., Almazan, F., Enjuanes, L. and Belak, S., (2012). Molecular characterization of feline infectious peritonitis virusStrain DF-2 and studies of the role of ORF3 abc in viral cell tropism. *Journal of Virology* **86**: 6258 – 6267.

Baranov, P., Henderson, C., Anderson, C., Gesteland, R., Atkins, J. and Howard, M. (2005). Programmed ribosomal frameshifting in decoding the SARS-CoV genome. *Virology* **332**: 498 – 510.

Bárcena, M., Oostergetel, G., Bartelink, W., Faas, F., Verkleij, A., Rottier, P., Koster, A. and Bosch, B. (2009). Cryo-electron tomography of mouse hepatitis virus: Insights into the structure of the coronavirion. *Proceedings of National Academy of Sciences United States of America* **106**: 582 – 587.

Baric, R., Nelson, G., Fleming, J., Deans, R., Keck, J., Casteel, N. and Stohlman, S. (1988). Interactions between coronavirus nucleocapsid protein and viral RNAs: Implications for viral transcription. *Journal of Virology* **62**: 4280 – 4287.

Basso, L., Vicente, E., Crusca, E., Cilli, E. and Costa-Filho, A. (2016) SARS-CoV fusion peptides induce membrane surface ordering and curvature. *Scientific reports* **6**: 37131.

Bayry, J., Goudar, M., Nighot, P., Kshirsagar, S., Ladman, B., Gelb, J., Ghalsasi, G. and Kolte, G. (2005). Emergence of a nephropathogenic avian infectious bronchitis virus with a novel genotype in India. *Journal of Clinical Microbiology* **43**: 916 – 918.

Beato, M.S., De Battisti, C., Terregino, C., Drago, A., Capua, I. and Ortali, G. (2005). Evidence of circulation of a Chinese strain of infectious bronchitis virus (QXIBV) in Italy. *The Veterinary Record* **156:**720.

Beaudette, F. and Hudson, C. (1937). Cultivation of the virus of infectious bronchitis. *Journal of the American Veterinary Medical Association* **90:** 51 – 60.

Becares, M., Pascual-Iglesias, A., Nogales, A., Sola, I., Enjuanes, L. and Zuñiga, S. (2016). Mutagenesis of coronavirus nsp14 reveals its potential role in modulation of the innate immune response. *Journal of Virology* **90**: 5399 – 5414.

Becker, M., Graham, R., Donaldson, E., Rockx, B., Sims, A., Sheahan, T., Pickels, R., Corti, D., Johnson, R., Baric, R. and Denision, M. (2008). Synthetic recombinant bat SARS-like coronavirus is infectious in cultured cells and in mice. *Proceedings of the National Academy of Science USA* **105**: 19944 – 19949.

Belouzard, S., Millet, J., Licitra, B. and Whittaker, G. (2012). Mechanisms of coronavirus cell entry mediated by the viral spike protein. *Viruses* **4**: 1011 –0 1033.

Belshe, R., Mendelman, P., Treanor, J.,King, J., Gruber, W., Piedra, P., Bernstein, D., Hayden, F., Kotloff, K., Zangwill, K., Iacuzio, D. and Mark Wolff, M. (1998). The efficacy of live attenuated, cold-adapted, trivalent, intranasal Influenza virus vaccine in children. *The New England Journal of Medicine* **338**: 1405 – 1412.

Bentely, K. (2012). IBV: Potential as a vaccine vector and identification of a novel subgenomic mRNA. *PhD thesis.* University of Warwick.

Bentley, K., Armesto, M. and Britton, P. (2013). Infectious Bronchitis Virus as a vector for the expression of heterologous genes. *Plos One* **6**: e67875.

Bentley, K., Keep, S., Armesto, M. and Britton, P. (2013B). Identification of a noncanonically transcribed subgenomic mRNA of infectious bronchitis virus and other gammacoronaviruses. *Journal of Virology* **4:** 2128 – 2136.

Benyeda, Z., Mato, T., Suveges, T., Szabo, E., Kardi, V., Abonyi-Toth, Z., Rusvai, M. and Palya, V. (2009). Comparison of the pathogenicity of QX-like, M41 and 793/B infectious bronchitis strains from different pathological conditions. *Avian Pathology* **38**: 449 – 56.

Bhardwaj, K., Guarino, L. and Kao, C. (2004). The severe acute respiratory syndrome coronavirus Nsp 15 protein is an endoribonuclease that prefers manganese as a cofactor. *Journal of Virology* **78**: 12218 – 12224.

Bickerton E, Dowgier G, Britton P. (2018). Recombinant infectious bronchitis viruses expressing heterologous S1 subunits: potential for a new generation of vaccines that replicate in Vero cells. *Journal of General Virology* **99**: 1681 – 1685.

Bickerton, E., Maier, H.J., Stevenson-Leggett, P., Armesto, M., Britton P. (2018B). The S2 subunit of infectious bronchitis virus Beaudette is a determinant of cellular tropism. Journal of Virology **92**: e01044-01018.

Bijlenga, G., Cook, J., Gelb, J. and de Wit, J. (2004). Development and use of the H strain of avian infectious bronchitis virus from the Netherlands as a vaccine: a review. *Avian Pathology* **33**: 550 – 557.

Bingham., R., Madge, H. and Tyrrell, D. (1975). Haemagglutination by Avian Infectious Bronchitis Virus- a Coronavirus. *Journal of General Virology* **28**: 381 – 390.

Binns, M., Boursnell., M., Cavanagh, D., Darryl, J. (1985). Cloning and sequencing of the gene encoding the spike protein of the Coronavirus IBV. *Journal of General Virology* **66**: 719 – 726.

Bisht, H., A. Roberts, L. Vogel, A. Bukreyev, P. L. Collins, B. R. Murphy, K. Subbarao, and Moss, B. (2004). Severe acute respiratory syndrome coronavirus spike protein expressed by attenuated vaccinia virus protectively immunizes mice. *Proceedings of the National Academy of Sciences the USA* **101**: 6641–6646.

Boots., A.M.H., Kusters, J.G., Vannoort, J.M., Zwaagstra, K.A., Rijke, E., Vanderzeijst,. B.A.M. and Hensen, E.J. (1991). Localization of a T-Cell epitope within the nucleocapsid protein of avian coronavirus. *The Journal of Immunology* **74**: 8 – 13.

Bonavia, A., Zelus, B., Wentworth, D., Talbot, P. and Holmes, K. (2003). Identification of a Receptor-Binding Domain of the Spike Glycoprotein of Human Coronavirus HCoV-229E. *Journal of Virology* **77**: 2530 – 2538.

Boursnell, M., Brown, T., Foulds, I., Green, P., Tomley. F. and Binns, M. (1987). Completion of the sequence of the genome of the coronavirus avian infectious bronchitis virus. Journal of General *Virology* **68**: 57 – 77.

Bosch, B., van der Zee, R., de Haan, C. and Rottier, P. (2003). The coronavirus spike protein is a class I virus fusion protein: structural and functional characterization of the fusion core complex. *Journal of Virology* **77**: 8801 – 8811.

Bourogâa , H., Larbi, I., Miled, K., Kort Hellal, Y., Hassen, J., Behi, I., Nsiri, J. and Ghram, A. (2014). Evaluation of protection conferred by a vaccination program based on the H120 and CR88 commercial vaccines against a field variant of avian infectious bronchitis virus. *Journal of Applied Poultry Research* **23**: 156 – 164.

Bouvet, M., Debarnot, C., Imbert, I., Selisko, B., Snijder, E. J., Canard, B. and Decroly, E. (2010) In vitro reconstitution of SARS-Coronavirus mRNA cap methylation. *PLoS Pathogens* **6**: e1000863.

Bouvet, M., Imbert, I., Subissi, L., Gluais, L., Canard, B. and Decroly, E. (2012). RNA -3'-end mismatch excision by the severe acute respiratory syndrome Coronavirus nonstructural protein nsp10/nsp14 exoribonuclease complex. *Proceedings of the National Academy of Science USA* **109**: 9372 – 9377.

Bouvet, M., Lugari, A., Posthuma, C., Zevenhoven, J., Bernard, S., Betzi, S., Imbert, I., Canard, B., Guillemot, J., Lécine, P., Pfefferle, S.,Drosten, C., Snijder, E., Decroly, E. and Morelli, X. (2014). Coronavirus Nsp10, a critical co-factor for activation of multiple replicative enzymes. *The Journal of Biological Chemistry* **289**: 25783 – 25796.

Bradel-Tretheway, B., Kelley, Z., Chakraborty-Sett, S., Takimoto, T., Kim, B. and Dewhurst, S. (2008). The human H5N1 influenza A virus polymerase complex is active *in vitro* over a broad range of temperatures, in contrast to the WSN complex, and this property can be attributed to the PB2 subunit. *Journal of General Virology* **89**: 2923 – 2932.

Brian, D. and Baric R. (2005). Coronavirus genome structure and replication. *Current topics in Microbiology and Immunology* **287**: 1 – 30.

Broadbent, A., Santo, C., Godbout, R. and Subbara, K. (2014). The temperature-sensitive and attenuation phenotypes conferred by mutations in the Influenza Virus PB2, PB1, and NP genes are influenced by the species of origin of the PB2 Gene in reassortant viruses derived from Influenza A/California/07/2009 and A/WSN/33 viruses. *Journal of Virology* **88**: 12339 – 12347.

Brierley, I., Boursnell, M., Binns, M., Bilimoria, B., Blok, V., Brown, T. and Inglis, S. (1987). An efficient ribosomal frame-shifting signal in the polymerase encoding region of the coronavirus IBV. *EMBO Journal* **6**: 3779 – 3785.

Brierley, I., Digard, P. and Inglis, S. (1989). Characterization of an efficient coronavirus ribosomal frameshifting signal: requirement for an RNA pseudoknot. *Cell* **57**: 537 – 547.

Britton, P. and Cavanagh, D. (2008). Nidovirus genome organization and expression mechanisms. In: Perlman, S., Gallagher, T. and Snijder, E. Nidoviruses. Washington, DC: ASM Press.

Britton, P., Evan, S., Dove, B., Davies, M., Casais, R. and Cavanagh, D. (2005). Generation of a recombinant avian coronavirus infectious bronchitis virus using transient dominant selection. *Journal of Virological Methods* **123**: 203 – 211.

Britton, P., Green, P., Kottier, S., Mawditt, K., Penzes, Z., Cavanagh, D. and Skinner, M. (1996). Expression of bacteriophage T7 RNA polymerase in avian and mammalian cells by a recombinant fowlpox virus. *Journal of General Virology* **77**: 963 – 967.

Bru, T., Vila, R., Cabana, M. and Geerligs, H.J. (2017). Protection of chickens vaccinated with combinations of commercial live infectious bronchitis vaccines containing Massachusetts, Dutch and QX-like serotypes against challenge with virulent infectious bronchitis viruses 793B and IS/1494/06 Israel variant 2. *Avian Pathology* **46**:52-58

Buchholz, U., Bukreyev, A., Yang, L., Lamirande, E., Murphy, B., Subbarao, K. and Collins, P. (2004). Contributions of the structural proteins of severe acute respiratory syndrome coronavirus to protective immunity. *PNAS* **101**: 9804 – 9809.

Burke-Schinkel, S., Rubin, S. and Wright, K. (2017). Mechanisms of temperature sensitivity of attenuated Urabe mumps virus. *Virus Research* **227**: 104 – 109.

Bukreyev, A., Lamirande, E., Buchholz, U., Vogel, L., Elkins, W., St Claire, M., Murphy, B., Subbaraoo, K. and Collins, P. (2004).Mucosal immunisation of African green monkeys (Cercopithecusaethiops) with an attenuated parainfluenza virus expressing the SARS coronavirus spike protein for the prevention of SARS. *The Lancet* **363**: 2122 – 2127.

Cao, J., Wu, C. and Lin, T. (2008). Turkey coronavirus non-structure protein NSP 15 – An endoribonuclease. *Intervirology* **51**: 342 – 351.

Cao, J. and Zhang, X., (2012). Comparative in vivo analysis of the nsp15 endoribonuclease of murine, porcine and severe acute respiratory syndrome coronaviruses. *Virus Research* **167**: 247 – 258.

Capua, I., Minta, Z., Karpinska, E., Mawditt, K., Britton, P., Cavanagh, D. and Gough, R. (1999). Co-circulation of four types of infectious bronchitis virus (793/B, 624/I, B1648 and Massachusetts). *Avian Pathology* **28**: 587 – 592.

Carstens, E. (2010). Ratification vote on taxonomic proposals to the International Committee on Taxonomy of Viruses (2009). *Archives of Virology* **155**: 133 – 146.

Casais, R., Davies, M., Cavanagh, D. and Britton, P. (2005). Gene 5 of the Avian Coronavirus Infectious Bronchitis Virus is not essential for replication. *Journal of Virology* **13**: 8065 – 8078.

Casais, R., Dove, B., Cavanagh, D. and Britton, P. (2003). Recombinant avian infectious bronchitis virus expressing a heterologous spike gene demonstrates that the spike protein is a determinant of cell tropism. *Journal of Virology* **77**: 9084 – 9089.

Casais, R., Thiel, V., Siddell, S., Cavanagh, D. and Britton, P. (2001). Reverse Genetics System for the Avian Coronavirus Infectious Bronchitis Virus. *Journal of Virology* **75**: 12359 – 12369.

Cavanagh, D. (2003). Severe acute respiratory syndrome vaccine development: experiences of vaccination against avian infectious bronchitis coronavirus. *Avian Pathology* **32**: 567 – 582.

Cavanagh, D. (2007). Coronavirus avian infectious bronchitis virus. *Veterinary Research* **38**: 1 – 17.

Cavanagh, D. and Davis, P. (1986). Coronavirus IBV: removal of the spike glycopolypeptide S1 by urea abolishes infectivity and haemagglutination but not attachment to cells. *Journal of General Virology* **67**: 1443 – 1448.

Cavanagh, D., Davis, P. and Mockett, A. (1988). Amino acids within hypervariable region 1 of avian coronavirus IBV (Massachusetts serotype) spike glycoprotein are associated with neutralization epitopes. *Virus Research* **11**: 141 – 150.

Cavanagh, D. and Naqi, S. (2003). Infectious bronchitis In: SAIF, Y. M., BARNES, H. J., GLISSON, J. R., FADLY, A. M., MCDOUGALD, L. R. & SWAYNE, D. E. (eds.) Diseases of Poultry. Ames, Iowa: Iowa State University Press.

Cavanagh, D., Davis, P., Darbyshire, J. and Peters, R. (1986B). Coronavirus IBV: virus retaining spike glycopolypeptide S2 but not S1 is unable to induce virus-neutralizing or haemagglutination-inhibiting antibody, or induce chicken tracheal protection. *Journal of General Virology* **67**: 1435 – 1442.

Cavanagh, D., Davis, P., Cook, J., Li, D., Kant, A. and Koch, G. (1992). Location of the amino acid differences in the S1 spike glycoprotein subunit of closely related serotypes of infectious bronchitis virus. *Avian Pathology* **21**: 33 – 43.

Cavanagh, D., Darbyshire, J., Davies, P. and Peters, R. (1984). Induction of humoral neutralising and haemagglutination-inhibiting antibody by the spike protein of avian infectious bronchitis virus. *Avian Pathology* **13**: 573 – 583.

Cavanagh, D., Davis, P., Pappin, D., Binns, M., Boursnell, M. and Brown, T. (1986B). Coronavirus IBV: partial amino terminal sequencing of spike polypeptide S2 identifies the sequence Arg-Arg-Phe-Arg-Arg at the cleavage site of the spike

precursor polypeptide of IBV strains Beaudette and M41. *Virus Research* **4**: 133 – 143.

Cavanagh, D., Ellis, M. and Cook, J. (1997). Relationship between sequence variation in the S1 spike protein of infectious bronchitis virus and the extent of cross-protection in vivo. *Avian Pathology* **26**: 63 – 74.

Cavanagh, D., Picault, J., Gough, R., Hess, M., Mawditt, K. and Britton, P., (2005). Variation in the spike protein of the 793/B type of infectious bronchitis virus, in the field and during alternate passage in chickens and embryonated eggs. *Avian Pathology* **34**: 20 – 25.

Chang, H., Egberink, H., Halpin, R., Spiro, D. and Rottier, P. (2012). Spike protein fusion peptide and Feline Coronavirus virulence. *Emerging Infectious Diseases* **18**: 1089 – 1095.

Chen, Y., Cai, H., Pan, J., Xiang, N., Tien, P., Ahola, T. and Guo, D. (2009). Functional screen reveals SARS coronavirus nonstructural protein nsp14 as a novel cap N7 methyltransferase. *PNAS* **106**: 3484–3489.

Chen, Y., Su, C., Ke, M., Jin, X., Xu, L., Zhang, Z., Wu, A., Sun, Y., Yang,Z., Tien, P., Ahola, T., Liang, Y., Liu, X. and Guo, D. (2011). Biochemical andstructural insights into the mechanisms of SARS coronavirus RNA ribose 2_-O-methylation by nsp16/nsp10 protein complex. *PLoS Pathogens* **7**: e1002294.

Chen, Y., Tao, J., Sun, Y., Wu, A., Su, C., Gao, G., Cai, H., Qiu, S., Wu, Y., Ahola, T. and Guo, D. (2013). Structure-function analysis of severe acute respiratory syndrome coronavirus RNA cap guanine-N7-methyltransferase. *Journal of Virology* **87**: 6296–6305.

Chen, H., Yanga, M., Cuia, B., Cuib, P., Shengb, M., Chenb, G., Wanga, S. and Genga, J. (2010). Construction and immunogenicity of a recombinant fowlpox vaccinecoexpressing S1 glycoprotein of infectious bronchitis virus and chicken IL-18. *Vaccine* **28**: 8112 – 8119.

Chu, V., Mcerlroy, L., Chu, V., Bauman, B. and Whittaker, G. (2006). The avian coronavirus infectious bronchitis virus undergoes direct low-pH-dependent fusion activation during entry into host cells. **Journal of Virology 80**: 3180 – 8.

Clementz, M., Kanjanahaluethai, A., O'Brien, T. and Baker, S. (2008). Mutation in murine coronavirus replication protein nsp4 alters assembly of double membrane vesicles. *Virology* **375**: 118 – 129.

Cook, J., Orbell, S., Woods, M. and Huggins, M. (1999). Breadth of protection of the respiratory tract provided by different live-attenuated infectious bronchitis vaccines against challenge with infectious bronchitis viruses of heterologous serotypes. *Avian Pathology* **28**: 477 – 485.

Cook, J., Chesher, J., Baxendale, W., Greenwood, N., Huggins, M., and Orbell, S. (2001). Protection of chickens against renal damage caused by a nephropathogenic infectious bronchitis virus. *Avian Patholathogy* **30:** 423 – 426.

Cook, J., Darbyshire, J. and Peters, R. (1976). The use of chicken tracheal organ cultures tor the isolation and assay of avian Infectious Bronchitis Virus. *Archives of Virology* **50**: 1 09 – 118.

Cook, J., Jackwood, M. and Jones, R. (2012). The long view: 40 years of infectious bronchitis research. *Avian Pathology* **41**: 239 – 50.

Coley, S., Lavi, E., Sawicki, S., Fu, L., Schelle, B., Karl, N., Siddell, S. and Thiel, V. (2005). Recombinant mouse hepatitis virus strain A59 from cloned, full-length cDNA replicates to high titers *in vitro* and is fully pathogenic *in vivo*. *Journal of Virology* **79**: 3097 – 3106.

Collisson, E.W., Pei, J., Dzielawa, J. and Seo, S.H. (2000). Cytotoxic T lymphocytes are critical in the control of infectious bronchitis virus in poultry. *Developmental and Comparative Immunology* **24**:187-200.

Corse, E. and Machamer, C. (2000). Infectious bronchitis virus E protein is targeted to the golgi complex and directs release of virus-like particles. *Journal of Virology* **74**: 4319 – 4326.

Corse, E. and Machamer, C. (2003). The cytoplasmic tails of infectious bronchitis virus E and M proteins mediate their interaction. *Virology* **312**: 25 – 34.

Dalton, R., Mullin, A., Amorim, M., Medcalf, E., Tiley, L. and Digard, P. (2006). Temperature sensitive influenza A virus genome replication results from low thermal stability of polymerase-cRNA complexes. Virology Journal **3**: 58.

Daniel, C., Anderson, R., Buchmeier, M. Fleming, J. Spaan, W., Wege, H. and Talbot, P. (1993) Identification of an immunodominant linear neutralization domain on the S2 portion of the murine coronavirus spike glycoprotein and evidence that it forms part of complex tri dimensional structure. *Journal of Virology* **67**: 1185 – 1194.

Darbyshire, J. (1980). Assessment of cross-immunity dm chickens to strains of avian infectious bronchitis virus using tracheal organ cultures. *Avian Pathology* **9**: 179 – 184.

Darbyshire, J., Rowell, J., Cook, J. and Peters, R. (1979). Taxonomic studies on strains of avian infectious bronchitis virus using neutralisation tests in tracheal organ cultures. *Archives of Virology* **61**: 227 – 238.

Decroly, E., Debarnot, C., Ferron, F., Bouvet, M., Coutard, B., Imbert, I., Gluais, L., Papageorgiou, N., Sharff, A., Bricogne, G., Ortiz-Lombardia, M., Lescar, J. and Canard, B. (2011). Crystal structure and functional analysis of the SARS-Coronavirus RNA cap 2-O-methyltransferase nsp10/nsp16 complex. *PLoS Pathogens* **7**: e1002059.

Decroly, E., Ferron, F., Lescar, J., and Canard, B. (2012). Conventional and unconventional mechanisms for capping viral mRNA. *Nature Reviews Microbiology* **10**: 51 – 65.

Decroly, E., Imbert, I., Coutard, B., Bouvet, M., Selisko, B., Alvarez, K., Gorbalenya, A., Snijder, E. and Canard, B. (2008). Coronavirus nonstructural protein 16 is a cap-0 binding enzyme possessing (nucleoside-2'O)-methyltransferase activity. *Journal of Virology* **82**: 8071 – 8084.

DeDiego, M., Nieto-Torres, J., Jimenez-Guardeno, J., Regla-Nava, J., Alvarez, E., Oliveros, J., Zhao, J., Fett, C., Perlman, S. and Enjuanes, L. (2011). Severe acute respiratory syndrome coronavirus envelope protein regulates cell stress response and apoptosis. *PLoS pathogens* **7**:e1002315.

DeDiego, M., Nieto-Torres, J., Jimenez-Guardeño, J., Regla-Nava, J., Castaño-Rodriguez, C., Fernandez-Delgado, R., Usera, F. and Enjuanes, L. (2014). Coronavirus virulence genes with main focus on SARS-CoV envelope gene. *Virus Research* **194**: 124 – 37.

DeDiego, M., Nieto-Torres, J., Regla-Nava, J., Jimenez-Guardeno, J., Fernandez-Delgado, R., Fett, C., Castano-Rodriguez, C., Perlman, S. and Enjuanes, L. (2014B). Inhibition of NF-kappaB mediated inflammation in severe acute respiratory syndrome coronavirus-infected mice increases survival. Journal of Virology **88**: 913 – 924.

DEFRA (2005). Economic assessment of livestock diseases in Great Britain, 2000 – 2002. *http://www.defra.gov.uk/science/Project_Data/DocumentLibrary/ZZ0102/ZZ0102_1215_FRP.doc*

de Haan, C., Smeets, M., Vernooij, F., Vennema, H. and Rottier, P. (1999). Mapping of the coronavirus membrane protein domains involved in interaction with the spike protein. *Journal of Virology* **73**: 7441 – 7452.

de Haan, C., Stadler, K., Godeke, G., Bosch, B. and Rottier, P. (2004). Cleavage inhibition of the murine coronavirus spike protein by a furin-like enzyme affects cell-cell but not virus-cell fusion. *Journal of Virology* **78**: 6048 – 6054.

de Haan, C., Vennema, H. and Rottier, P. (2000). Assembly of the coronavirus envelope: homotypic interactions between the M proteins. *Journal of Virology* **74**: 4967 – 4978.

Deng, X. and Baker, S. (2018). An "Old" protein with a new story: Coronavirus endoribonuclease is important for evading host antiviral defences. *Virology* **517**: 157 – 163.

Deng, X., Hackbart, M., Mettelman, R., O'Brien, A., Mielech, A., Yi, G., Kao, C. and Baker, S. (2017). Coronavirus nonstructural protein 15 mediates evasion of dsRNA sensors and limits apoptosis in macrophages. *Proceedings of National Academy of Sciences USA* **114**: 4251 – 4260.

Deng, X., Mettelman, R., O'Brien, A., Thompson, J., O'Brien, T. and Baker, S. (2019). Analysis of coronavirus temperature-sensitive mutants reveals an interplay between the macrodomain and papain-like protease impacting replication and pathogenesis. *Journal of Virology* doi:**10**.1128/JVI.02140-18

de Wit, J. (2000). Technical Review. Detection of infectious bronchitis virus. *Avian Pathology* **29**: 71 – 93.

de Wit, J., Boelm, G., van Gerwe, T. and Swart, W. (2013). The required sample size in vaccination-challenge experiments with infectious bronchitis virus, a meta-analysis. *Avian Pathology* **42**: 9 – 16.

de Wit, J., Cook, J. and van der Heijden, H. (2011). Infectious bronchitis virus variants: a review of the history, current situation and control measures. *Avian Pathology* **40**: 223 – 235.

de Wit, J., Nieuwenhuisen-van Wilgen, J., Hoogkamer, A., van de Sande, H., Zuidam, G. and Fabri, T. (2011B) Induction of cystic oviducts and protection

against early challenge with infectious bronchitis virus serotype D388 (genotype QX) by maternally derived antibodies and by early vaccination. *Avian Pathology* **40(5):**463 – 471.

de Wit, J. and Cook, J. (2014). Factors influencing the outcome of infectious bronchitis vaccination and challenge experiments. *Avian Pathology* **43**: 485 – 497.

Dhinaker, R. and Jones, R. (1997). Infectious bronchitis virus: immunopathogenesis of infection in the chicken *Avian Pathology* **26**: 677 – 706.

Doms, R., Lamb, R., Rose, J. and Helenius, A. (1993). Folding and assembly of viral membrane proteins. *Virology* **193**: 545 – 562.

Donaldson, E., Graham, R., Sims, A., Denison, M. and Baric, R. (2007). Analysis of murine hepatitis virus strain A59 temperature-sensitive mutant TS-LA6 suggests that nsp10 plays a critical role in polyprotein processing. *Journal of Virology* **81**: 7086 – 7098.

Donaldson, E., Sims, A., Graham, R., Denison, M. and Baric, S. (2007). Murine hepatitis virus replicase protein nsp10 is a critical regulator of viral RNA synthesis. *Journal of Virology* **81**: 6356 – 6368.

Donaldson, E., Yount, B., Sims, A., Burkett, S., Pickles, R. and Baric, R. (2008). Systematic assembly of a full-length infectious clone of human coronavirus NL63. *Journal of Virology* **82**: 11948 – 11957.

Doyle, N., Neuman,B., Simpson, J., Hawes, J., Mantell, J., Verkade, P., Alrashedi, H. and Maier, H. (2018). Infectious Bronchitis Virus nonstructural protein 4 alone induces membrane pairing. *Viruses* **10**: 477

Eckerle, L., Becker, M., Halpin, R., Li, K., Venter, E., Lu, X., Scherbakova, S., Graham, R., Baric, R., Stockwell, T., Spiro, D. and Denison, M. (2010). Infidelity of SARS-CoV Nsp14 exonuclease mutant virus replication is revealed by complete genome sequencing. *PLoS Pathogens* **6**:1000896.

Eckerle, L., Lu, X., Sperry, S., Choi, L. and Denison, M. (2007). High fidelity of murine hepatitis virus replication is decreased in nsp14 exoribonuclease mutants. *Journal of Virology* **81**:12135 – 12144.

Egloff, M., Malet, H., Putics, A., Heinonen, M., Dutartre, H., Frangeul, A., Gruez, A., Campanacci, V., Cambillau, C., Ziebuhr, J., Ahola, T. and Canard, B. (2006). Structural and functional basis for ADP-ribose and poly(ADP-ribose) binding by viral macro domains. *Journal of Virology* **80**: 8493 – 8502.

Eldaghayes, I., Rothwell, L., Williams, A., Withers, D., Balu, S., Davison, F. and Kaiser, P. (2006). Infectious bursal disease virus: strains that differ in virulence differentially modulate the innate immune response to infection in the chicken bursa. *Viral Immunology* **19**: 83 – 91.

Eldemery, F., Joiner, K., Toro, H. and van Santen, V. (2017). Protection against infectious bronchitis virus by spike ectodomain subunit vaccine. *Vaccine* **35**: 5864 – 5871.

Ellis., S., Keep, S., Britton, P., de Wit, S., Bickerton, E., and Vervelde L. (2018). Recombinant Infectious Bronchitis Viruses expressing chimeric spike glycoproteins

induces partial protective immunity against homologous challenge despite limited replication *in vivo*. *Journal of Virology* **92**: e01473-18.

Enjuanes, L., Zuñiga, S., Castaño-Rodriguez, C., Gutierrez-Alvarez, J., Canton, J. and Sola, I. (2016). Molecular basis of coronavirus virulence and vaccine development. *Advances in Virus Research* **96**: 245 – 286.

Eriksson, K., Cervantes-Barragan, L., Ludewig, B. and Thiel, V. (2008). Mouse hepatitis virus liver pathology is dependent on ADP-ribose-1''-phosphatase, a viral function conserved in the alpha-like supergroup. *Journal of Virology* **82**: 12325 – 12334.

European Pharmacoepia 6.1. (2010). Avian infectious bronchitis vaccine (live), p 3371 – 3373. European Directorate for the Quality of Medicines and HealthCare (EDQM), Council of Europe, Strasbourg, France.

Falkner, G. and Moss, B. (1988). Escherichia coli gpt gene provides dominant selection for vaccinia virus open reading frame expression vectors. *Journal of Virology* **62**: 1849 – 1854.

Falkner, G. and Moss, B. (1990). Transient dominant selection of recombinant vaccinia viruses. *Journal of Virology* **64:** 3108 – 3111.

Fang, S., Chen, B., Tay, F. and Liu D. (2007) An Arginine-to-Proline mutation in a domain with undefined functions within the helicase protein (NSP 13) is lethal to the coronavirus Infectious Bronchitis Virus in cultured cells. *Virology* **358**: 136–147.

Fehr, A., Athmer, J., Channappanavar, R., Phillips, J., Meyerholz, D. and Perlman, S. (2015). The nsp3 macrodomain promotes virulence in mice with coronavirus-induced encephalitis. *Journal of Virology* **89**: 1523 – 1536.

Fehr, A., Channappanavar, R., Jankevicius, G., Fett, C., Zhao, J. et al. (2016). Athmer, J., Meyerholz, D., Ahel, I. and Perlman, S. (2016). The conserved coronavirus macrodomain promotes virulence and suppresses the innate immune response during severe acute respiratory syndrome coronavirus infection. *MBio* **7**: e01721-16.

Fehr, A. and Perlman, S. (2015). Coronaviruses: an overview of their replication and pathogenesis. *Methods in Molecular Biology* **1282**: 1 – 23.

Feller, J., Smallwood, S., Skiadopoulos, M., Murphy, B. and Moyer, S. (2000). Comparison of identical temperature-sensitive mutations in the L polymerase proteins of Sendai and Parainfluenza3 viruses. *Virology* **276**: 190 – 201.

Frana, M., Behnke, J., Sturman, L. and Holmes, K. (1985). Proteolytic cleavage of the E2 glycoprotein of murine coronavirus: host-dependent differences in proteolytic cleavage and cell fusion. *Journal of Virology* **56:** 912 – 920.

Foxman, E., Storera, J., Fitzgerald, M., Wasike, B., Houf, L., Zhaof, H., Turnere, P., Pyle, A. and Iwasakia, A. (2015). Temperature-dependent innate defense against the common cold virus limits viral replication at warm temperature in mouse airway cells. PNAS **112**: 827 – 832.

Frazatti-Gallina, N., Mourao-Fuches, R., Paoli, R., Silva, M., Miyaki, C. and Valentini, E. (2004). Vero-cell rabies vaccine produced using serum free media. *Vaccine* **23**: 511 – 517.

Frieman, M., Ratia, K., Johnston, R., Mesecar, A. and Baric, R. (2009). Severe acute respiratory syndrome coronavirus papain-like protease ubiquitin-like domain and catalytic domain regulate antagonism of IRF3 and NF-kappaB signaling. *Journal of Virology* **83**: 6689 – 6705.

Gelb, J., Lunt, R., Metz, A. and Fries, P. (1991). Attenuation of avian Infectious Bronchitis Virus by cold-adaptation. *Avian Diseases* **35**: 847 – 853.

Geilhausen, H., Ligon, F. and Lukert, P. (1973). The pathogenesis of virulent and avirulent avian infectious bronchitis virus. *Archives of Virology* **40**:285 – 290.

Geerligs, H., Boelm, G., Meinders, C., Stuurman, B., Symons, J., Tarres-Call, J., Bru, T., Vila, R., Mombarg, M., Karaca, K., Wijmenga, W. and Kumar, M. (2011). Efficacy and safety of an attenuated live QX-like infectious bronchitis virus strain as a vaccine for chickens. *Avian Pathology* **40**: 93 – 102.

Gonzalez, J., Penzes, Z., Almazan, F., Calvo, E. and Enjuanes, L., (2002). Stabilization of a full-length infectious cDNA clone of transmissible gastroenteritis coronavirus by insertion of an intron. *Journal of Virology* **76**: 4655 – 4661.

Gorbalenya, A., Enjuanes, L., Ziebuhr, J. and Snijder, E. (2006). Nidovirales: evolving the largest RNA virus genome. *Virus Research* **117**: 17 – 37.

Gough, R., Cox, W., de, B., Welchman, D., Worthington, K. and Jones, R. (2008). Chinese QX strain of infectious bronchitis virus isolated in the UK. *The Veterinary Record* **162**: 99 – 100.

Gosert, R., Kanjanahaluethai, A., Egger, D., Bienz, K. and Baker, S. (2002). RNA replication of mouse hepatitis virus takes place at double-membrane vesicles. *Journal of Virology* **76**: 3697 – 3708.

Graham, R., Becker, M., Eckerle, L., Bolles, M., Denison, M. and Baric, R. (2012). A live, impaired-fidelity coronavirus vaccine protects in an aged, immunocompromised mouse model of lethal disease. *Nature Medicine* **18**: 1820 – 1826.

Griffon, A., Moy, M., Yadav, K., Velasquez, M., Buchmeier, J., Stevens, R. and Kuhn, P. (2006) Crystal structure of non-structural protein 10 from the severe acute respiratory syndrome Coronavirus reveals a novel fold with two zinc binding motifs. *Journal of Virology* **80**: 7894 – 7901.

Gurjar, R.S., Gulley, S.L. and van Ginkel, F.W. (2013). Cell-mediated immune responses in the head-associated lymphoid tissues induced to a live attenuated avian coronavirus vaccine. *Developmental and Compartivie Immunology* **41**:715-722

Haijema, B., Volders, H. and Rottier, P. (2003). Switching species tropism: an effective way to manipulate the feline coronavirus genome. *Journal of Virology* **77**: 4528 – 4538.

Hall, R. (2017). The role of infectious bronchitis virus accessory proteins 3a, 3b and 4b. *PhD thesis,* University of Liverpool.

Hall, S., Stokes, A. Tierney, E., London, W., Belshe, R. Newman, F. and Murphy, B. (1992). Cold-passaged human parainfluenza type 3 viruses contain ts and non-ts mutations leading to attenuation in rhesus monkeys. *Virus Research* **22**: 173 – 184.

Han, D., Lohani, M. and Cho, M. (2007). Specific asparagine-linked glycosylation sites are critical for DC-SIGN- and L-SIGN-mediated severe acute respiratory syndrome coronavirus entry. Journal of Virology **81**: 12029 – 12039.

Hatta, M., Hatta, Y., Kim, J., Watanabe, S., Shinya, K., Nguyen, T., Lien, P., Le, Q. and Kawaoka, Y. (2007). Growth of H5N1 influenza A viruses in the upper respiratory tracts of mice. PLoS Pathogens **3**: 1374 – 1379.

He,Y., Li, J., Heck, S., Lustigman, S.and Jiang, S. (2006). Antigenic and immunogenic characterization of recombinant baculovirus-expressed Severe Acute Respiratory Syndrome Coronavirus spike protein: Implication for vaccine design. *Journal of Virology* **80**: 5757 – 5767.

Hennion, R. (2015). The preparation of chicken tracheal orgran cultures for virus isolation, propagation, and titration. Coronaviruses: Methods and protocols. *Methods in molecular biology* **1282**: Doi10.1007/978-1-4939-2438-7_5

Hennion, R. and Hill, G. (2015). The Preparation of Chicken Kidney Cell Cultures for Virus Propagation, p 57 - 62. *In* Maier HJ, Bickerton E, Britton P (ed), Coronaviruses: Methods and Protocols, vol 1282. Springer, Methods in Molecular Biology.

Heusipp, G., Grötzinger, C., Herold, J., Siddell, S. and Ziebuhr J. (1997). Identification and subcellular localization of a 41 kDa, polyprotein 1ab processing product in human coronavirus 229E-infected cells. *Journal of General Virology* **78**: 2789 – 2794.

Hodgson, T., Britton, P. and Cavanagh, D. (2006). Neither the RNA nor the proteins of open reading frames 3a and 3b of the coronavirus infectious bronchitis virus are essential for replication. *Journal of Virology* **80**: 296 – 305.

Hodgson, T., Casais, R., Dove, B., Britton, P. and Cavanagh, D. (2004). Recombinant infectious bronchitis coronavirus Beaudette with the spike protein gene of the pathogenic M41 strain remains attenuated but induces protective immunity. *Journal of Virology* **78**: 13804 – 13811.

Hoekstra, J. and Rispens, B. (1960). Infectieuze bronchitis bij pluimvee I. Laboratorium-experimenten met een sterkwerkende entstam (Infectious bronchitis in poultry. I. Laboratory experiments with a medium-virulent vaccine strain). *Tijdschrift voor Diergeneeskunde* **85**: 279 – 284.

Hofmann, H., Pyrc, K., van der Hoek, L., Geier, M., Berkhout, B. and Pohlmann, S. (2005). Human coronavirus NL63 employs the severe acute respiratory syndrome coronavirus receptor for cellular entry. *PNAS* **102**: 7988–93.

Hogue, B. and Machamer, C. (2008). Coronavirus Structural Proteins and Assembly. In: Perlman, SG., editor. The Nidoviruses. American Society for Microbiology Press 179 – 200.

Hsue, B. and Masters, P. (1997). A bulged stem-loop structure in the 3' untranslated region of the genome of the coronavirus mouse hepatitis virus is essential for replication. *Journal of virology* **71**: 7567 – 7578.

Huo, Y., Huanga, Q., Wu, M., Lin, S., Zhu, F., Zhang, X., Huang, Y., Yang, S. and Xu, C. (2016). Attenuation mechanism of virulent infectious bronchitis virus strain with QX genotype by continuous passage in chicken embryos. *Vaccine* **34**: 83 – 89.

International Committee for the Taxonomy of Viruses, (ICTV; 2018). https://talk.ictvonline.org/ictv-reports/ictv_9th_report/positive-sense-rna-viruses-2011/w/posrna_viruses/219/nidovirales. Viewed 19th June 2019.

Ignjatovic, J. and Galli, L. (1994). The S1 glycoprotein but not the N or M proteins of avian infectious bronchitis virus induces protection in vaccinated chickens. *Archives of Virology* **138**: 117 – 134.

Ignjatovic, J. and Sapats, S. (2005). Identification of previously unknown antigenic epitopes on the S and N proteins of avian infectious bronchitis virus. *Archives of Virology* **150**:1813-1831.

Ivanov, K., Hertzig, T., Rozanov, M., Bayer, S., Thiel, V. and Gorbalenya, A. (2004). Major genetic marker of nidoviruses encodes a replicative endoribonuclease. *Proceedings of National Academy of Sciences* **101**: 12694 – 12699.

Jackwood, M., Hilt, D., Callison, S., Lee, C., Plaza, H. and Wade, E. (2001). Spike glycoprotein cleavage recognition site analysis of infectious bronchitis virus. *Avian Diseases* **45**: 366 – 72.

Jackwood, M., Jordan, B., Roh, H., Hilt, D. and Williams, S. (2015). Evaluating protection against infectious bronchitis virus by clinical signs, ciliostasis, challenge virus detection, and histopathology. *Avian Diseases* **59**: 368 – 374.

Jackwood, M., Yousef, N. and Hilt, D. (1997). Further development and use of a molecular serotype identification test for infectious bronchitis virus. *Avian Diseases* **41**: 105 – 110.

Jeffers, S., Hemmila, E. and Holmes, K. (2006). Human coronavirus 229E can use CD209L (L-SIGN) to enter cells. *Advances in Experimental Medicine and Biology* **581**: 265 – 269.

Jeffers, S., Tusell, S., Gillim-Ross, L., Hemmila, E., Achenbach, J., Babcock, G., Thomas, W., Thackray, L., Young, M., Mason, R., Ambrosino, D., Wentworth, D., DeMartini, J. and Holmes, K. (2004). CD209L (L-SIGN) is a receptor for severe acute respiratory syndrome coronavirus. *PNAS* **101**: 15748 – 15753.

Jimenez-Guardeño, J., Regla-Nava, J., Nieto-Torres, J., DeDiego, M., Castaño-Rodriguez, C., Fernandez-Delgado, R., Perlman, S. and Enjuanes, L. (2015). Identification of the mechanisms causing reversion to virulence in an attenuated SARS-CoV for the design of a genetically stable vaccine. *PLoS Pathogens* **11**: e1005215.

Jin, X., Chen, Y., Sun, Y., Zeng, C., Wang, Y., Tao, J., Wu, A., Yu, X., Zhang, Z., Tian, J. and Guo, D. (2013). Characterization of the guanine-N7 methyltransferase activity of coronavirus nsp14 on nucleotide GTP. *Virus Research* **176**: 45 – 52.

Jin, H., Lu, B., Zhou, H., Ma, C., Zhao, J., Yang, C., Kemble, G. and Greenberg, H. (2003). Multiple amino acid residues confer temperature sensitivity to human influenza virus vaccine strains (FluMist) derived from cold-adapted A/AnnArbor/6/60.*Virology* **306**: 18 – 24.

Johnson, M., Pooley, C., Ignjatovic, J. and Tyack, S. (2003). A recombinant fowl adenovirus expressing the S1 gene of infectious bronchitis virus protects against challenge with infectious bronchitis virus. *Vaccine* **21**: 2730–2736.

Jones, R. and Jordan, F. (1970) The exposure of day-old chicks to infectious bronchitis and subsequent development of the oviduct. *Veterinary Record* **87**: 504 – 505.

Jones, R. and Jordan, F. (1971) The site of replication of infectious bronchitis virus in the oviducts of experimentally infected hens. *Veterinary Record* **89**: 317 – 318.

Jordan, B. (2017). Vaccination against infectious bronchitis virus: A continuous challenge*. Veterinary Microbiology* **206**: 137 – 143.

Joseph, J., Saikatendu, K., Subramanian, V., Neuman, B., Brooun, A., Griffith, M., Moy, K., Yadav, M., Velasquez, J., Buchmeier, M., Stevens, R. and Kuhn, P. (2006). Crystal structure of nonstructural protein 10 from the severe acute respiratory syndrome coronavirus reveals a novel fold with two zinc-binding motifs. *Journal of Virology* **80**: 7894 – 7901.

Juhasz, K., Whitehead, S., Boulanger, C., Firestone, C., Collins, P. and Murphy B. (1999). The two amino acid substitutions in the L protein of cpts530/1009, a live-attenuated respiratory syncytial virus candidate vaccine, are independent temperature-sensitive and attenuation mutations. *Vaccine* **17**:1416 – 1424.

Jones, R. (1974). Nephrosis in laying chickens caused by Massachusetts type Infectious Bronchitis Virus. *The Veterinary Record* **5**: 319.

Kang, H., Bhardwaj, K., Li, Y., Palaninathan, S., Sacchettini, J., Guarino, L., Leibowitz, J. and Cheng Kao, C., (2007). Biochemical and genetic analyses of murine hepatitis virus Nsp 15 endoribonuclease. *Journal of Virology* **81**: 13587 – 13597.

Kant, A., Koch, G., van Roozelaar, D., Kusters, J., Poelwijk, F. and van der Zeijst, B. (1992). Location of antigenic sites defined by neutralising monoclonal antibodies on the S1 avian infectious bronchitis virus glycopolypeptide. *Journal General Virology* **73**: 591 – 596.

Keane, S. and Giedroc, D. (2013). Solution structure of mouse hepatitis virus (MHV) nsp3a and determinants of the interaction with MHV nucleocapsid (N) protein. *Journal of Virology* **87**: 3502 – 3515.

Keep, S. (2013). Modifications of the IBV S glycoprotein. *MSc Thesis* Liverpool John Moores University.

Keep, S., Bickerton, E., Armesto, M. and Britton, P. (2018). The ADRP domain from a virulent strain of infectious bronchitis virus is not sufficient to confer a pathogenic phenotype to the attenuated Beaudette strain. *Journal of General Virology* **99**: 1097 – 1102.

Keep, S., Bickerton, E. and Britton, P. (2015). Transient dominant selection for the modification and generation of recombinant infectious bronchitis virus. Coronaviruses: Methods and Protocols. *Methods in Molecular Biology*. Springer. 1282: 115 – 133.

Kindler, E., Gil-Cruz, C., Spanier, J., Li, Y., Wilhelm, J., Rabouw, H., Züst, R., Hwang, M., V'kovski, P., Hanspeter Stalder, H., Marti, S., Habjan, M., Cervantes-Barragan, L., Elliot, R., Karl, N., Gaughan, C., van Kuppeveld, F., Silverman, R., Keller, M., Ludewig, B., Bergmann, C., Ziebuhr, J., Weiss, S., Kalinke, U. and Thiel, V. (2017). Early endonuclease-mediated evasion of RNA sensing ensures efficient coronavirus replication. *PLoS Pathogens* **13**: e1006195.

Kint, J., Dickhout, A., Kutter, J., Maier, H., Britton, P., Koumans, J., Pijlman, G., Fros, J., Wiegertjes, G. and Forlenza, M. (2015). Infectious Bronchitis Coronavirus Inhibits STAT1 Signaling and Requires Accessory Proteins for Resistance to Type I Interferon Activity. *Journal of Virology* **89**: 12047 – 57.

Kint, J., Langereis, M., Maier, H., Britton, P. van Kuppeveld, F., Koumans, J., Wiegertjes, G. and Forlenza, M. (2016). Infectious Bronchitis Coronavirus Limits Interferon Production by Inducing a Host Shutoff That Requires Accessory Protein 5b. *Journal of Virology* **90**: 7519 – 7528.

Kirchdoerfer, R., Cottrell, C., Wang, N., Pallesen, J., Yassine, H., Turner, H., Corbett, K., Graham, B., McLellan, J. and Ward, A. (2016). Pre-fusion structure of a human coronavirus spike protein. *Nature* **531**: 118 – 121.

Klumperman, J., Locker, J., Meijer, A., Horzinek, M., Geuze, H. and Rottier, P. (1994). Coronavirus M proteins accumulate in the Golgi complex beyond the site of virion budding. Journal of *Virology* **68:** 6523 – 6534.

Knoops, K., Kikkert, M., Worm, S., Zevenhoven-Dobbe, J., Van der Mer, Y., Kostr, A., Mommaas, A. and Snijder, E. (2008). SARS-coronavirus replication is supported by a reticulovesicular network of modified endoplasmic reticulum. *PLoS Biology* **6**: e226.

Koch, G., Hartog, L., Kant, A. and van Roozelaar, D. (1990). Antigenic domains of the peplomer protein of avian infectious bronchitis virus: correlation with biological function. *Journal of General Virology* **71**: 1929 – 1935.

Koetzner, C., Parker, M., Richard, C., Sturman, L. and Masters, P. (1992). Repair and mutagenesis of the genome of a deletion mutant of the coronavirus mouse hepatitis virus by targeted RNA recombination. *Journal of Virology* **66**: 1841 – 1848.

Krijnse-Locker J., Ericsson, M., Rottier, P. and Griffiths, G. (1994). Characterization of the budding compartment of mouse hepatitis virus: evidence that transport from the RER to the Golgi complex requires only one vesicular transport step. *Journal of Cell Biology* **124**: 55 – 70.

Kubo, H., Yamada, Y. and Taguchi, F. (1994). Localization of neutralizing epitopes and the receptor-binding site within the amino-terminal 330 amino acids of the murine coronavirus spike protein. *Journal of Virology* **68**: 5403 – 5410.

Kuo, L., Godeke, G., Raamsmanm M., Masters, P. and Rottier, P. (2000). Retargeting of coronavirus by substitution of the spike glycoprotein ectodomain: crossing the host cell species barrier. *Journal of Virology* **74**: 1393 – 1406.

Kuo, L. and Masters, P. (2002). Genetic evidence for a structural interaction between the carboxy termini of the membrane and nucleocapsid proteins of mouse hepatitis virus. *Journal of Virology* **76**: 4987 – 4999.

Kuri, T., Eriksson, K., Putics, A., Züst, R., Snijder, E. Davidson, A., Siddell, S., Thiel, V., Ziebuhr, J. and Weber, F. (2011). The ADPribose- 1''-monophosphatase domains of severe acute respiratory syndrome coronavirus and human coronavirus 229E mediate resistance to antiviral interferon responses. *Journal of General Virology* **92**: 1899 – 1905.

Kusters, J., Niesters, H., Lenstra, J., Horzinek, M. and van der Zeijst, B. (1989). Phylogeny of antigenic variants of avain coronavirus IBV. *Virology* **169**: 217 – 221.

Ladman, B., Loupos, A. and Gelb, J. (2006). Infectious bronchitis virus S1 gene sequence comparison is a better predictor of challenge of immunity in chickens than serotyping by virus neutralization. *Avian Pathology* **35**: 127 – 133.

Laconi, A., van Beurden, S., Berends, A., Kramer-Kuhl, A., Jansen, C., Spekreijse, D., Chenard, G., Phillip, H., Mundt, E., Rotteir, P. and Verheije, H. (2018). Deletion of accessory genes 3a, 3b, 5a or 5b from avian coronavirus infectious bronchitis virus induces an attenuated phenotype both *in vitro* and *in vivo*. *Journal of General Virology* **99**: 1381 – 1390.

Lambrechts, C., Pensaert, M. and Ducatelle, R. (1993). Challenge experiments to evaluate cross-protection induced at the trachea and kidney level by vaccine strains and Belgian nephropathogenic isolates of avian infectious bronchitis virus. *Avian Pathology* **22**: 577 – 590.

Lee, H., Shieh, A., Gorbalenya, A., Koonin, E., Monica, N., Tuler, J., Bagdzhadzhyan, A. and Lai, M. (1991). The complete sequence (22 kilobases) of murine coronavirus gene 1 encoding the putative proteases and RNA polymerase. *Virology* **180**: 567–582.

Lei, J., Kusov, Y. and Hilgenfeld, R. (2018). Nsp3 of coronaviruses: structures and functions of a large multi-domain protein. *Antiviral Research* **149**: 58 – 74.

Lei, Y., Moore, C., Liesman, R., O'Connor, B., Bergstralh, D., Chen, Z., Pickles, R. and Ting, J. (2009). MAVS-mediated apoptosis and its inhibition by viral proteins. *PLoS One* **4**:e5466.

Li, W., Moore, M., Vasilieva, N., Sui, J., Wong, S., Berne, M., Somasundaran, M., Sullivan, J., Luzuriaga, K., Greenough, T., Choe, H. and Farzan, M. (2003). Angiotensin-converting enzyme 2 is a functional receptor for the SARS coronavirus. *Nature* **426** : 450–54.

Li, W., Zhang, C., Sui, J., Kuhn, J., Moore, M., Luo, S., Wong, S., Huang, I., Xu, K., Vasilieva, N., Murakami, A., He, Y., Marasco, W., Guan, Y., Choe, A. and

Farzan, M. (2005). Receptor and viral determinants of SARS-coronavirus adaptation to human ACE2. *The EMBO Journal* **24**: 1634 – 1643.

Lim, T.H., Kim, M.S., Jang, J.H., Lee, D.H., Park, J.K., Youn, H.N., Lee, J.B., Park, S.Y., Choi, I.S. and Song, C.S. (2012). Live attenuated nephropathogenic infectious bronchitis virus vaccine provides broad cross protection against new variant strains. Poult Sci **91**:89 – 9.

Lim, K and Liu, D. (2001). The missing link in coronavirus assembly: retention of the avian coronavirus infectious bronchitis virus envelope protein in the pre- Golgi compartments and physical interaction between the envelope and membrane proteins. *Journal of Biology and Chemistry* **276**: 17515 – 23.

Liu, C., Tang, J., Ma, Y., Liang, X., Yang, Y., Peng, G., Qi, Q., Jiang, S., Li, J., Du, L. and Li, F. (2015). Receptor usage and cell entry of porcine epidemic diarrhea coronavirus. *Journal of Virology* **89**: 6121 – 6125.

Liu, Q., Johnson, R. and Leibowitz, J. (2001). Secondary structural elements within the 3' untranslated region of mouse hepatitis virus strain JHM genomic RNA. *Journal of virology* **75**: 12105 – 12113.

Liu, S. and Kong, X. (2004). A new genotype of nephropathogenic infectious bronchitis virus circulating in vaccinated and nonvaccinated flocks in China *Avian Pathology* **33**: 321–327.

Liu, S., Zhang, Q., Chen, J., Han, X., Liu, X., Feng, L., Shao, Y., Rong, J., Kong, X. and Tong, G. (2006). Genetic diversity of avian infectious bronchitis coronavirus strains isolated in China between 1995 and 2004. *Archives of Virology* **151**: 1133 – 1148.

Liu, S., Zhang, X., Wang, Y., Li, C., Liu, Q., Han, Z., Zhang, Q., Kong, X. and Tong, G. (2009). Evaluation of the protection conferred by commercial vaccines and attenuated heterologous isolates in China against the CK/CH/LDL/97I strain of infectious bronchitis coronavirus. *The Veterinary Journal* **179**: 130 – 136.

Liu, S., Zhang, Q., Chen, J., Han, X., Liu, X., Feng, L., Shao, Y., Rong, J., Kong, X. and Tong, G. (2006). Genetic diversity of avian infectious bronchitis coronavirus strains isolated in China between 1995 and 2004. *Archives of Virology* **151**: 1133 – 1148.

Lugari, A., Betzi, S., Decroly, E., Bonnaud, E., Hermant, A., Guillemot, J., Debarnot, C., Borg, J., Bouvet, M., Canard, B., Morelli, X. and Lecine, P. (2010) Molecular mapping of the RNA Cap 2′-O-methyltransferase activation interface between severe acute respiratory syndrome coronavirus nsp10 and nsp16. *Journal of Biology and Chemistry* **285**: 33230 – 33241.

Luo, Z. and Weiss, S. (1998). Roles in cell-to-cell fusion of two conserved hydrophobic regions in the murine coronavirus spike protein. *Virology* **244**: 483 – 494.

Ma, Y., Wub, L., Shawc, N., Gaoa, Y., Wangd, J., Sunc, Y., Loua, Z., Yana, L., Zhang, R. and Raoa, Z. (2015). Structural basis and functional analysis of the SARS coronavirus nsp14–nsp10 complex. *Proceedings of the National Academy of Science USA* **112**: 9436 – 9441.

Madu, I., Roth., S., Belouzard, S. and Whittaker, G. (2009). Characterization of a highly conserved domain within the severe acute respiratory syndrome coronavirus spike protein S2 domain with characteristics of a viral fusion peptide. *Journal of Virology* **83**: 7411 – 7421.

Maier, H., Hawes, P., Cottam, E., Mantell, J., Verkade, P., Monaghan, P., Wileman, T. and Britton, P. (2013). Infectious Bronchitis Virus Generates Spherules from Zippered Endoplasmic Reticulum Membranes. *mBio* **5**: e00801-13.

Maier, H., Neuman, B. Bickerton, E., Keep, S., Alrashedi, H., Hall, R. and Britton, P. (2016). Extensive coronavirus-induced membrane rearrangements are not a determinant of pathogenicity. *Scientific Reports* **6**: 27126.

Mihindukulasuriya, K., St. Leger, W., Nordhausen, R. and Wang, D. (2008). Identification of a novel coronavirus from a beluga whale by using a panviral microarray. *Journal Virology* **82**: 5084 – 5088.

Makadiya, N., Brownlie, R., van den Hurk, J., Berube, N., Allan, B., Gerdts, V. and Zakhartchouk, A. (2016). S1 domain of the porcine epidemic diarrhea virus spike protein as a vaccine antigen. *Virology Journal* DOI 10.1186/s12985-016-0512-8.

Massin, P., Kuntz-Simon, G., Barbezange C., Deblanc, C., Oger, A., Marquet-Blouin, E., Bougeard, S., van der Werf, S and Jestin, V. (2010). Temperature sensitivity on growth and/or replication of H1N1, H1N2 and H3N2 influenza A viruses isolated from pigs and birds in mammalian cells. *Veterinary Microbiology* **142**: 232 – 241.

Maassab, H. (1967). Adaptation and growth characteristics of influenza virus at 25°C. *Nature* **213**: 612 – 614.

Maassab, H. (1968). Plaque formation of influenza virus at 25°C. Nature 219: 645 – 646.

Maassab, H. and Bryant, M. (1999). The development of live attenuated cold-adapted influenza virus vaccine for humans. *Reviews in Medical Virology* **9**: 237 – 244.

Madu, I., Chu, V., Lee, H., Regan, A., Bauman, B. and Whittaker, G. (2007). Heparan sulfate is a selective attachment factor for the avian coronavirus infectious bronchitis virus Beaudette. *Avian Diseases* **51**: 45 – 51.

Matthijs, M., van Eck, J., Landman, W., and Stegeman, J. (2003). Ability of Massachusetts-type infectious bronchitis virus to increase colibacillosis susceptibility in commercial broilers: a comparison between vaccine and virulent field virus. *Avian Pathol*ogy **32**: 473 – 481.

Matthijs, M.G., Ariaans, M.P., Dwars, R.M., van Eck, J.H., Bouma, A., Stegeman, A. and Vervelde L. (2009). Course of infection and immune responses in the respiratory tract of IBV infected broilers after superinfection with E. coli. *Veterinary Immunology and Immunopathology* **127:**77-84.

McBride, R. Van Zyl, M. and Fielding, B. (2014). The coronavirus nucleocapsid is a multifunctional protein. *Viruses* **6**: 2991 – 3018.

Menachery, V., Debbinka, K. and Baric, R. (2014). Coronavirus non-structural protein 16: Evasion, attenuation, and possible treatments. *Virus Research* **19**: 191 – 199.

Menachery, V., Gralinski, L., Mitchell, H., Deinnon, K., Leist, S., Yount, B., McAnarney, E., Graham, R., Waters, K. and Baric, R. (2018). Combination attenuation offers strategy for live attenuated coronavirus vaccines. *Journal of Virology* **92**: e00710 – 18.

Meir, R., Krispel, S., Simanov, L., Eliahu, D., Maharat, O. and Pitcovski, J. (2012). Immune Responses to mucosal vaccination by the Recombinant S1 and N Proteins of Infectious Bronchitis Virus. *Viral Immunology* **25**: 55 – 62.

Meulemans, G., Carlier, M., Gonze, M., Petit, P and Vanderbroeck, M. (1987). Incidence, characterization and prophylaxis of nephropathogenic avian infectious bronchitis viruses. Veterinary Record **120**: 205 – 206.

Mielech, A., Deng, X., Chen, Y., Kindler, E., Wheeler, D., Mesecar, A., Thiel, V., Perlman, S. and Baker S. (2015). Murine coronavirus ubiquitin-like domain is important for papain-like protease stability and viral pathogenesis. *Journal of Virology* **89**: 4907 – 4917.

Minskaia, E., Hertzig, T., Gorbalenya, A., Campanacci, V., Cambillau, C., Canard, B. and Ziebuhr, J. (2006). Discovery of an RNA virus 3' → 5'exoribonuclease that is critically involved in coronavirus RNA synthesis. *Proceedings of the National Academy of Science USA* **103**: 5108 – 5113.

Miura, T., Travanty, E., Oko, L., Bielefeldt-Ohmann, H., Weiss, S., Beauchemin, N. and Holmes, K. (2008). The spike glycoprotein of murine coronavirus MHV-JHM mediates receptor independent infection and spread in the central nervous systems of Ceacam1a-/- Mice. *Journal of Virology* **82**: 755 – 763.

Mockett, A., Cavanagh, D. and Brown T. (1984). Monoclonal Antibodies to the S1 Spike and Membrane Proteins of Avian Infectious Bronchitis Coronavirus Strain Massachusetts M41. *Journal of General Virology* **65**: 2281 – 2286.

Molenkamp, R. and Spaan, W. (1997). Identification of a specific interaction between the coronavirus mouse hepatitis virus A59 nucleocapsid protein and packaging signal. *Virology* **239**: 78 – 86.

Montagnon, B., Fanget, B. and Nicolas, A. (1981). The large-scale cultivation of Vero cells in microcarrier culture for virus vaccine production. Preliminary results for killed poliovirus vaccine. *Development in Biological Standardisation* **47**: 55 – 64.

Moore, K., Jackwood, M. and Hilt, D. (1997). Identification of amino acids involved in a serotype and neutralization specific epitope within the s1 subunit of avian infectious bronchitis virus. *Archives of Virology* **142**: 2249 – 2256.

Narayanan, K., Maeda, A., Maeda, J. and Makino, S. (2000). Characterization of the coronavirus M protein and nucleocapsid interaction in infected cells. *Journal of Virology* **74**: 8127 – 8134.

Neuman, B., Adair, B., Yosjioka, C., Quispe, J., Orca, G., Kuhn P., Milliagan R., Yeagerm M. and Buchmeier, M. (2006). Supramolecular architecture of Severe

Acute Respiratory Syndrome Coronavirus revealed by Electron Cryo-microscopy. *Journal of Virology* **80**: 7918 – 7928.

Neuman, B., Joseph, J., Saikatendu, K., Serrano, P., Chatterjee, A., Johnson, M., Liao, L., Klaus, J., Yates, J., Wuthrich, K., Stevens, R., Buchmeier, M. and Kuhn, P. (2008). Proteomics analysis unravels the functional repertoire of coronavirus nonstructural protein 3. *Journal of virology* **82**: 5279 – 5294.

Neuman, B., Kiss, G., Kunding, A., Bhella, D., Baksh, M., Connelly, S., Droese, B., Klaus, J., Makino, S., Sawicki, S., Siddell, S., Stamou, D., Wilson, I., Kuhn, P. and Buchmeier, M. (2011). A structural analysis of M protein in coronavirus assembly and morphology. *Journal of structural biology* **174**: 11 – 22.

Niesters, H., Lenstra, J., Spaan, W., Zijderveld, A., Bleumink-Pluym, N., Hong, F., van Scharrenburg, G., Horzinek, M. and van der Zeijst, B. (1986). The peplomer protein sequence of the M41 strain of coronavirus IBV and its comparison with Beaudette strains. *Virus research* **5**: 253 – 26.

Nogales, A., Rodriguez L., Chauché, C., Huang K., Reilly, E.,Topham D., Murcia, P., Parrish, C. and Martínez-Sobrido, L. (2017).Temperature sensitive live-attenuated canine influenza virus H3N8 vaccine. *Journal of Virology* **91**:e02211-16.

Oade, M., Keep, S., Freimanis, G., Orton, R., Britton, P., Hammond, J. and Bickerton, E. (2019). Attenuation of infectious bronchitis virus in eggs results in different patterns of genomic variation across multiple replicates. *Journal of Virology* DOI: 10.1128/JVI.00492-19

Opstelten, D., Raamsman, M., Wolfs, K., Horzinek, M. and Rottier, P. (1995). Envelope glycoprotein interactions in coronavirus assembly. *Journal of Cell Biology* **131**: 339 – 349.

Ou, X., Zheng, W., Shan, Y., Mu, Z., Dominguez, S., Holmes K. and Qian, Z. (2016). Identification of the fusion peptide-containing region in betacoronavirus spike glycoproteins. *Journal of Virology* **90**: 5586 – 5600.

Pardo, J., Bosque, A., Brehm, R., Wallich, R., Naval, J., Mullbacher, A., Anel, A. and Simon, M. (2004). Apoptotic pathways are selectively activated by granzyme A and/or granzyme B in CTL mediated target cell lysis. *The Journal of Cell Biology* **167**: 457 – 468.

Peacock, T., Reddy, K., James, J., Adamiak, B., Barclay, W., Shelton, H. and Iqbal, M. (2016). Antigenic mapping of an H9N2 avian influenza virus reveals two discrete antigenic sites and a novel mechanism of immune escape. *Scientific Reports* doi:10.1038/srep18745

Pei, J., Briles, E. and Collisson, E. (2003). Memory T cells protect chicks from acute infectious bronchitis virus infection. *Virology* **306**: 376 – 384.

Pei, J., Sekellick, M., Marcus, P., Choi, I. and Collisson, E. (2004). Chicken Interferon Type I inhibits Infectious Bronchitis Virus replication and associated respiratory illness. *Journal of Interferon & Cytokine* **21**: 1071 – 1077.

Pensaert, M., Callebaut, P. and Vergote, J. (1986). Isolation of a porcine respiratory, non-enteric coronavirus related to transmissible gastroenteritis. *Veterinary Quarterly* **8**: 257 – 261.

Perlman, S., Gallagher, T. and Snijder, E. (2008). Nidoviruses, Washington DC, ASM Press.

Pharmacopeia E. (2010). Avian infectious bronchitis vaccine (live). European Directorate for the Quality of Medicines and HealthCare (EDQM), Council of Europe, Strasbourg, France.

Phillips, J., Chua, M., Lavi, E. and Weiss, S. (1999). Pathogenesis of Chimeric MHV4/MHV-A59 Recombinant Viruses: the Murine Coronavirus Spike Protein Is a Major Determinant of Neurovirulence. *Journal of Virology* **73**: 7752 – 7760.

Piotrowski, Y., Hansen, G., Boomaars-van der Zanden, A., Snijder, E., Gorbalenya, A. and Hilgenfeld, R. (2009). Crystal structures of the X-domains of a group-1 and a group-3 coronavirus reveal that ADP-ribose-binding may not be a conserved property. *Protein Science* **18**: 6–16.

Promkuntod N, Wickramasinghe IN, de Vrieze G, Grone A, Verheije MH. 2013. Contributions of the S2 spike ectodomain to attachment and host range of infectious bronchitis virus. Virus Research **177:**127-137.

Promkuntod, N., van Eijndhoven, R., de Vrieze, G., Gröne A. and Verheije, M. (2014). Mapping of the receptor-binding domain and amino acids critical for attachment in the spike protein of avian coronavirus Infectious Bronchitis Virus. *Virology* **448**: 26 – 32.

Putics, A., Filipowicz, W., Hall, J., Gorbalenya, A. and Ziebuhr, J. (2005). ADPribose-1"-monophosphatase: a conserved coronavirus enzyme that is dispensable for viral replication in tissue culture. *Journal of Virology* **79**: 12721 – 12731.

Raj, V., Mou, H., Smits, S., Dekkers, D., Müller, M,. Dijkman, R., Muth, D., Demmers, J., Zaki, A., Fouchier, R., Thiel, V., Drosten, C., Rottier, P., Osterhaus, A., Bosch, B. and Haagmans, B. (2013). Dipeptidyl peptidase 4 is a functional receptor for the emerging human coronavirus-EMC. *Nature* **495**: 251–54.

Rasschaert, D. Duarte, M. and Laude, H. (1990). Porcine respiratory coronavirus differs from transmissible gastroenteritis virus by a few genomic deletions. *Journal of General Virology* **71**: 2599 – 2607.

Ray, R., Galinski, M., Heminway, B., Meyer, K., Newman, F. and Belse, R. (1996). Temperature-sensitive phenotype of the human parainfluenza virus type 3 candidate vaccine strain (cp45) correlates with a defect in the L gene. *Journal of Virology* **70**: 580 – 584.

Ray, R., Meyer, K., Newman, F. and Belshe, R. (1995). Characterization of a live, attenuated human parainfluenza type 3 virus candidate vaccine strain. *Journal of Virology* **69**: 1959 – 1963.

Reed, L. and Muench, H. (1938). A simple method of estimating fifty percent endpoints. *American Journal of Hygiene* **27**: 493 – 497.

Reddy, V., Trus, I., Desmarets, M., Li, Y., Theuns, S. and Nauwynck, H. (2016). Productive replication of nephropathogenic infectious bronchitis virus in peripheral blood monocytic cells, a strategy for viral dissemination and kidney infection in chickens. *Veterinary Research* **47**: 70

Regla-Nava, J., Nieto-Torres, J., Jimenez-Guardeño, J., Fernandez-Delgado, R., Fett, C., Castaño-Rodríguez, C., Perlman, S., Enjuanes, and DeDiegoa, M. (2015). SARS coronaviruses with mutations in E protein are attenuated and promising vaccine candidates. *Journal of Virology* **89**: 3870 – 3887.

Rota, P., Oberste, S., Monroe, S., Nix, A., Campagnoli, R., Icenogle, J., Peñaranda, S., Bankamp, B., Maher, K., Chen, M., Tong, S., Tamin, A., Lowe, L., Frace, M., DeRisi, J., Chen, Q., Wang, D., Erdman, D., Peret, T., Burns, C., Ksiazek, T., Rollin, P., Sanchez, A., Liffick, S., Holloway, B., Limor, J., McCaustland, K., Olsen-Rasmussen, M., Fouchier, R., Gunther, S., Osterhaus, A., Drosten, C., Pallansch, M., Anderson, L. and Bellini, W. (2003). Characterisation of a novel coronavirus associated with severe acute respiratory syndrome. *Science* **300**: 1394 – 1399.

Rottier, P. (1995). The coronavirus membrane protein. The Coronaviridae. *New York, Plenum Press.*

Ruch, T. and Machamer, C. (2011). The hydrophobic domain of infectious bronchitis virus E protein alters the host secretory pathway and is important for release of infectious virus. *Journal of Virology* **85**: 675 – 685.

Ruch, T. and Machamer, C. (2012). The coronavirus E protein: assembly and beyond. *Viruses* **4**: 363 – 82.

Sainz, B., Rausch, J., Gallaher, W., Garry, R. and Wimley, W. (2005). The aromatic domain of the coronavirus class I viral fusion protein induces membrane permeabilization: putative role during viral entry. Biochemistry 44: 947 – 958.

Saikatendu, K., Joseph, J., Subramanian, V., Clayton, T., Griffith, M., Moy, K., Velasquez, J., Neuman, B., Buchmeier, M., Stevens, R. and Kuhn, P. (2005). Structural basis of severe acute respiratory syndrome coronavirus ADP-ribose-1''-phosphate dephosphorylation by a conserved domain of nsP3. *Structure* **13**: 1665 – 1675.

Sanchez, C., Izeta, A., Sanchez-Morgado, J., Alonso, S., Sola, I., Balasch, M., Plana-Duran, J. and Enjuanes, L. (1999). Target recombination demonstrates that the spike gene of transmissible gastroenteritis coronavirus is a determinant of its enteric tropism and virulence. *Journal of Virology* **73**: 7607 – 7618.

Sawicki, S. and Sawicki, D. (1995). Coronaviruses use discontinuous extension for synthesis of subgenome-length negative strands. *Advances in Experimental Medicine and Biology* **380**: 499 – 506.

Sawicki, S., Sawicki, D. and Siddell, S. (2007). A contemporary view of coronavirus transcription. *Journal of Virology* **81**: 20 – 9.

Schalk, A. and Hawn, M. (1931). An apparently new respiratory disease of baby chicks. Journal of American Veterinary Medical Association. **78**: 413 – 422.

Schultze, B., Cavanagh, D. and Herrler, G. (1992). Neuraminidase treatment of avian infectious bronchitis coronavirus reveals a hemagglutinating activity that is dependent on sialic acid-containing receptors on erythrocytes. *Virology* **189**: 792–794.

Schultze, B., Krempl, C., Ballesteros, M., Shaw, L., Schauer, R., Enjuanes, L. and Herrler, G. (1996). Transmissible gastroenteritis coronavirus, but not the related porcine respiratory coronavirus, has a sialic acid (N-glycolylneuraminic acid) binding activity. *Journal of Virology* **70**: 5634 – 5637.

Scobey, T., Yount, B., Sims, A., Donaldson, E., Agnihothram, S., Menachery,V., Graham, R., Swanstrom, J., Bove, P., Kim, J., Grego, S., Randell, S. and Baric, R. (2013). Reverse genetics with a full-length infectious cDNA of the Middle East respiratory syndrome coronavirus. *Proceedings of National Academy of Sciences of United States of America* **110**: 16157 – 16162.

Seo, S. and Collisson, E.W. (1997). Specific cytotoxic T lymphocytes are involved in *in vivo* clearance of infectious bronchitis virus. *Journal of Virology* **71**:5173-5177.

Seo, S., Pei, J., Briles, W., Dzielawa, J. and Collisson, E. (2000). Adoptive transfer of infectious bronchitis virus primed $\alpha\beta$ T cells bearing CD8 antigen protects chicks from acute infection. *Virology* **269**: 183 – 189.

Seo. S., Wang, L., Smith, R. and Collisson, E. (1997). The Carboxyl-Terminal 120-Residue Polypeptide of Infectious Bronchitis Virus Nucleocapsid Induces Cytotoxic T Lymphocytes and Protects Chickens from Acute Infection. *Journal of Virology* **71**: 7889 – 7894.

Senanayake, S. and Brian, D. (1999). Translation from the 59 untranslated region (UTR) of mRNA 1 is repressed, but that from the 59 UTR of mRNA 7 Is stimulated in coronavirus-infected cells. *Journal of Virology* **73**: 8003 – 8009.

Sevajol, M., Subissi, L., Decroly, E., Canard, B. and Imbert, I. (2014).Insights into RNA synthesis, capping, and proofreading mechanisms of SARS-coronavirus. *Virus Research* **194**: 90 – 99.

Shang, J., Zheng, Y., Yang, Y., Liu, C., Geng, Q., Luo, C., Zhang, W. and Li, F. (2018). Cryo-EM structure of infectious bronchitis coronavirus spike protein reveals structural and functional evolution of coronavirus spike proteins. *PLoS Pathogens* **14**: e1007009.

Shi, S., Schiller, J., Kanjanahaluethai, A., Baker, S., Oh, J. and Lai, M. (1999). Colocalization and membrane association of murine hepatitis virus gene 1 products and De novo-synthesized viral RNA in infected cells. *Journal of Virology* **73**: 5957 – 5969.

Shirvani, E., Paldurai, A., Manoharan, V., Varghese, B. and & Samal, S. (2018). A Recombinant Newcastle Disease Virus (NDV) expressing S protein of Infectious Bronchitis Virus (IBV) protects chickens against IBV and NDV. *Scientific Reports* DOI:10.1038/s41598-018-30356-2

Shang, J., Zheng, Y., Yang, Y., Liu, C., Geng, Q., Luo, C., Zhang, W. and Fang, Li. (2018). Cryo-EM structure of infectious bronchitis coronavirus spike protein reveals structural and functional evolution of coronavirus spike proteins. *PLoS Pathogens* **14**: e1007009.

Shang, J., Zheng, Y., Yang, Y., Liu, C., Geng, Q., Tai, W., Du, L., Zhou, Y., Zhangm W. and Li, F. (2018B). Cryo-electron microscopy structure of porcine deltacoronavirus spike protein in the prefusion state. *Journal of Virology* **92**: e01556-17.

Shulla, A. and Gallagherm T. (2009). Role of spike protein endodomains in regulating coronavirus entry. *The Journal of Biological Chemistry* **284**: 32725 – 32734.

Smith, H., Cook, J. and Parsell, Z. (1985). The experimental infection of chickens with mixtures of infectious bronchitis virus and Escherichia coli. *Journal of General Virology* **66**: 777 – 786.

Sola, I., Almazán,F., Zúñiga, S. and Enjuanes, L. (2015). Continuous and discontinuous RNA synthesis in coronaviruses. *Annual Reviews in Virology* **2**: 265 – 288.

Sola, I., Mateos-Gomez, P., Almazan, F., Zuñiga, S. and Enjuanes, L. (2011). RNA-RNA and RNA-protein interactions in coronavirus replication and transcription. *RNA Biology* **8**: 237 – 248.

Song, C., Lee, Y., Lee, C., Sung, H., Kim, J., Mo, I., Izumiya, Y., Jang, H. and Mikami, T. (1998). Induction of protective immunity in chickens vaccinated with infectious bronchitis virus S1 glycoprotein expressed by a recombinant baculovirus. *Journal of General Virology* **79**: 719 – 723.

Snijder, E., Bredenbeek, P., Dobbe, J., Thiel, V., Ziebuhr, J., Poon, L., Guan, Y., Rozanov, M., Spaan, W. and Gorbalenya, A. (2003). Unique and conserved features of genome and proteome of SARS-coronavirus, an early split-off from the coronavirus group 2 lineage. *Journal of Molecular Biology* **331**: 991 – 1004.

Sparks J., Donaldson, E., Lu, X., Baric, R. and Denison, M. (2008). A novel mutation in murine hepatitis virus nsp5, the viral 3C-like proteinase, causes temperature-sensitive defects in viral growth and protein processing. *Journal of Virology* **82**: 5999 – 6008.

Sperry, S., Kazi, L., Graham, R., Baric, R. and Weiss, S. (2005). Single-amino-acid substitutions in Open Reading Frame (ORF) 1b-nsp14 and ORF 2a proteins of the coronavirus Mouse Hepatitis Virus are attenuating in mice. *Journal of Virology* : 3391 – 3400.

Stevenson-Leggett, P. (2018). Investigation into Infectious Bronchitis Virus (IBV) spike glycoprotein glycosylation, pathogenicity and tropism. PhD thesis. *University of Liverpool.*

St-Jean, J., Desforges, M., Almazan, F., Jacomy, H. and Enjuanes. (2006). Recovery of a neurovirulent human coronavirus OC43 from an infectious cDNA clone. *Journal of Virology* **80:** 3670 – 3674.

Stobart, C., Lee, A., Lu, X. and Denison, M. (2012). Temperature-sensitive mutants and revertants in the coronavirus nonstructural protein 5 protease (3CLpro) define residues involved in long-distance communication and regulation of protease activity. *Journal of Virology* **86**: 4801– 4810.

Stohlman, S., Baric, R., Nelson, G., Soe, L., Welter, L., Deans, R. (1988). Specific interaction between coronavirus leader RNA and nucleocapsid protein. *Journal of virology* **62**: 4288 – 4295.

Su, D., Lou, Z., Sun, F., Zhai, Y., Yang, H., Zhang, R., Joachimiak, A., Zhang, X., Bartlam, M. and Rao, Z. (2006). Dodecamer structure of severe acute respiratory syndrome Coronavirus nonstructural protein nsp10. *Journal of Virology* **80**: 7902 – 7908.

Surjit, M., Liu, B., Kumar, P., Chow, V. and Lal, S. (2004). The nucleocapsid protein of the SARS coronavirus is capable of self-association through a C-terminal 209 amino acid interaction domain. *Biochemical and Biophysical Research Communications* **317**: 1030 – 1036.

Tan, T., Fang, S., Fan, H., Lescar, J. and Liu D. (2006). Amino acid residues critical for RNA-binding in the N-terminal domain of the nucleocapsid protein are essential determinants for the replication and infectivity of coronavirus in cultured cells. *Nucleic Acids Research* **34**: 4816–4825.

Tekes, G., Hofmann-Lehmann, R., Bank-Wolf, B., Maier, R., Thiel, H. and Thiel, V. (2010). Chimeric feline coronaviruses that encode type II spike protein on type I genetic background display accelerated viral growth and altered receptor usage. *Journal of Virology* **84**: 1326 – 1333.

Tekes, G., Hofmann-Lehmann, R., Stallkamp, I., Thiel, V. and Thiel, H. (2008). Genome organization and reverse genetic analysis of a type I feline coronavirus. *Journal of Virology* **82**: 1851 – 1859.

Tekes, G., Spies, D., Bank-Wolf, B., Thiel, V. and Thiel, H. (2012). A reverse genetics approach to study feline infectious peritonitis. *Journal of Virology* **86**: 6994 – 6998.

Tanga, X., Agnihothramb, S., 1, Jiaoa, Y., Stanhopea, J., Grahamb, R., Petersona, E., Avnira, Y., Tallaricoa, A., Sheehana, J., Zhua, Q., Baricb, R. and Marascoa, W. (2014). Identification of human neutralizing antibodies against MERS-CoV and their role in virus adaptive evolution. *PNAS* doi: 10.1073/pnas.1402074111

Terregino, C., Toffan, A., Beato, M., De Nardi, R., Vascellari, M., Meini, A., Ortali, G., Mancin, M. and Capua, I. (2008). Pathogenicity of a QX strain of infectious bronchitis virus in specific pathogen free and commercial broiler chickens, and evaluation of protection induced by a vaccination programme based on the Ma5 and 4/91 serotypes. Avian Pathology 37: 487 – 493.

Thiel, V., Herold, J., Schelle, B. and Siddell, S. (2001). Infectious RNA transcribed in vitro from a cDNA copy of the human coronavirus genome cloned in vaccinia virus. *Journal of General Virology* **82**: 1273 – 1281.

Tooze, J., Tooze, S. and Fuller, S. (1987). Sorting of progeny coronavirus from condensed secretory proteins at the exit from the trans-Golgi network of AtT20 cells. *The Journal of Cell Biology* **105**: 1215 – 1226.

Toro, H., Zhao, W., Breedlove, C., Zhang, Z., van Santen, V. and Yu, Q. (2014). Infectious bronchitis virus S2 expressed from recombinant virus confers braod protectection against challenge. *Avain Diseases* **58**: 83 – 89.

Tusell, S., Schittone, S. and Holmes, K. (2007).Mutational analysis of aminopeptidase N, a receptor for several group 1 coronaviruses, identifies key determinants of viral host range. *Journal of Virology* **81**: 1261 – 1273.

Tylor, S., Andonov, A., Cutts, T., Cao, J., Grudesky, E., Van Domselaar, G., Li, X. and He, R. (2009). The SR-rich motif in SARS-CoV nucleocapsid protein is important for virus replication. Canadian *Journal of Microbiology* **55**: 254 – 260.

Ulasli, M., Verheije, M., de Haan, C. and Reggiori, F. (2010). Qualitative and quantitative ultrastructural analysis of the membrane rearrangements induced by coronavirus. *Cell Microbiology* **12**: 844 – 861.

van Ginkel, F., van Santen, V., Gulley, S. and Toro, H. (2008). Infectious Bronchitis Virus in the chicken Harderian Gland and Lachrymal Fluid: viral load, infectivity, immune cell responses, and effects of viral immunodeficiency. *Avian Diseases* **52**: 608 – 617.

Valastro, V., Holmes, E., Britton, P., Fusaro, A., Jackwood, M., Cattoli, G. and Monne, I. (2016). S1 gene-based phylogeny of infectious bronchitis virus: An attempt to harmonize virus classification. *Infection, Genetics and Evolution* **39**: 349 – 364.

van Beurden, S., Berends, A., Krämer-Kühl, A., Spekreijse, D., Chénard, G., Philipp, H., Mundt, E., Rottier, P. and Verheije, M. (2017). A reverse genetics system for avian coronavirus infectious bronchitis virus based on targeted RNA recombination. *Virology Journal* **14**: 109.

van Beurden, S., Berends, A., Kramer-Kuhl, A., Spekreigse, D., Chenard, G., Phillip, H. Mundt, E., Rottier, P. and Verheije, H. (2018). Recombinant live attenuated avian coronavirus vaccines with deletions in the accessory genes 3ab and/or 5ab protect against infectious bronchitis in chickens. *Vaccine* **36**: 1085 – 1092.

van den Worm, S., Eriksson, K., Zevenhoven, J., Weber, F., Zust, R., Kuri, T.,Dijkman, R., Chang, G., Siddell, S., Snijder, E., Thiel, V. and Davidson, A. (2012).Reverse genetics of SARS-related coronavirus using vaccinia virus-based recombination. *PLoS ONE* **7**: e32857

Vennema, H., Godeke, G., Rossen, J., Voorhout, W., Horzinek, M., Opstelten, D. and Rottier, J. (1996). Nucleocapsid-independent assembly of coronavirus-like particles by co-expression of viral envelope protein genes. *The EMBO Journal* **15**: 2020 – 2028.

Verheije, M., Hagemeijer, M., Ulasli, M., Reggiori, F., Rottier, P., Masters, P. and de Haan, C. (2010). The coronavirus nucleocapsid protein is dynamically associated with the replication-transcription complexes. *Journal of Virology* **84**: 11575 – 11579.

Vervelde, L., Matthijs, M.G., van Haarlem, D.A., de Wit, J.J., Jansen, C.A. (2013). Rapid NK-cell activation in chicken after infection with infectious bronchitis virus M41. *Veterinary Immunology and Immunopathology* **151:**337-341.

Walls, A., Tortorici, A., Bosch, B., Frenz,. B., Rottier, P., DiMaio, F., Rey, F. and Veesler, D. (2016). Cryo-electron microscopy structure of a coronavirus spike glycoprotein trimer*. Nature* **531**: 114 – 1

Walls, A., Tortorici, M., Snijdner, J., Xiong, X., Bosch, B., Rey, F. and Veesler, D. (2017). Tectonic conformational changes of a coronavirus spike glycoprotein promote membrane fusion. *Proceedings of the National Academy of Science USA* **114**: 11157 – 11162.

Wang, C., Hsieh, M. and Chang, P. (1996). Isolation, pathogenicity, and H120 protection efficacy of infectious bronchitis viruses isolated in Taiwan. *Avian Diseases* **40**: 620 – 625.

Wang, D., Fan, J., Fang, L., Luo, R., Ouyang, H., Ouyang, C., Zhang, H., Chen, H., Li, K. and Xiao, S. (2015). The nonstructural protein 11 of porcine reproductive and respiratory syndrome virus inhibits NF-κB signaling by means of its deubiquitinating activity. *Molecular Immunology* **68**: 357 – 366.

Wang, Y., Sun, Y., Wu, A., Xu, S., Pan, R., Zeng, C., Jin, X., Ge, X., Shi, Z., Ahola, T., Chen, Y. and Guo, D. (2015B). Coronavirus nsp10/nsp16 methyltransferase can be targeted by nsp10-derived peptide *in vitro* and *in vivo* to reduce replication and pathogenesis. *Journal of Virology* **89**: 8416 – 8427.

Wang, Y., Wang, Y., Zhang, Z., Fan, G., Jiang, Y., Liu, X,. Ding, J. and Wang, S. (1998). Isolation and identification of glandular stomach type IBV (QX IBV) in chickens. *Chinese Journal of Animal Quarantine* **15**:1 – 3.

Weiss, S and Navas-Martin, S. (2005). Coronavirus pathogenesis and the emerging pathogen severe acute respiratory syndrome coronavirus. *Microbiology and Molecular Biology Reviews* **69**: 635 – 664.

Williams, G., Chang, R. and Brian, D. (1999). A phylogenetically conserved hairpin-type 3′ untranslated region pseudoknot functions in coronavirus RNA replication. *Journal of Virology* **73**: 8349 – 55.

Williams, R., Jiang, G. and Holmes, K. (1991). Receptor for mouse hepatitis virus is a member of the carcinoembryonic antigen family of glycoproteins. *PNAS* **88**: 5533–36.

Winter, C., Herrler, G. and Neumann, U. (2008). Infection of the tracheal epithelium by infectious bronchitis virus is sialic acid dependent. *Microbes and Infection* **10**: 367 – 373.

Winter, C., Schwegmann-Weßels, C., Cavanagh, D., Neumann, U. and Herrler, G. (2006). Sialic acid is a receptor determinant for infection of cells by avian Infectious bronchitis virus. *Journal of General Virology* **5**: 1209 – 1216.

Weiss, S and Navas-Martin, S. (2005). Coronavirus pathogenesis and the emerging pathogen severe acute respiratory syndrome coronavirus. *Microbiology and Molecular Biology Reviews* **69**: 635 – 664.

Williams, G., Chang, R. and Brian, D. (1999). A phylogenetically conserved hairpin-type 3' untranslated region pseudoknot functions in coronavirus RNA replication. *Journal of virology* **73**: 8349 – 8355.

Wilson, L., Gage, P. and Ewart, G. (2006). Hexamethylene amiloride blocks E protein ion channels and inhibits coronavirus replication. *Virology* **353**: 294 – 306.

Wilson, L., McKinlay, C., Gage, P. and Ewart, G. (2004) SARS coronavirus E protein forms cation-selective ion channels. *Virology* **330**: 322 – 331.

Woo, P., Lau, S., Lam, C., Lai, K., Huang, Y., Lee, P., Luk, G., Dyrting, K., Chan, K. and Yuen, K. (2009). Comparative analysis of complete genome sequences of three Avian coronaviruses reveals a novel group 3c coronavirus. *Journal of Virology* **83**: 908 – 917.

Wong, S., Li, W., Moore, M., Choe, H. and Farzan, M. (2004). A 193-amino acid fragment of the SARS coronavirus S protein efficiently binds angiotensin-converting enzyme 2*. *The Journal of Biological Chemistry* **279**: 3197 – 3201.

Worthington, K.J., Currie, R.J. and Jones, R.C. (2008). A reverse transcriptase-polymerase chain reaction survey of infectious bronchitis virus genotypes in Western Europe from 2002 to 2006. *Avian Pathology* **37**:247-257.

Xu, Y., Cong, L., Chen, C., Wei, L., Zhao, Q., Xu, X., Ma, Y., Bartlam, M. and Rao, Z. (2009). Crystal structures of two coronavirus ADP-ribose-1''-monophosphatases and their complexes with ADP-ribose: a systematic structural analysis of the viral ADRP domain. *Journal of Virology* **83**: 1083 – 1092.

Yachida, S., Aoyama, N., Takahashi, N., Iritani, Y. and Katagiri, K. (1981). Influence of temperature of incubation on chicken embryo tracheal organ cultures and chick embryos infected with strains of avian Infectious Bronchitis Virus. *Research in Veterinary Science* **31**: 14 – 18.

Yamada, Y. and Liu, D. (2009). Proteolytic activation of the spike protein at a novel RRRR/S motif is implicated in furin-dependent entry, syncytium formation, and infectivity of coronavirus infectious bronchitis virus in cultured cells. *Journal of Virology* **83**: 8744 – 8758.

Yan, F., Zhao, Y., Hu, Y., Qiu, j., Lei, W., Ji, W., Li, X., Wu, Q., Shi, X. and Li, Z. (2013). Protection of chickens against infectious bronchitis virus with a multivalent DNA vaccine and boosting with an inactivated vaccine. *Journal of Veterinary Science* **14**: 53 – 60.

Yang, Z., Kong, W., Huang, Y., Roberts, A., Murphy, B., Subbarao, K. and Nabel, G. (2004). A DNA vaccine induces SARS coronavirus neutralization and protective immunity in mice. *Nature* **428**: 561–564.

Ye, Y. and Hogue, B. (2007) Role of the coronavirus E viroporin protein transmembrane domain in virus assembly. *Journal of Virology* **81**: 3597 – 3607.

Youn, S., Leibowitz, J. and Collisson, E. (2005). *In vitro* assembled, recombinant infectious bronchitis viruses demonstrate that the 5a open reading frame is not essential for replication. *Virology* **332**: 206 – 215.

Yount, B., Curtis, K. and Baric, R. (2000). Strategy for systematic assembly of largeRNA and DNA genomes: the transmissible gastroenteritis virus model. *Journal of Virology* **74**: 10600 – 10611.

Yount, B., Curtis, K., Fritz, E., Hensley, L., Jahrling, P., Prentice, E., Denision, M., Geisbert, T. and Baric, R. (2003). Reverse genetics with a full-length infectious cDNA of severe acute respiratory syndrome coronavirus. *Proceedings of the National Academy of Science USA* **100**: 12995 – 13000.

Yount, B., Denison, M., Weiss, S. and (Baric) R. (2002). Systematic assembly of afull-length infectious cDNA of mouse hepatitis virus strain A59. *Journal of Virology* **76**: 11065 – 11078.

Yudong, W., Yonglin, W., Zichun, Z., Genche, F., Yihai, J., Xiange, L., Jiang, D. and Shushuang, W. (1998). Isolation and identification of glandular stomach type IBV (QX IBV) in chickens. Chinese *Journal of Animal Quarantine* **15**.

Zhao, R., Sun, J., Qi, T., Zhao, W., Han, Z., Yang, X. and Liu, S. (2017). Recombinant Newcastle disease virus expressing the infectious bronchitis virus S1 gene protects chickens against Newcastle disease virus and infectious bronchitis virus challenge. *Vaccine* **35**:2435-2442.

Zhang, Y., Buckles, E. and Whittaker, G. (2012). Expression of the C-type lectins DC-SIGN or L-SIGN alters host cell susceptibility for the avian coronavirus, infectious bronchitis virus. *Veterinary Microbiology* **157**: 285 – 293.

Zhang H, Wang, G., Li, J., Nie, Y., Shi, X., Lain, G., Wang, W., Yin, X., Zhao, Y., Qu, X., Ding, M. and Deng, H. (2004). Identification of an antigenic determinant on the S2 domain of the severe acute respiratory syndrome coronavirus spike glycoprotein capable of inducing neutralizing antibodies. *Journal of Virology* **78**: 6938 – 6945.

Ziebuhr, J., Snijder, E. and Gorbalenya, A. (2000). Virus-encoded proteinases and proteolytic processing in the Nidovirales. *Journal of General Virology* **81**: 853 – 879.

Ziebuhr, J. Thiel, V. and Gorbalenya, A. (2001). The autocatalytic release of a putative RNA virus transcription factor from its polyprotein precursor involves two paralogous papain-like proteases that cleave the same peptide bond. *Journal of Biology Chemistry* **276**: 33220 –33232.

Zhong, Y., Wah Tan, Y. and Liu, D. (2012). Recent Progress in Studies of Arterivirus- and Coronavirus-Host Interactions. *Viruses* **4**: 980 – 1010.

Zuniga, S., Sola, I., Alonso, S. and Enjuanes, L. (2004). Sequence motifs involved in the regulation of discontinuous coronavirus subgenomic RNA synthesis. *Journal of Virology* **78**: 980 – 994.

Zust, R., Cervantes-Barragan, L., Habjan, M., Maier, R., Neuman, B., Ziebuhr, J., Szretter, K., Baker, S., Barchet, W., Diamond, M., Siddell, S., Ludewig, B. and Thiel, V. (2011). Ribose 2-O-methylation provides a molecular signature for the distinction of self and non-self mRNA dependent on the RNA sensor Mda5. *Nature Immunology* **12**:137 – 143.

Zust, R., Dong, H., Li, X., Chang, D., Zhang, B., Balakrishnan, T., Toh, Y., Jiang, T., Li, S., Deng, Y., Ellis, B., Ellis, E., Poidinger, M., Zolezzi, F., Qin, C., Shi, P. and Fink, K. (2013) Rational design of a live attenuated dengue vaccine: 2′O-methyl-transferase mutants are highly attenuated and immunogenic in mice and macaques. *PLoS Pathogens* **9**:e1003521.